DISSERTATION

TROPICAL FOREST ROOT CHARACTERISTICS AND RESPONSES TO DRYING ACROSS ENVIRONMENTAL GRADIENTS

Submitted by

Amanda Longhi Cordeiro

Graduate Degree Program in Ecology

In partial fulfillment of the requirements

For the Degree of Doctor of Philosophy

Colorado State University

Fort Collins, Colorado

July 2024

Doctoral Committee:

Advisor: Daniela F. Cusack

Dennis Ojima
M.Francesca Cotrufo
Richard Conant

ABSTRACT

TROPICAL FOREST ROOT CHARACTERISTICS
AND RESPONSES TO DRYING ACROSS
ENVIRONMENTAL GRADIENTS

Fine roots represent the interface between plants and soils, and as such regulate all major biogeochemical cycles in terrestrial ecosystems, including tropical forests. Tropical forests play a crucial role in global carbon (C) cycling, largely due to their extensive root biomass and significant soil C stocks. However, these ecosystems have been experiencing more frequent severe droughts across some regions and are predicted to continue experiencing these extreme drought events in the future. This dissertation seeks to contribute to the understanding and synthesis of tropical root responses to drying in varying environmental conditions. In chapter 1, I gave an introduction about the importance of fine roots to ecosystem function and the impacts of drying in tropical forests. In chapter 2, I characterized root biomass, morphology, nutrient content, colonization to 1.2 meters depth as well as and arbuscular mycorrhizal fungal (AMF) to 20 cm depth in 32 plots across four distinct lowland Panamanian forests which are representative of the vast variation in soil fertility and mean annual precipitation (MAP) found across tropical forests. Root characteristics measurements, such as morphology and chemistry, at soil layers deeper than 30 cm have been rarely documented and to the best of knowledge this is the first study in tropical forests. I observed that that some root traits changed with soil depth similarly across sites while others had site-specific variation. I also observed larger variation at the soil surface and that morphological traits, in addition to root biomass can affect soil C stocks. In chapter 3, the effects of experimental and

seasonal drying on fine root dynamics were explored using a partial throughfall reduction experiment across the same 32 plots as in chapter 2. I found that chronic drying impacted root biomass, productivity, morphology and arbuscular mycorrhizal fungi (AMF) colonization. Root biomass and characteristics also changed across seasons with different dynamics across depths. Chapter 4 focused on the effects of drought on tropical seedling development in a controlled chamber environment. I observed that drying decreased seedling growth, but high soil fertility and AMF inoculation mitigated these effects. I also observed changes in root morphology, leached C, new C allocation patterns, and aboveground traits in response to drought, but with usually interacting effects with fertility and AMF inoculation. Chapter 5 contributes a tropical root database (TropiRoot 1.0 database) with root data extracted from scientific papers across different countries and continents. Overall, this dissertation provides novel results and insights into the variation in root characteristics among tropical forests and their responses to climatic drying with interacting effects of fertility, symbionts and soil depth effects. It brings novel measurements that have never been published in tropical forest studies. In chapter 2, I found novel results about how different tropical forests had similar patterns of root variation with depth. It indicated differences in resources acquisition at the soil surface (likely for nutrients) and at deeper soil layers (likely for water) that are usually less investigated. I also showed a large variation of roots at surface soil across different forests that may influence forest responses to global change factors. In chapter 3, I supported some results across the literature such as drying decreasing root growth at the soil surface. However, I added new results such as drying decreasing root productivity at deeper soil layers, and changing root morphology and associations with symbionts probably to compensate the lower root growth. All together I observed that drying promoted changes in acquisition strategies and also that fertile forests may respond differently to drying. In chapter 4, I showed

some clear tradeoffs in plant traits providing evidence that they are constantly changing in response to the environment. Also, I provided some novel results on the mechanisms, such as nutrient retention, on how mycorrhizal and fertility mitigated some negative effects of drying on plant growth. This aligns with the field study showing some possible resilience in the fertile forests to drying. The findings highlight the complex interactions between root traits and environmental conditions, offering important implications for predicting tropical forest responses to changing moisture and nutrient availability. All these chapters together provided a good understanding on how different forests respond to environmental changes. These impacts on soil C storage, links with root function and possible larger vulnerability of some forests are great topics for future studies.

ACKNOWLEDGEMENTS

I would like to thank many people for helping me with this PhD. I feel grateful and fulfilled to have made so many friends and collaborators through this journey. So many people inspired me, gave me strengthen or simply were there to help me navigate grad school. First, I must thank Dr. Daniela Cusack, my advisor; who has given me this opportunity, been supportive, always providing advice for my career, feedback, teaching me and clearly demonstrating how she wants to see her students successful. I am grateful for her mentorship, for the collaborations we made together and for being there in all the moments in this journey. I have learned so much! I also would like to thank my committee members for their support, feedback, and advice: Dr. Francesca Cotrufo, Dr. Dennis Ojima and Dr. Richard Conant. My committee members were very kind, empathetic and with great scientific contributions during my time at CSU. They have encouraged me to think about diverse topics in science and about my future. A special thanks to Dr. Francesca Cotrufo for her collaboration in one of my chapters and constantly feedback. I also would like to thanks all the people who have worked at Cusack lab, for either their help on my work, their company, time spent together and support. Special thanks to Dr. Lee Dietterich who has been an amazing mentor and who I had the pleasure to work with during the year I lived in Panama to conduct my field work. He is a person who I want to always learn from. Also, a special thanks to: Emily Blackaby for helping me analyzing some samples and for her partnership and friendship during our time spent together at CSU and to Avishesh Neupane and Alex Headpetch who coordinated the root processing for one semester while I was doing my field work in Panama and have been amazing lab partners and friends. Next, I'd like to thank all the 45 students/technichians from UCLA,

Panama and who had worked in the lab or in the field in the project: Alex Smilor, Alyssa Schaefer, Andres Rodriguez, Avery Schell, Bianco, Carina Easton, Daniel D. Vidal, Delisa Mambeche, Dulce Dharma, Edwin, Eric Valdes, Erinn Hayward, Eugenio, Gabriela Quesada, Gabriel Oppler, Hayden Warner, Hilary Johnson, Ilana Vargas, Isabella Felsing, J Reu, Johnny Linares, Julia Perbohner, Kathryn Smith, Kevin Neung, Kimmie Pham, Kori Valencia, Laura Lenhart, Layna Webb, Leo Thomas, Lily Colburn, Lily Daniels, Lovisa Duck, Makenna Brown, Maira Oliveira, Mason McKinzie, Minh Quang Nguyen, Natalie Namba, Parker Neal, Quin Noel, Riley Krudop, Ryan Bridges, Sebastian Bravo, Weronika Konwent. It has been a wonderful experience to be a part of this lab, and that is in part because of the great people I had the opportunity to work with. There are many other people who made this research possible: Michelle Haddix, Dan Reuss, Guy Beresford, Rod Simpson, Lauren Hibbard, Lauren Ackein, Jennifer Neuwald, Jonathan Straube who I also would like to thank. I'd also like to acknowledge the Graduate Degree Program in Ecology (GDPE) and Department of Ecosystem Science and Sustainability here at CSU – for their funding, support, and opportunities to engage with other scientists. I also want to thanks the professor Alan Knapp and Dr. Olivia Hajek for letting me borrow their Li-Cor equipment and for my personal great friend André Araújo and his professors Dr Todd Gaines for lending me the leaf area meter from weed science lab. I would like to thank the professors of classes I TA'ed who have touch me so much (Dr. Stacy Linn, Dr. Robin Reid, Dr. Amanda Shores, Dr. Daniela Cusack) and my TA colleagues, especially Jemma Fadum who helped me so much during my first-time teaching. Special thanks to friends from ESS who have been in this journey with me. I have been able to build an amazing and diverse ecology community during my time at CSU which I'm very grateful for. Further, I'd like to acknowledge the Smithsonian Tropical Research

Institute who have me support during my field work. Special thanks to Dr. Joe Wright as my host and advisor during the time I was living in Panama. I also want to thanks all the people who have helped me in Panama and the very supportive community from Gamboa. I also want to thank all the members from the TropiRoot group who I had the pleasure to collaborate with during the past 4 years and who I've learnt so much from. I will never forget to thanks my previous advisors (Dr. Richard Norby, Dr. Beto Quesada and Dr. Kelly Andersen) who encouraged me to start this PhD journey and have been incredibly supportive during all these years! I would like to thank the love and support that I have received from my friends. Thanks to my old friends from school, university, masters, internships abroad and my newer friends from LA, Panama and Fort Collins. A special thanks to Cindy Guillaume who has always seen the best on me and helped guiding me to thriving mindset and Robin Reid also helped me to thrive in challenging moments. A special thanks to all my friends from Fort Collins where I was lucky to make an international + American community of friends who I want to bring with me for the rest of my life. Thanks also to the Brazilian community in Fort Collins who made me feel at home. Finally, I want to thanks my family. I am very lucky to have an amazing family who has always supported me and understood the times when I could not be present. My partner Nathan Borges Gonçalves who have been on my side since we were doing our master's degree together, has collaborated with me on research, ideas and especially has been my biggest company always supporting and encouraging me. My grandparents, Ivette Maria Bonato, Nelson Longhi, parents, Mariangela Longhi and Renato Campello Cordeiro, sibling, Daniel Longhi Cordeiro, have been the best friends and greatest supporters in my life, and this endeavor has been no different. I can't thank my friends and family enough!

TABLE OF CONTENTS

CHAPTER 1: INTRODUCTION

Fine roots represent the interface between plants and soils, and as such regulate all major biogeochemical cycles in tropical forests. Root dynamics and characteristics are important components to study in response to changes in environmental conditions as they play a crucial role in the cycling of water, nutrients, and carbon (C) (McCormack *et al.*, 2015) and are likely the primary inputs of C to soils (Rasse *et al.*, 2005). Across diverse tropical forests in Panama, fine roots were the best predictor of soil C (Cusack, *et al.*, 2018). These roots are expected to change dynamics, morphological and physiological traits or their distribution in response to environmental factors such as drought which may help with nutrients and water acquisition and avoid or delay negative effects of drought (Comas *et al.*, 2013; Cusack *et al.*, 2021). Given the importance of root dynamics and traits in the cycling of C and nutrients, its crucial to study how roots respond to global change factors, especially in C rich ecosystems.

Tropical forests are critical reservoirs of C stocks, accounting for 25-40% of the world's terrestrial C pools (Field *et al.*, 1998; Jobbagy & Jackson, 2000) with most of the C being stored belowground (Crowther *et al.*, 2019). These biomes are also vital in regulating global water, nutrient, and C cycles, with an important role in global climate regulation (Artaxo *et al.*, 2022b) being an important C sink over the last decades (Brienen *et al.*, 2015). However, these regions have experienced ongoing climate change, with climate extremes becoming increasingly more common which have had large impacts in forest structure and function. For example, disturbance and climate change are affecting tropical forest's C sink with this C sink decreasing in some regions (Brienen *et al.*, 2015; Hubau *et al.*, 2020) with some parts of the Amazonia even starting to act as a C source (Gatti *et al.*, 2021). One important disturbance that appears to influence these

C dynamics in tropical forests is the intensification of the dry season and increased drought extreme events.

Some regions of tropical forests have experienced increased duration of the dry season and more frequent severe droughts (Artaxo *et al.*, 2022a; Artaxo *et al.*, 2022b). There is evidence that in some regions, drier months have become drier while wetter months have become wetter (Marengo, 2004; Gloor *et al.*, 2013; Marengo & Espinoza, 2016) with also variability in precipitation anomalies across different regions (Marengo, 2004). A review shows that drought is expected to intensify during the 21st century (Marengo & Espinoza, 2016), but there has been large range of uncertainty, especially in the tropics (Kharin *et al.*, 2007). Although of the remaining uncertainty, climate models consistently project that large rainfall changes will occur for a considerable proportion of tropical land (Chadwick *et al.*, 2015). These changes have important impacts on tropical forests dynamics and function.

Across a growing body of tropical field studies, drying appears to negatively affect tropical plant growth, reducing ecosystem C storage in plants and soils, and biodiversity (Cusack, *et al.*, 2016). Even intact tropical rainforests have become increasingly vulnerable to drought (Tao *et al.*, 2022). Drier conditions are expected to increase tree mortality rates (Nepstad *et al.*, 2007; da Costa *et al.*, 2010; Rowland *et al.*, 2015) and alter fire regimes, biodiversity and nutrient availability (Bonal *et al.*, 2016; Cusack, *et al.*, 2016). Also, there is evidence of experimental drying changing soil respiration (Cusack *et al.*, 2023); microbial communities (Chacon *et al.*, 2023); decreasing microbial biomass and dissolved organic carbon (DOC) inputs to soil and changing nutrient cycling (Dietterich *et al.*, 2022) which also showed in some cases specific responses to drought in different tropical forests. Also, experimental drying generally reduces root stocks and productivity across different tropical regions (Metcalfe *et al.*, 2008; Moser *et al.*, 2014; Zhou *et al.*, 2019), with

rainfall frequency and volume and its interaction with other treatments appearing to influence fine root biomass responses to moisture availability (Deng *et al.*, 2018). These changes can lead to a reduction in the C storage capabilities of these forests (Brodribb *et al.*, 2020) contributing to the decrease in C sink in some regions.

Tropical forests are expected to respond differently to changes in precipitation due to their high variability. These forests are diverse, both for species richness and the range of environmental conditions including mean annual precipitation (MAP), soil fertility, and structural complexity (Holdridge *et al.*, 1971; FAO, 2012). Different responses to drought have been observed in a modeling study showing that frequent droughts led to different biomass, structure and composition responses of drier vs wetter forests with the wet site showing insensitivity to drought scenarios (Longo *et al.*, 2018). Also, forests with easier access to groundwater are expected to be less vulnerable to drought but under severe drought conditions, these patterns can be reversed as forests not often exposed to drought are expected to have drought-intolerant traits (Costa *et al.*, 2023). These responses are also expected to interact with soil fertility as it can also influence plant traits (Cusack *et al.*, 2021; Oliveira *et al.*, 2021; Costa *et al.*, 2023). Therefore, given the expected variation in plant responses to drought across different forests and the importance of fine roots to C and nutrient cycling, it is essential to understand drying effects on roots across different tropical forests. These variations in responses can have implications for forest structure and function and can impact not only local areas, but also have the potential to affect global C, water and nutrients cycles.

Despite the recognized importance of drying effects on tropical forests' structure, there is a gap in our understanding of root responses, particularly at the community level across different tropical forests and at deeper soil layers (Bonal *et al.*, 2016). Also, there is general less research

on belowground responses than aboveground (Iversen *et al.*, 2017), and less belowground data representation in models (Cusack *et al.*, 2024) probably because studying belowground responses is often more time consuming (Judd *et al.*, 2015), especially in deeper soil layers. Root variation across depths, root phenology, root traits variation across different environmental conditions as well as their links with aboveground traits are paramount to understand how different forests can respond to drying and also increase roots representation in vegetation models (Cusack *et al.*, 2024) and improve model predictions.

This dissertation contributes to the fields of tropical forest ecology, root biology, and biogeochemistry by pushing forward our understanding and synthesis of tropical root responses to drying in varying environmental conditions as well as shifts in root dynamics and characteristics across depths. The dissertation provides: 1. a large body of new data with novel root measurements at deeper soil layers across different tropical forests (chapter 2), 2. A multi-year time series of new data for field responses of roots to experimental and seasonal drying (chapter 3). 3. integrated measures of belowground and aboveground tropical seedling responses to drying with interacting effects with fertility and symbionts (chapter 4), and 4. a new database of published data that will be available to the scientific community (chapter 5). Together, these areas of investigation advance the fields of knowledge represented here.

Chapter 2 presents research on root characteristics in a broad spatial scale, not only across different tropical forests, but also at deeper soils. For this chapter I measured live and dead root biomass, morphology, chemistry, and AMF colonization rates to 1.2 m depths in 32 plots across four lowland Panamanian forests that represent the broader – scale variation in rainfall, dry season length, and soil fertility in the region (Cusack, *et al.*, 2018). I explored patterns and tradeoffs in root characteristics by depth and among sites, as well as relationships among root characteristics,

and with soil C stocks. These measurements provide unprecedented detail about root characteristics in deeper soil layers that have rarely been documented in the scientific literature in the tropics. I observed that specific root length (SRL) increased with depth while root tissue density (RTD), coarse root biomass, and AMF colonization decreased systematically across sites while fine root biomass, diameter and chemistry varied differently by depth among sites. These characteristics varied more at the soil surface than deeper and tradeoffs among traits were observed which were likely related to resource acquisition. Fertile forests had less surface fine root biomass but a more homogeneous distribution of roots across depths and larger deep root radiocarbon values, indicating older roots and more productivity at deeper layers which can confer more resilience to drying under fertile conditions. On the other hand, infertile forests appeared to rely more on superficial roots likely making them more vulnerable to environmental changes. Soil C stocks were positively related to root biomass and negatively related to SRL indicating root morphology can also contribute to soil C storage variation. These results show that tropical forests employ diverse resource acquisition and conservation strategies that vary with soil depth—often overlooked in measurements. This study discovered emergent properties of tropical forests belowground, such as some root traits changed with soil depth similarly across forests, while other characteristics had site-specific variation. These patterns could offer insights into root function, transfer of root C to soil, and how different forests might differ in vulnerability to climate change.

Chapter 3 explores the impacts of drying on root systems in a field-scale drought experiment, providing new, high-resolution spatial and temporal data across different forests and seasons. Specifically, this study presents new results from experimental and seasonal drying on fine root productivity, mortality, stocks, turnover, morphology, chemistry and arbuscular mycorrhizal fungi (AMF) across various tropical forest sites and soil depths, where I also dig

deeper investigating roots to ~1-m depth. I used a partial throughfall reduction experiment across 32 plots in four different lowland seasonal forests varying in fertility and mean annual precipitation. I collected soil and fine roots data using various methods (minirhizotron, ingrowth core, sequential coring) during years 1-5 of the experiment. Therefore, this chapter provides results from diverse methods, in a high-resolution spatial scale (both across forests and depths) and also temporal scale. Throughfall exclusion consistently reduced root stocks and productivity across all depths, with more pronounced effects at the soil surface and in infertile forests. Seasonal trends indicated peak productivity in surface soils during the early wet season, likely related to nutrient acquisition and higher root stocks in deeper soils during the dry season, likely related to water uptake, revealing different root function across depths. Experimental drying generally increased fine root diameter and decreased RTD which may be related to the increased AMF colonization under chronic drying. Drying effects from chronic drying and seasonal drying did not always follow the same direction suggesting a complex response to drying depending on the variable measured. Root productivity, mortality, stocks and turnover decreased with depth and root dynamics distribution depended on soil fertility. This research provides direct evidence of drying effects on root characteristics in tropical forests, especially at the soil surface. It contributes crucial data about which root characteristics, depths, and forest types respond more strongly to drying.

Chapter 4 presents research in a controlled environment in a greenhouse where I could assess drought effects on a relatively abundant Neotropical tree seedling species, comparing interacting effects of soil fertility and AMF inoculation. I was able to conduct belowground and aboveground measurements using a whole-plant approach to link changes in biomass allocation with above-belowground coordination in trait responses. I measured whole-plant C and nutrient dynamics (e.g., biomass, root:shoot ratios, photosynthetic rates), plant traits (e.g. specific leaf area

[SLA, cm2 g-1], SRL), and transfer of plant C into soils (e.g., root leachate, extractable soil C). This chapter provide new insights into how tropical seedlings adjust their root and shoot characteristics in response to drying, offering valuable data on plant C and nutrient dynamics. I was able to demonstrate the capacity of tropical seedlings to adjust their growth, photosynthesis, leaf and root characteristics, and nutrient dynamics in reaction to drought conditions. I also showed shifts in C allocation between seedlings in drought conditions compared to those in moist environments, with rapid allocation of newly fixed C to both leaves and roots under drought. The impact of drought on various metrics was substantially influenced by soil fertility and AMF inoculation, often surpassing the direct effects of drought itself. Drying increased leached C in the end of the experiment as did soil fertility, whereas AMF suppressed it decreasing plant C expenditure in exudates showing implications on fluxes of C to soil. Also, plant association with symbionts increased photosynthesis and plant growth even though plants displayed more conservative morphological root traits. These results revealed the role of fertility and symbionts to mitigate some drying effects of seedlings that offers insight on how tropical seedlings might respond to drought across site-scale environmental variation.

Chapter 5 contributes to the scientific community by providing a database (TropiRoot 1.0 database) with data extracted from 106 new sources, resulting in more than 8000 rows of data (either species or community data). Most of the data includes root characteristics such as root biomass, morphology, root dynamics, mass fraction, architecture, anatomy, physiology and root chemistry with data collected from 25 different countries across different continents. This initiative represents a 30% increase of the currently available data for tropical roots available in the Fine root ecological database (FRED) (Iversen *et al.*, 2017) which can be used to move the field of tropical root ecology forward through large synthesis analyses.

In summary, I was able to demonstrate that not only biomass, but also root productivity, mortality and turnover as well as root characteristics vary with depth and that these characteristics can influence soil C stocks (chapter 2 and 3). I also demonstrated that chronic and seasonal drying affect root dynamics and characteristics including deeper soil layers that are rarely measured. I also found that drying effects on roots can be partially reduced by fertility and symbionts association, in specific conditions such as in seedlings and in the field at some depending on when and where roots were measured (chapter 3 and 4). I also observed tradeoffs in root characteristics at both community (chapter 2) and species (chapter 4) levels which are likely related to resource acquisition strategies. I also provided a root database contributing with new data to researchers that want to investigate root dynamics and traits globally (chapter 5). This dissertation provided comprehensive insights into fine root dynamics and characteristics under different environmental conditions, especially drying, thus improving our understanding of tropical forest responses to environmental changes and contributing valuable data for ecosystem modeling and climate change mitigation strategies.

LITERATURE CITED

Artaxo P, Hansson H-C, Andreae MO, Bäck J, Alves EG, Barbosa HMJ, Bender F, Bourtsoukidis E, Carbone S, Chi J, et al. 2022a. Tropical and Boreal Forest – Atmosphere Interactions: A Review. *Tellus B: Chemical and Physical Meteorology* 74(1).

Artaxo P, Hansson HC, Machado LAT, Rizzo LV. 2022b. Tropical forests are crucial in regulating the climate on Earth. *PLOS Climate* 1(8).

Bonal D, Burban B, Stahl C, Wagner F, Herault B. 2016. The response of tropical rainforests to drought-lessons from recent research and future prospects. *Ann For Sci* 73: 27-44.

Brienen RJ, Phillips OL, Feldpausch TR, Gloor E, Baker TR, Lloyd J, Lopez-Gonzalez G, Monteagudo-Mendoza A, Malhi Y, Lewis SL, et al. 2015. Long-term decline of the Amazon carbon sink. *Nature* 519(7543): 344-348.

Brodribb TJ, Powers J, Cochard H, Choat B. 2020. Hanging by a thread? Forests and drought. *Science* 368(6488): 261-+.

Chacon SS, Cusack DF, Khurram A, Bill M, Dietterich LH, Bouskill NJ. 2023. Divergent responses of soil microorganisms to throughfall exclusion across tropical forest soils driven by soil fertility and climate history. *Soil Biology and Biochemistry* 177.

Chadwick R, Good P, Martin G, Rowell DP. 2015. Large rainfall changes consistently projected over substantial areas of tropical land. *Nature Climate Change* 6(2): 177-181.

Comas LH, Becker SR, Cruz VV, Byrne PF, Dierig DA. 2013. Root traits contributing to plant productivity under drought. *Frontiers in Plant Science* 4: 16.

Costa FRC, Schietti J, Stark SC, Smith MN. 2023. The other side of tropical forest drought: do shallow water table regions of Amazonia act as large-scale hydrological refugia from drought? *New Phytol* 237(3): 714-733.

Crowther TW, van den Hoogen J, Wan J, Mayes MA, Keiser AD, Mo L, Averill C, Maynard DS. 2019. The global soil community and its influence on biogeochemistry. *Science* 365(6455).

Cusack D, Karpman J, Ashdown D, Cao Q, Ciochina M, Halterman S, Lydon S, Neupane A. 2016. Global change effects on humid tropical forests: Evidence for biogeochemical and biodiversity shifts at an ecosystem scale. *Reviews of Geophysics* 54(3): 523-610.

Cusack D, Markesteijn L, Condit R, Lewis O, Turner B. 2018. Soil carbon stocks in tropical forests of Panama regulated by base cation effects on fine roots. *Biogeochemistry* 137(1-2): 253-266.

Cusack DF, Addo-Danso SD, Agee EA, Andersen KM, Arnaud M, Batterman SA, Brearley FQ, Ciochina MI, Cordeiro AL, Dallstream C, et al. 2021. Tradeoffs and Synergies in Tropical Forest Root Traits and Dynamics for Nutrient and Water Acquisition: Field and Modeling Advances. *Frontiers in Forests and Global Change* 4: 704469.

Cusack DF, Christoffersen B, Smith-Martin CM, Andersen KM, Cordeiro AL, Fleischer K, Wright SJ, Guerrero-Ramirez NR, Lugli LF, McCulloch LA, et al. 2024. Toward a coordinated understanding of hydro-biogeochemical root functions in tropical forests for application in vegetation models. *New Phytol*.

Cusack DF, Dietterich LH, Sulman BN. 2023. Soil Respiration Responses to Throughfall Exclusion Are Decoupled From Changes in Soil Moisture for Four Tropical Forests, Suggesting Processes for Ecosystem Models. *Global Biogeochemical Cycles* 37(4).

Cusack DF, Karpman J, Ashdown D, Cao Q, Ciochina M, Halterman S, Lydon S, Neupane A. 2016. Global change effects on humid tropical forests: Evidence for biogeochemical and biodiversity shifts at an ecosystem scale. *Reviews of Geophysics* 54(3): 523-610.

Cusack DF, Markesteijn L, Condit R, Lewis OT, Turner BL. 2018. Soil carbon stocks across tropical forests of Panama regulated by base cation effects on fine roots. *Biogeochemistry* 137(1-2): 253-266.

da Costa AC, Galbraith D, Almeida S, Portela BT, da Costa M, Silva Junior Jde A, Braga AP, de Goncalves PH, de Oliveira AA, Fisher R, et al. 2010. Effect of 7 yr of experimental drought on vegetation dynamics and biomass storage of an eastern Amazonian rainforest. *New Phytol* 187(3): 579-591.

Deng Q, Zhang D, Han X, Chu G, Zhang Q, Hui D. 2018. Changing rainfall frequency rather than drought rapidly alters annual soil respiration in a tropical forest. *Soil Biology and Biochemistry* 121: 8-15.

Dietterich LH, Bouskill NJ, Brown M, Castro B, Chacon SS, Colburn L, Cordeiro AL, Garcia EH, Gordon AA, Gordon E, et al. 2022. Effects of experimental and seasonal drying on soil microbial biomass and nutrient cycling in four lowland tropical forests. *Biogeochemistry* 161(2): 227-250.

FAO. 2012. Global Ecological Zones for FAO Forest Reporting: 2010 Update. Forest Resources Assessment Working Paper Rome: Food and Agriculture Organication of the United Nations.

Field CB, Behrenfeld MJ, Randerson JT, Falkowski P. 1998. Primary production of the biosphere: Integrating terrestrial and oceanic components. *Science* 281(5374): 237-240.

Gatti LV, Basso LS, Miller JB, Gloor M, Gatti Domingues L, Cassol HLG, Tejada G, Aragao L, Nobre C, Peters W, et al. 2021. Amazonia as a carbon source linked to deforestation and climate change. *Nature* 595(7867): 388-393.

Gloor M, Brienen RJW, Galbraith D, Feldpausch TR, Schöngart J, Guyot JL, Espinoza JC, Lloyd J, Phillips OL. 2013. Intensification of the Amazon hydrological cycle over the last two decades. *Geophysical Research Letters* 40(9): 1729-1733.

Holdridge L, Grenke W, Hatheway W, Liang T, Tosi J. 1971. *Forest environments in tropical life zones*. New York: Pergamon Press.

Hubau W, Lewis SL, Phillips OL, Affum-Baffoe K, Beeckman H, Cuni-Sanchez A, Daniels AK, Ewango CEN, Fauset S, Mukinzi JM, et al. 2020. Asynchronous carbon sink saturation in African and Amazonian tropical forests. *Nature* 579(7797): 80-87.

Iversen CM, McCormack ML, Powell AS, Blackwood CB, Freschet GT, Kattge J, Roumet C, Stover DB, Soudzilovskaia NA, Valverde-Barrantes OJ, et al. 2017. A global Fine-Root Ecology Database to address belowground challenges in plant ecology. *New Phytologist* 215(1): 15-26.

Jobbagy EG, Jackson RB. 2000. The vertical distribution of soil organic carbon and its relation to climate and vegetation. *Ecological Applications* 10(2): 423-436.

Judd LA, Jackson BE, Fonteno WC. 2015. Advancements in Root Growth Measurement Technologies and Observation Capabilities for Container-Grown Plants. *Plants* 4(3): 369-392.

Kharin VV, Zwiers FW, Zhang X, Hegerl GC. 2007. Changes in temperature and precipitation extremes in the IPCC ensemble of global coupled model simulations. *Journal of Climate* 20(8): 1419-1444.

Longo M, Knox RG, Levine NM, Alves LF, Bonal D, Camargo PB, Fitzjarrald DR, Hayek MN, Restrepo-Coupe N, Saleska SR, et al. 2018. Ecosystem heterogeneity and diversity mitigate Amazon forest resilience to frequent extreme droughts. *New Phytologist* 219(3): 914-931.

Marengo JA. 2004. Interdecadal variability and trends of rainfall across the Amazon basin. *Theoretical and Applied Climatology* 78(1-3).

Marengo JA, Espinoza JC. 2016. Extreme seasonal droughts and floods in Amazonia: causes, trends and impacts. *International Journal of Climatology* 36(3): 1033-1050.

McCormack ML, Dickie IA, Eissenstat DM, Fahey TJ, Fernandez CW, Guo D, Helmisaari H-S, Hobbie EA, Iversen CM, Jackson RB, et al. 2015. Redefining fine roots improves understanding of below-ground contributions to terrestrial biosphere processes. *New Phytologist* 207(3): 505-518.

Metcalfe DB, Meir P, Aragao L, da Costa ACL, Braga AP, Goncalves PHL, Silva JD, de Almeida SS, Dawson LA, Malhi Y, et al. 2008. The effects of water availability on root growth and morphology in an Amazon rainforest. *Plant and Soil* 311(1-2): 189-199.

Moser G, Schuldt B, Hertel D, Horna V, Coners H, Barus H, Leuschner C. 2014. Replicated throughfall exclusion experiment in an Indonesian perhumid rainforest: wood production, litter fall and fine root growth under simulated drought. *Global Change Biology* 20(5): 1481-1497.

Nepstad DC, Tohver IM, Ray D, Moutinho P, Cardinot G. 2007. Mortality of large trees and lianas following experimental drought in an amazon forest. *Ecology* 88(9): 2259-2269.

Oliveira RS, Eller CB, Barros FV, Hirota M, Brum M, Bittencourt P. 2021. Linking plant hydraulics and the fast-slow continuum to understand resilience to drought in tropical ecosystems. *New Phytol* 230(3): 904-923.

Rasse DP, Rumpel C, Dignac MF. 2005. Is soil carbon mostly root carbon? Mechanisms for a specific stabilisation. *Plant and Soil* 269(1-2): 341-356.

Rowland L, da Costa AC, Galbraith DR, Oliveira RS, Binks OJ, Oliveira AA, Pullen AM, Doughty CE, Metcalfe DB, Vasconcelos SS, et al. 2015. Death from drought in tropical forests is triggered by hydraulics not carbon starvation. *Nature* 528(7580): 119-122.

Tao S, Chave J, Frison PL, Le Toan T, Ciais P, Fang J, Wigneron JP, Santoro M, Yang H, Li X, et al. 2022. Increasing and widespread vulnerability of intact tropical rainforests to repeated droughts. *Proc Natl Acad Sci U S A* 119(37): e2116626119.

Zhou L, Liu Y, Zhang Y, Sha L, Song Q, Zhou W, Balasubramanian D, Palingamoorthy G, Gao J, Lin Y, et al. 2019. Soil respiration after six years of continuous drought stress in the tropical rainforest in Southwest China. *Soil Biology & Biochemistry* 138.

CHAPTER 2: ROOT CHARACTERISTICS VARY WITH DEPTH ACROSS FOUR LOWLAND SEASONAL TROPICAL FORESTS[1]

2.1 Summary

Tropical forests contain some of the largest root biomass stocks globally, contributing to large soil carbon (C) stocks. Variation in root characteristics among tropical forests and with depth is poorly characterized. We characterized root biomass, morphology, nutrient content, and arbuscular mycorrhizal fungal (AMF) colonization rates to 1.2m depths in 32 plots across four distinct lowland Panamanian forests, and related root characteristics to soil C stocks. We hypothesized that: (H1) root characteristics vary systematically with depth, exhibiting tradeoffs related to resource acquisition, and (H2) variation in root characteristics is strongest in surface soils, reflecting site-scale resource differences. We used principal components analysis (PCA) and cluster analyses to assess overall patterns, and then compared individual characteristics by site and depth. We observed systematic variation in root characteristics by depth: specific root length (SRL) increased with depth, whereas root tissue density (RTD), coarse root biomass, and AMF colonization declined with depth. PCA showed tradeoffs for diameter versus SRL and biomass, and AMF colonization rates versus SRL. Among sites, the fertile forest had the least surface fine root biomass (0–10cm) and largest deep-root radiocarbon ages, the driest forest had the smallest root diameter (0–60cm), and the wettest, most infertile forest had the most surface root biomass and smallest SRL (0–120cm). Soil C stocks were positively related to root biomass and negatively related to SRL. These results provide novel data on how roots change across depths in Panamanian tropical forest, with indications of different acquisition strategies across sites and depths.

[1] Cordeiro, A.L et al. 2024. Root Characteristics Vary with Depth Across Four Lowland Seasonal Tropical Forests. Manuscript under review by Ecosystems

2.2 Introduction

Tropical forests have the largest fine root biomass stocks globally (Jackson *et al.*, 1996), likely contributing to large soil carbon (C) stocks in tropical forests, which contain one third of global terrestrial C stocks. Tropical forests also have the largest net primary production (NPP) globally (Field *et al.*, 1998; Jobbagy & Jackson, 2000; Hengl *et al.*, 2017), with over one third of NPP typically allocated to roots (Aragao *et al.*, 2009; Malhi *et al.*, 2011; Cordeiro *et al.*, 2020; Huaraca Huasco *et al.*, 2021). Fine roots, often defined as < 2 mm in diameter or the first branching orders (Guo *et al.*, 2008; McCormack *et al.*, 2015; Freschet *et al.*, 2021a), are the primary interface between plants and soils, and thus mediate both C transfer from plants to soils as well as acquisition of soil resources like water and nutrients for plants. While the relationship between root biomass and soil C stocks has been established for tropical forests (Cusack *et al.*, 2018; Cusack & Turner, 2020), root traits beyond biomass are also important for resource acquisition in tropical forests (Cusack *et al.*, 2021), and could also influence how root detritus is retained as soil C.

Lowland tropical forests are typically warm, wet ecosystems, but there is large variation in moisture and nutrient availability among lowland tropical forest sites, and with depth, which likely influence root characteristics. Mean annual precipitation (MAP) in moist and wet tropical forests ranges from 2,000 to over 8,000 mm globally (Holdridge *et al.*, 1971), with dry seasons ranging from 0 – 5 months (FAO, 2012). Water resources in tropical forests can also vary greatly with depth, with moisture in surface soils declining sharply during dry seasons (Cusack *et al.*, 2019; Cusack, *et al.*, 2019; Spanner *et al.*, 2022), and belowground water tables common in many lowland tropical forests (Fan *et al.*, 2017). Tropical forests also occur across large ranges of soil fertility, such as the more than 250 fold difference in soil available phosphorus (P) and base cations observed across the Panamanian lowlands and the Amazon Basin (Turner & Engelbrecht, 2011;

Cusack *et al.*, 2018; Quesada *et al.*, 2020). The vertical distribution of nutrients in the soil profile also varies, with notable depletion of P and base cations at depth in heavily weathered soils, compared to more uniform nutrient depth distributions in fertile tropical soils (Cusack & Turner, 2020). Despite these large environmental gradients within and among tropical forests, little is known about how root characteristics beyond biomass vary with depth and among sites.

A framework of root trait tradeoffs has been presented as different strategies for belowground resource acquisition, following aboveground traits frameworks that describe "fast" versus "slow" lifestyles growth strategies (Wright *et al.*, 2004; Reich, 2014; Diaz *et al.*, 2016). Conflicting findings suggest root traits diverge from the simple fast – slow spectrum devised for aboveground traits, likely related to different evolutionary pressures belowground (Kramer-Walter *et al.*, 2016; Weemstra *et al.*, 2016; Bergmann *et al.*, 2020; Weemstra *et al.*, 2020; Laughlin *et al.*, 2021). Newer frameworks for understanding root tradeoffs center around water and nutrient acquisition, with one axis mirroring the fast-slow axis used aboveground, and a second axis representing symbiotic associations. In this second axis, plant invest either in root structures specialized for resource acquisition (e.g. roots with high specific root length [SRL]), or invest in symbiotic associations, such as C transfer to arbuscular mycorrhizal fungi (AMF) (Hodge, 2004; Eissenstat *et al.*, 2015; Ma *et al.*, 2018; Bergmann *et al.*, 2020; Weigelt *et al.*, 2021). The first fast-slow axis is often represented as a tradeoff between high root tissue density (RTD; $g\ cm^{-3}$), which might indicate longer root lifespans (“slow”), versus high fine root nitrogen (N) concentrations, which might indicate higher metabolic rates, and turnover times (“fast”), and a more acquisitive life strategy. These tradeoffs have been illustrated globally at species level (Bergmann et al., 2020), but have not been tested across tropical forest types, deeper soil layers, or at the community-scale. A drawback of these approaches has been that they are typically limited to root morphology and

nutrient content, without considering root biomass stocks or depth distributions, or other characteristics like symbiotic associations. Here, we use the term root characteristics in some instances to include root biomass measurements (live, dead, and coarse), morphological root traits (e.g., SRL, RTD), root nutrient content, and root symbiotic colonization rates by AMF.

According to the optimal partitioning theory plant biomass allocation can be flexible allowing plants to optimize resource acquisition, depending on which resource is most limiting, for example increasing belowground allocation if soil resources are limiting (Bloom *et al.*, 1985). While coarse roots are less critical for resource acquisition than fine roots, they are essential for storing reserves such as C stocks, distributing resources within the plant, and providing physical support for anchorage (McCormack *et al.*, 2015; Fantozzi *et al.*, 2024). For resources acquisition, plants are more likely to change fine root structures. For example, a study across 50 distinct Panamanian forests showed larger fine root biomass in low fertility versus high fertility tropical sites, with no change in aboveground biomass (Cusack *et al.*, 2018; Cusack & Turner, 2020), suggesting greater relative allocation of biomass belowground when soil resources are scarce. However, less is known about how plant allocate this biomass to different types of root structures, or to root symbionts. The development of different types of root structures and morphologies in response to resource scarcity has been documented across tropical and temperate forests, but patterns are not consistent according to specific resources (Addo-Danso *et al.*, 2020; Cusack *et al.*, 2021; Freschet *et al.*, 2021b), and different suites of characteristics appear to respond to nutrient or water scarcity availability (Dallstream *et al.*, 2023). For example, specific root length (SRL; cm mg^{-1}) can increase in response to drought in tropical forests (Metcalfe *et al.*, 2008), and also to respond to changes in nutrient availability in some cases but not others in Panama, Brazil, and across pan – tropical forest sites (Wurzburger & Wright, 2015; Addo-Danso *et al.*, 2020; Lugli *et*

al., 2021). Most of these studies focused on the surface soil, and did not consider changes with depth, despite large resource gradients in tropical forests with depth as described above.

Investment by plants in different types of root structures or symbioses could have downstream effects on soil C storage, since fresh C input into mineral soils appears to originate primarily from roots (Rasse *et al.*, 2005; Jackson *et al.*, 2017; Dijkstra *et al.*, 2021). For example, thinner and longer roots (i.e., higher SRL) could promote soil aggregate production through physical entanglement of soil particles, subsequently promoting physical protection of soil C from decomposition as suggested in a review (Poirier *et al.*, 2018). Root nutrient content and organic chemistry have also been related to soil C stocks, as reviewed by Poirier *et al.* (2018). Investment by plant in fungal root symbionts could also help promote soil C storage, since fungal biomass is more N – rich and has been shown to contribute an important component of soil C via exudation or biomass itself (Wu *et al.*, 2023). Thus, understanding spatial variation in fine root biomass as well as other morphological and chemical traits could help us better predict tropical forest soil C storage.

To improve our understanding of variation in root characteristics within and among tropical forests, we measured live and dead root biomass, morphology, chemistry, and AMF colonization rates to 1.2 m depths in 32 plots across four lowland Panamanian forests. We selected forests that represent the broader scale variation in rainfall, dry season length, and soil fertility in the region (Cusack *et al.*, 2018). We explored patterns and tradeoffs in root characteristics by depth and among sites, as well as relationships among root characteristics, and with soil C stocks. We hypothesized that: (H1) root characteristics vary systematically with depth, exhibiting tradeoffs related to resource acquisition, and (H2) variation in root characteristics is strongest in surface soils, reflecting site – scale resource differences. We predicted that the most fertile forest would

have the most unique root characteristics among the four forests. We also predicted that in addition to the positive correlation between root biomass and soil C stocks, as previously demonstrated for these sites (Cusack *et al.*, 2018), root morphologies with thicker diameter and denser tissues would also be positively associated with soil C stocks because these are more resistant to decomposition.

2.3 Methods

Study sites

Our forest sites are part of a larger network of ~50 long term 1 ha forest dynamics sites maintained by the Smithsonian Tropical Research Institute. Across the Panamanian lowlands there is more than a 250 – fold variation in soil extractable P and base cations (Turner & Engelbrecht, 2011; Turner *et al.*, 2018; Cusack *et al.*, 2021) and a rainfall gradient from approximately 1,750 mm/year on the Pacific coast to about 4,000 mm/year on the Caribbean coast (Engelbrecht et al., 2007; Pyke et al., 2001). The forests have a tropical monsoon climate and are classified as tropical moist broadleaf forests (Holdridge et al., 1971). The Caribbean coast has a shorter dry season (about 115 days) compared to the Pacific coast (about 150 days).

All sites are classified as tropical moist forests (Holdridge *et al.,* 1971) with a mean annual temperature of 26°C (Windsor, 1990). Aboveground biomass does not vary significantly among sites or across the broader rainfall and soil fertility gradients (Pyke *et al.*, 2001; Cusack *et al.*, 2018). Tree species composition shifts across the broader rainfall and fertility gradients of the Isthmus, predominantly influenced by species – specific affinities for moisture and P (Engelbrecht *et al.*, 2007; Condit *et al.*, 2013b; Turner *et al.*, 2018), and our forests are typical of this rapid turnover in tree species (Cusack *et al.*, 2023).

The Isthmus of Panama features a wide range of soil weathering statuses and fertility levels

(Condit *et al.,* 2013; Cusack *et al.,* 2018; Turner & Engelbrecht, 2011; Turner *et al.,* 2018). Nutrients derived from rocks (such as phosphorus and base cations) are primarily related to geological substrates and are not directly influenced by rainfall (Pyke *et al.,* 2001; Stewart *et al.,* 1980; Turner & Engelbrecht, 2011). This allowed the selection of forests where rainfall varies independently from soil fertility. Our sites represent a subset of the variation across the Isthmus of Panama with 10 – fold variation in resin P and 24 – fold variation in base cations to 1 – m depth and sites receiving between 2,350 and 3,400 mm of annual rainfall. Our sites also represent a subset of the global variation of moist and wet tropical forests that span a range of 2,000 to >8,000 mm of MAP (Holdridge et al., 1971) and more than 50% of tropical forests occur on the two most strongly weathered soil orders in USDA soil taxonomy: Ultisols and Oxisols (Holzman, 2008), represented by three of our sites. The remaining tropical forests grow on a wide range of soil types that are less weathered and more fertile in P and bases (e.g., Alfisols, Mollisols), but where N is typically more scarce (Sayer & Banin, 2016; Fujii *et al.,* 2018; Turner & Engelbrecht, 2011; Cusack *et al.,* 2018; Quesada *et al.,* 2020). Our forest sites include: Gigante Peninsula (GIG, 2350 MAP, infertile, Oxisol), plot 12 (2600 MAP, infertile, Ultisol), plot 13 (P13, 2600 MAP, fertile, Alfisol), and Sherman Crane (SC, a.k.a. San Lorenzo, 3421 MAP, infertile, Oxisol) (Table 2.1, Figure 2.1). The four sites are situated at low elevations and consist of mature forests. These areas exhibit significant species turnover and host a limited number of common tree species (Cusack *et al.,* 2023).

Root collection

Root standing stocks to a depth of 1.2 m were collected using a 5 – cm diameter hand auger. These collections coincided with the subsequent installation of minirhizotron tubes into the holes, which were installed at a 45° angle to the soil surface (Norby *et al.*, 2004). Since soils were

sampled at an angle, we collected in 14.1 cm length intervals so that the true vertical depths were in 10 – cm intervals. Soil samples were collected from one hole per plot, and plots were located > 20 m apart in each forest. Soils were then stored in plastic bags at 4° C until processing. Soils were collected in September 2017 (P12), December 2017 (P13), February 2018 (SC), and October 2018 (GIG). These dates correspond to the late wet season for P12, P13 and GIG, and the transition to the dry season in SC while soils were still wet enough to sample (Paton, 2023a; Paton, 2023b). In total, root samples were collected from 32 plots across the four forests in 12 depth increments from 0 – 1.2 m (384 samples).

Additional root samples were collected from each plot to measure AMF colonization by taking sequential cores from 0 – 10 cm and 10 – 20 cm depth in three locations per plot using a 3.81 cm diameter constant volume corer. Collection dates for AMF samples were September 2018 (P12, P13, and SC) and December 2018 (GIG) – all during the wet season. Fine roots were separated from the soil and stored in plastic cassettes in tap water at 4°C until staining for colonization counts (see below).

Root processing

The wet weight of all field samples was measured, then subsamples of 3 – 4 g of root-free, fresh soil were oven-dried at 105°C until constant weight to calculate the mass of dry soil for each depth increment.

Soils were gently rinsed through a 0.25 mm diameter sieve to remove soil from roots, and remaining roots were then cleaned by hand using paint brushes and water. Roots were divided into fine roots (< 2 mm in diameter) and coarse-roots (> 2 mm in diameter) using a caliper. In general, the coarse roots collected in our cores were no larger than 3mm, such that we collected a relatively

small-diameter portion of the coarse root stock. Fine roots were then separated into live or dead using visual and mechanical assessments. Live roots were determined based on being more turgid, not easily broken, and the cortex and periderm could not be separated easily (Freschet *et al.*, 2021a). Live fine roots were then scanned to assess morphology (see below), and dried at 60^{o} C until constant weight to measure root biomass per sample. Root biomass per mass of soil was then calculated using dry root and dry soil mass per sample (g-biomass / kg dry soil). We calculated biomass in Mg/ha by dividing the fine root biomass summer for the whole soil profile by the soil core surface area. Then we calculated root biomass in g-Carbon (Mg C/ha), by multiplying g-biomass by site-average fine root %C.

Root morphology, chemistry and AMF colonization

Live fine root samples were scanned fresh at 800 dpi on a 9800XL plus – Microtek – TMA 1600 II scanner. Images were analyzed using WinRHIZO (WinRHIZO Regular, Regent Instruments, Canada) to determine SRL, specific root area (SRA), RTD, and mean root diameter. SRL (cm * mg^{-1}) was calculated as root length per dry mass; SRA (cm^2 * mg^{-1}) as root surface area per dry mass; and RTD (g * cm^{-3}) as root dry mass per volume.

After oven drying, live root tissues were finely cut into fine pieces for elemental C and N analysis on a Carlo – Erba NA1500 at the Environmental Stable Isotope Laboratory at Duke University, USA. Root chemistry was analyzed for all depths in 4-5 plots per site, with site selection for these analyses depending on tissue availability.

To further explore differences in deep root characteristics among sites, we also measured radiocarbon content (fraction modern [FM] and $\Delta^{14}C$) and $\delta^{13}C$ on fine (< 2 mm) live deep roots (>80cm depth) for a subset of plots (n = 5 for GIG, P12 and P13, n = 4 for SC). Roots were prepared

for analysis by sealed-tube combustion to CO_2 in the presence of CuO and Ag, cryogenically purified, and reduced to graphite on Fe powder in the presence of H_2 (Vogel *et al.*, 1984). $\delta^{13}C$ values were measured on a split of purified CO_2 at the Stable Isotope Geosciences Facility at Texas A&M University on a Thermo Scientific MAT 253 Dual Inlet Stable Isotope Ratio Mass Spectrometer. ^{14}C samples were measured as graphite on the 10 MV Van de Graaff FN or the 1MV NEC Compact accelerator mass spectrometer at Lawrence Livermore National Laboratory (Broek *et al.*, 2021). ^{14}C values were corrected for mass dependent fractionation using measured $\delta^{13}C$ values and are reported here as $\Delta^{14}C$ corrected to the year of measurement of 2022 or 2023 (Stuiver & Polach, 1977) and as fraction modern, also referred to as FM or $F^{14}C$ (Reimer *et al.*, 2004). The purpose of these radiocarbon analyses is to determine the age and carbon cycling characteristics of fine deep roots to understand their role in soil carbon storage.

For AMF colonization, roots were cleared and stained using standard protocols modified for field-collected tropical roots (Giovannetti & Mosse, 1980; Koske & Gemma, 1989; INVAM, 2023). Roots were cleared in 10% KOH at ~60 °C for ~7 days and bleached in ~3% household H_2O_2 at room temperature for 30 – 60 minutes, until appropriately cleared. Roots were then thoroughly rinsed in tap water, acidified in 1% HCl for 30 – 60 minutes. Next, they were stained with 0.05% trypan blue in 10:9:1 glycerol: deionized water: 1% HCl at ~60 °C for 30 – 60 minutes until appropriately stained, rinsed again in tap water, and stored in tap water at 4 °C until visual scoring under a microscope was completed. AMF colonization was estimated as the percentage of root length containing AMF structures using the gridline-intersect method (Giovannetti & Mosse, 1980), and plot-level colonization rates were calculated as the proportion of scorable intersections in which AMF structures were observed for each plot and soil depth, averaged across the three subsamples per plot.

Soil C stocks

We used previously reported soil C stocks at each site for depth intervals of 0–10, 10–20, 20–50 and 50–100 cm (Cusack & Turner, 2020) to explore relationships with the root characteristics collected here.

Statistical analyses

To assess coordination and tradeoffs in root characteristics across depths and sites, we used principal components analysis (PCA) and cluster analysis. For these analyses we used data from all depth increments, as well as whole-profile data (summed root biomass and averages for other traits). All variables were scaled and centered prior to analysis. We followed these analyses with multiple analysis of variance (MANOVA) using all root characteristics as response variables, with post hoc Hotteling's T-squared test. We then conducted post-hoc mixed model nested ANOVA for each root characteristic separately, nesting plots within the site, including a random effect of plot, and using site (categorical) and depth (continuous) as predictors. When there were site*depth interactions we then applied post-hoc Tukey Honest Significant Difference (HSD) means separation tests to explore differences among sites for each depth. If there was no interaction, Tukey HSD tests were run for the whole soil profile (0 – 1.2 m). We also created correlation matrices of all one-to-one comparisons to assess relationships among root characteristics. Root characteristics for these analyses included: live fine root biomass, dead fine root biomass, coarse root biomass, dead:total fine root biomass ratio, total fine root length, SRL, SRA, RTD, root diameter, AMF colonization, root %N, root %C, and root C:N ratios. All raw data is available in Table SI 1.1.

For initial PCA all characteristics were used, and then subsequent tests were conducted removing auto-correlated characteristics (Pearson correlation coefficient $>|0.8|$ or $R^2>0.64$). For cluster analyses, we first identified clusters by depth, then by site, both using all available data 0 – 1.2 m, and then with additional tests including AMF for only 0 – 10 and 10 – 20 cm depths. We repeated PCA and cluster analyses after removing fine root biomass to assess patterns in root morphology, and then performed additional tests adding root chemistry for available plots (Table SI 1.2).

The smaller dataset for deep root radiocarbon and $\delta^{13}C$ values was analyzed separately. Given the small sample size, large range, and non-normal distribution of the deep root radiocarbon data, we used the non-parametric Kruskal-Wallis test to assess differences among sites. Post-hoc pairwise comparisons between all pairs of sites were conducted using the Wilcoxon Method.

Root characteristics were then assessed as predictors of soil C stocks by depth increment using forward stepwise model building. Response variables were total soil C (TC, g/kg) and dissolved organic C (DOC, mg C/kg), and we used all of the above-listed root characteristics for the initial model building exercise. The final most parsimonious significant model is reported.

All data were assessed for normal distribution. Log transformations were applied when variables were non-normal. The significance level was $p<0.05$, except for multiple comparisons we used Bonferroni corrections, and these significance levels are presented. Unless otherwise noted, we present mean ± standard error (SE).

Analyses were conducted in R studio version "*Already Tomorrow"* 4.3.0 (R Core Team, 2023) or JMP 17.0 software (SAS Institute, 2023). The R scales package, *cmdscale* and *dist* functions were used for the cluster analysis; the *emmeans* package and *cld* function were employed for pairwise comparisons of site means; the *ggfortify* package was utilized for the PCA analyses;

the lme4 package was applied for the mixed models; and the *stepAIC* function from the *MASS* package was used for the stepwise model building.

2.4 Results

Overall, live fine root biomass stocks to 1.2 m depths across the four forests varied from 2.7 to 6.5 g-biomass/kg-soil (Table 2.2, Table 2.3), representing 3.5 – 7.4 Mg-biomass/ha (1.4 – 3.0 Mg-C/ha), with significant differences among sites and the largest fine root biomass stocks in the wettest, infertile forest (SC). Across the 32 plots, this represents a range of 1.64 to 14.08 Mg-biomass/ha, or 0.67 to 5.82 Mg-root C/ha (Table SI 1.1). Dead roots typically represented ~1/3 of total root biomass (live + dead), and coarse root biomass was similar to or larger than live fine root biomass across the sites, with the largest coarse root biomass in SC (Table 2.3). Overall, there were significant site effects for all root morphological and chemical traits except AMF colonization rates, and there were significant depth effects for all root biomass and trait data except dead:total fine root ratios and root %C (Table 2.5). Interacting effects of site*depth were present for live and dead fine root biomass, total root length, diameter, %N, and C:N ratios. Also, there were consistent patterns by depth across sites for coarse root biomass, SRL, SRA, RTD and AMF colonization (Table 2.6). Raw data for root biomass, morphology, and chemistry are available in Table SI 1.1.

Coordination and tradeoffs among root characteristics in tropical forests

The first two axes of the final PCA analysis for all data 0 – 1.2 m depth explained ~50% of the variation in root characteristics, with the third axis explaining an additional 19% (Table 2.4, Figure 2.2a). Similarly, the first two axes of the PCA for 0 – 20 cm depths, including AMF

colonization, explained 49% of the variation (Table 2.4, Figure 2.2b). The additional PCA that added auto-correlated factors gave similar results (Figure SI 1.2, Table SI 1.3), as did the PCA with removal of root biomass measurements (Table SI 1.4, Figure SI 1.3).

Opposite loadings of different root characteristics on PCA axes suggest tradeoffs in plant belowground strategies, which were explored further with correlation matrices. For the full soil profile (0 – 1.2 m depth), axis PC1 had strong opposite loadings for SRL (0.689) versus fine root diameter (-0.450), axis PC2 had strong opposite loadings of fine root diameter (0.454) versus live fine root biomass (-0.547), and axis PC3 had strong opposite loadings for RTD (-0.295) versus root %C (0.737). The first relationship is implicit in that higher SRL indicates long thinner (i.e., smaller diameter) roots. The second relationship, however, is more novel and suggests that sites and depths with greater live root biomass contained roots with larger diameter. For the PCA of 0 – 20 cm depth with AMF, the most novel tradeoff appeared on axis PC3, with strong opposite loadings for AMF (-0.616) versus SRL (0.366, Table 2.4). Some of the relationship identified in the PCA are reflected in bivariate correlations (Figure SI 1.1), although relationships from PCA identified in the second or higher axis are not typically matched by simple correlations, since PCA identifies tradeoffs in the context of the entire data set

Depth effects on tropical forest root characteristics

Cluster analysis for all depth increments and sites across 32 plots indicated that surface roots were different for each depth increment to 60 cm depths, after which root characteristics were similar to 1.2m depth (Figure 2.3, Table SI 1.5). The MANOVA for these data support the clusters, with depth being a significant main effect across root characteristics. Hotteling's T-squared test showed that 10 cm increments from the surface to 60 cm depth were each distinct, whereas deeper

than 60 cm root characteristics were relatively constant with depth. These results were similar for the different combinations of data used (e.g., removing live root biomass or including root C and N, Table SI 1.5, Figure 2.3).

Similar cluster analyses conducted for each site separately indicated that the most root variation among surface depth increments was at the driest, infertile site (GIG), where each surface depth increment was unique down to 60 cm depth, whereas in the most fertile site (P13) only the surface 0 – 10 cm had unique root characteristics relative to the rest of the profile (Table SI 1.5, Figure SI 1.4).

Below, we present the patterns with depth for each root characteristic individually, since all characteristics varied by depth and/or had a depth*site interaction except dead:total fine root biomass ratios and root %C (Table 2.2, Table 2.6). We also presented gravimetric soil moisture variation at depth when soil samples were collected (Figure SI 1.8) and monthly precipitation around the collection dates (Table SI 1.15).

Consistent depth effects on root characteristics across four tropical forests

Across sites, coarse and fine root biomass (live and dead), RTD, and AMF colonization decreased with depth, whereas SRL and SRA increased with depth (Figure 2.4, Figure SI 1.5, Table 2.5, Table SI 1.6). Thus, the relatively small stocks of deeper roots were longer and thinner, less dense, and with less AMF colonization, whereas the larger surface root stocks across the sites were shorter, denser, and had higher rates of AMF colonization (Table 2.6). None of these root characteristics had an interaction of depth*site except live and dead fine root biomass (see below). Thus, these important root morphological and symbiotic characteristics varied with depth in a consistent manner across these tropical forest sites, regardless of local rainfall and soil fertility.

Interacting effects of site and depth on tropical forest root characteristics

In addition to live and dead fine root biomass, there were also site*depth interactions for total fine root length per sample, fine root diameter, fine root %N, and fine root C:N ratios (Table 2.5, Figure 2.5). Separate regressions for each site for these root characteristics vs depth indicated that live and dead fine root biomass, as well as total fine root length, all decreased with depth at all sites, but there was significantly less surface fine root biomass and length in the most fertile site (P13), so the slope of the decline with depth was less steep (Figure 2.5, Table SI 1.6). Fine root diameter generally did not change with depth, except in the driest site where it increased with depth (GIG, Figure 2.5, Table SI 1.6). Fine root %N generally decreased with depth, while C/N increased with depth, with the strongest changes at the driest and wettest sites (GIG and SC, Figure 2.5, Table SI 1.6). Thus, depth patterns for root biomass and length were generally similar across sites, except that surface root biomass appeared to vary with site fertility, and fine root %N generally decreased with depth, but the magnitude of the decline was different across sites. For these characteristics with site*depth interactions, Tukey HSD tests indicated that the largest variation among sites was in surface to mid-depth soils (0 – 60 cm depth, Figure 2.5), following results from the cluster analysis.

Summarizing root variation by depth across these four forests, live and dead fine root biomass declined with depth, as did total root length and coarse root biomass, RTD and AMF colonization. Meanwhile, SRL and SRA increased with depth. Fine root %N tended to decline with depth and C:N ratios increased with depth, but there was substantial variation in the magnitude of the change with depth among sites. Finally, root diameter generally did not change with depth, except for a dramatic shift in the driest site.

Spatial variation in root characteristics among four tropical forests

Cluster analysis using root biomass and morphological characteristics showed separation among the four forests, with the strongest separation for the driest infertile site (GIG), followed by the wettest infertile site (SC, Figure 2.6, Table SI 1.7). The MANOVA results supported the cluster analysis, showing that site was a significant main effect for predicting overall variation in root characteristics (Table SI 1.7, Figure 2.6, Figure SI 1.7). Same results were found when considering only morphological variables and excluding fine root biomass (Table SI 1.8) or when including chemistry data that is not available for all sites and depths (Table SI 1.9).

As indicated above, most variation in root characteristics was for surface soils, and this was where most separation among the sites occurred (Table SI 1.10; Figure 2.6). Hotteling's tests by depth increments highlight that the most distinct surface root characteristics (0 – 10 cm depth) were in the driest infertile site (GIG), with some separation also for the wettest infertile site (SC, Table SI 1.10). In particular, the driest site had smaller surface fine root diameter, whereas the wettest site had the largest surface live and dead fine root biomass, and the largest surface total root length (Table 2.6, Figure 2.5).

While most deep root characteristics were similar among the sites (Table SI 1.7), an exception emerged from the deep root radiocarbon data. Deep root radiocarbon averages varied significantly among sites (ChiSquare 8.69, DF = 3, p = 0.03). The most fertile site had the highest fraction modern and $\Delta^{14}C$ (P13: 1.09 ± 0.04 FM, or $\Delta^{14}C$ 81.62 ± 35.10‰), with the lowest fraction modern and $\Delta^{14}C$ in its paired infertile site (P12: 1.01 ± 0.006 FM, or $\Delta^{14}C$ 3.38 ± 6.66‰), and intermediate values for deep roots in the driest and wettest infertile sites (GIG: 1.05 ± 0.02, or $\Delta^{14}C$ 41.74 ± 24.47‰; SC: 1.04 ± 0.02 FM, or $\Delta^{14}C$ 35.85 ± 16.81‰ Table SI 1.13. Pairwise Wilcoxon comparisons indicated that the significant difference between was for P13 (fertile)

versus P12 (paired infertile, $Z = 2.4$, $p = 0.01$). The variation among measurements for each site was large except for P12, with overall values across all sites and plots ranging from 0.99 – 1.22 FM and $\Delta^{14}C$ -10.6 to 213.5 ‰, indicating a broad range of deep root ages. Using age conversions for modern radiocarbon values (Reimer *et al.*, 2004; Reimer & Reimer, 2024), the site-level averages indicate that deep roots from P12 are constructed from very recent photosynthate (past 5 years). Values for GIG and SC are slightly older than 5 years, and P13 values suggest they grew from photosynthate that was fixed around the year 2000. The $\delta^{13}C$ of deep roots did not vary among sites (Table SI 1.13).

Post-hoc tests assessing root characteristics individually indicated that site was a significant main effect for all root characteristics except AMF colonization rates (Table 2.2, Table 2.5, Table 2.6). In many cases there was a main effect of site with no site*depth interaction, including for SRL, SRA, RTD, root %C, coarse root biomass, and dead:total fine root biomass (Table 2.6, Figure 2.7, Figure 2.5, Figure SI 1.12). For these characteristics that had no interaction, Tukey HSD tests for the whole soil profile indicated the wettest, infertile site (SC) had the overall smallest average SRL and SRA, the largest coarse root biomass, and the largest dead:total fine root biomass ratios (Figure. 2.7). Meanwhile, the driest infertile site (GIG) had the highest average RTD (Figure 2.7). Fine root %C was also lower in the driest and the wettest sites (GIG and SC) compared to the two mid-rainfall sites (P12 and P13, Figure 2.7, Table 2.2, Table 2.3, Table 2.6).

Summarizing site-scale differences, the wettest and most infertile site (SC), which was characterized by the largest surface root biomass (live and dead), also had overall more coarse roots, a larger proportion of dead:total fine roots, and generally shorter, thicker roots than other sites. The driest site (GIG) was distinguished by having higher RTD overall, smaller surface root diameter, lower surface root C:N ratios, and a strong decline in root %N from the surface to depth.

Finally, the most fertile site, which had the smallest surface root biomass, was not distinct from other sites in most other root characteristics, except older radiocarbon values for deep roots.

Root characteristics as predictors of soil C stocks

The forward stepwise model with the lowest Akaike Information Criterion (AIC) highlighted that depth, live fine root biomass, and SRL were significant predictors of total soil C (Table SI 1.11, Figure 2.8). For extractable dissolved organic C (DOC), a measure of C available to microbes, SRL was the only significant predictor. Post – hoc regressions showed that live fine root biomass was strongly positively correlated to soil C stocks ($R^2 = 0.60$, Figure 2.8a, Table SI 1.11) while SRL was negatively correlated with soil C stocks ($R^2 = 0.31$, Figure 2.8b, Table SI 1.11). Post – hoc regressions also showed that SRL was negatively correlated to DOC ($R^2 = 0.34$, Figure 2.8c, Table SI 1.11). Thus, root biomass as well as fine root morphology predicted soil C stocks, with longer, thinner roots associated with smaller soil C and DOC stocks. Complete data is shown in Table SI 1.12.

2.5 Discussion

The results from this study showed important contributions of new data on how root characteristics are different across depths and across sites at the soil surface which are likely related to different strategies in resources uptake. Also, we present here a homogeneous variation of roots with depth indicating different tropical forests have similar variations across depth. We provide more details below.

Root biomass stocks across tropical forests

Overall, root biomass and trait values in these four Panamanian forests were representative of published data across broader seasonal tropical forests. For example, live fine root biomass stocks across the 32 plots in our study ranged from 1.64 to 14.08 Mg/ha to 1.2 m depths, which is similar to the published range of live root biomass stocks for a broader set of 43 Panamanian lowland forests (1.14 to 7.70 Mg/ha to 1m depths, Cusack *et al.*, 2018; Cusack & Turner, 2020). Our values also encompass the range across Amazonian studies: a seasonal mature Brazilian forest in Central Amazon (~3-month dry season; 1,900 to 2,400 mm) had live root biomass stocks similar to our higher range (13.1 Mg/ha to 90 cm depth, Cordeiro *et al.*, 2020), whereas a Brazilian forest in Eastern Amazonia with a longer dry season (~6 months) had live root biomass stocks similar to our lower range (1.7 Mg C/ha to 6m depth, Trumbore *et al.,* 2006).

More root biomass stock data is available across wet and seasonal tropical forests for depths <30 cm. Fine root biomass from 0 – 30 cm depth for 47 tropical forest plots in 22 sites across the Americas, Africa, and Asia had a range of 0.85 Mg C/ha for a wet Malaysian Bornean rainforest to 24.29 Mg C/ha for a wet eastern Amazonian lowland forest (fine root biomass estimated ~42 %C) (Huaraca Huasco *et al.*, 2021). Converting our biomass values to similar units gives a range of 0.67 to 5.82 Mg C/ha for the four Panama forests, indicating that our sites to 1.2 m depth have root C stocks near the lower end indicated in this pan-tropical study, which extended to much wetter sites and did not go as deep. Another study found root biomass to 30 cm depth ranging from 0.89 ± 0.08 Mg/ha in a dry tropical forest to 1.49 ± 0.11 Mg/ha in a drier forest in Ghana (MAP range from 1700 to 2000) (Ibrahim *et al.*, 2020), near the low end of stocks in our Panama study. Another drier tropical forest in Southern Mexico (MAP range from 900 to 1400) had average fine root biomass stock was 4.29 Mg/ha to 30 cm depth, also near the lower end of

our range (Sarai *et al.*, 2022). Thus, our forest sites, while providing a relatively large range in root biomass stocks over a small spatial area, are also typical for lower to mid-rainfall seasonal tropical forests.

Root morphological, chemical, and symbiotic traits across tropical forests

Our study greatly expands the available data for tropical forest deep root morphological and chemical traits. Across all forests, plots and depths, SRL ranged from 0.09 to 14.7 cm/mg, SRA ranged from 0.04 to 3.12 cm^2/mg, fine root diameter ranged from 0.28 to 1.44 mm, and RTD ranged from 0.02 to 1.62 g/cm^3. To compare with most other studies that have focused on surface soils, ranges in the 0 – 30 cm depth comprised the smaller end of our total range for SRL (0.39 to 3.5 cm/mg) and SRA (0.1 to 0.63 cm^2/mg), but were toward the middle of our total range for fine root diameter (0.34 to 1.13 mm) and RTD (0.10 to 0.86 g/cm^3). Thus, measuring deep roots contributed more of the extreme values for root morphology to the overall data set, and these are missed in studies of shallow soils only.

Comparing our fine root morphology values from the soil surface (0 – 30 cm) with a large-scale database assessment of 59 tropical forest sites across the Americas, Africa, and Asia to this depth, our ranges were toward the bottom of the global range for SRL of 0.74 to 7.93 cm/mg, but toward the middle of the global range for SRA of 0.079 to 0.879 cm^2/mg, fine root diameter of 0.2 to 1.8 mm, and RTD of 0.13 to 0.68 g/cm^3 (Addo-Danso *et al.*, 2020). Specifically, previous tropical studies reviewed in Addo-Danso *et al.* (2020) to 30 cm depth have reported ranges of SRL (cm/mg) from 0.74 to 7.93 for surface soils, whereas here we expand this range to include 0.39 to 3.5. Those same studies have reported ranges of RTD (g/cm3) from 0.13 to 0.68, whereas here we expand this range to include 0.1 to 0.86; ranges of root diameter (mm) from 0.2 to 1.8, but here

we did not expand this range since our values fall within that range (0.34 to 1.13); and ranges of SRA (cm2/mg) from 0.079 to 0.879, whereas here we also did not expand this range since our values fall within that range (0.1 to 0.63). The global review noted that variation in surface root morphology within continents was likely related to variation in soil properties (Addo-Danso *et al.,* 2020), which is similar to the surface root morphological variation found across our distinct forests. More data on deep root morphological traits is needed to assess whether these are as constrained globally as we observed in our four forests. Therefore, this study significantly expanded the ranges for SRL and RTD across tropical forests, but did not expand the ranges for root diameter and SRA since the whole variation across other studies already included the values found in this study.

The root chemistry values reported here are also similar to other tropical forests. Across all forests, plots and depths, fine roots had a range of 32.81 to 52.41 % C and 0.41 to 2.05 % N in our Panama study. The shallower roots to 30 cm depth (35.30 to 48.22 % C; and 0.66 to 1.80 % N) had ranges toward the middle of the whole – soil profile range, indicating that the deep roots also contributed to extremes to the overall root chemistry data set. Our fine root %N values across surface soils were near the high end of fine root values of 0.3 to 1.9 % N reported across six pine/mahogany plantations, and two mature tropical forests to 30 cm depth (MAP 3500 mm) from a review from Puerto Rico (Yaffar & Norby, 2020). The root %C and %N values were similar to values from lowland seasonal tropical forest in Brazil at 30 cm depth, which had an average of 43.82 ± 0.19 % C and 0.74 ± 0.13 % N (Lugli *et al.*, 2021). Six other forests in China ranging from seasonal rainforest to subtropical evergreen have fine roots with 46.68 % C and 1.93 % N to 20 cm depth (Kong *et al.*, 2014), which is similar to our values. In summary, previous tropical studies to 30 cm depth have reported ranges of %C from 43.82 to 46 (Kong *et al.*, 2014; Lugli *et al.*, 2021),

whereas here we expand this range to include 32.81 to 52.41. Previous tropical studies have reported ranges of %N from 0.3 to 1.93 (Kong *et al.*, 2014; Yaffar & Norby, 2020; Lugli *et al.*, 2021), whereas here we expand this range to include 0.41 to 2.05. Thus, this study expanded the ranges for %C and %N across tropical forests.

Coordination and tradeoffs in tropical fine root characteristics

The tradeoffs suggested in our PCA analyses were similar in some respects to results using global fine root databases (McCormack & Iversen, 2019; Bergmann *et al.*, 2020). Generally, these studies indicate a tradeoff between high SRL for root exploration of soils, versus large diameter, similar to the dominant tradeoff observed on our PC1 axis. This tradeoff has been posited to be related to AMF colonization and "outsourcing" of soil exploration, such that plants either invest in roots with high SRL for resource exploration ("do it yourself"), or they transfer C to AMF, which might require larger diameter roots for colonization (Bergmann *et al.*, 2020). Species-level measurements with >100,000 observations from a database including major vegetated biomes (but with the tropics poorly represented) showed a positive relationship between AMF colonization and root diameter (McCormack and Iversen, 2019). Alternatively, the inverse relationship between SRL and root diameter could reflect their mathematical relationship (i.e., diameter is implicated in SRL) (Ostonen *et al.*, 2007). Supporting this second idea, our study did not demonstrate a relationship between root diameter and AMF colonization at the community-scale, and neither did another community-scale study in Central Amazonia (Lugli *et al.*, 2020). There was some indication of a relationship between AMF colonization rate and SRL in our PCA, but the relationships were not strong. Further exploration into functional relationships among AMF, fine root diameter, and SRL in tropical forests is warranted.

Another common tradeoff presented in the literature at the species-level is high RTD with a conservative ("slow") root strategy, versus a high %N and rapid turnover ("fast") root strategy (McCormack & Iversen, 2019; Bergmann *et al.*, 2020). Our data did not support this trend, with fine root %N loading opposite to fine root diameter, rather than RTD. Rather than simple tradeoffs in morphological traits, new frameworks for tropical fine root strategies suggests that suites of traits, including morphology, symbioses, turnover, and depth distributions, are used by different species in tropical forests to acquire scarce resources like water (in seasonal forests), and phosphorus (on strongly weathered soils) (Cusack *et al.*, 2021; Dallstream *et al.*, 2023). Understanding coordination and tradeoffs in complex, highly diverse tropical forests will likely require expanding root research to include more functional traits (e.g., nutrient uptake rates, production of decomposition enzymes) (Cusack *et al.*, 2024), which is indicated by the divergence of patterns in this Panama root data set from patterns observed dominantly in other biomes.

Systematic depth variation of tropical forest root characteristics

Our assessment identified emergent patterns of root characteristics with depth across tropical forests, despite substantial variation among site in moisture and nutrient availability. Our observation that live and dead fine root biomass and coarse root biomass declined with depth is similar to depth distributions identified in other tropical forests studies in Panama (Cusack & Turner, 2020), Brazil (Cordeiro *et al.*, 2020), Puerto Rico (Yaffar & Norby, 2020; Cabugao *et al.*, 2021), and more broadly across terrestrial ecosystems (Jackson *et al.*, 1996).

More novel here were the general increases in fine root SRL and SRA, and declines in fine root RTD with depth. These shifts suggest a change in resource acquisition strategy from the surface to depth across the tropical forests. Surface roots are most likely formed primarily for

nutrient acquisition, since the deeper soils in these forests are typically poorer in rock-derived nutrients like P than surface soils, particularly for the strongly-weathered soil orders (Cusack & Turner, 2020). Deeper fine roots are more likely formed primarily for water acquisition in these seasonal forests, since surface soils tend to dry out seasonally in these Panama forests (Cusack, DF *et al.*, 2019), but deep soil moisture or standing water tables are common in seasonal tropical forests (Fan *et al.*, 2017). Deep water acquisition during the dry season has been demonstrated for a Panama forest near our BCNM sites using natural abundance $\delta^{18}O$ measurements that indicated trees were accessing water from > 1 m depths during the dry season (Meinzer *et al.*, 1999; Andrade *et al.*, 2005).

The higher SRL and SRA at depth in our study in particular could be related to plant exploration for water. Larger SRL increases root contact area with soils per unit biomass, and can help plants acquire resources (Hodge, 2004), especially water in deeper soil layers (Jackson *et al.*, 2000). Our trend for SRL with depth differs from the lack of a depth trend in a Puerto Rican forests from 0 – 30 cm depth (Cabugao *et al.*, 2021) and other ecosystems from three climatic zones (tropical, mediterranean and montane) where shallow roots (0-20 cm) and deep roots (100–150 cm) were measured (Prieto *et al.*, 2015). Similar to our results, SRL increased with depth to 3m in a Brazilian Eucalyptus plantation (1,360 mm MAP) (Maurice *et al.*, 2010), possibly related to water acquisition. A broader assessment of deep root morphology across seasonal and wet tropical forests could help us better understand the role of deep root morphology in water acquisition.

The depth pattern we observed for fine root RTD could also be related to moisture, but in a different way. Greater fine root RTD generally represents more robust tissues that can resist desiccation as well as herbivory (Birouste *et al.*, 2014; Freschet *et al.*, 2021b), both of which are more prevalent at the soil surface. Specifically, higher RTD had been associated with greater

content of secondary compounds for protection against root grazers (Xia *et al.*, 2021), and a longer root lifespan (Freschet *et al.*, 2021b). Thus, while plants might allocate more biomass to surface roots per segment for defense, allocation to deeper roots appears to be allocated to more delicate tissues for exploration of scarce resources where herbivory and desiccation are less likely.

Generally, root %N declined with depth and C:N ratios increased, as would be expected, but there was site-scale idiosyncrasy in root chemistry across depths, with this pattern driven by the driest and wettest infertile forests (GIG and SC). This result might reflect the stronger reduction in soil N content with depth in infertile versus fertile Panamanian forests (Cusack & Turner, 2020). Fine root N content in these relatively N-rich forests is likely a reflection of nutrient availability, as there is not a clear functional role for N in roots. The results from our infertile forests aligns with findings from Puerto Rican forests to 70 cm depths (Yaffar & Norby, 2020) and across broader ecosystem types to 150 cm depths (Prieto *et al.*, 2015) which also observed a decrease of root %N with depth. Root %N is interesting in relating to tissue quality for herbivores and decomposers, with low-nutrient root detritus likely decomposing more slowly than high-N root detritus (Throop & Lerdau, 2004). Thus, fine root %N is useful as an indication of N availability in soils, and litter quality for decomposers, but we did not find an indication that root N plays a strong role in root trait tradeoffs.

Variation in tropical forest root characteristics among forests

There were several differences in root characteristics among our forests (sites), many of which did not occur across the entire soil profile (i.e., site*depth interactions). The most notable differences were: the most fertile forest had the least surface live and dead fine root biomass (0 – 10 cm); the driest forest had the smallest surface fine root diameter (0 – 60 cm), and the highest

overall RTD (0 – 120 cm); the wettest forest overall had the smallest SRL and the most coarse roots throughout the soil profile (0 – 120 cm). The smaller surface root biomass in the most fertile forest follows plant optimal partitioning theory, in which less biomass is allocated to roots when soil resources are plentiful (Bloom *et al.*, 1985), and follows the inverse relationship between rock-derived nutrients and live root biomass stock sizes across 42 Panamanian forests (Cusack & Turner, 2020). The smaller fine root diameter in our driest forest (GIG) could be related to increased moisture uptake, with smaller diameter reducing the apoplastic barrier for water to enter the xylem (Comas *et al.*, 2013). The larger RTD in the driest forests could have served as protection against desiccation, as discussed above for trends with depth. The overall smaller SRL in the wettest, most infertile forest was unexpected since larger SRL is usually associated soil exploration for scarce resources. This forest also had the largest surface root biomass, the most coarse roots, and the largest dead:total fine root biomass. The larger surface root biomass, regardless of morphology, likely served the role of soil exploration without large SRL. More broadly, SRL does not vary consistently with natural shifts in tropical forest soil fertility, as demonstrated in a large-scale pantropical assessment (Addo-Danso *et al.*, 2020). Greater coarse root biomass in the wet, infertile forest could serve different functions, including water and nutrient transport, and long-term nutrient storage in biomass (McCormack *et al.*, 2015; Fantozzi *et al.*, 2024). Thus, the site-scale differences in root characteristics generally followed our understanding of belowground plant responses to shifts in soil resources, with several different strategies employed in response to changing moisture and nutrient availability among our forests.

Overall, the variation in root characteristics among the four Panamanian forests is likely related to a combination of shifts in soil fertility, rainfall, and tree species community composition. Our forests range a 1.5-fold increase in MAP, 24-fold variation in total extractable base cations,

10-fold variation in resin-extractable P, and turnover of most tree species (Turner & Engelbrecht, 2011; Condit *et al.*, 2013a; Cusack *et al.*, 2018; Turner *et al.*, 2018; Cusack, *et al.*, 2023). Similar to the landscape-scale relationship between rock-derived nutrient availability and root biomass stocks across the Panamanian lowlands (Cusack *et al.*, 2018; Cusack & Turner, 2020), low soil potassium corresponded to larger root biomass stocks across 47 plots in 22 tropical forests across the Americas, Africa, and Asia, with no significant relationship of root stocks to climate variables (Huaraca Huasco *et al.*, 2021). Research in Ghana found that root biomass stocks were positively associated with increasing MAP from 1700 to 2000 mm (Ibrahim *et al.*, 2020).

Also of note was the lack of difference between the most fertile forest (P13) versus its paired infertile forest (P12) for all root morphological traits, despite the fertile forest having ~4.5x more soil resin-extractable P and ~8x more extractable base cations. In a nearby Panamanian forest, nutrient additions increased fine root SRL and decreased RTD (Wurzburger & Wright, 2015). In an Amazonian forest root diameter increased with base cation and P additions (Lugli *et al.*, 2021). Across global tropical forests there have been correlations of soil fertility with SRL and SRA, primarily in relation to base cations (Addo-Danso *et al.*, 2020; Cusack *et al.*, 2021). So, in some tropical forests, root morphology is often sensitive to soil fertility, both over long-term adaptation and with sudden changes, but this was not apparent in the four forests here.

Our radiocarbon data provided the main difference we observed for deep root characteristics among forests, and was also the only difference for fertile forest versus the infertile forests other than surface root biomass. The highest radiocarbon values were for deep roots in the most fertile forest (P13), with the lowest values in the paired infertile forest (P12), indicating a difference in the average age of deep root biomass stocks at the two forests. The low values for P12 suggest either very recent photosynthate (past five years) or ~75-year-old photosynthate,

depending on which side of the bomb curve is used (Reimer *et al.*, 2004; Reimer & Reimer, 2024). A model-data study in three temperate forests suggested that fine root stock ages can range from 5 – 13 years old for depths up to 60 cm, with 20% of roots turning over in one year and 80% turning over on decadal timescales (Gaudinski *et al.*, 2010). Thus, it seems unlikely that our deep roots in P12 are from 1950s photosynthate. Rather, P12 likely had the youngest deep live fine roots among forests, constructed from recent photosynthate. This forest also had much less within-site variation in deep root radiocarbon values compared with other forests. Thus, we conclude that the higher radiocarbon values for our most fertile forest (P13) represent relatively older deep roots compared with the other forests, on average ~20 years old. This finding is surprising, since we expected that roots in the most fertile forest have the highest production and turnover rates, following the "fast" plant growth lifestyle strategy common in higher resource conditions (Wright *et al.*, 2004; Aragao *et al.*, 2009; Reich, 2014; Diaz *et al.*, 2016). Possibly, plants in the most fertile forest, where both shallow and deep soils contain high nutrient concentrations relative to the other forests (Cusack & Turner, 2020), have less need for continual production of new roots for soil exploration and nutrient uptake. Rather, deep root production in these forests could be more responsive to moisture changes, with the higher fertility supporting greater flushing of roots at the beginning of the wet season and subsequent die back. The highest rates of root production and new flushing has been observed at the beginning of the wet season in a nearby Panamanian forest (Yavitt & Wright, 2001), so by our sampling date late in the wet season these newer roots might have died back in the fertile forest, leaving only older, higher order roots behind. In contrast, the infertile forests might maintain newer deep roots on an ongoing basis through the wet season for both water and nutrient uptake. Further assessment of deep root productivity and turnover at these forests could help clarify the meaning of our deep root radiocarbon data.

The lack of forest-scale variation in AMF colonization rate was also surprising, since the number of soil fungal taxa increase significantly with increasing MAP across the Isthmus of Panama (McGuire *et al.*, 2012), and our fertile forest (P13) had greater overall fungal diversity compared to the infertile forests according to genetic assessment (Chacon *et al.*, 2023). An Amazonian review across soil P gradients showed that AMF colonization rates increased with declining soil P (Reichert et al., 2022), and we expected to see a similar pattern with our strong site-scale variation in P availability. Similar to our study, other tropical forest studies found no change in AMF colonization rate with soil fertility, including a natural soil fertility gradient and fertilization study in Hawai'i (Treseder & Allen, 2002), and a comparison between two mature lowland Costa Rican forests that varied in soil fertility (Nasto *et al.*, 2014). We note that our measurements for AMF colonization rates, like other measurements in this study, were during the wet season. There might be more site-scale variation during the dry season if these AMF are responsive to moisture. Also, AMF colonization is not necessarily indicative of AMF functional activity (Cusack *et al.*, 2024). Further investigation in the functional activity of root symbionts across tropical forest moisture and fertility gradients could help clarify their role and tradeoffs with other root characteristics.

Relationships of Fine root Characteristics with Soil C Stocks

The positive relationship we observed here between root biomass stocks and soil C stocks follows broader-scale patterns across 50 forest plots on the Isthmus of Panama (Cusack *et al.*, 2018; Cusack & Turner, 2020), and support the hypothesis that roots provide the primary inputs of fresh C to mineral soils (Rasse *et al.*, 2005). The more novel finding here was that fine root SRL is negatively correlated to soil C stocks and extractable DOC, with SRL adding predictive power in these

analyses beyond live root biomass stocks alone. Thus, soil profiles characterized by longer, thinner roots had smaller soil C stocks, whereas soil profiles with larger root biomass stocks had larger soil C stocks. This finding was opposite of our prediction, that higher SRL would promote aggregate formation and C protection from decomposition. There was a negative correlation between SRL and live root biomass across our forests and soil depths, but this relationship was not particularly strong ($R^2 = 0.37$), and the stepwise model building activity identified SRL as the most significant predictor of soil C stocks after live root biomass and soil depth. For extractable DOC, SRL was the single strongest predictor. Here, SRL was also negatively correlated with RTD, indicating that the longer, thinner roots are also likely more labile and easily decomposed. A temperate tree study found that high SRL was correlated to shorter root lifespans (McCormack *et al.*, 2012), which could represent a more consistent input of labile C into soils, possibly promoting priming effects and faster overall decomposition of soil C (Fontaine *et al.*, 2004; Nottingham *et al.*, 2009), primarily in the rhizosphere (Cheng *et al.*, 2014). Beyond root biomass, our results call for further exploration of root morphology and other traits as drivers of soil C storage in tropical forests.

2.6 Conclusion

This study provides novel data for systematic depth variation of root characteristics across tropical forests for all variables measured, except dead:total fine root biomass ratios and fine root %C. The most notable patterns with depth were: increasing SRL and C:N ratios, and declining RTD and AMF colonization. These patterns add to the observed and previously characterized patterns of declining live, dead, and coarse root biomass in forest ecosystems. The first hypothesis that root characteristics vary systematically with depth, exhibiting trade – offs related to resource acquisition was partially supported, because most root characteristics varied with depth systematically across sites, but some root characteristics presented site-specific variation. Across sites, trade-offs of surface root characteristics (likely for nutrient uptake) vs deeper root characteristics (likely for water uptake) were observed. Variation in root characteristics among the four tropical forests indicated the influence of local moisture and nutrient availability on root characteristics like diameter, SRL, and allocation to surface root biomass. Most of the overall variation in root characteristics occurred in surface soils. Some characteristics, however, like SRL, RTD, coarse root biomass, and dead:total fine root biomass were distinct among forests throughout the soil profile, suggesting that these are emergent ecosystem properties of tropical forests, likely resulting from combinations of resource availability and tree species composition. The second hypothesis that variation in root characteristics is strongest in surface soils, reflecting site – scale resource differences was supported. However, the prediction that the most fertile forest would have the most unique root characteristics among the four forests, was not supported. Variation of root characteristics was strongest in surface soils, but the most distinct characteristics were in the driest, infertile site (GIG, not the fertile P13). The main distinct characteristic in fertile sites was larger radiocarbon ages at deeper soil layers. Multivariate assessment of root characteristics in this study

supports the global-scale pattern of a strong SRL vs. diameter tradeoff axis, and we observed an additional axis for diameter vs. live fine root biomass. However, we did not find that root diameter was positively related to AMF colonization, which has been posited as an explanation for the SRL vs. diameter axis. Rather, we identified an axis opposing AMF colonization vs. SRL, indicating that there may be an "outsourcing" versus "do-it-yourself" tradeoff in these forests, but diameter is not a good proxy for root symbiosis. Finally, our data indicate that root traits such as SRL can be important determinants of tropical forest soil C stock sizes, in addition to the importance total root biomass. Overall, this study indicates that root characteristics in tropical forests are in part related to resource availability, but also likely emerge from species composition. An important question going forward is the capacity for root characteristics to respond to changing resource availability across tropical forests with different baseline conditions. Conceptual figures with main results and conclusions can be found in figures 2.9 and 2.10.

2.7 Figures

Figure 2.1.

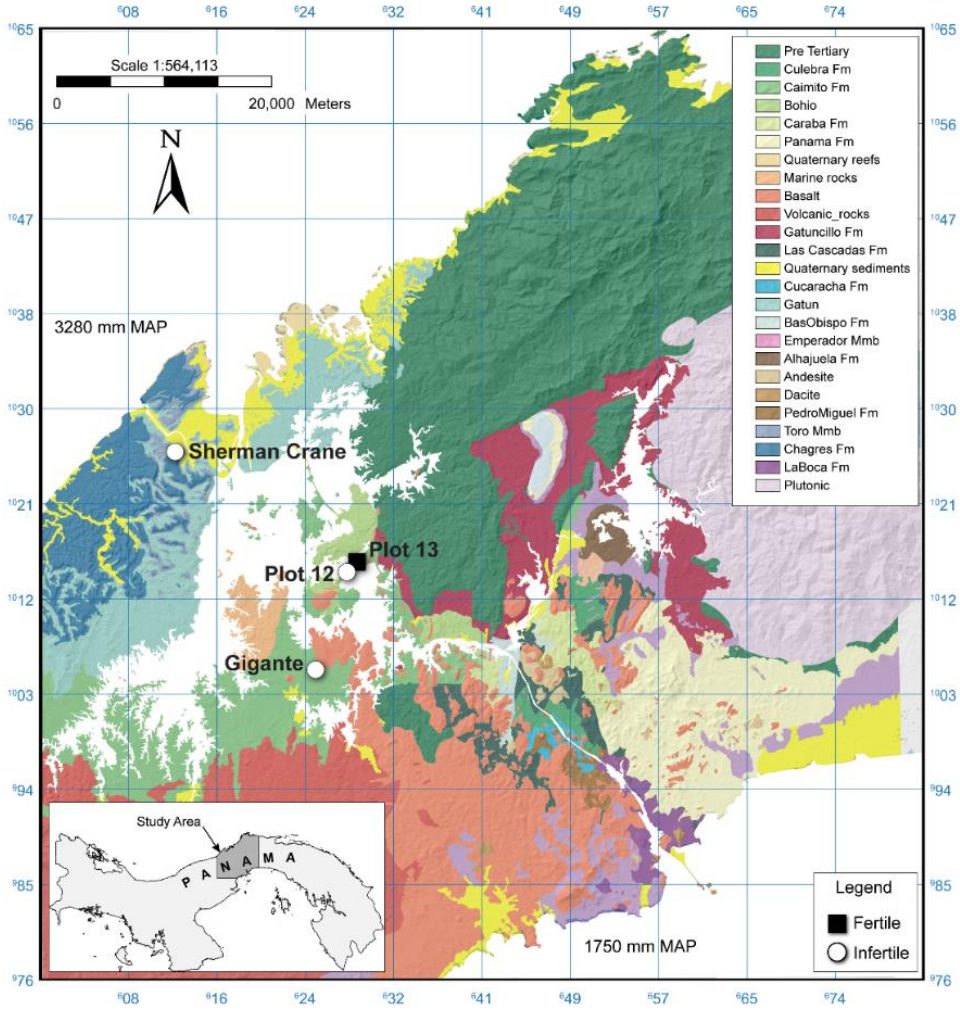

Figure 2.1: The four lowland tropical forest study forest sites are shown along a rainfall gradient on the Isthmus of Panama. Geological substrates and formations (Fm, shown in different colors) give rise to large variation in soil fertility, which is not correlated with the rainfall gradient. Rainfall increases from 1750 mm mean annual precipitation (MAP) on the Pacific coast to >3200 on the Caribbean coast, with sites for this study ranging from 2350 (Gigante) to 3400 (Sherman Crane). Soil fertility for the study sites is shown as fertile (black squares) or infertile (white circles). Citation: Geología de la República de Panamá, digitalizada del mapa Geológico de Panamá, 1:250,000 preparado por el Ministerio de Comercio e Industrias, Dirección General de Recursos Minerales, año 1990. Ministerio de Comercio e Industrias, Dirección General de Recursos Minerales, año 1990. Site details are presented in Table 2.1.

Figure 2.2.

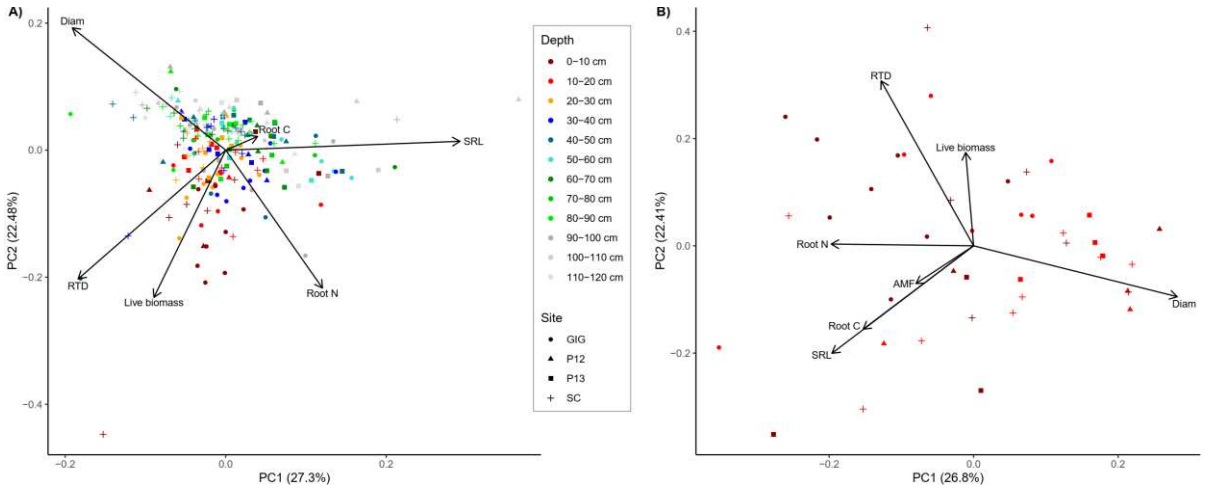

Figure 2.2: Tradeoffs in root characteristics are shown using principal components analyses (PCA) for 32 plots across four distinct tropical forests, including Gigante (GIG), plot 12 (P12), plot 13 (P13), and Sherman Crane (SC, details in Table 2.1) to 120 cm depths (10 cm increments shown in different colors). The percent variance explained by each component is shown on the axis. A) PCA results using root data to 1.2 m depths in 10 cm increments for live fine root biomass (live biomass), specific root length (SRL), root tissue density (RTD), root diameter (Diam), root %N (Root N), and root %C (Root C). This analysis illustrates separation in root traits by depth along axis 2, with shallow roots in particular separating out (brown markers). Axis 2 shown a tradeoff for SRL and root %N versus diameter, RTD, and live root biomass. Root characteristics that were strongly autocorrelated with other those shown were not used here (see Tables SI 2 – 4 for details). B) PCA results including AMF colonization rates to 20 cm depth with other characteristics to that depth show that AMF varied in the same direction as SRL and root %C, and AMF did not vary with diameter as had been expected. In this shallow depth analysis, the separation of the two depths is also apparent.

Figure 2.3.

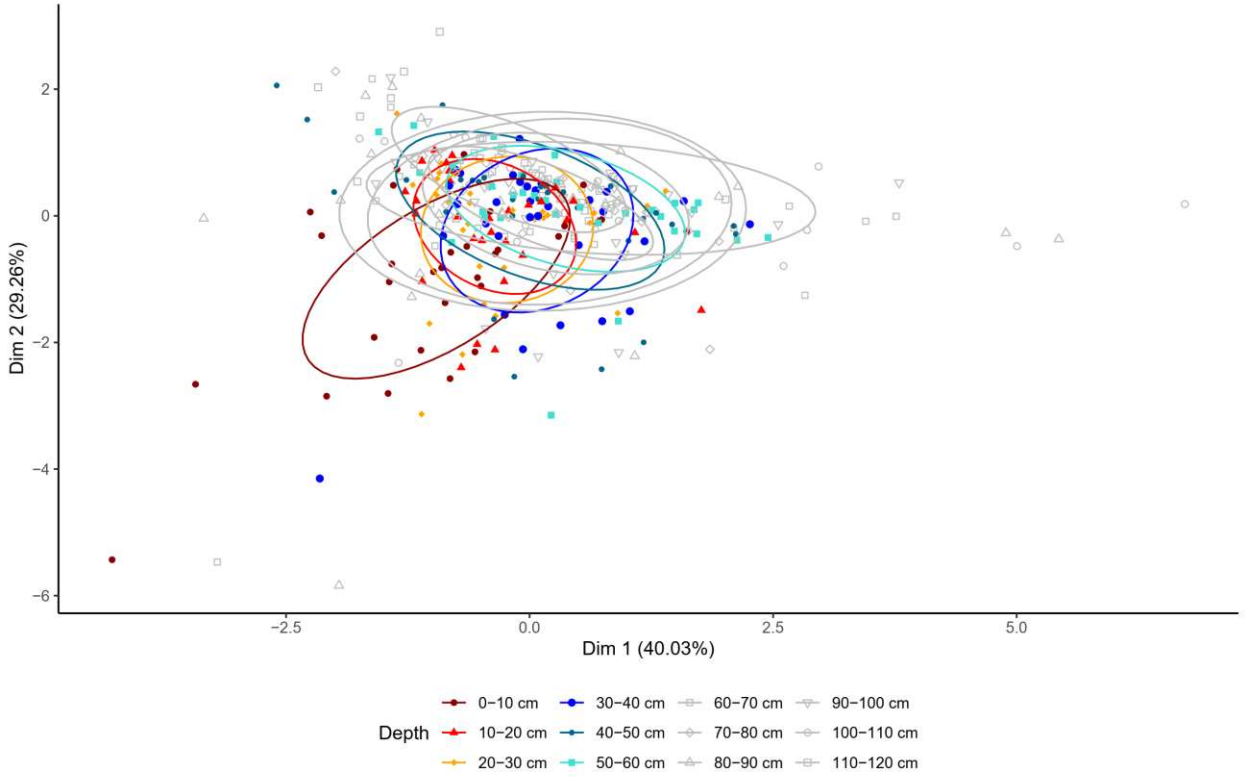

Figure 2.3: A cluster analysis is shown for fine root characteristics for 32 plots across four distinct tropical forests including Gigante (GIG), plot 12 (P12), plot 13 (P13), and Sherman Crane (SC, details in Table 2.1) to 120 cm depths (10 cm increments shown in different colors). Root data included live fine root biomass, specific root length (SRL), fine root diameter, and root tissue density (RTD). Depths not significantly different from each other are shown in gray, such that all surface depth increments were distinct, and depth >60 cm were not different. The percentage of variance explained by the first and second dimensions is shown in the axis labels. The ellipses shown confidence level = 0.50 around the center of each group (n = 32 per depth). A Euclidean distance metric was used to separate the 12 clusters by depth (k = 12).

Figure 2.4.

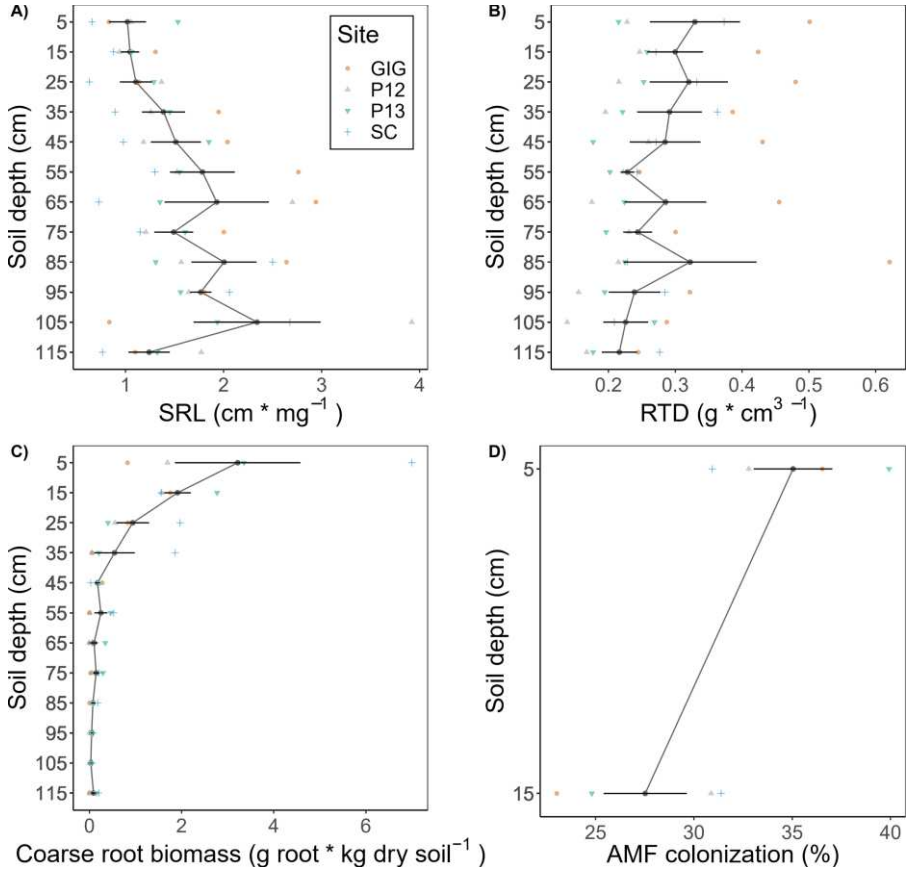

Figure 2.4: Root characteristics that varied significantly by depth similarly across all forest sites (no interaction with site) are shown, with depth on the y axis and root characteristic values on the x axis. Depth increments are presented as midpoints of depth intervals (i.e.: 5 cm for 0 – 10 cm depth interval). a) Site and depth predicted SRL, without interaction; b) Site and depth predicted RTD, without interaction; c) Site and depth predicted coarse root biomass, without interaction; d) Depth predicted AMF, without effect of site or interaction. The AMF data were collected only 0 – 10 and 10 – 20 cm depths. Black dots and bars represent mean ± SE across sites (n = 4 sites per depth). Colored markers show the average from 8 plots per site for each variable and depth. A similar figure for SRA, the only other root characteristic which also had significant effects of site and depth but not interaction, is in Figure SI 1.5.

Figure 2.5.

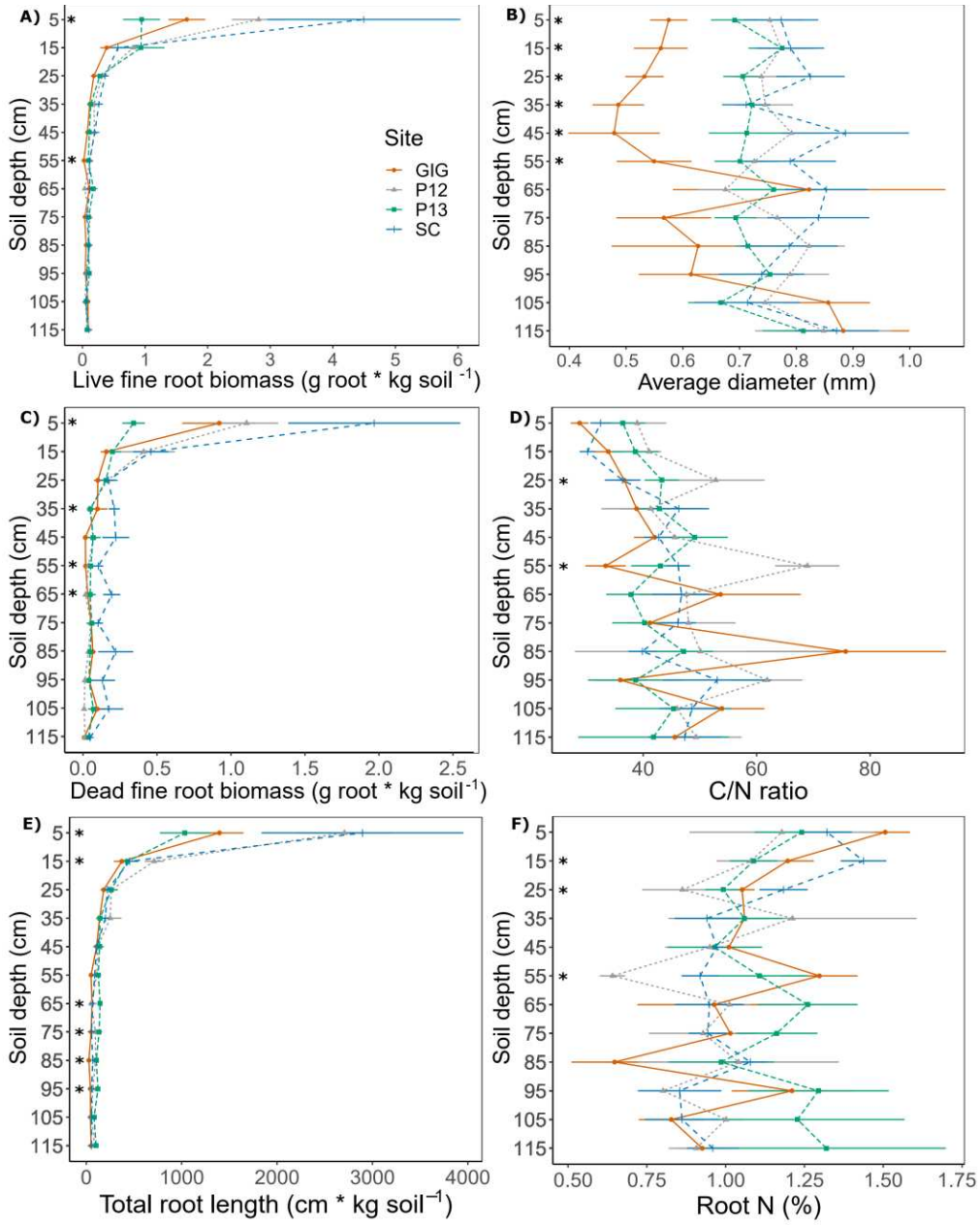

Figure 2.5: Root characteristics are shown by depth and forest site where there was a significant depth*site interaction. Soil depth is on the y axis and root characteristic values are on the x axis, with depth increments presented as midpoints of sampled depth intervals (i.e.: 5 cm for 0 – 10 cm depth). Asterisks (*) show significant means separation of sites within depths using Tukey's HSD test. Colored symbols and bars give mean ± SE for each site and depth (n = 8 plots per site).

Figure 2.6.

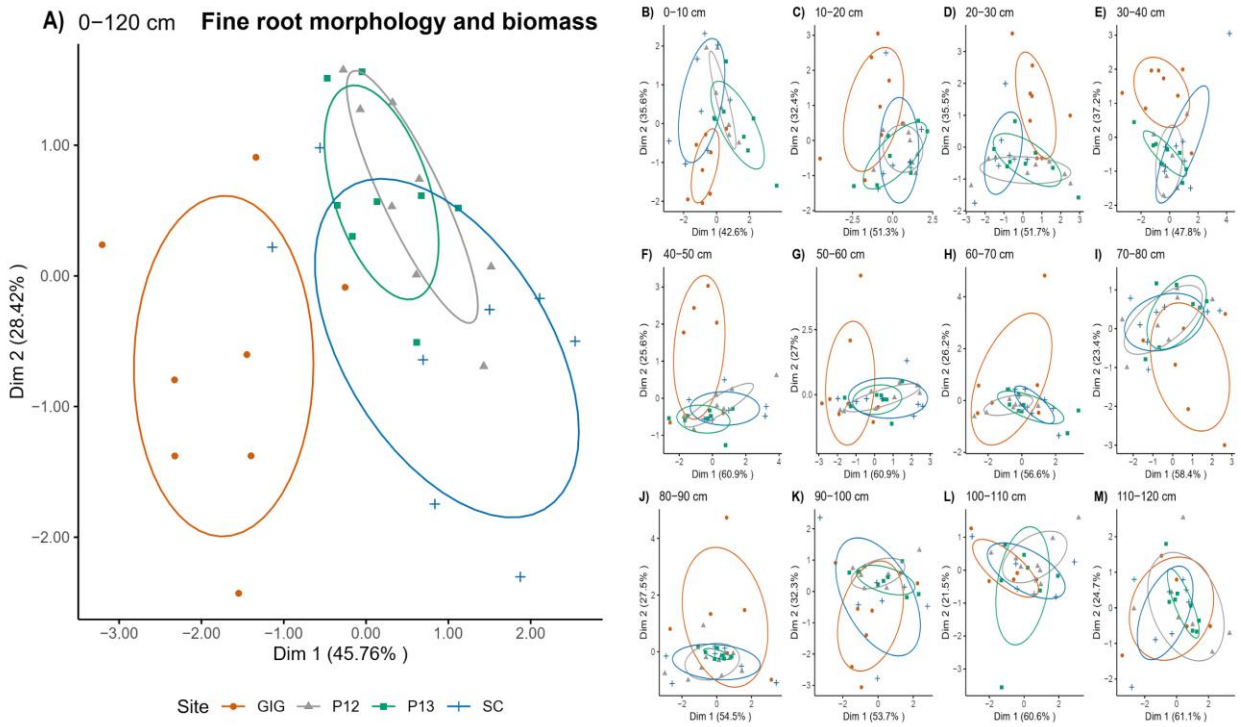

Figure 2.6: Results are given from cluster analysis comparing root characteristics among four distinct Panamanian forests in the four colors. A) separation among forest sites is shown for all root data 0 – 1.2 m depths including summed live fine root biomass, and average SRL, root diameter, and RTD. B to M) show the same analysis for depth increments separately to show the trend with depth, with the least separation among sites for deeper soil layers. The percentage of variance explained by the first and second dimensions is shown in the axis labels. The ellipses show confidence level = 0.50 around the center of each site (n = 8 per site). Cluster analysis used principal coordinates analysis (PCoA) and k – means clustering on scaled data, using a Euclidean distance metric to divide the data into four distinct clusters corresponding to the four forests (k = 4).

Figure 2.7.

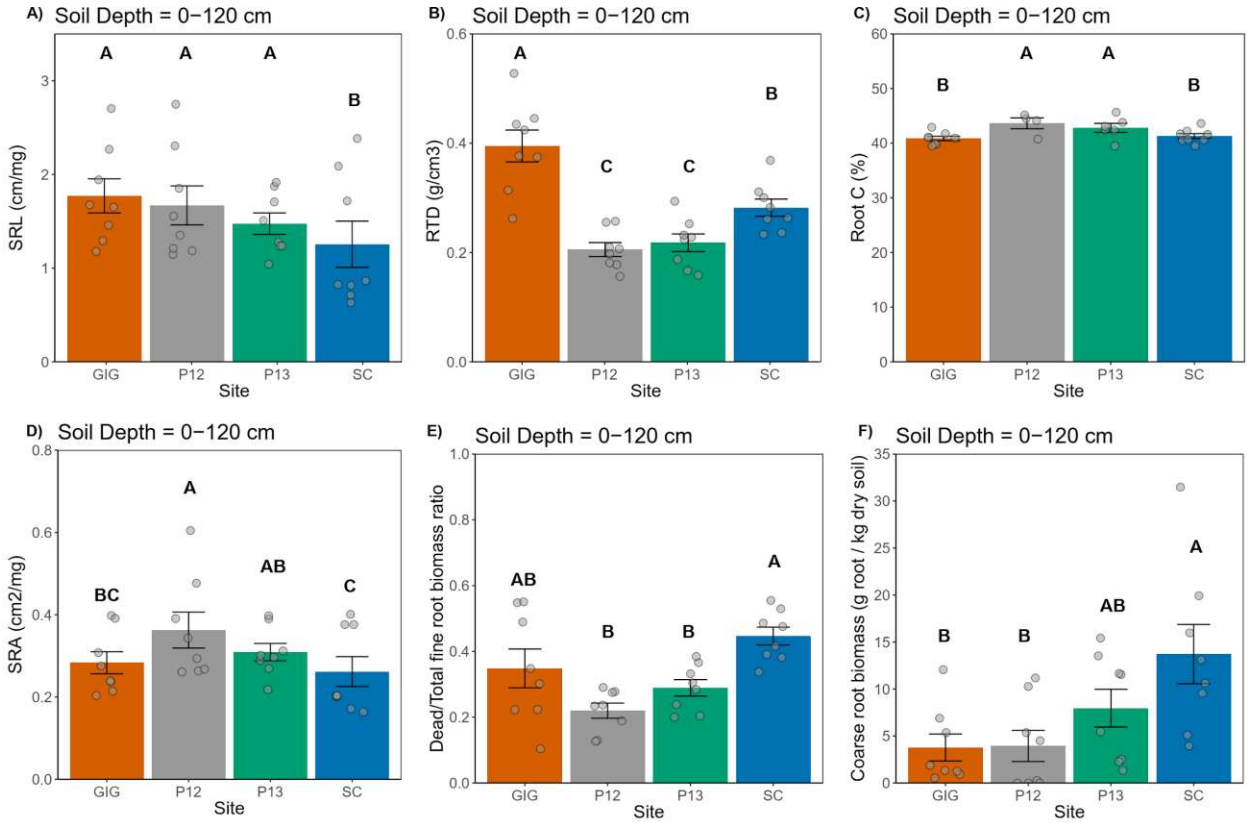

Figure 2.7: Average values for root characteristics are compared by forest site the whole soil profile 0 – 1.2 m depth, including root characteristics with no site * depth interactions. Sites are arranged in order of increasing MAP (GIG < [P12, P13] < SC). Data are mean ± SE (n = 8 per site). Letters show differences using Tukey's HSD means separation tests.

Figure 2.8.

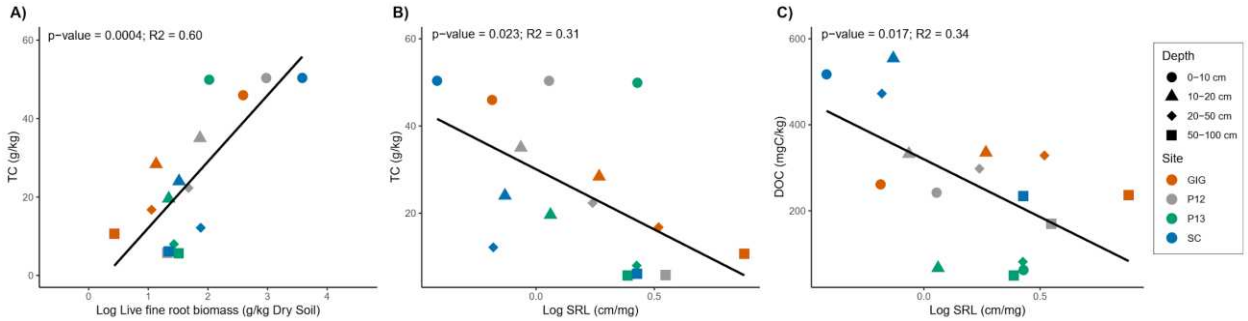

Figure 2.8: The most significant predictors of total soil C (TC) stocks selected using forward stepwise tests (Table SI 1.11) are shown, including a) live fine root biomass (g/kg – soil), and B) specific root length (SRL, cm/mg). Similarly, the most significant predictor of DOC (mg C/kg – soil) was SRL. One – way regression p – values and R2 are given on each figure, with symbols showing depth increments and colors representing the four forests.

Figure 2.9.

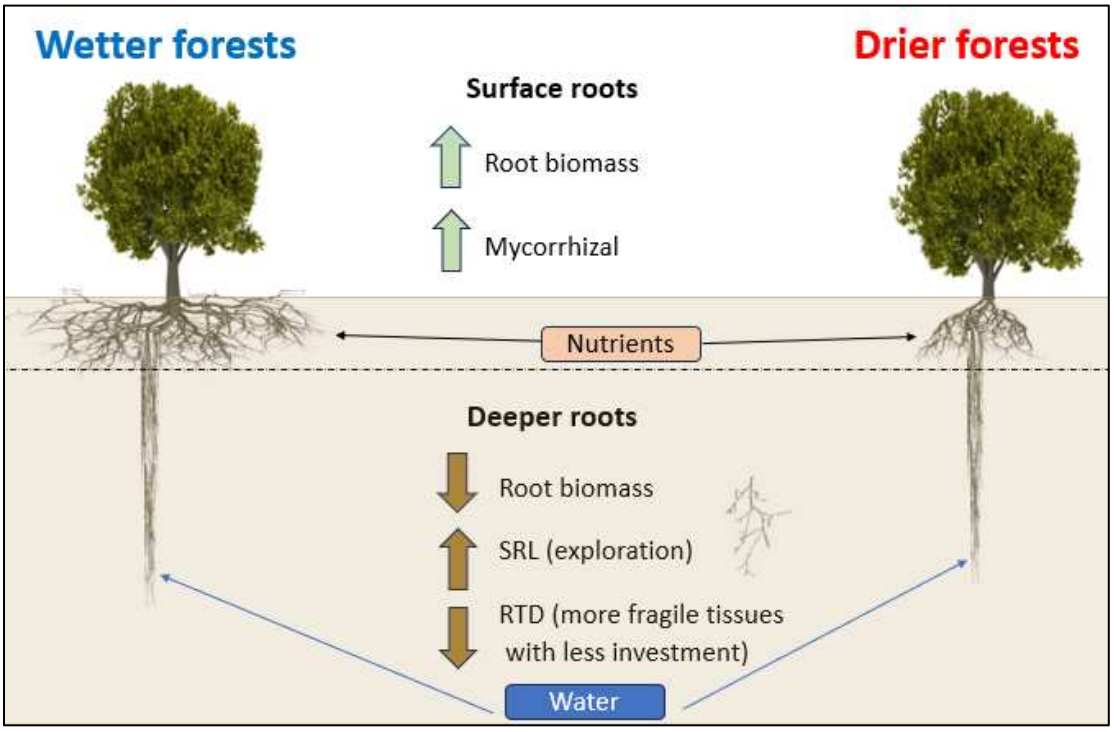

Figure 2.9: Conceptual figure from chapter 2. This chapter showed that most root characteristics exhibited similar variations with depth across various forests. It has been observed that root biomass generally decreases with depth, a trend consistent across tropical forests. More notably, there has been a general increase in fine root specific root length (SRL) and a decrease in fine root root tissue density (RTD) with depth. Surface roots are primarily formed for nutrient acquisition, given that deeper soils in these forests typically contain fewer nutrients compared to the surface. The larger biomass and higher arbuscular mycorrhizal fungi (AMF) colonization at the soil surface likely play a crucial role in nutrient acquisition. In contrast, deeper roots may be more focused on water acquisition since surface soils tend to dry out during the dry season, whereas deeper soil moisture remains more consistent. Consequently, the higher SRL and more delicate tissues with lower RTD at deeper levels could be adaptations allowing plants to explore for water with less biomass investment. The first hypothesis that **root characteristics vary systematically with depth, exhibiting trade – offs related to resource acquisition** was partially supported, because most root characteristics varied with depth systematically across sites, but some root characteristics presented site-specific variation. Across sites, trade-offs of surface root characteristics (likely for nutrient uptake) vs deeper root characteristics (likely for water uptake) were observed.

Figure 2.10.

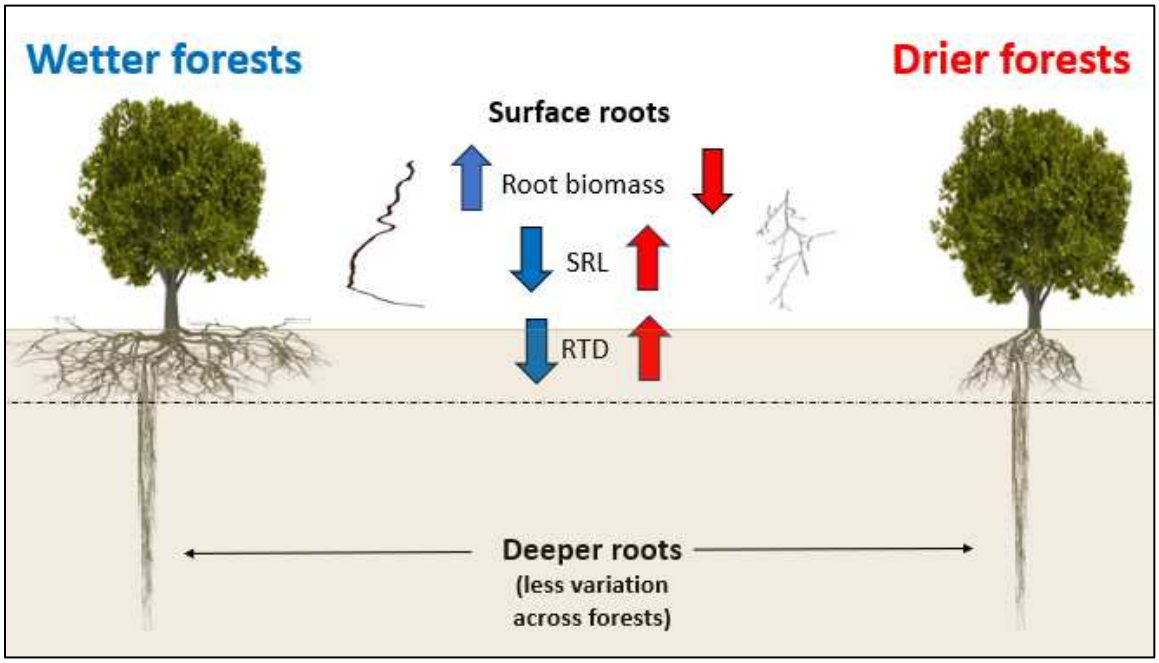

Figure 2.10: Conceptual figure for chapter 2. This chapter also showed that plants adapted to drier conditions tend to exhibit reduced biomass and a higher specific root length (SRL), likely as a compensatory mechanism for their lower biomass. Additionally, these plants often have a larger root tissue density (RTD), which likely serves as a form of protection. There is a significant variation in root characteristics at the soil surface, which could have crucial implications for forest responses to extreme drought events. Lower root biomass may increase the vulnerability of forests; however, the presence of longer and thinner roots might enable plants to explore deeper soil layers where resources are still available. Moreover, denser roots may help plants conserve resources, offer more protection, and penetrate dry soils, potentially increasing their resilience. At deeper soil layers, however, there was less variation in root characteristics across different sites, indicating a more uniform response to environmental conditions at these depths. The second hypothesis that **variation in root characteristics is strongest in surface soils, reflecting site – scale resource differences** was supported**.** However, the prediction that **the most fertile forest would have the most unique root characteristics among the four forests**, was not supported. Variation of root characteristics was strongest in surface soils, but the most distinct characteristics were in the driest, infertile site (GIG, not the fertile P13). The main distinct characteristic in fertile sites was larger radiocarbon ages at deeper soil layers.

2.8 Tables

Table 2.1. Forest Site characteristics are given for the four tropical forests used in this study (Cusack et al., 2018)

Site	Latitude North	Longitude East	Soil order	Fertility	MAP (mm)	Profile Clay% 1.0m	Above ground biomass (Mg /ha) >10cm dbh	SOC to 1 m kg/ m2	Total N to 1 m kg/ m2	Total P to 1 m g/m2	resin-extractable P to 1 m AEM Pi gP/m2	DOC to 1 m g/m2	Total Extractable Bases to 1 m kg/m2
GIG	9.09918	-79.8540	Oxisol	Infertile	2350	86.129	201.8	19	2.01	152.95	0.25	318.32	1.37
P12	9.17936	-79.8296	Ultisol	Infertile	2600	52.298	212.8	19	1.45	241.66	0.33	267.33	0.63
P13	9.18788	-79.821	Alfisol	Fertile	2600	49.228	260.2	12	1.01	204.13	1.58	65.32	5.29
SC	9.28087	-79.9747	Oxisol	Infertile	3421	78.217	304.9	13	1	233.59	0.15	375.3	0.22

Table 2.2: Root characteristics are compared among forest sites for each response variable for the whole soil profile from 0 – 1.2 m depth, using summed values for biomass, and average values for other traits. Mean ± SE are given, with letters in columns giving significant differences among sites using Tukey's HSD test. Total fine root length and AMF results are shown in Table 2.6. If variable had also a depth effect, a * is given in the column header, and if there was interaction between site and depth # is given. All raw data by depth is provided in Table SI 1.I1.

Site	Live fine root biomass (g/kg-dry-soil) *#	Dead fine root biomass (g/kg-dry-soil) *#	Coarse root biomass (g/kg-dry-soil) *	Dead:total fine root biomass ratio	SRL (cm/mg) *	SRA (cm2/mg) *	RTD (g/cm3) *	Diameter (mm) *#	N content (%) *#	C content (%)	C/N ratio *#
GIG	2.72 ± 0.45 B	1.49 ± 0.32 B	3.78 ± 1.44 B	0.35 ± 0.06 AB	1.77 ± 0.18 A	0.28 ± 0.03 B	0.39 ± 0.03 A	0.6 ± 0.02 B	1.1 ± 0.03 AB	40.87 ± 0.4 B	40.46 ± 0.78 B
P12	4.52 ± 0.73 AB	1.79 ± 0.42 B	3.95 ± 1.66 B	0.22 ± 0.02 B	1.75 ± 0.22 A	0.34 ± 0.03 A	0.21 ± 0.01 C	0.77 ± 0.02 A	0.93 ± 0.07 B	43.61 ± 0.97 A	50.46 ± 2.97 A
P13	2.64 ± 0.43 B	1.09 ± 0.12 B	7.97 ± 2.01 AB	0.29 ± 0.02 B	1.47 ± 0.12 A	0.31 ± 0.02 A	0.22 ± 0.02 C	0.73 ± 0.02 A	1.07 ± 0.11 A	42.82 ± 0.83 A	43.38 ± 3.58 B
SC	6.52 ± 1.65 A	3.91 ± 0.77 A	13.72 ± 3.15 A	0.44 ± 0.03 A	1.26 ± 0.25 B	0.26 ± 0.04 B	0.28 ± 0.02 B	0.8 ± 0.04 A	1.07 ± 0.05 AB	41.31 ± 0.44 B	41.72 ± 2.26 B

Table 2.3: Root biomass to 1.2 m depths is given as Mg/ha, summed for the whole soil profile (0 – 1.2 m), with means and standard errors (SE, n = 8 plots per site). Letters give significant differences among sites using Tukey's HSD test. Total biomass values were calculated by summing root biomass across depth increments in grams, then dividing by the soil core surface area (5 cm diameter).

Site	**Live Fine Root biomass (Mg/ha)**		**Live Fine Root biomass (Mg C/ha)**		**Dead Fine Root biomass (Mg/ha)**		**Coarse Fine Root biomass (Mg/ha)**		**Total biomass (Mg/ha)**	
	Mean	*SE*	*Mean*	*SE*	*Mean*	*SE*	*Mean*	*SE*	*Mean*	*SE*
GIG	3.49 **C**	0.51	1.43 **C**	0.21	1.96 **B**	0.39	6.43 **B**	2.50	11.88 **B**	2.36
P12	6.72 **AB**	0.63	2.93 **AB**	0.28	2.58 **B**	0.47	5.75 **B**	2.42	15.04 **B**	2.55
P13	4.14 **BC**	0.58	1.17 **BC**	0.25	1.69 **B**	0.19	12.31 **AB**	2.95	18.14 **AB**	3.20
SC	7.36 **A**	1.17	3.04 **A**	0.48	5.49 **A**	0.89	19.36 **A**	4.43	32.21 **A**	4.28

Table 2.4: Loadings for root characteristics are given for the axes of the PCA for the whole soil profile (0 – 1.2 m depth) using 10 cm depth increments, and for the soil surface (0 – 20 cm depth) using 10 cm depth increments and including AMF colonization rates. The most positive and negative loadings are in bold for emphasis on tradeoffs. Cumulative proportions of variance and other test statistics are given below.

Depth	Variable	PC1	PC2	PC3	PC4	PC5	PC6	PC7
0-120 cm	Live biomass	-0.211	**-0.547**	0.292	0.472	-0.590	-0.018	
	SRL	**0.689**	0.033	-0.101	0.085	-0.278	0.656	
	RTD	-0.434	-0.478	**-0.295**	-0.469	0.063	0.522	
	Diam	**-0.451**	**0.454**	0.377	0.346	0.187	0.542	
	Root N	0.284	-0.512	0.365	0.184	0.698	0.054	
	Root C	0.094	0.051	**0.737**	-0.630	-0.220	0.001	
0-20 cm	Live biomass	-0.024	0.386	-0.452	-0.715	0.101	-0.352	-0.015
	SRL	-0.435	**-0.445**	**0.366**	-0.266	-0.033	-0.372	-0.519
	RTD	-0.284	**0.682**	0.061	0.215	-0.161	0.231	-0.569
	Diam	**0.626**	-0.211	-0.264	0.052	0.301	0.073	-0.629
	Root N	**-0.437**	0.007	-0.181	0.258	0.840	-0.017	0.060
	Root C	-0.339	-0.345	-0.421	-0.273	-0.161	0.696	-0.064
	AMF	-0.177	-0.156	**-0.616**	0.476	-0.375	-0.441	-0.057
Depth	**Importance of components:**	**PC1**	**PC2**	**PC3**	**PC4**	**PC5**	**PC6**	**PC7**
0-120 cm	Proportion of Variance	0.273	0.2248	0.1878	0.1414	0.1143	0.05861	
	Cumulative Proportion	0.273	0.4978	0.6857	0.8271	0.9414	1	
	Standard deviation	1.28	1.1614	1.0616	0.9211	0.8281	0.593	
	Eigenvalues	**1.6384**	**1.34885**	**1.126995**	0.848425	0.68575	0.351649	
0-20 cm	Proportion of Variance	0.268	0.2241	0.1864	0.1167	0.1101	0.08415	0.0107
	Cumulative Proportion	0.268	0.492	0.6784	0.7951	0.9052	0.9893	1
	Standard deviation	1.37	1.2524	1.1422	0.9036	0.8779	0.76749	0.2737
	Eigenvalues	**1.8769**	**1.568506**	**1.304621**	0.816493	0.770708	0.589041	0.074912

Table 2.5: Mixed model results for different root characteristics. Alpha = 0.05, but after applying a Bonferroni correction, the significance level for the multiple comparisons was 0.004.

Dependent	Independent	Chisq	Df	p-value
Log Live fine root biomass	Site	13.827	3	0.003
	Depth	55.374	1	0.000
	Site:Depth	14.294	3	0.003
Coarse root biomass	Site	13.244	3	0.004
	Depth	62.272	1	0.000
Log Dead fine biomass	Site	30.982	3	0.000
	Depth	10.833	1	0.001
	Site:Depth	15.748	3	0.001
Dead:Total fine biomass ratio	Site	21.718	3	0.000
	Depth	0.0644	1	0.800
Log Total root length	Site	7.5465	3	0.046
	Depth	111.87	1	0.000
	Site:Depth	19.457	3	0.000
Log SRL	Site	12.433	3	0.006
	Depth	5.1076	1	0.024
Log SRA	Site	13.704	3	0.003
	Depth	13.966	1	0.000
Log Diameter	Site	47.42	3	0.000
	Depth	13.473	1	0.000
	Site:Depth	9.2996	3	0.026
Log RTD	Site	35.846	3	0.000
	Depth	27.653	1	0.000
Root N	Site	9.8261	3	0.020
	Depth	18.091	1	0.000
	Site:Depth	20.399	3	0.000
Root C	Site	25.459	3	0.000
	Depth	1.3092	1	0.253
Root CN	Site	9.4041	3	0.024
	Depth	20.684	1	0.000
	Site:Depth	8.056	3	0.045
AMF colonization	Site	0.2187	3	0.975
	Depth	4.9127	1	0.027

Table 2.6: Mean ± SE for each response variable, across different forest sites and depths. Depth was a significant main effect for all characteristics except dead:total fine root biomass ratio, and root %C. Site had a significant main effect for all characteristics except AMF colonization rate. Columns marked with ^ indicate root characteristics for which there was a significant effect of depth. Columns marked with *** indicate root characteristics for which there was a significant interaction between depth and site. For these characteristics, we present comparisons of means among sites for each depth separately, shown in rows in bold text, with by significance letters from Tukey's HSD tests. For variables involving an interaction between site and depth, we specifically highlight in bold those sites where the variable significantly varies by depth. For columns without ***, there was no interaction between depth and site. Since the effect of the site was significant across most variables, we present results from means comparisons for the summed or averaged profile (0 – 1.2 m depth) in the bottom row.

Soil depth	**Live fine root biomass (g/Dry soil kg) ^ *****			
	GIG	P12	P13	SC
0-10 cm	**1.67 ± 0.29 B**	**2.81 ± 0.49 AB**	**0.94 ± 0.3 B**	**4.5 ± 1.54 A**
10-20 cm	0.39 ± 0.1	0.81 ± 0.11	0.55 ± 0.15	0.57 ± 0.11
20-30 cm	0.18 ± 0.05	0.31 ± 0.11	0.28 ± 0.08	0.36 ± 0.04
30-40 cm	0.12 ± 0.04	0.19 ± 0.07	0.13 ± 0.03	0.26 ± 0.06
40-50 cm	0.08 ± 0.03	0.19 ± 0.08	0.11 ± 0.04	0.2 ± 0.06
50-60 cm	**0.02 ± 0 B**	**0.12 ± 0.04 A**	**0.1 ± 0.02 A**	**0.12 ± 0.03 A**
60-70 cm	0.08 ± 0.03	0.04 ± 0.01	0.18 ± 0.06	0.12 ± 0.03
70-80 cm	0.04 ± 0.02	0.12 ± 0.03	0.1 ± 0.02	0.07 ± 0.02
80-90 cm	0.05 ± 0.03	0.1 ± 0.03	0.09 ± 0.02	0.11 ± 0.04
90-100 cm	0.05 ± 0.02	0.06 ± 0.02	0.11 ± 0.02	0.07 ± 0.03
100-110 cm	0.09 ± 0.04	0.04 ± 0.02	0.06 ± 0.02	0.06 ± 0.02
110-120 cm	0.09 ± 0.06	0.09 ± 0.04	0.07 ± 0.01	0.1 ± 0.05
0-120	**2.72 ± 0.45 B**	**4.52 ± 0.73 AB**	**2.64 ± 0.43 B**	**6.52 ± 1.65 A**
Soil depth	**Total fine root length (cm/kg Soil) ^ *****			
	GIG	P12	P13	SC
0-10 cm	**1395.76 ± 251.18 AB**	**2706.82 ± 492.88 A**	**1033.58 ± 261.94 B**	**2895.8 ± 1057.48 A**
10-20 cm	**372.56 ± 83.57 B**	**711.15 ± 99.02 A**	**432.97 ± 68.6 B**	**454.2 ± 91.96 B**
20-30 cm	182.56 ± 33.78	262.21 ± 58.39	260.16 ± 69.73	220.13 ± 34.05

30-40 cm	139.38 ± 35.94	250.4 ± 118.16	143.21 ± 38.97	199.12 ± 34.78
40-50 cm	107.39 ± 22.72	120.8 ± 20.72	138.16 ± 45	109.4 ± 23.45
50-60 cm	50.56 ± 8.67	109.96 ± 27.76	125.6 ± 28.35	88.07 ± 14.36
60-70 cm	**59.27 ± 9.79 B**	**53.35 ± 18.42 B**	**144.25 ± 24.57 A**	**68.24 ± 12.89 B**
70-80 cm	**51.44 ± 19.11 B**	**94.62 ± 15.16 AB**	**133.87 ± 31.06 A**	**54.46 ± 10.75 B**
80-90 cm	**27.26 ± 6.34 B**	**97.64 ± 17.43 A**	**104.6 ± 20.99 A**	**68.84 ± 7.65 AB**
90-100 cm	**43.87 ± 11.5 B**	**67.85 ± 13.35 B**	**121.99 ± 24.92 A**	**55.9 ± 17.76 B**
100-110 cm	44.51 ± 8.39	57.69 ± 14.82	81.87 ± 25.03	54.14 ± 6.4
110-120 cm	50.96 ± 14.97	86.09 ± 23.25	101.57 ± 29.1	53.33 ± 22.19
0-120	2428.38 ± 361.96 A	4262.96 ± 573.71 A	2740.74 ± 431.83 A	4314.64 ± 1213.73 A
Soil depth	**Dead fine root biomass (g/Dry soil kg) ^ *****			
	GIG	P12	P13	SC
0-10 cm	**0.91 ± 0.25 B**	**1.09 ± 0.21 AB**	**0.34 ± 0.08 B**	**1.94 ± 0.57 A**
10-20 cm	0.15 ± 0.04	0.4 ± 0.21	0.2 ± 0.06	0.45 ± 0.12
20-30 cm	0.1 ± 0.03	0.16 ± 0.07	0.15 ± 0.05	0.17 ± 0.05
30-40 cm	**0.09 ± 0.07 AB**	**0.04 ± 0.02 B**	**0.05 ± 0.02 B**	**0.21 ± 0.04 A**
40-50 cm	0.01 ± 0.01	0.07 ± 0.05	0.07 ± 0.05	0.22 ± 0.09
50-60 cm	**0.02 ± 0.01 B**	**0.04 ± 0.01 B**	**0.05 ± 0.02 AB**	**0.1 ± 0.03 A**
60-70 cm	**0.03 ± 0.02 B**	**0.02 ± 0 B**	**0.05 ± 0.04 B**	**0.19 ± 0.06 A**
70-80 cm	0.05 ± 0.03	0.05 ± 0.02	0.06 ± 0.03	0.1 ± 0.03
80-90 cm	0.06 ± 0.02	0.03 ± 0.01	0.05 ± 0.02	0.22 ± 0.12
90-100 cm	0.04 ± 0.01	0.01 ± 0	0.04 ± 0.01	0.13 ± 0.08
100-110 cm	0.09 ± 0.06	0.01 ± 0	0.07 ± 0.03	0.17 ± 0.1
110-120 cm	0.01 ± 0	0.01 ± 0	0.03 ± 0.02	0.05 ± 0.02
0-120	**1.49 ± 0.32 B**	**1.79 ± 0.42 B**	**1.09 ± 0.12 B**	**3.91 ± 0.77 A**
Soil depth	**Coarse root biomass (g/Dry soil kg) ^**			
	GIG	P12	P13	SC
0-10 cm	0.83 ± 0.53	1.69 ± 1.15	3.35 ± 1.26	7 ± 1.96
10-20 cm	1.76 ± 1.06	1.57 ± 1.25	2.77 ± 1.37	1.55 ± 0.78

20-30 cm	0.84 ± 0.47	0.55 ± 0.49	0.4 ± 0.15	1.97 ± 1.24
30-40 cm	0.06 ± 0.04	0.06 ± 0.06	0.2 ± 0.18	1.86 ± 1.14
40-50 cm	0.28 ± 0.24	0.17 ± 0.17	0.22 ± 0.2	0.03 ± 0.03
50-60 cm	0 ± 0	0.01 ± 0.01	0.46 ± 0.3	0.53 ± 0.35
60-70 cm	0 ± 0	0 ± 0	0.34 ± 0.14	0.06 ± 0.04
70-80 cm	0.02 ± 0.02	0.05 ± 0.05	0.3 ± 0.22	0.21 ± 0.1
80-90 cm	0 ± 0	0.05 ± 0.03	0.07 ± 0.04	0.18 ± 0.12
90-100 cm	0.06 ± 0.06	0 ± 0	0.04 ± 0.03	0.08 ± 0.06
100-110 cm	0.02 ± 0.02	0 ± 0	0.03 ± 0.02	0.06 ± 0.06
110-120 cm	0 ± 0	0 ± 0	0.15 ± 0.13	0.2 ± 0.2
0-120	**3.78 ± 1.44 B**	**3.95 ± 1.66 B**	**7.97 ± 2.01 AB**	**13.72 ± 3.15 A**
Soil depth	**Dead/total fine root biomass ratio**			
	GIG	P12	P13	SC
0-10 cm	0.35 ± 0.08	0.29 ± 0.04	0.34 ± 0.07	0.35 ± 0.08
10-20 cm	0.32 ± 0.09	0.25 ± 0.07	0.27 ± 0.08	0.42 ± 0.07
20-30 cm	0.36 ± 0.08	0.36 ± 0.08	0.4 ± 0.1	0.28 ± 0.09
30-40 cm	0.31 ± 0.11	0.2 ± 0.05	0.27 ± 0.09	0.48 ± 0.06
40-50 cm	0.25 ± 0.12	0.15 ± 0.04	0.26 ± 0.11	0.44 ± 0.12
50-60 cm	0.27 ± 0.11	0.2 ± 0.06	0.29 ± 0.08	0.47 ± 0.06
60-70 cm	0.33 ± 0.15	0.32 ± 0.11	0.13 ± 0.05	0.56 ± 0.09
70-80 cm	0.44 ± 0.19	0.32 ± 0.09	0.22 ± 0.11	0.54 ± 0.09
80-90 cm	0.53 ± 0.14	0.27 ± 0.08	0.3 ± 0.1	0.46 ± 0.11
90-100 cm	0.46 ± 0.12	0.09 ± 0.03	0.31 ± 0.11	0.44 ± 0.16
100-110 cm	0.34 ± 0.09	0.04 ± 0.03	0.46 ± 0.11	0.56 ± 0.09
110-120 cm	0.15 ± 0.11	0.16 ± 0.06	0.22 ± 0.09	0.35 ± 0.08
0-120	**0.35 ± 0.06 AB**	**0.22 ± 0.02 B**	**0.29 ± 0.02 B**	**0.44 ± 0.03 A**
Soil depth	**SRL (cm/mg) ^**			
	GIG	P12	P13	SC
0-10 cm	0.83 ± 0.08	1.06 ± 0.15	1.53 ± 0.31	0.66 ± 0.08

10-20 cm	1.31 ± 0.35	0.94 ± 0.1	1.06 ± 0.28	0.88 ± 0.13
20-30 cm	1.14 ± 0.18	1.37 ± 0.28	1.29 ± 0.29	0.63 ± 0.1
30-40 cm	1.95 ± 0.42	1.26 ± 0.16	1.45 ± 0.34	0.89 ± 0.08
40-50 cm	2.04 ± 0.53	1.18 ± 0.33	1.85 ± 0.42	0.98 ± 0.25
50-60 cm	2.76 ± 0.44	1.52 ± 0.41	1.55 ± 0.31	1.3 ± 0.38
60-70 cm	2.94 ± 1.17	2.7 ± 0.88	1.35 ± 0.25	0.73 ± 0.11
70-80 cm	2 ± 0.6	1.21 ± 0.3	1.61 ± 0.27	1.15 ± 0.38
80-90 cm	2.64 ± 1.5	1.57 ± 0.4	1.31 ± 0.21	2.5 ± 1.29
90-100 cm	1.8 ± 0.52	1.64 ± 0.31	1.56 ± 0.35	2.06 ± 1.07
100-110 cm	0.83 ± 0.32	3.92 ± 1.69	1.94 ± 0.65	2.68 ± 1.16
110-120 cm	1.1 ± 0.43	1.77 ± 0.5	1.32 ± 0.24	0.77 ± 0.13
0-120	**1.77 ± 0.18 A**	**1.75 ± 0.22 A**	**1.47 ± 0.12 A**	**1.26 ± 0.25 B**
Soil depth	**SRA (cm2/mg) ^**			
	GIG	P12	P13	SC
0-10 cm	0.15 ± 0.01	0.24 ± 0.02	0.31 ± 0.05	0.16 ± 0.02
10-20 cm	0.2 ± 0.04	0.22 ± 0.01	0.23 ± 0.04	0.21 ± 0.03
20-30 cm	0.19 ± 0.03	0.29 ± 0.05	0.27 ± 0.06	0.16 ± 0.02
30-40 cm	0.29 ± 0.07	0.29 ± 0.03	0.31 ± 0.06	0.2 ± 0.02
40-50 cm	0.28 ± 0.08	0.26 ± 0.06	0.36 ± 0.05	0.22 ± 0.04
50-60 cm	0.45 ± 0.07	0.32 ± 0.07	0.32 ± 0.04	0.27 ± 0.05
60-70 cm	0.45 ± 0.17	0.52 ± 0.15	0.29 ± 0.04	0.18 ± 0.02
70-80 cm	0.29 ± 0.06	0.27 ± 0.05	0.34 ± 0.05	0.24 ± 0.05
80-90 cm	0.4 ± 0.24	0.36 ± 0.08	0.28 ± 0.04	0.46 ± 0.19
90-100 cm	0.29 ± 0.08	0.37 ± 0.05	0.34 ± 0.06	0.44 ± 0.23
100-110 cm	0.2 ± 0.06	0.86 ± 0.36	0.37 ± 0.1	0.44 ± 0.15
110-120 cm	0.25 ± 0.07	0.39 ± 0.08	0.31 ± 0.04	0.2 ± 0.03
0-120	**0.28 ± 0.03 BC**	**0.34 ± 0.03 A**	**0.31 ± 0.02 AB**	**0.26 ± 0.04 C**
Soil depth	**RTD (g/cm3) ^**			
	GIG	P12	P13	SC

0-10 cm	0.5 ± 0.05	0.23 ± 0.01	0.22 ± 0.03	0.37 ± 0.06
10-20 cm	0.42 ± 0.06	0.25 ± 0.02	0.26 ± 0.03	0.27 ± 0.04
20-30 cm	0.48 ± 0.08	0.22 ± 0.02	0.25 ± 0.03	0.33 ± 0.05
30-40 cm	0.39 ± 0.06	0.2 ± 0.02	0.22 ± 0.03	0.36 ± 0.12
40-50 cm	0.43 ± 0.09	0.26 ± 0.04	0.18 ± 0.02	0.27 ± 0.04
50-60 cm	0.25 ± 0.08	0.22 ± 0.03	0.2 ± 0.02	0.24 ± 0.03
60-70 cm	0.46 ± 0.24	0.18 ± 0.03	0.22 ± 0.03	0.29 ± 0.03
70-80 cm	0.3 ± 0.04	0.23 ± 0.03	0.2 ± 0.03	0.25 ± 0.03
80-90 cm	0.62 ± 0.21	0.21 ± 0.04	0.22 ± 0.03	0.23 ± 0.05
90-100 cm	0.32 ± 0.06	0.16 ± 0.01	0.19 ± 0.03	0.28 ± 0.07
100-110 cm	0.29 ± 0.05	0.14 ± 0.03	0.27 ± 0.1	0.21 ± 0.03
110-120 cm	0.24 ± 0.05	0.17 ± 0.03	0.18 ± 0.01	0.28 ± 0.03
0-120	**0.39 ± 0.03 A**	**0.21 ± 0.01 C**	**0.22 ± 0.02 C**	**0.28 ± 0.02 B**
Soil depth	**Diameter (mm) ^ *****			
	GIG	P12	P13	SC
0-10 cm	**0.58 ± 0.03 B**	**0.75 ± 0.06 A**	**0.69 ± 0.04 AB**	**0.77 ± 0.07 A**
10-20 cm	**0.56 ± 0.05 B**	**0.77 ± 0.05 A**	**0.77 ± 0.06 A**	**0.79 ± 0.06 A**
20-30 cm	**0.53 ± 0.03 B**	**0.74 ± 0.05 A**	**0.71 ± 0.03 A**	**0.82 ± 0.06 A**
30-40 cm	**0.49 ± 0.05 B**	**0.75 ± 0.05 A**	**0.72 ± 0.03 A**	**0.71 ± 0.04 A**
40-50 cm	**0.48 ± 0.08 B**	**0.79 ± 0.06 A**	**0.71 ± 0.07 AB**	**0.89 ± 0.11 A**
50-60 cm	**0.55 ± 0.07 B**	**0.73 ± 0.04 A**	**0.7 ± 0.05 A**	**0.79 ± 0.08 A**
60-70 cm	0.59 ± 0.09	0.68 ± 0.05	0.76 ± 0.07	0.85 ± 0.07
70-80 cm	0.57 ± 0.08	0.77 ± 0.05	0.69 ± 0.04	0.84 ± 0.09
80-90 cm	0.63 ± 0.15	0.82 ± 0.06	0.71 ± 0.02	0.79 ± 0.09
90-100 cm	0.61 ± 0.09	0.79 ± 0.07	0.75 ± 0.05	0.74 ± 0.08
100-110 cm	0.86 ± 0.07	0.75 ± 0.04	0.67 ± 0.06	0.71 ± 0.09
110-120 cm	0.88 ± 0.12	0.85 ± 0.12	0.81 ± 0.07	0.87 ± 0.07
0-120	**0.6 ± 0.02 B**	**0.77 ± 0.02 A**	**0.73 ± 0.02 A**	**0.8 ± 0.04 A**
Soil depth	**N content (%) ^ *****			
	GIG	P12	P13	SC

0-10 cm	1.51 ± 0.08	1.18 ± 0.29	1.24 ± 0.15	1.32 ± 0.08
10-20 cm	**1.2 ± 0.08 B**	**1.08 ± 0.11 B**	**1.09 ± 0.08 B**	**1.44 ± 0.07 A**
20-30 cm	**1.05 ± 0.04 AB**	**0.86 ± 0.13 B**	**0.99 ± 0.06 AB**	**1.18 ± 0.08 A**
30-40 cm	1.06 ± 0.08	1.21 ± 0.39	1.06 ± 0.12	0.94 ± 0.1
40-50 cm	1.01 ± 0.08	0.95 ± 0.14	0.97 ± 0.15	0.97 ± 0.05
50-60 cm	**1.3 ± 0.12 A**	**0.64 ± 0.04 C**	**1.11 ± 0.15 AB**	**0.92 ± 0.06 BC**
60-70 cm	0.96 ± 0.24	1.01 ± 0.07	1.26 ± 0.16	0.95 ± 0.11
70-80 cm	1.01 ± 0.08	0.93 ± 0.17	1.16 ± 0.13	0.94 ± 0.06
80-90 cm	0.65 ± 0.14	1.04 ± 0.32	0.99 ± 0.17	1.08 ± 0.05
90-100 cm	1.21 ± 0.19	0.8 ± 0.04	1.29 ± 0.22	0.85 ± 0.13
100-110 cm	0.83 ± 0.1	1 ± 0.05	1.23 ± 0.34	0.86 ± 0.12
110-120 cm	0.93 ± 0.08	0.91 ± 0.09	1.32 ± 0.38	0.96 ± 0.08
0-120	**1.1 ± 0.03 AB**	**0.93 ± 0.07 B**	**1.07 ± 0.11 A**	**1.07 ± 0.05 AB**
Soil depth	**C content (%)**			
	GIG	P12	P13	SC
0-10 cm	42.55 ± 0.79	42.27 ± 0.61	43.95 ± 0.35	41.81 ± 0.52
10-20 cm	39.5 ± 1.07	43.84 ± 2.2	40.95 ± 1.54	42.63 ± 0.9
20-30 cm	38.17 ± 0.6	43.15 ± 0.99	42 ± 1.02	41.62 ± 1.11
30-40 cm	39.68 ± 1.11	42.84 ± 3.65	43.12 ± 1.01	40.67 ± 1.81
40-50 cm	41.21 ± 0.49	41.05 ± 1.49	43.97 ± 1.14	40.88 ± 1.69
50-60 cm	40.92 ± 0.63	43.59 ± 2.86	44.54 ± 1.84	41.75 ± 1.06
60-70 cm	42.09 ± 2.29	47.64 ± 1.25	44.29 ± 1.02	40.95 ± 1.25
70-80 cm	40.88 ± 1.28	43.09 ± 0.56	44.6 ± 1.31	42.57 ± 1.32
80-90 cm	44.18 ± 0.77	44.99 ± 7.01	43.17 ± 1.54	42.34 ± 1.59
90-100 cm	39.54 ± 0.99	48.99 ± 2.32	42.94 ± 0.69	41.67 ± 0.75
100-110 cm	42.27 ± 0.76	45.55 ± 0.25	42.78 ± 2.45	38.6 ± 0.67
110-120 cm	40.76 ± 1.19	43.43 ± 3.17	45.67 ± 2.4	39.57 ± 2
0-120	**40.87 ± 0.4 B**	**43.61 ± 0.97 A**	**42.82 ± 0.83 A**	**41.31 ± 0.44 B**
Soil depth	**C/N ratio ^ *****			

	GIG	P12	P13	SC
0-10 cm	28.79 ± 1.55	38.95 ± 5.12	36.41 ± 3.91	32.48 ± 1.78
10-20 cm	33.86 ± 2.57	41.06 ± 2.08	38.63 ± 4.08	30.19 ± 1.38
20-30 cm	**36.66 ± 1.34 B**	**52.79 ± 8.6 A**	**43.27 ± 3.02 AB**	**36.38 ± 3.14 B**
30-40 cm	38.85 ± 2.84	41.3 ± 8.66	42.85 ± 4.4	46.28 ± 5.32
40-50 cm	42.03 ± 3.64	45.55 ± 5.42	49.09 ± 5.83	42.73 ± 2.64
50-60 cm	**33.38 ± 3.55 B**	**68.94 ± 5.66 A**	**43.01 ± 5.11 B**	**46.18 ± 2.06 B**
60-70 cm	53.63 ± 14.14	47.61 ± 4.17	37.84 ± 4.35	46.74 ± 5.04
70-80 cm	41.18 ± 3.96	47.98 ± 8.3	40.25 ± 5.7	46.12 ± 3.15
80-90 cm	75.7 ± 17.69	50.1 ± 22.12	47.1 ± 5.21	39.84 ± 2.42
90-100 cm	35.97 ± 4.49	61.85 ± 6.22	38.69 ± 8.4	53.06 ± 9.5
100-110 cm	53.89 ± 7.48	45.98 ± 2.51	45.34 ± 10.25	48.57 ± 5.73
110-120 cm	45.57 ± 4.55	49.34 ± 7.97	41.81 ± 13.26	47.33 ± 6.4
0-120	**40.46 ± 0.78 B**	**50.46 ± 2.97 A**	**43.38 ± 3.58 B**	**41.72 ± 2.26 B**
Soil depth	**AMF colonization (%) ^**			
	GIG	P12	P13	SC
0-10 cm	36.53 ± 3.60	23.44 ± 3.37	39.92 ± 5.05	30.46 ± 2.79
10-20 cm	23.02 ± 5.12	25.14 ± 3.16	24.80 ± 4.90	28.39 ± 5.36
20-30 cm	NA	NA	NA	NA
30-40 cm	NA	NA	NA	NA
40-50 cm	NA	NA	NA	NA
50-60 cm	NA	NA	NA	NA
60-70 cm	NA	NA	NA	NA
70-80 cm	NA	NA	NA	NA
80-90 cm	NA	NA	NA	NA
90-100 cm	NA	NA	NA	NA
100-110 cm	NA	NA	NA	NA
110-120 cm	NA	NA	NA	NA
0-120	**NA**	**NA**	**NA**	**NA**

LITERATURE CITED

Addo-Danso SD, Defrenne CE, McCormack ML, Ostonen I, Addo-Danso A, Foli EG, Borden KA, Isaac ME, Prescott CE. 2020. Fine-root morphological trait variation in tropical forest ecosystems: an evidence synthesis. *Plant Ecology* 221(1): 1-13.

Andrade JL, Meinzer FC, Goldstein G, Schnitzer SA. 2005. Water uptake and transport in lianas and co-occurring trees of a seasonally dry tropical forest. *Trees-Structure and Function* 19(3): 282-289.

Aragao L, Malhi Y, Metcalfe DB, Silva-Espejo JE, Jimenez E, Navarrete D, Almeida S, Costa ACL, Salinas N, Phillips OL, et al. 2009. Above- and below-ground net primary productivity across ten Amazonian forests on contrasting soils. *Biogeosciences* 6(12): 2759-2778.

Bergmann J, Weigelt A, van der Plas F, Laughlin DC, Kuyper TW, Guerrero-Ramirez N, Valverde-Barrantes OJ, Bruelheide H, Freschet GT, Iversen CM, et al. 2020. The fungal collaboration gradient dominates the root economics space in plants. *Science Advances* 6(27): eaba3756.

Birouste M, Zamora-Ledezma E, Bossard C, Pérez-Ramos IM, Roumet C. 2014. Measurement of fine root tissue density: a comparison of three methods reveals the potential of root dry matter content. *Plant and Soil* 374(1-2): 299-313.

Bloom AJ, Chapin FS, Mooney HA. 1985. Resource limitation in plants - an economic analogy. *Annual Review of Ecology and Systematics* 16: 363-392.

Broek TAB, Ognibene TJ, McFarlane KJ, Moreland KC, Brown TA, Bench G. 2021. Conversion of the LLNL/CAMS 1 MV biological AMS system to a semi-automated natural abundance (14)C spectrometer: system optimization and performance evaluation. *Nucl Instrum Methods Phys Res B* 499: 124-132.

Cabugao KG, Yaffar D, Stenson N, Childs J, Phillips J, Mayes MA, Yang X, Weston DJ, Norby RJ. 2021. Bringing function to structure: Root–soil interactions shaping phosphatase activity throughout a soil profile in Puerto Rico. *Ecology and Evolution* 11(3): 1150-1164.

Chacon SS, Cusack DF, Khurram A, Bill M, Dietterich LH, Bouskill NJ. 2023. Divergent responses of soil microorganisms to throughfall exclusion across tropical forest soils driven by soil fertility and climate history. *Soil Biology and Biochemistry* 177.

Cheng W, Parton WJ, Gonzalez-Meler MA, Phillips R, Asao S, McNickle GG, Brzostek E, Jastrow JD. 2014. Synthesis and modeling perspectives of rhizosphere priming. *New Phytologist* 201(1): 31-44.

Comas LH, Becker SR, Cruz VV, Byrne PF, Dierig DA. 2013. Root traits contributing to plant productivity under drought. *Frontiers in Plant Science* 4: 16.

Condit R, Engelbrecht BM, Pino D, Perez R, Turner BL. 2013a. Species distributions in response to individual soil nutrients and seasonal drought across a community of tropical trees. *Proc Natl Acad Sci U S A* 110(13): 5064-5068.

Condit R, Engelbrecht BMJ, Pino D, Perez R, Turner BL. 2013b. Species distributions in response to individual soil nutrients and seasonal drought across a community of tropical trees. *Proceedings of the National Academy of Sciences of the United States of America* 110(13): 5064-5068.

Cordeiro AL, Norby RJ, Andersen KM, Valverde-Barrantes O, Fuchslueger L, Oblitas E, Hartley IP, Iversen CM, Gonçalves NB, Takeshi B, et al. 2020. Fine-root dynamics vary with soil

depth and precipitation in a low-nutrient tropical forest in the Central Amazonia. *Plant-Environment Interactions* 1(1): 3-16.

Cusack D, Ashdown D, Dietterich L, Neupane A, Ciochina M, Turner B. 2019. Seasonal changes in soil respiration linked to soil moisture and phosphorus availability along a tropical rainfall gradient. *Biogeochemistry* 145: 235-254.

Cusack D, Dietterich L, Valdes E 2023. Data set: Tropical Tree Species Identity and Diameter at Breast Height in a Throughfall-Reduction Drying Experiment in Four Lowland Panamanian Forests; Grant: Consequences of Plant Nutrient Uptake for Soil Carbon Stabilization.In Energy DO. *Environmental System Science - Data Infrastructure for a Virtual Ecosystem (ESS-DIVE) Repository*. https://data.ess-dive.lbl.gov/datasets/doi:10.15485/1960043.

Cusack D, Markesteijn L, Condit R, Lewis O, Turner B. 2018. Soil carbon stocks in tropical forests of Panama regulated by base cation effects on fine roots. *Biogeochemistry* 137(1-2): 253-266.

Cusack DF, Addo-Danso SD, Agee EA, Andersen KM, Arnaud M, Batterman SA, Brearley FQ, Ciochina MI, Cordeiro AL, Dallstream C, et al. 2021. Tradeoffs and Synergies in Tropical Forest Root Traits and Dynamics for Nutrient and Water Acquisition: Field and Modeling Advances. *Frontiers in Forests and Global Change* 4.

Cusack DF, Ashdown D, Dietterich LH, Neupane A, Ciochina M, Turner BL. 2019. Seasonal changes in soil respiration linked to soil moisture and phosphorus availability along a tropical rainfall gradient. *Biogeochemistry* 145(3): 235-254.

Cusack DF, Christoffersen B, Smith-Martin CM, Andersen KM, Cordeiro AL, Fleischer K, Wright SJ, Guerrero-Ramirez NR, Lugli LF, McCulloch LA, et al. 2024. Toward a coordinated understanding of hydro-biogeochemical root functions in tropical forests for application in vegetation models. *New Phytol*.

Cusack DF, Dietterich L, Sulman BN. 2023. Soil Respiration Responses to Throughfall Exclusion Are Decoupled From Changes in Soil Moisture for Four Tropical Forests, Suggesting Processes for Ecosystem Models. *Global Biogeochemical Cycles* 37: e2022GB007473.

Cusack DF, Turner BL. 2020. Fine Root and Soil Organic Carbon Depth Distributions are Inversely Related Across Fertility and Rainfall Gradients in Lowland Tropical Forests. *Ecosystems* 24(5): 1075-1092.

Dallstream C, Weemstra M, Soper FM. 2023. A framework for fine-root trait syndromes: syndrome coexistence may support phosphorus partitioning in tropical forests. *Oikos* 2023(1).

Diaz S, Kattge J, Cornelissen JH, Wright IJ, Lavorel S, Dray S, Reu B, Kleyer M, Wirth C, Prentice IC, et al. 2016. The global spectrum of plant form and function. *Nature* 529(7585): 167-171.

Dietterich LH, Bouskill NJ, Brown M, Castro B, Chacon SS, Colburn L, Cordeiro AL, Garcia EH, Gordon AA, Gordon E, et al. 2022. Effects of experimental and seasonal drying on soil microbial biomass and nutrient cycling in four lowland tropical forests. *Biogeochemistry* 161(2): 227-250.

Dijkstra FA, Zhu B, Cheng W. 2021. Root effects on soil organic carbon: a double-edged sword. *New Phytol* 230(1): 60-65.

Eissenstat DM, Kucharski JM, Zadworny M, Adams TS, Koide RT. 2015. Linking root traits to nutrient foraging in arbuscular mycorrhizal trees in a temperate forest. *New Phytologist* 208(1): 114-124.

Engelbrecht BMJ, Comita LS, Condit R, Kursar TA, Tyree MT, Turner BL, Hubbell SP. 2007. Drought sensitivity shapes species distribution patterns in tropical forests. *Nature* 447(7140): 80-U82.

Fan Y, Miguez-Macho G, Jobbagy EG, Jackson RB, Otero-Casal C. 2017. Hydrologic regulation of plant rooting depth. *Proceedings of the National Academy of Sciences of the United States of America* 114(40): 10572-10577.

Fantozzi D, Montagnoli A, Trupiano D, Di Martino P, Scippa GS, Agosto G, Chiatante D, Sferra G. 2024. A systematic review of studies on fine and coarse root traits measurement: towards the enhancement of urban forests monitoring and management. *Frontiers in Forests and Global Change* 7.

FAO. 2012. Global Ecological Zones for FAO Forest Reporting: 2010 Update. Forest Resources Assessment Working Paper Rome: Food and Agriculture Organication of the United Nations.

Field CB, Behrenfeld MJ, Randerson JT, Falkowski P. 1998. Primary production of the biosphere: Integrating terrestrial and oceanic components. *Science* 281(5374): 237-240.

Fontaine S, Bardoux G, Abbadie L, Mariotti A. 2004. Carbon input to soil may decrease soil carbon content. *Ecology Letters* 7(4): 314-320.

Freschet GT, Pages L, Iversen CM, Comas LH, Rewald B, Roumet C, Klimesova J, Zadworny M, Poorter H, Postma JA, et al. 2021a. A starting guide to root ecology: strengthening ecological concepts and standardising root classification, sampling, processing and trait measurements. *New Phytol* 232(3): 973-1122.

Freschet GT, Roumet C, Comas LH, Weemstra M, Bengough AG, Rewald B, Bardgett RD, De Deyn GB, Johnson D, Klimesova J, et al. 2021b. Root traits as drivers of plant and ecosystem functioning: current understanding, pitfalls and future research needs. *New Phytol* 232(3): 1123-1158.

Gaudinski JB, Torn MS, Riley WJ, Dawson TE, Joslin JD, Majdi H. 2010. Measuring and modeling the spectrum of fine-root turnover times in three forests using isotopes, minirhizotrons, and the Radix model. *Global Biogeochemical Cycles* 24(3): GB3029.

Giovannetti M, Mosse B. 1980. An Evaluation of Techniques for Measuring Vesicular Arbuscular Mycorrhizal Infection in Roots. *New Phytologist* 84(3): 489-500.

Guo D, Xia M, Wei X, Chang W, Liu Y, Wang Z. 2008. Anatomical traits associated with absorption and mycorrhizal colonization are linked to root branch order in twenty-three Chinese temperate tree species. *New Phytologist* 180(3): 673-683.

Hengl T, Mendes de Jesus J, Heuvelink GB, Ruiperez Gonzalez M, Kilibarda M, Blagotic A, Shangguan W, Wright MN, Geng X, Bauer-Marschallinger B, et al. 2017. SoilGrids250m: Global gridded soil information based on machine learning. *Plos One* 12(2): e0169748.

Hodge A. 2004. The plastic plant: root responses to heterogeneous supplies of nutrients. *New Phytologist* 162(1): 9-24.

Holdridge L, Grenke W, Hatheway W, Liang T, Tosi J. 1971. *Forest environments in tropical life zones*. New York: Pergamon Press.

Huaraca Huasco W, Riutta T, Girardin CAJ, Hancco Pacha F, Puma Vilca BL, Moore S, Rifai SW, del Aguila-Pasquel J, Araujo Murakami A, Freitag R, et al. 2021. Fine root dynamics across pantropical rainforest ecosystems. *Global Change Biology* 27(15): 3657-3680.

Ibrahim F, Adu-Bredu S, Addo-Danso SD, Duah-Gyamfi A, Manu EA, Malhi Y. 2020. Patterns and controls on fine-root dynamics along a rainfall gradient in Ghana. *Trees-Structure and Function* 34(4): 917-929.

INVAM ICoVAMF. 2023. Staining of Mycorrhizal Roots.
Jackson RB, Canadell J, Ehleringer JR, Mooney HA, Sala OE, Schulze ED. 1996. A global analysis of root distributions for terrestrial biomes. *Oecologia* 108(3): 389-411.
Jackson RB, Lajtha K, Crow SE, Hugelius G, Kramer MG, Piñeiro G. 2017. The Ecology of Soil Carbon: Pools, Vulnerabilities, and Biotic and Abiotic Controls. *Annual Review of Ecology, Evolution, and Systematics* 48(1): 419-445.
Jackson RB, Schenk HJ, Jobbagy EG, Canadell J, Colello GD, Dickinson RE, Field CB, Friedlingstein P, Heimann M, Hibbard K, et al. 2000. Belowground consequences of vegetation change and their treatment in models. *Ecological Applications* 10(2): 470-483.
Jobbagy EG, Jackson RB. 2000. The vertical distribution of soil organic carbon and its relation to climate and vegetation. *Ecological Applications* 10(2): 423-436.
Kong D, Ma C, Zhang Q, Li L, Chen X, Zeng H, Guo D. 2014. Leading dimensions in absorptive root trait variation across 96 subtropical forest species. *New Phytol* 203(3): 863-872.
Koske RE, Gemma JN. 1989. A MODIFIED PROCEDURE FOR STAINING ROOTS TO DETECT VA-MYCORRHIZAS. *Mycological Research* 92: 486-505.
Kramer-Walter KR, Bellingham PJ, Millar TR, Smissen RD, Richardson SJ, Laughlin DC, Mommer L. 2016. Root traits are multidimensional: specific root length is independent from root tissue density and the plant economic spectrum. *Journal of Ecology* 104(5): 1299-1310.
Laughlin DC, Mommer L, Sabatini FM, Bruelheide H, Kuyper TW, McCormack ML, Bergmann J, Freschet GT, Guerrero-Ramirez NR, Iversen CM, et al. 2021. Root traits explain plant species distributions along climatic gradients yet challenge the nature of ecological tradeoffs. *Nature Ecology & Evolution* 5(8): 1123-+.
Lugli LF, Andersen KM, Aragao L, Cordeiro AL, Cunha HKV, Fuchslueger L, Meir P, Mercado LM, Oblitas E, Quesada CA, et al. 2020. Multiple phosphorus acquisition strategies adopted by fine roots in low-fertility soils in Central Amazonia. *Plant and Soil* 450(1-2): 49-63.
Lugli LF, Rosa JS, Andersen KM, Di Ponzio R, Almeida RV, Pires M, Cordeiro AL, Cunha HFV, Martins NP, Assis RL, et al. 2021. Rapid responses of root traits and productivity to phosphorus and cation additions in a tropical lowland forest in Amazonia. *New Phytol* 230(1): 116-128.
Ma Z, Guo D, Xu X, Lu M, Bardgett RD, Eissenstat DM, McCormack ML, Hedin LO. 2018. Evolutionary history resolves global organization of root functional traits. *Nature*.
Malhi Y, Doughty C, Galbraith D. 2011. The allocation of ecosystem net primary productivity in tropical forests. *Philos Trans R Soc Lond B Biol Sci* 366(1582): 3225-3245.
Maurice J, Laclau J-P, Scorzoni Re D, de Moraes Goncalves JL, Nouvellon Y, Bouillet J-P, Stape JL, Ranger J, Behiing M, Chopart J-L. 2010. Fine root isotropy in Eucalyptus grandis plantations. Towards the prediction of root length densities from root counts on trench walls. *Plant and Soil* 334(1-2): 261-275.
McCormack ML, Adams TS, Smithwick EAH, Eissenstat DM. 2012. Predicting fine root lifespan from plant functional traits in temperate trees. *New Phytologist* 195(4): 823-831.
McCormack ML, Dickie IA, Eissenstat DM, Fahey TJ, Fernandez CW, Guo D, Helmisaari H-S, Hobbie EA, Iversen CM, Jackson RB, et al. 2015. Redefining fine roots improves understanding of below-ground contributions to terrestrial biosphere processes. *New Phytologist* 207(3): 505-518.

McCormack ML, Iversen CM. 2019. Physical and Functional Constraints on Viable Belowground Acquisition Strategies. *Frontiers in Plant Science* 10: 12.

McGuire KL, Fierer N, Bateman C, Treseder KK, Turner BL. 2012. Fungal community composition in neotropical rain forests: the influence of tree diversity and precipitation. *Microb Ecol* 63(4): 804-812.

Meinzer FC, Andrade JL, Goldstein G, Holbrook NM, Cavelier J, Wright SJ. 1999. Partitioning of soil water among canopy trees in a seasonally dry tropical forest. *Oecologia* 121(3): 293-301.

Metcalfe DB, Meir P, Aragao L, da Costa ACL, Braga AP, Goncalves PHL, Silva JD, de Almeida SS, Dawson LA, Malhi Y, et al. 2008. The effects of water availability on root growth and morphology in an Amazon rainforest. *Plant and Soil* 311(1-2): 189-199.

Nasto MK, Alvarez-Clare S, Lekberg Y, Sullivan BW, Townsend AR, Cleveland CC. 2014. Interactions among nitrogen fixation and soil phosphorus acquisition strategies in lowland tropical rain forests. *Ecology Letters* 17(10): 1282-1289.

Norby RJ, Ledford J, Reilly CD, Miller NE, O'Neill EG. 2004. Fine-root production dominates response of a deciduous forest to atmospheric CO2 enrichment. *Proceedings of the National Academy of Sciences of the United States of America* 101(26): 9689-9693.

Nottingham AT, Griffiths H, Chamberlain PM, Stott AW, Tanner EVJ. 2009. Soil priming by sugar and leaf-litter substrates: A link to microbial groups. *Applied Soil Ecology* 42(3): 183-190.

Ostonen I, Püttsepp Ü, Biel C, Alberton O, Bakker MR, Lõhmus K, Majdi H, Metcalfe D, Olsthoorn AFM, Pronk A, et al. 2007. Specific root length as an indicator of environmental change. *Plant Biosystems* 141(3): 426-442.

Paton S. 2023a. Meteorological and hydrological summary for Barro Colorado Island. *Smithsonian Tropical Research Institute*: 42.

Paton S 2023b. Meteorological and hydrological summary for the San Lorenzo/Fort Sherman canopy crane: Panama: Smithsonian Tropical Research Institute. Retrieved from https ….

Poirier V, Roumet C, Munson AD. 2018. The root of the matter: Linking root traits and soil organic matter stabilization processes. *Soil Biology and Biochemistry* 120: 246-259.

Prieto I, Roumet C, Cardinael R, Dupraz C, Jourdan C, Kim JH, Maeght JL, Mao Z, Pierret A, Portillo N, et al. 2015. Root functional parameters along a land-use gradient: evidence of a community-level economics spectrum. *Journal of Ecology* 103(2): 361-373.

Pyke CR, Condit R, Aguilar S, Lao S. 2001. Floristic composition across a climatic gradient in a neotropical lowland forest. *Journal of Vegetation Science* 12(4): 553-566.

Quesada CA, Paz C, Oblitas Mendoza E, Phillips OL, Saiz G, Lloyd J. 2020. Variations in soil chemical and physical properties explain basin-wide Amazon forest soil carbon concentrations. *Soil* 6(1): 53-88.

Rasse DP, Rumpel C, Dignac MF. 2005. Is soil carbon mostly root carbon? Mechanisms for a specific stabilisation. *Plant and Soil* 269(1-2): 341-356.

Reich PB. 2014. The world-wide 'fast-slow' plant economics spectrum: a traits manifesto. *Journal of Ecology* 102(2): 275-301.

Reimer RW, Brown, Reimer PJ. 2004. Discussion: Reporting and Calibration of Post-Bomb14C Data. *Radiocarbon* 46: 1299-1304.

Reimer RW, Reimer PJ 2024. CALIBomb.

Sarai S-S, De Jong BHJ, Esperanza H-L, Jorge M-V, Danilo M-R, Aryal DR. 2022. Fine root biomass stocks but not the production and turnover rates vary with the age of tropical successional forests in Southern Mexico. *Rhizosphere* 21.

Spanner GC, Gimenez BO, Wright CL, Menezes VS, Newman BD, Collins AD, Jardine KJ, Negron-Juarez RI, Lima AJN, Rodrigues JR, et al. 2022. Dry Season Transpiration and Soil Water Dynamics in the Central Amazon. *Front Plant Sci* 13: 825097.

Stuiver M, Polach HA. 1977. Reporting of C-14 data. *Radiocarbon* 19(3): 355-363.

Throop HL, Lerdau MT. 2004. Effects of Nitrogen Deposition on Insect Herbivory: Implications for Community and Ecosystem Processes. *Ecosystems* 7(2).

Treseder KK, Allen MF. 2002. Direct nitrogen and phosphorus limitation of arbuscular mycorrhizal fungi: a model and field test. *New Phytol* 155(3): 507-515.

Trumbore S, Da Costa ES, Nepstad DC, De Camargo PB, Martinelli L, Ray D, Restom T, Silver W. 2006. Dynamics of fine root carbon in Amazonian tropical ecosystems and the contribution of roots to soil respiration. *Global Change Biology* 12(2): 217-229.

Turner BL, Brenes-Arguedas T, Condit R. 2018. Pervasive phosphorus limitation of tree species but not communities in tropical forests. *Nature* 555(7696): 367-+.

Turner BL, Engelbrecht BMJ. 2011. Soil organic phosphorus in lowland tropical rain forests. *Biogeochemistry* 103(1-3): 297-315.

Vogel JS, Southon JR, Nelson DE, Brown TA. 1984. Performance of catalytically condensed carbon for use in accelerator mass-spectrometry. *Nuclear Instruments & Methods in Physics Research Section B-Beam Interactions with Materials and Atoms* 5(2): 289-293.

Weemstra M, Kiorapostolou N, Ruijven J, Mommer L, Vries J, Sterck F, Weiser M. 2020. The role of fine-root mass, specific root length and life span in tree performance: A whole-tree exploration. *Functional Ecology* 34(3): 575-585.

Weemstra M, Mommer L, Visser EJW, van Ruijven J, Kuyper TW, Mohren GMJ, Sterck FJ. 2016. Towards a multidimensional root trait framework: a tree root review. *New Phytologist* 211(4): 1159-1169.

Weigelt A, Mommer L, Andraczek K, Iversen CM, Bergmann J, Bruelheide H, Fan Y, Freschet GT, Guerrero-Ramírez NR, Kattge J, et al. 2021. An integrated framework of plant form and function: the belowground perspective. *New Phytologist* 232(1): 42-59.

Windsor DM. 1990. Climate and moisture availability in a tropical forest, long term record for Barro Colorado Isalnd, Panama. *Smithsonian Contributions to Earth Science* 29(1-145).

Wright IJ, Reich PB, Westoby M, Ackerly DD, Baruch Z, Bongers F, Cavender-Bares J, Chapin T, Cornelissen JH, Diemer M, et al. 2004. The worldwide leaf economics spectrum. *Nature* 428(6985): 821-827.

Wu S, Fu W, Rillig MC, Chen B, Zhu YG, Huang L. 2023. Soil organic matter dynamics mediated by arbuscular mycorrhizal fungi - an updated conceptual framework. *New Phytol*.

Wurzburger N, Wright SJ. 2015. Fine-root responses to fertilization reveal multiple nutrient limitation in a lowland tropical forest. *Ecology* 96(8): 2137-2146.

Xia M, Valverde-Barrantes OJ, Suseela V, Blackwood CB, Tharayil N. 2021. Coordination between compound-specific chemistry and morphology in plant roots aligns with ancestral mycorrhizal association in woody angiosperms. *New Phytologist* 232(3): 1259-1271.

Yaffar D, Norby RJ. 2020. A historical and comparative review of 50 years of root data collection in Puerto RicoPalabras Clave. *Biotropica* 52(3): 563-576.

Yavitt JB, Wright SJ. 2001. Drought and irrigation effects on fine root dynamics in a tropical moist forest, Panama. *Biotropica* 33(3): 421-434.

CHAPTER 3: ROOT DYNAMICS RESPOND TO EXPERIMENTAL AND SEASONAL DRYING IN FOUR DISTINCT LOWLAND TROPICAL FORESTS

3.1 Summary

Tropical forests fine roots are the active interface between plants and soils, and also represent a primary input of carbon to long–term soil pools. Climatic drying, which is increasing in many tropical regions, is likely to shift root dynamics, with cascading effects on other ecosystem processes. To better understand these root responses to drying, we investigated the effects of experimental and seasonal drying on fine root productivity, mortality, stocks, turnover, morphology, chemistry and arbuscular mycorrhizal fungi (AMF) across various tropical forest sites in Panama and soil depths. We hypothesized that: H1) Chronic and seasonal drying decreases root production and stocks at the soil surface and increases at depth where soil moisture is greater; H2) Chronic and seasonal drying leads to changes in root morphology and symbionts association, with traits shifting toward greater resource acquisition per unit of biomass invested. H3) Drying effects on root dynamics, morphology and association with symbionts are greater in wetter forests because roots in these forests are less adapted to dry conditions. We used a drying experiment in four lowland seasonal forests that vary in soil fertility and rainfall. We collected root biomass and images during years 1–5 of the experiment. Experimental drying consistently reduced root stocks and productivity across the four forests to 1.2 m depths, with stronger effects in infertile versus fertile soils, but increased turnover with drying in a fertile forest. Seasonal trends showed peak productivity in surface soils during the early wet season, and higher productivity in deeper soils during the dry season, suggesting shifts in water acquisition strategies. The drying treatment had mixed effects on root morphology and chemistry, but generally increased fine root diameter and decreased root tissue density, together with increased AMF colonization with experimental drying.

Root stocks and productivity generally declined with depth. These results clearly indicate a strong effect of drying on tropical forest root dynamics and characteristics, which could alter plant resource acquisition and transfer of root carbon to soils.

3.2 Introduction

Fine roots represent the interface between plants and soils, and as such regulate all major biogeochemical cycles in tropical forests. They play a crucial role in the cycling of water, nutrients, and carbon (McCormack *et al.*, 2015) and are a primary input of fresh plant carbon (C) into soil C stocks (Rasse *et al.*, 2005). These root functions are likely responding to climate change in tropical forests (Comas *et al.*, 2013), which are undergoing chronic drying and increased drought events (Kharin *et al.*, 2007; Magrin *et al.*, 2014; Chadwick *et al.*, 2015; Tao *et al.*, 2022). Root changes can include shifts in production and mortality, biomass depth distributions, and morphological traits related to resource acquisition. There is still great uncertainty in how tropical roots will respond to the drying trends prevalent across tropical regions.

Experimental drying studies in tropical forests at the community level have presented root biomass, productivity and morphological responses to drying. For example, a recent review has presented variable results on the impact of drought on root biomass (Yaffar *et al.,* 2024). It showed that biomass generally decreased or did not change in response to drying with some of the divergence in results attributed to the different soil depths collected, duration and intensity of drought. In addition to root biomass, drying have been reported to affect root growth and morphology (Yaffar *et al.,* 2024) with some possible compensatory mechanisms on these changes. For example, in a throughfall experiment in Brazil, drier conditions decreased total fine root

growth at 30 cm depth (Metcalfe *et al.*, 2008). Notably, wet season root growth in drought–exposed plots exhibited a compensatory increase, suggesting an adaptive mechanism to counterbalance reduced annual growth. Also, in this same experiment, dry conditions led to an increase in specific root length and area indicating morphological changes likely to increase nutrients and water uptake with no extra carbon cost. Therefore, plants appear to be able to modify their structures in response to drying, but it is unclear if this happens in particular conditions and depths or it these responses are general across forests.

In addition to changes in biomass and morphology, plants may change their relationships with symbionts, and alter their nutrition status in response to drought. For example, a global meta–analysis with 460 field and greenhouse studies indicates that plants increase drought resistance when their roots are associated with arbuscular mycorrhizal fungi (AMF) colonization as this symbiosis can affect stomatal behavior and photosynthesis of host plants (Auge *et al.*, 2015). Regarding plant nutrition, there is only one greenhouse experiment in Brazil, showing that seedlings from native and invasive species showed reduced root potassium (K) concentrations under four months of drought but there were no significant differences for phosphorus (P) and nitrogen (N) root content (Barros *et al.*, 2020). Although plant nutrition responses, and changes in AMF colonization appear to be important parameters to investigate in response to drying, there is no current study showing in situ responses in the tropics.

Generally, root dynamics, except biomass, are usually investigated at depths to no more than 30 cm. However, at humid forests, rooting depth appear to be a major factor contributing to water acquisition (Nepstad *et al.*, 1994; Cusack *et al.*, 2021) and can vary across different environments. For example, a survey of root biomass for 62 tropical tree seedlings showed generally shallower, more lateral rooting structures in wetter versus more seasonal forests

(Markesteijn & Poorter, 2009). Also, across a rainfall and fertility gradient in Panama, although fertile tropical forests presented less fine root biomass at the soil surface, they presented a larger root distribution at deeper soil layers when compared to infertile forests (Cusack & Turner, 2020) which can play an important role on plant water balance. The shallower rooting structure is likely to make root biomass in wetter and infertile forests more vulnerable to decreased soil moisture than deeper roots in seasonal or fertile tropical forests. For example, during the 1998 El Niño drought, sapling species with shallow roots experienced more water stress and more mortality in a tropical forest in Borneo (Cao, 2000). On the other hand, species with shallow roots and more surface root biomass might recover faster after drought as they have first access to rainfall (Cao, 2000). Therefore, analyzing not only biomass, but also root dynamics responses at deeper soil layers and in different tropical forests may be crucial to understand forests vulnerability do drying.

This study utilized an ongoing chronic drying experiment, Panama Rainforest Changes with Experimental Drying (PARCHED), in four seasonal lowland forests across a natural rainfall gradient and with variation in soil fertility. The overall hypothesis of this study was that drying shifts root characteristics toward greater resource acquisition, including changes in biomass, morphological traits, and depth distributions. Specifically, We hypothesized: H1) Chronic and seasonal drying decrease root production and stocks at the soil surface and increase these at depth where soil moisture remains higher; H2) Chronic and seasonal drying lead to changes in root morphology and symbiotic associations, with root shifting toward greater resource acquisition traits such as higher SRL and AMF colonization rates; H3) Drying effects on root dynamics, morphology, and symbiotic associations are greater in wetter versus drier tropical forests because of less adapted to dry conditions. We also predicted that roots in more fertile forest soils would be more resilient to drying because of overall higher resource conditions. We analyzed root

productivity, mortality, and turnover during wet and dry seasons using sequential coring, root ingrowth cores, and minirhizotron images in 10–cm increments to 110 cm depths over years 2 to 4 of chronic drying.

3.3 Methods

Study sites

This study was conducted across a natural rainfall gradient with variation in soil fertility on the Isthmus of Panama. The forests are classified as tropical moist forests (Holdridge *et al.*, 1971) with a mean annual temperature of 26°C (Windsor, 1990). The region presents a rainfall gradient of ~1,750 mm $year^{-1}$ MAP on the Pacific coast, with longer dry season (~150 days) to ~4,000 mm $year^{-1}$ MAP on the Caribbean coast with shorter dry seasons (~ 115 days) (Pyke *et al.*, 2001; Engelbrecht *et al.*, 2007). Also, across this region there is more than a 250–fold variation in soil extractable phosphorus (P) and base cations (Turner & Engelbrecht, 2011; Turner *et al.*, 2018; Cusack *et al.*, 2023). The Isthmus of Panama features a wide range of soil weathering statuses and fertility levels (Condit *et al.,* 2013; Cusack *et al.,* 2018; Turner & Engelbrecht, 2011; Turner *et al.,* 2018). Nutrients derived from rocks (such as phosphorus and base cations) are primarily related to geological substrates and are not directly influenced by rainfall (Pyke *et al.,* 2001; Stewart *et al.,* 1980; Turner & Engelbrecht, 2011). This allowed the selection of forests where rainfall varies independently from soil fertility.

Tree species composition change across the gradient, and are influenced by the species affinities for moisture and P (Engelbrecht *et al.*, 2007; Condit *et al.*, 2013; Turner *et al.*, 2018). However, aboveground biomass does not vary significantly among sites or according to rainfall or

soil fertility (Pyke *et al.*, 2001; Cusack *et al.*, 2018). Other site characteristics, including aboveground biomass, MAP, root biomass, soil C stocks, soil nutrients, and other soil properties, have been described for the ~50 long-term 1-ha plots in more details in other studies (Engelbrecht *et al.*, 2007; Condit *et al.*, 2013; Cusack *et al.*, 2018; Cusack & Turner, 2020).

For the present study, we used a subset of four forests from the ~50 long–term 1–ha forest dynamics plots maintained by the Smithsonian Tropical Research Institute across the rainfall and fertility gradient (Cusack *et al.*, 2018) (Figure 3.1). Our sites represent a subset of the variation across the Isthmus of Panama with 10 – fold variation in resin P and 24 – fold variation in base cations to 1 – m depth and sites receiving between 2,350 and 3,400 mm of annual rainfall. Our sites also represent a subset of the global variation of moist and wet tropical forests that span a range of 2,000 to >8,000 mm of MAP (Holdridge *et al.,* 1971) and more than 50% of tropical forests occur on the two most strongly weathered soil orders in USDA soil taxonomy: Ultisols and Oxisols (Holzman, 2008), represented by three of our sites. The remaining tropical forests grow on a wide range of soil types that are less weathered and more fertile in P and bases (e.g., Alfisols, Mollisols), but where N is typically more scarce (Sayer &Banin, 2016; Fujii *et al.,* 2018; Turner & Engelbrecht, 2011; Cusack et al., 2018; Quesada et al., 2020). Our forest sites include: Gigante Peninsula (GIG, 2350 MAP, infertile, Oxisol), plot 12 (2600 MAP, infertile, Ultisol), plot 13 (P13, 2600 MAP, fertile, Alfisol), and Sherman Crane (SC, a.k.a. San Lorenzo, 3421 MAP, infertile, Oxisol) (Table 3.1, Figure 3.1). The four sites are situated at low elevations and consist of mature forests. These areas exhibit significant species turnover and host a limited number of common tree species (Cusack *et al.*, 2023).

We separated seasons into four periods based on prior work showing distinct shifts in soil respiration rates and soil moisture from dry to early wet season, and from early to mid and late wet season (Cusack *et al.*, 2023): dry season (20 December to 10 May), early wet season (11 May to 1 July), mid wet season (2 July to 10 October), and late wet season (11 October to 19 December). For the ingrowth core method, since there was an overlap of seasons within each period of collection that encompass 3 – 4 months, we classified seasons only in wet and dry. The ingrowth core periods of March – June 2018 and December–April 2019 were considered as dry periods. The other periods (June – September 2018; September – December 2018; April – August 2019; August – December 2019) were considered as wet ones. More information about the periods of collections from the different methods can be found in Table 3.2.

Throughfall exclusion experimental design

In the four sites from this study, we constructed four partial throughfall exclusion plots at each site that were paired with control plots (total plots=32, n=4). Each structure in drying plots excluded ~50% of rainfall from the forest floor. The structeres extended 12 m x 12 m over the 10 m x 10 m plot so that the structure extended 1 m beyond the plot edge in every direction to avoid edge effects. We also trenched the exclusion plots to a depth of 50 cm, lining the vertical trench walls with heavy-duty plastic, and backfilling the trenches. This design prevented plants within the exclusion plots from accessing water beyond the plot boundaries. The setup aimed to simulate a chronic drying scenario by redirecting throughfall away from each plot. We referred to this partial throughfall exclusion experiment as the PAnama Rainforest CHanges with Experimental Drying (PARCHED). We completed plot construction in 2018 on May 16 (P13), June 12 (P12), July 26 (SC), and December 3 (GIG). Every three weeks, leaf litter was cleared from the roofing and

redistributed evenly across the plots using broom heads attached to telescoping poles. The roofing laminates were regularly cleaned to prevent the accumulation of moss and mold. Additionally, any damage to the plots caused by fallen trees, branches, or large fruits was promptly repaired, with inspections and maintenance conducted monthly. Further information about these sites and partial throughfall exclusion construction details can be found in previous publications (Dietterich *et al.*, 2022; Cusack *et al.*, 2023). Also, baseline data showed that there were no differences in root biomass or morphology between treatments from soils collected before the throughfall exclusion treatment was installed.

Ingrowth core root productivity collection

New roots were collected using ingrowth cores (Metcalfe *et al.*, 2007). In each plot five ingrowth mesh traps 20 cm–deep by 5 cm–diameter were installed using 0.25–inch mesh (HDPE hardware cloth) and filled with root–free soil collected from outside of the plots at each site in 2018 and 2019 (Table 2). Soils were collected in the months prior to each installation, kept at ambient moisture in closed plastic bins, and hand–picked with tweezers to remove all visible roots. Ingrowth cores were installed in the center of each plot and distributed across the core area, avoiding ~2m near edges. Ingrowth cores were collected after 3 – 4 months from March 2018 to January 2020, representing the first and second years of the experiment. Harvested ingrowth cores were divided into depth intervals (0–10 and 10–20 cm) and stored in a 5°C fridge until processed. In total, GIG had two collections dates, SC had four collection dates, and P12 and P13 had six.

Sequential coring root stock collection

Total standing root stocks were collected using sequential coring from 0 – 10 cm and 10 –

20 cm depths. In each plot three 1.5 inch–diameter cores were taken every 3–4 months from September 2018 until January 2020, representing years 1 to 5 of the experiment. Cores were collected avoiding plot edges as above, and stored at 5° C until processed. Baseline samples were collected prior to construction of the treatment structures when minirhizotron tubes were installed (see below), using soils from the minirhizotron holes as baseline samples. These results are reported for live and dead fine root biomass, root morphology and root chemistry.

Soil and root processing for productivity and stocks

Soils samples from ingrowth cores and soil cores were washed through a 0.25mm mesh size sieve to remove mineral soil. Roots were then picked out from other debris by hand using tweezers. Paint brushes were used to gently clean any remaining soil from roots. Roots were separated into fine roots (< 2 mm in diameter) and coarse roots (> 2 mm in diameter) using a caliper. Live fine roots were then separated from dead fine roots based on visual and mechanical consistency: live roots are more turgid, not easily broken, and the cortex and periderm are not easily separated (Vogt, 1991). Live fine roots were scanned for morphological analysis (see below), and then dried at 60°C until constant weight to determine dry root mass (mg). Root productivity from ingrowth cores was calculated as dry mass of live or dead roots produced per day per dry soil weight for each depth interval. Root stocks from sequential coring were calculated as dry mass of live or dead root stocks per dry soil weight for each depth interval. Calculations of root dry mass per core volume were also performed and had the same patterns as per dry soil weight.

Root morphology

Live fine root samples from three ingrowth cores per plot and all three standing root stock cores for both depths per plot were scanned using the 9800XL plus – Microtek –TMA 1600II scanner at 600 dpi on Barro Colorado Island. All images were then analyzed using WinRHIZO (WinRHIZO Regular, Regent Instruments, Canada) at Colorado State University to determine specific root length (SRL), specific root area (SRA), root tissue density (RTD) and mean root diameter (Metcalfe *et al.*, 2008). SRL (cm / mg) was calculated as root length per dry mass; SRA (cm^2 / mg) as root surface area per dry mass; and RTD (mg / cm^3) as root dry mass per volume. Root morphology data from ingrowth cores were collected for 3 collection periods for P12 and P13 (Mar–Jun 2018, Jun–Sep 2018 and Apr–Aug 2019), and 1 collection period (Apr–Aug 2019) for GIG and SC. Root morphology data from sequential cores were collected for 3 collection dates (Sep-Dec 2018, Mar 2022 and Jul 2022) for all sites.

Minirhizotron

Fine root dynamics were measured using minirhizotrons (Johnson *et al.*, 2001). In 2017 – 2018, acrylic minirhizotron tubes with 5 cm inner diameter and 2 m length were installed in each of the 32 plots at approximately 120 cm depth and 45° angle using a hand auger (Norby *et al.*, 2004). Tubes were installed in September 2017 (P12), December 2017 (P13), February 2018 (SC), and October 2018 (GIG) near the center of each plot. Insertion angles were measured during and after installation. The aboveground outlet of each tube was covered with a fitted PVC cap, black foam, and an aluminum can to exclude light, rain, and protect from damage from animals. After ~ 1 year waiting period for initial disturbance of tube installation to subside (except for GIG), images were recorded every three weeks from February 2019 to March 2020 and from October 2021 to

October 2022, representing years 2 – 3 and 4 – 5 of the experiment. Images were collected with a RhizoSystems, LLC minirhizotron camera at 230 continuous viewing windows per tube (image size: 8.4 mm x 6.3 mm) at 96 dpi, with a total viewing area across the tube of 0.0122 m^2. Pictures were taken at the same position and direction for each time point to observe root dynamics down the soil profile over time. A total of 237,360 images were analyzed for the 32 tubes for 33 sample collection periods. All images were analyzed by the lead author using Rootfly software (http://www.plant-image-analysis.org/software/rootfly). The length and diameter of each fine root segment were measured, and the incremental growth, death, or disappearance between collection times was recorded. Root length production per minirhizotron window area per day (mm–root / m^2 – viewing area / day) and standing stock (m–root/m^2 – viewing area) were calculated for each sample date. Root mortality (mm / m^2 – viewing area / day) was considered when the entire root or a part of the root disappeared from one date to the other. Roots were not considered dead until they disappeared, so we conservatively equate "disappearance" with "mortality." Root standing stock, productivity, mortality, and turnover were aggregated by depth intervals (every 10 cm) to 120 cm depth.

Root turnover calculations

We used two methods to calculate fine root turnover, first with minirhizotron data, and second with root ingrowth core data. For minirhizotrons, we calculated annual fine root turnover with fine root productivity summed across the year (mm / m^2 /year) divided by peak root standing stock of root length (mm / m^2) which is the date of the maximum standing stock (Iversen, Ledford, & Norby, 2008). We also calculated fine root turnover across seasons with fine root productivity averaged across months in each season (mm / m^2 /month) divided by peak root standing stock of

root length (mm / m^2) from each season. Second, we calculated biomass turnover by dividing fine root biomass productivity from ingrowth cores (g root / kg dry soil /year) by fine root peak standing stock from sequential coring root biomass stock (g root / kg dry soil). Calculations for peak standing crop were taken from the same period that we had data for ingrowth cores (2018 – 2019). In this case, turnover was calculated for years 2018 and 2019 (for P12 and P13) and 2019 (for P12, P13 and SC).

Arbuscular mycorrhizal fungal colonization

Using split samples from our sequential root biomass stock cores (see above), we measured colonization rates for AMF. The root samples analyzed for AMF colonization included all four sites for the mid to late wet season of 2018 (September for P12, P13, and SC, and December for GIG), P12 for the dry season (April 2019), and SC for the early wet season (May 2019). We separated fine roots from soil by washing (see above) and stored them in plastic cassettes in tap water at 4 °C until staining. We cleared and stained roots using standard protocols modified for field–collected tropical roots (Giovannetti & Mosse, 1980; Koske & Gemma, 1989; INVAM, 2023). We cleared roots in 10% KOH at ~60 °C for ~7 d and bleached them in ~3% household H_2O_2 at room temperature for 30 – 60 minutes, checking frequently, until appropriately cleared. We then rinsed roots thoroughly in tap water, acidified them in 1% HCl for 30 – 60 minutes, and stained them with 0.05% trypan blue in 10:9:1 glycerol: deionized water: 1% HCl at ~60 °C for 30 – 60 minutes until appropriately stained, rinsed again in tap water, and stored in tap water at 4 °C until scoring was completed. We scored AMF colonization using the gridline–intersect method (Giovannetti & Mosse, 1980), and calculated plot–level colonization rates as the proportion of scorable intersections from a given plot and soil depth in which we observed AMF structures.

Root chemistry

Fine roots from 0 – 10 cm soil depth from ingrowth cores (Aug–Dec 2019 collection) and sequential coring (Oct/Nov 2021 and July 2022 collections) were analyzed for C, N, and P content. Root samples were dried in coin envelopes at 60°C until constant weight. Before chemical analyses, roots from all cores per plot for the same depth were pooled into one composite sample, cut with scissors into small fragments to homogenize, and shipped to Baylor University for analyses, where samples were redried for 24 hours and weighed into tin capsules. Fine root C and N content were measured simultaneously with a Thermo–Finnegan Flash 1200 elemental analyzer (ThermoQuest, Milan, Italy). For fine root total P content, samples were placed in 15 mL distilled water with 1.8 mL of a mixture of peroxodisulphate (30 g L)1 $K_2S_2O_8$), boric acid (50 g L)1 H_3BO_3) and sodium hydroxide (15 g L)1 NaOH), and then autoclaved (121 _C, 1 h) (Færøvig & Hessen, 2003). P content was estimated via colorimetry by the ascorbic acid–molybdate method on a Lachat 8500 flow–injection autoanalyzer with an ASX–520 autosampler (Hach Co., Loveland, Colorado). Both analyses were done at Baylor University in the CRASR Recharge Center Analytical Lab.

Statistical analysis

To assess changes in root dynamics over time, we used repeated measures multivariate analysis of variance (MANOVA) analysis with including treatment, site, depth, and time as factors. For time points, we used monthly imaging sessions for minirhizotron data (n = 28 periods), quarterly collections for sequential root coring (n = 12 periods), and three–month collection intervals for root ingrowth cores (n = 6 periods). To ensure balanced data with consistent session counts and depths across all minirhizotron tubes, we restricted our analyses to 28 collections, each

extending to a depth of 90 cm. Response variables for MANOVA were: 1) fine root productivity from the minirhizotron, 2) fine root productivity from root ingrowth cores, 3) fine root mortality from the minirhizotron, 4) root length stocks from the minirhizotron, 5) live and dead fine root biomass from sequential coring. We used 10–cm depth increments as well as summed or averaged values for whole–profile analyses.

All data were first assessed for normal distribution using goodness of fit Shapiro–Wilk test and diagnostic plots. Because of a large abundance of zero values in minirhizotron data across time, especially deep in the soil profile, these data were transformed to presence/absence data for initial MANOVA. Whole–profile summed and averaged data, sequential coring, ingrowth core, and root characteristics were generally acceptable as normally distributed. Cube root transformations were needed for fine root productivity, mortality and stock from minirhizotrons at the whole soil profile and at the soil surface (0-10 and 10-20 cm depth) (Table SI 15). Natural log transformations were needed for root morphology and from ingrowth core and sequential cores (see Table SI 16 and Table SI 18), but no transformations were needed for root chemistry.

When site, depth, treatment or time were a significant effect in the initial repeated measures MANOVA, we conducted post hoc tests assessing differences among years, seasons, treatments, sites, and depths using ANOVA or Tukey HSD means separation tests. We used transformed data for these analyses as above. When depth was significant in the initial model, we conducted subsequent ANOVA per depth increment (0 – 10, 10 – 20, 20 – 50 and 50 – 90 cm depth intervals). For the minirhizotron data, these analyses averaging by season and year (rather than each time point) did not have a large abundance of zero values, except at deeper soil layers. In these deeper layers, we used generalized linear models with presence/absence data and ANOVA models excluding zero values.

The subset of data for root morphology (3 periods from sequential coring and 3 periods from ingrowth core) and chemistry (2 periods from sequential coring and 1 period from ingrowth core) were analyzed using ANOVA, with site, depth, sampling date, and treatment as predictors of plot–scale average values, because there were not enough time points to merit repeated measures MANOVA. For the AMF colonization data, we used a generalized linear model with a logit link function to analyze the proportion of mycorrhizal colonization. This approach was chosen over a traditional linear model because the dependent variable in the study followed a binomial distribution, which violates the normality assumption. The logit link function was used, making it possible to model the odds of colonization as a function of the predictor variables, making sure that predicted values stay within a 0 to 1 range.

Statistical analyses were conducted using R studio (2023.03.0 Build 386, "Cherry Blossom") and JMP (SAS Institute, 2023). Means are given ± one standard error, and the significance level for all tests was $p < 0.05$ unless otherwise noted.

3.4 Results

The drying treatment was a significant effect for root productivity, mortality, stocks, and turnover for both minirhizotron, ingrowth, and sequential coring data, as were time, site, and depth. Overall, posthoc tests indicated that the drying treatment suppressed root productivity across different methods, with details below. In addition, treatment was significant for AMF colonization rates, root diameter, and RTD; site was significant for root chemistry and morphology; depth was significant for turnover from all methods, AMF colonization, and RTD; time was significant for root chemistry, AMF colonization, and root morphology. There were also numerous interactions among site, depth, treatment, and time, as described below. Repeated measures analyses showed

time was a significant predictor for all variables measured. Both year and season were significant aspects of the time effect (Table SI 15, Table SI 16 and Table SI 18). Details of results from post hoc analyses conducted after the repeated measures analyses, including season and year as main effects are presented below. All raw data are presented in Table SI 1 (minirhizotron), Table SI 2 (ingrowth core), Table SI 3 (sequential coring), Table SI 4 (AMF) and Table SI 5 (root chemistry).

3.4.1. Minirhizotron root data

Fine root productivity

Fine root productivity to 90 cm depths

Fine root length productivity to 90 cm depth across all depths from our data set ranged from 0 ± 0 to 116.84 ± 90.89 mm / m^2 /day over the study period (Table SI 2.6). Post–hoc tests revealed that season and year were significant components of time, as well as treatment, site, depth, and multiple interactions for predicting fine root productivity (Figure 3.3, Figure 3.4, Figure SI 2.1, Table SI 2.15). Fine root productivity decreased with depth. The site*depth interaction occurred because fertile sites had a larger productivity than infertile sites at deeper soil layers. The site*depth*season interaction occurred because fine root productivity decreased with depth for all sites across all seasons, except in the fertile site (P13) where productivity was more homogeneous across depths during the dry and late wet season.

Fine root productivity summed by profile

For fine root productivity summed across the soil profile to 90 cm, significant effects were

site, season, year, treatment*site, and site*year interactions for predicting fine root productivity (Table SI 2.15). Treatment had a marginally significant effect alone (p=0.08), as well as its significance in interactions. The whole–profile productivity was least in the driest site (GIG), followed by the wettest site (SC) with similarly high productivity at the two mid rainfall sites (P12 and P13). The highest rates of fine root productivity overall were in the early wet season, intermediate rates in the mid wet seasons, and the lowest rates were in the late wet season and dry season. The treatment*site interaction occurred because the drying treatment suppressed fine root productivity for the whole soil profile only in the wettest site (SC). Also, site differences were most prominent in the drying treatment with larger fine root productivity in treated plots of the fertile site (P13), intermediate in P12, and lower in GIG and SC but. The site*year interaction reveals that this differences among sites occurred only in the first year of manipulation (2019–2020).

Fine root length productivity within soil depths

Because of the numerous interactions of other factors with depth, we explored trends among different depths. For the 0 – 10 cm depth, significant effects were season and site for fine root productivity with no interactions (Figure 3.3, Figure 3.4, Figure SI 2.1, Table SI 2.15). There was larger fine root productivity in the wettest, infertile site (SC), intermediate in the mid rainfall sites (P12 and P13) and lower productivity in the drier site (GIG). Productivity was also smaller during the late wet season and dry season and was larger during the mid wet and early wet season this depth, following overall trends (above).

For the 10 – 20 cm depth, significant effects were treatment, season, site, and interactions for fine root productivity (Figure 3.3, Figure 3.4, Figure SI 2.1, Table SI 2.15). The drying

treatment decreased fine root productivity at this depth, similar to the overall patterns, and productivity was larger during the early wet season. There was larger fine root productivity at this depth in the infertile, intermediate rainfall site (P12) when compared to the other sites, and the interaction with year revealed that these differences only occurred in the second year of measurements (2021–2022). The treatment*site interaction revealed that drying treatment decreased productivity primarily in the wettest, infertile site (SC) for this depth.

For the 20 – 50 cm depth, a large abundance of zero values necessitated using presence–absence data. Site was the only significant effect for predicting fine root productivity at this depth (Figure 3.3, Figure 3.4, Figure SI 2.1, Table SI 2.15). Productivity was smaller in the wettest, infertile site (SC) and larger in all the other sites. A subsequent ANOVA test considering only the positive values of productivity and eliminating the zero values, showed that year was a significant effect of productivity with larger productivity during 2019-2020.

For the 50 – 90 cm depth, season was the only significant effect in the presence/absence analysis of fine root productivity (Figure 3.3, Figure 3.4, Figure SI 2.1, Figure SI 2.2, Table SI 2.15). Productivity was larger at this depth during the dry season, intermediate during early and mid–wet and smaller during the late wet season, showing an opposite pattern from surface root productivity over seasons. A subsequent ANOVA test eliminating the zero values, showed that site, year, treatment*site and treatment*year interactions were significant effects for productivity, such that productivity was larger in the fertile site and smaller in the other sites at this depth (Figure SI 2.3). The treatment*site interaction occurred because drying treatment suppressed root productivity driven by the wettest, infertile site (SC) in these deep soils.

Fine root mortality

Fine root length mortality to 90 cm depths

Fine root length mortality to 90 cm depth across all depths from our data set ranged from 0 ± 0 to 107.77 ± 81.28 mm / m^2 /day (Table SI 2.6). Post–hoc tests indicated that year and season were both important aspects of the time effect, as well as treatment, site, depth and interactions for predicting fine root mortality (Figure 3.5, Figure 3.6, Figure SI 2.4, Table SI 2.15). Fine root mortality decreased with depth across sites and had different treatment effects across depths, further explored below.

Fine root mortality summed by profile

For fine root mortality summed across the soil profile to 90 cm, significant effects were site, year, treatment*site, site*year and treatment*year (Table SI 2.15). Fine root mortality was overall lowest in the driest site (GIG), followed by the wettest site (SC), and intermediate in the two mid–rainfall sites. Drying decreased fine root mortality for the whole soil profile primarily in one of the mid rainfall sites (P12).

Fine root length mortality variation within depths

Because of the complex interactions with depth, we also assessed mortality within each depth separately. For the 0 – 10 cm depth, the significant effects were site, year, treatment*site and treatment*year interactions for fine root mortality (Figure 3.5, Figure 3.6, Figure SI 2.4, Table SI 2.15). Root mortality was lowest at GIG, followed by the two mid–rainfall sites, and highest at the wettest site (SC). The treatment*site interaction indicated that drying increased root mortality

primarily in P13 and SC. Also, the treatment*year interaction indicated that drying increased root mortality primarily in 2021–2022.

For the 10 – 20 cm depth, the significant effects were site, year, treatment*site, and other interactions for fine root mortality (Figure 3.5, Figure 3.6, Figure SI 2.4, Table SI 2.15). Contrary to the 0 – 10 cm depth, drying treatment decreased fine root mortality at 10 – 20 cm. Also, mortality was lowest at GIG, followed by SC, and highest at the two mid–rainfall sites. Drying decreased mortality primarily in P12 at this depth.

For the 20 – 50 cm depth, a large abundance of zero values necessitated using presence–absence data, and site and site*season were significant effects for fine root mortality at this depth (Figure 3.5, Figure 3.6, Figure SI 2.4, Table SI 2.15).

For the 50 – 90 cm depth, season was the only significant effect for presence/absence data of fine root mortality (Figure 3.5, Figure 3.6, Figure SI 2.4, Table SI 2.15). Mortality was larger during the dry season at this depth, intermediate during early and mid–wet and smaller during the late wet season. A subsequent ANOVA using the positive data indicated that site, year, treatment*site and treatment*year interactions were significant effects of mortality, with greater mortality in the fertile site (P13), and drying decreasing root mortality at this depth primarily in the wettest site (SC).

Fine root stocks

Fine root length stocks to 90 cm depths

Fine root peak length stocks to 90 cm depth across all depths from our data set ranged from 0 ± 0 to 14464.98 ± 4158.44 mm/m^2 (Table SI 2.6). Year (but not season) was a significant

component of the time effect for predicting root length stocks in the whole profile, as well as treatment, site and interactions (Figure 3.7, Figure 3.8, Figure SI 2.5, Table SI 2.15). Root stock generally decreased with depth across sites. The treatment*depth interaction indicated that drying led to a more pronounced suppression of root stocks at the soil surface, with fewer differences in deeper soils.

Fine root length stocks summed by profile

For fine root length stocks summed by soil profile, the significant effects were treatment, site, year, and interactions (Table SI 2.15). Drying generally suppressed fine root length stock. Root stocks were smaller in GIG and SC and larger in P12 and P13. The treatment*site interaction indicated that drying decreased fine root length stocks most strongly in the wettest site (SC).

Fine root length stock variation within depths

Because of extensive interactions with depth, we analyzed each depth separately, as for other minirhizotron data. For the 0 – 10 cm depth, the significant effects were treatment, year (but not season), site, and interactions among these factors (Figure 3.7, Figure 3.8, Figure SI 2.5, Table SI 2.15). The drying treatment suppressed fine root length stock, with some variation in the magnitude of the effect among sites between the two years. Root length stock also generally was lowest in the driest site (GIG), followed by the fertile site (P13), the wettest site (SC), and the largest biomass was in the infertile, mid–rainfall site.

For the 10 – 20 cm depth, the significant effects were treatment, site, and interactions with year (Figure 3.7, Figure 3.8, Figure SI 2.5, Table SI 2.15). Drying treatment suppressed root length stock, with some variation among sites and years. Also, it was lowest in the wettest site (SC),

followed by the fertile (P13) and driest site (GIG) and the largest biomass was in the infertile, mid-rainfall site (P12).

For the 20 – 50 cm depth, a large abundance of zero values necessitated using presence–absence data. There were no significant effects using presence/absence data, but available continuous data had significant effects of site, season, year, and interactions with treatment were significant effects for predicting root length stock (Figure 3.7, Figure 3.8, Figure SI 2.5, Table SI 2.15). Root stocks were smaller in SC and larger in the other sites at this depth. Lastly, root stocks were smaller during the early wet season, intermediate at late and mid wet season and larger during the dry season.

For the 50 – 90 cm depths, there was no significant effects using presence/absence data, but analyses with continuous positive data showed significant effects of treatment, site, season, year, and interactions (Figure 3.7, Figure 3.8, Figure SI 2.5, Table SI 2.15). Drying treatment decreased root stocks at this depth when there were roots present. Also root stock was smaller in GIG and SC, intermediate in P12 and larger in the fertile site (P13). Lastly, similarly as the 20 – 50 cm depth, root stocks were smaller during the early wet season, intermediate at late and mid wet season and larger during the dry season in these deeper layers.

Fine root turnover

Annual fine root turnover

Depth and the treatment*depth interaction predicted annual fine root turnover. The drying treatment overall increased fine root annual turnover, with some variation by depth. When

considering analysis by season, depth, season and year*season predicted seasonal fine root turnover with no drying treatment effects (Table SI 2.7, Figure SI 2.6). These two different analyses are further explored below.

Annual fine root turnover to 90 cm depths

Fine root annual turnover to 90 cm depth across our data set ranged from 0 ± 0 to 1.58 ± 0.26 $year^{-1}$ when summarizing across years (Table SI 2.7). Depth and treatment*depth were significant factors for predicting annual fine root turnover (Figure SI 2.6, Table SI 2.15). Turnover generally decreased with depth. The treatment*depth interaction occurred because fine root turnover was only significantly affected by the drying treatment at the soil surface where drying increased turnover.

Annual fine root turnover variation within depths

Also because of interactions with depth, we analyzed each depth separately, as for other minirhizotron data. For the 0 – 10 cm depth, the significant effects were treatment, site, treatment*site and site*year interactions for predicting annual fine root annual turnover (Figure SI 2.6, Table SI 2.15). The drying treatment increased root turnover. Also, the fertile site (P13) had the largest turnover, the wettest, infertile site (SC) had an intermediate and the drier, infertile sites (GIG, P12) had smaller turnover at this depth. The treatment*site interaction revealed that the drying treatment increased root turnover driven by the fertile site (P13). This interaction also revealed that root turnover in control plots was not different across sites. Differences in turnover across sites occurred only at the drying treatment plots.

For the 10 – 20 cm depth, there were no significant effects (Figure SI 4).

For the 20 – 50 cm depth, the site*year interaction was the only significant factor (Figure SI 2.6, Table SI 2.15). Turnover was lowest in the infertile, mid–rainfall site (P12), followed by the fertile site (P13) and the wettest site (SC), and the largest turnover was in the driest site (GIG).

For the 50 – 90 cm depth there were no significant effects (Figure SI 2.6).

Fine root turnover considering seasons

Seasonal fine root turnover to 90 cm depths

Seasonal fine root turnover to 90 cm depth across our data set ranged from 0 ± 0 to 0.34 ± 0.22 month^{-1} (Table SI 2.8). Depth, season, and year*season interaction were significant factor for predicting seasonal fine root turnover (Figure 3.9, Figure 3.10). Turnover decreased with depth and it was larger during the wet season. Since depth did not interact with any other factor, we did not proceed with analysis for each depth separately.

3.4.2. Ingrowth core root dynamics

Fine root biomass productivity to 20 cm depth across our data set ranged from 1.85 ± 0.60 to 17.12 ± 1.69 mg root / kg dry soil /day (Table SI 2.9). Fine root biomass mortality to 20 cm depth across our data set ranged from 0.02 ± 0.01 to 0.99 ± 0.23 mg root / kg dry soil / day (Table SI 2.9). The drying treatment generally suppressed fine root mortality with site interactions.

The drying treatment generally suppressed fine root biomass productivity and fine root biomass mortality with site interactions, also suppressing root length productivity in specific dates with site interaction. Depth was a significant effect for fine root biomass and length productivity

where productivity was always larger at the 0-10 cm depth compared to the 10-20 cm, but depth did not affect root biomass mortality. Site was also significant effects on fine root productivity and mortality and season only affected fine root productivity. There were also interactions among factors as described below.

Fine root biomass productivity

Across the six collection periods, the drying treatment, site, season, depth and interactions with season were significant predictors of fine root productivity from the mid-rainfall sites (Figure 3.11, Table SI 2.16). Fine root productivity declined with the drying treatment across all sites. P12 had larger fine root productivity when compared to P13; productivity was larger in the wet season when compared to the dry.

Across the four collection dates from three sites (P12, P13, and SC), the drying treatment, site, season, depth and interactions were significant predictors of root productivity (Figure 3.11, Table SI 2.16). Fine root productivity declined with the drying treatment. Productivity was larger in the wet season when compared to the dry. The interaction of treatment*site occurred because the drying treatment suppressed fine root productivity driven by the infertile sites (P12 and SC), but not at the fertile site (P13). Also, for the control plots, productivity was smaller in P13 and larger in P12 and SC, but no difference among sites in the drying plots. The site*season interaction occurred because productivity was larger during the wet season at P12 and P13 (with marginally significance in P13), but this pattern was reversed in the wettest site where productivity was larger during the dry season.

Across the two collection dates for which we had data for all four sites, date, site, treatment and depth were significant factors for predicting fine root productivity (Figure 3.11, Table SI 2.16).

The drying treatment decreased fine root productivity across all sites, except the fertile one (P13). For the control plots, productivity was smaller in P13 and GIG, intermediate in SC and larger in P12.

Fine root length productivity

Fine root scans at P12 and P13 across three dates showed that time, depth and site were significant factors for predicting total root length with no effect of the drying treatment and no interactions. P12 had larger root length than P13; and total root length was smallest in Mar–Jun 2018, intermediate in Jun–Sep 2018 and larger in Apr–Aug 2019.

For analyses with all sites for one date (Apr–Aug 2019) from ingrowth cores, depth, treatment, site and site*treatment interaction were significant factors for predicting total root length growth. The drying treatment declined root length growth driven by the most infertile sites (SC and GIG).

Fine root biomass mortality from ingrowth cores

For the three sites (P12, P13 and SC) and three collection dates, site and treatment were significant predictors of fine root mortality (Figure SI 2.7, Table SI 2.16). The drying treatment decreased fine root mortality. Also, for the control plots, mortality was smaller in P13 and larger in P12 and SC, but no difference among sites in the drying plots.

For one collection date across all four sites, only site was a significant predictor of fine root mortality. Also, there was a marginally significant effect of treatment ($p=0.05$) and treatment*site interaction ($p=0.05$) (Figure SI 2.7, Table SI 2.16). For the control plots, mortality was smaller in GIG, then P13, then P12 and was larger in SC, but no difference among sites in the drying plots.

Also, the marginally significant interaction of treatment*site occurred because the drying treatment decreased fine root mortality driven by the wettest infertile site (SC).

3.4.3. Sequential coring root stocks

Live fine root biomass stocks to 20 cm depth across our data set ranged from 0.45 ± 0.08 to 3.99 ± 0.52 g root / kg dry soil (Table SI 2.10). Dead fine root biomass stocks to 20 cm depth across our data set ranged from 0.45 ± 0.23 to 40.31 ± 32.09 mg root / kg dry soil (Table SI 2.10).

Drying decreased live fine root biomass and length stocks but did not affect dead fine root biomass.

Live fine root biomass

Site, depth, the drying treatment, and interactions were significant factors for predicting fine root biomass and total root length stocks from scans (Figure 3.12, Table SI 2.17). The drying treatment decreased fine root biomass and length stock from root scans. Root stocks were smaller in GIG, then P13 and larger in SC and P12. The treatment*site interaction revealed that the decrease of root stocks with the drying treatment were driven by the most infertile sites (GIG and SC). Also, fine root biomass and total fine root length stocks were larger at the soil surface (0 – 10 cm). Only for total fine root length, there was also an interaction of season*site with post hoc tests revealing that total fine root length was larger in the mid wet season driven by the driest, infertile site (GIG).

The baseline data showed that site and depth were significant factors affecting root biomass and total root length from scans but there was no effect of the drying treatment (Table SI 2.17).

Dead fine root biomass

Season, depth and year were significant predictors of dead fine root biomass (Figure SI 2.8, Table SI 2.17). Dead fine root biomass was larger at the soil surface (0 – 10 cm). It also varied across seasons being smaller during the early wet season, intermediate during late and mid wet season and being larger during the dry season.

The baseline data showed that site and depth were significant predictors of dead fine root biomass with no effect of the drying treatment.

3.4.4. Fine root biomass turnover

Fine root biomass turnover to 20 cm depth across our data set ranged from 0.50 ± 0.12 to 4.06 ± 2.70 $year^{-1}$ (Table SI 2.11). The drying treatment generally decreased root turnover.

For the two sites (P12 and P13) with two years of measurement, the drying treatment had a significant effect on fine root turnover. Contrary to results from minirhizotron, post hoc tests suggested that the drying treatment decreased surface root turnover (Table SI 2.11, Table SI 2.18). Sites, depth, and year were not significant factors predicting fine root turnover. When excluding two extreme outliers (turnover > 9) from year 2018, there was no significant effect of any factor on root turnover.

For the three sites (P12, P13 and SC) with one yar of measurement, the drying treatment had a significant effect on fine root turnover, decreasing it.

3.4.5. Fine root morphology

Live fine root morphology from ingrowth core

Fine root morphology from ingrowth cores to 20 cm depth across our data set ranged from 1.46 ± 0.26 to 5.30 ± 2.29 cm / mg for SRL, from 0.35 ± 0.03 to 0.57 ± 0.03 mm for root diameter and from 0.20 ± 0.02 to 0.52 ± 0.17 g / cm^3 for RTD (Table SI 2.12). The drying treatment generally decreased RTD, but not the other morphological traits.

For the two sites (P12 and P13) with three collection dates, site was the only significant factor affecting SRL. SRL was larger in P13. Collection date was the only significant factor affecting root diameter (Figure SI 2.9, Table SI 2.16). Root diameter was smaller in Apr–Aug 2019 (wet), intermediate in Jun–Sep 2018 (wet) and larger in Mar–Jun 2018 (dry). The drying treatment, site, site*time interaction were significant factors affecting RTD. The drying treatment decreased RTD and it was larger in the infertile site.

Across all four sites for one collection date, site was the only significant factor affecting SRL and diameter. The wettest site (SC) had the smallest SRL and largest diameter. Site, site*treatment and depth*site interactions were significant factors affecting RTD (Figure SI 2.9, Table SI 2.16). RTD was larger in the most infertile sites (GIG and SC). The interaction of site*treatment occurred because site differences occurred at the drying treatment; with no differences among sites in the control. The interaction of depth*site occurred because RTD was larger at the soil surface driven by the driest site (GIG).

Live fine root morphology from sequential coring

Fine root morphology to 20 cm depth across our data set ranged from 0.80 ± 0.12 to 5.50 ± 4.32 cm / mg for SRL, from 0.40 ± 0.01 to 0.81 ± 0.09 mm for root diameter and from 0.16 ± 0.02 to 1.09 ± 0.80 g / cm^3 for RTD (Table SI 2.12). The drying treatment generally increased root diameter with season interaction.

Site and season were significant predictors of SRL, root diameter and RTD and the interaction treatment*season was also a predictor of root diameter (Figure 3.13, Table SI 2.17). These traits were not affected by depth. There was a larger root diameter in the wettest site (SC), intermediate in P12 and lower in P13 and GIG; a larger RTD in GIG and a larger SRL in P13. For root diameter, the interaction of treatment*season occurred because the drying treatment increased fine root diameter during the late wet season (Sep–Dec 2018). RTD was larger while SRL and diameter were smaller in the late wet season (Sep–Dec 2018) when compared to mid wet (Jul–2022) and dry season (Mar–2022).

The baseline data showed that there was no significant effect of the drying treatment, depth or site on SRL. Diameter and RTD were only affected by site.

3.4.6. Live fine root AMF colonization

AMF colonization to 20 cm depth across our data set ranged from 12.13 ± 2.25 to 42.94 ± 10.73 % (Figure SI 2.10, Table SI 2.13). The drying treatment generally increased AMF colonization and there was greater AMF colonization in wet season than in dry season or transition.

Across all four sites in the wet season, the drying treatment, depth and interactions were significant effects for AMF colonization (Table 3.3, Table SI 2.19). The drying treatment increased AMF colonization rate and it was larger in the 0 – 10 soil depth. The site*treatment and site*treatment*depth interactions both appeared to be driven by the wettest, infertile (SC) site, in which the decline in AMF colonization with depth was reversed in the drying treatment plots (Table 3.3).

Considering SC samples collected in the wet season and dry–to–wet seasonal transition, the drying treatment increased AMF colonization (Table SI 2.19). Considering P12 samples

collected in both the wet and dry seasons, the drying treatment decreased AMF colonization contrasting with the increase in AMF colonization with the drying treatment when all sites were considered together in the wet season alone and in SC site during wet and dry season (Table SI 2.19). AMF colonization was larger during the wet season in both SC and P12.

3.4.7. Fine root chemistry

Live fine root chemistry from ingrowth core

Fine root chemistry to 10 cm depth across our data set ranged from 0.017 ± 0.001 to 0.022 ± 0.002 % for root %P; from 36.16 ± 2.17 to 45.31 ± 0.57 % for root %C; from 1.74 ± 0.09 to 2.12 ± 0.05 % for root %N; and from 18.47 ± 0.75 to 22.47 ± 1.34 for root C:N ratio (Table SI 2.14). The drying treatment did not affect root chemistry.

Site was a significant predictor of root %C and marginally significant predictor (p–value <0.1) of root %N, root %P and C/N ratio. Root %C was smaller in the fertile site (P13), intermediate in P12 and SC and larger in the drier, infertile site (GIG) (Figure SI 2.11, Table SI 2.16), but post hoc tests did not detect site differences for the other elements.

Live fine root chemistry from sequential coring

Fine root chemistry to 10 cm depth across our data set ranged from 0.018 ± 0.006 to 0.030 ± 0.002 % for root %P; from 40.23 ± 1.48 to 48.12 ± 0.79 % for root %C; from 1.24 ± 0.11 to 1.88 ± 0.26 % for root %N; and from 23.32 ± 0.21 to 38.80 ± 4.06 for root C:N ratio (Table SI 2.14). The drying treatment did not affect root chemistry.

Season predicted root %C; site predicted %N and C/N ratio and site*season predicted C/N

ratio (Figure SI 2.11, Table SI 2.17). Neither the drying treatment or site predicted root %P (Figure SI 2.11, Table SI 2.17). Root %C was larger in July 2022 (mid wet season) when compared to Oct/Nov 2021 (late wet season). Root %N was smaller in P12, intermediate in P13 and SC and larger in the drier site (GIG). GIG and SC presented smaller C/N ratios, P13 exhibited intermediate and P12 had the larger ratio. The interaction of site*season occurred because C:N ratio sites differences happened during the mid–wet season.

The baseline data showed that there was no significant effect of throughfall treatment or site on root %C, root %N and C/N ratio.

3.5 Discussion

Experimental drying effects on roots

Drying effects on tropical forest roots

Our study demonstrated that throughfall exclusion treatment generally suppressed fine root productivity and stocks consistently across the forests, with similar results from different methods. There were some site-specific, depth-specific, and seasonal interacting effects. Our findings align with other experimental drying studies at the soil surface, that also reported suppression of fine root productivity or stocks in pre-montane rainforest in Indonesia to 20 cm depth (Moser *et al.*, 2014), in a tropical rainforest in Southwest China to 10 cm depth (Zhou *et al.*, 2019), at an Amazon rainforest site in Brazil to 30 cm depth (Metcalfe *et al.*, 2008) and at a moist tropical Amazonian Forest to 1 m depth (Nepstad *et al.*, 2002; Davidson *et al.*, 2004). Although these two last studies did not report significance, they indicated decreased fine root biomass to 10 cm depth but similar

biomass at deeper layers (0.1 to 6.1 m) (Nepstad *et al.*, 2002; Davidson *et al.*, 2004). On the other hand, a study on dry forest tree plantations in Costa Rica showed no decrease in fine root productivity to 15 cm depth with drying (Vargas Gutiérrez *et al.*, 2023). The variation in responses suggest that drying can reduce biomass and productivity but may have variable impacts depending on forest type, experimental design, and drought severity. Our results contribute to this understanding by indicating that even within the same experiment, root system responses to drying are complex and site or depth specific.

Drying effects across depths

Our results also show interaction effects of drying with soil depth. For example, throughfall exclusion suppressed fine root length productivity at the soil surface across all forests using the minirhizotron method, did not affect length productivity at intermediate layers, and suppressed length productivity in deeper layers only in the wettest, infertile site (SC). These results suggest that experimental drying did not significantly impact deeper soil layers on most of our forests or that roots at these depths were more resilient to chronic drying. The suppressed root productivity in deeper soil layers at the wettest, infertile site also associated with decreased root stocks and decreased mortality may indicate that forests not used to longer drying periods (SC) may present lower resilience. Interestingly, this pattern is consistent with reduced soil respiration under throughfall exclusion, particularly in the wettest, infertile site (SC) (Cusack *et al.*, 2023). This may reflect reduced root activity and less CO_2 flux contributions from root respiration and microbial decomposition of root detritus (Davidson *et al.*, 2004). Therefore, the reduced root productivity at deeper soil layers in SC could have influenced the reduced soil respiration at this specific site.

Drying effects across forests with different fertility

Throughfall exclusion decreased surface fine root biomass productivity across all infertile forests but did not affect the fertile site (P13) in the second year of the experiment. Furthermore, the fertile site exhibited higher fine root productivity and stocks at deeper soil layers in drying plots, potentially delaying drying effects through drought avoidance or hydraulic lift (Oliveira *et al.*, 2005; Oliveira *et al.*, 2021). Another interesting pattern presented by the fertile site is that it did not show changes in microbial communities with drying, while the infertile forests converged to a common "drought microbiome" in response to experimental drying in this same experiment (Chacon *et al.*, 2023). Lastly, throughfall exclusion increased root turnover at the soil surface only in the fertile site. This may indicate that plants are trying to cope with the higher root mortality in response to drying by producing new roots, perhaps where water is more available at the soil surface. These results highlight the complementary nature of different root measurement methods and the site-specific responses to environmental conditions.

Symbiotic and morphological responses to experimental drying

Our results indicated that experimental drying did not significantly alter root morphological traits that are commonly associates with soil exploration (e.g., specific root length, SRL). Instead, plants increased symbiotic relationships with arbuscular mycorrhizal fungi (AMF), which is consistent with recent reviews highlighting AMF's role in promoting drought resilience (Kuyper & Jansa, 2023; Das & Sarkar, 2024). The observed increased fine root diameter and decreased root tissue density under experimental and seasonal drying in our experiment may optimize AMF habitat, supporting their colonization and increasing drought resilience (Brundrett, 2002; Kong *et al.*, 2014; Valverde-Barrantes *et al.*, 2016). These changes in root-AMF interactions could be a

way to optimize water acquisition from deeper or less accessible soil layers and from periods when water is more available, utilizing the AMF's ability to access these resources, but more research is needed to explore the mechanisms and how the symbiotic relationships may alter plant morphology.

Seasonal dynamics of fine roots

Seasonal tropical forest patterns

The seasonal patterns from our forests at the soil surface are a common pattern across tropical forests. Seasonal forests with longer dry seasons generally produce more roots during the wet season, while wetter forests with shorter dry seasons can also have large productivity during the dry season. This is similar to other studies in Panama, which found larger surface root productivity during the transition from dry to wet season marked by heavy rains or during the wet season (Cavelier *et al.*, 1999; Yavitt & Wright, 2001; Rodtassana & Tanner, 2018). Larger surface root productivity during wetter periods, especially after the dry season, has also been observed in other seasonal tropical forests (Green *et al.*, 2005; Espeleta & Clark, 2007; Cordeiro *et al.*, 2020). Therefore, seasonal forests with longer dry season in general produce more roots during the wet season, but wetter forests with shorter dry seasons can also have peaks of productivity during the dry season. This reversed pattern in the wettest site may be related to the fact that these soils can get often waterlogged (Cusack *et al.*, 2023). The results also align with results from peat swamp sites showing larger productivity during drier periods when the water table dropped below the surface (Sciumbata *et al.*, 2023). These patterns reveal different site responses to seasonal drying that may have important implications when interacting to long-term chronical drying.

Drying effects on nutrient availability

Patterns in root phenology are linked to plant resource acquisition strategies and C allocation which are relevant to understand when and where resources are being allocated. In Panamanian forests with similar mean annual precipitation as ours, peak litterfall production occurs during the dry season (Wright & Cornejo, 1990; Santiago & Mulkey, 2005), but litterfall production is more homogeneous in wetter forests (Santiago & Mulkey, 2005). During the dry season, nutrient accumulation was observed across our forests, although less seasonality was noted in the wettest site (Dietterich *et al.*, 2022). A study on seasonally dry tropical forests also found nutrient accumulation during dry seasons (Allen *et al.*, 2017). Thus, producing roots during the early wet season likely allows plants to benefit from greater water and nutrient uptake. The wettest site, however, may produce roots across different seasons when stressors like waterlogging are less available, and nutrients or water are more accessible.

Seasonal influence on root morphology and chemistry at the soil surface

Root morphology varied across collection periods, with sequential coring showing smaller RTD, larger SRL, and larger diameter during the dry and mid-wet seasons compared to the late wet season, revealing that root morphology may not follow a unidirectional pattern with seasonality. Younger roots from ingrowth cores were less responsive to seasonality, only showing an increase in diameter during the dry season similarly as the sequential coring method. Despite temporal variations, root morphology values remained within ranges reported for neotropical regions (Addo-Danso et al., 2020). Also, seasonal influences on root chemistry were noted such as larger %C in the mid wet season when compared to late wet season, highlighting the dynamic

nature of root chemical composition in response to temporal changes. Further research with more collection dates is needed to further investigate seasonal patterns in root morphology and chemistry.

Seasonal dynamics at deeper soil layers – shifts of function across depths

At deeper soil layers (50-90 cm), fine root productivity, mortality, and root stocks were larger during the dry season. Producing roots at these depths during drier periods may be advantageous as water may be available at those depths instead of at the surface. This shift in resource acquisition strategy from the surface to depth across tropical forests illustrates a change in root activity, from nutrient acquisition at the surface during wetter periods to water acquisition at depth during dry periods. Deep water acquisition during the dry season has been demonstrated in a Panama forest near our forests using natural abundance $\delta^{18}O$ measurements from xylem water, indicating trees accessed water from depths greater than 1 meter during the dry season (Meinzer *et al.*, 1999; Andrade *et al.*, 2005). These patterns indicate deeper fine roots are more likely formed primarily for water acquisition in these seasonal forests, since surface soils tend to dry out seasonally in these Panama forests (Nepstad *et al.*, 1994; Cusack *et al.*, 2019), and deep soil moisture are common in seasonal tropical forests (Fan *et al.*, 2017). Therefore, plants appear to shift from surface root activity during wet periods to deep root activity during dry periods.

Depth variation of root dynamics

Root dynamics presented overall depth variation consistent with other tropical forests, but our results revealed some site-specific differences in the magnitude of these changes with depth which is likely related to the variation in fertility and mean annual precipitation across our forests.

Root dynamics depth variation across tropical ecosystems

Our high-resolution assessment of root dynamics with minirhizotron cameras from 0 to 90 cm depth revealed similar patterns as observed in other tropical forests. Fine root productivity, mortality, stocks, and turnover decreased with depth across all forests which is consistent with other tropical forest studies in Panama (Cusack & Turner, 2020), Brazil (Cordeiro *et al.*, 2020), Puerto Rico (Yaffar & Norby, 2020; Cabugao *et al.*, 2021), and more broadly across terrestrial ecosystems (Jackson *et al.*, 1996). The slower turnover in deeper soil layers may be attributed to the reduced presence and activity of soil microorganisms (Taylor *et al.*, 2002) and the lower nutrient concentrations found at these depths (Cusack & Turner, 2020). These changes in root dynamics across depths and their variation across forests can change C fluxes from live roots to soils (Rasse *et al.*, 2005) which can impact soil C storage.

Site-specific depth variation

Productivity, mortality, and stocks revealed different patterns of decrease with depth across different forests. For example, root mortality decreased with depth across all forests, but the wettest infertile site (SC) had a more pronounced decrease due to lower stocks, mortality and productivity rates at deeper layers and generally large values at the soil surface. In the fertile site, the decrease in stocks and productivity with depth was more homogeneous, reflecting larger root productivity at deeper layers compared to other forests. This pattern aligns with findings from a Panamanian study, where fine root biomass distribution was more homogeneous in fertile forests, likely reflecting more uniform nutrient distribution across the soil profile (Cusack & Turner, 2020). This may indicate that while forests in fertile forests may rely on drought avoidance by roots

having access to water in deeper soil layers, forests in infertile soils may rely on drought resistance. This is especially alarming since forests that do not experience longer dry seasons such as the SC site, may not have specialized traits of drought resistance which may make them more vulnerable to long-term or more extreme drying.

Interaction of drying effects on roots

Similarly, experimental drying and seasonal drying both decreased root stocks, root productivity, and root tissue density (RTD) at the soil surface. Both drying types also led to an increase in root diameter at the soil surface. Conversely, experimental drying and seasonal drying led to different responses in the other measured variables. These findings highlight the complex and variable responses of root traits to different drying conditions across soil depths.

3.6 Conclusion

This chapter uncovered novel complexities in root responses to drying across different tropical forests, extending our previous understanding that plants alter their morphology to explore larger soil volumes to compensate for reduced growth and biomass. We now demonstrate that chronic drying not only decreases root growth and biomass but can increases arbuscular mycorrhizal fungi (AMF) colonization and alters root morphology in a way (larger diameter) that appear to predominantly support AMF functions rather than aiding plants in soil volume exploration by themselves. Additionally, root productivity and stocks were observed to be larger at deeper soil layers during the dry season, likely for water uptake. However, the suppression of these roots under chronic drying conditions may increase plant vulnerability. The study also indicates that fertile forests may possess some resilience to drying, as evidenced by their larger productivity at deeper

soil layers, which could be beneficial under drying conditions and did not show responses to chronic drying at some dates at the soil surface. The observed decrease in root stocks and productivity with drying might suggest a potential reduction in carbon inputs to the soil in tropical forests. Conversely, an increase in AMF colonization associated with drying could potentially enhance carbon inputs to the soil. These impacts on soil carbon storage warrant further investigation. The first hypothesis that chronic and seasonal drying decrease root production and stocks at the soil surface and increase these at depth where soil moisture is greater was partially supported. In support of the hypothesis, chronic drying generally decreased root productivity and stocks at surface. Also in support, seasonal drying decreased productivity (except in the wettest site), but seasonal drying did not change root stocks as hypothesized. Also contrary to the hypothesis, chronic drying decreased productivity and stocks at deeper soil layers, whereas seasonal drying increased deep root productivity and stocks. The second hypothesis that chronic and seasonal drying lead to changes in root morphology and symbiotic associations, with root shifting toward greater resource acquisition traits was partially supported. Chronic drying increased mycorrhizal colonization, but seasonal drying decreased it. Chronic drying did not increase SRL and seasonal drying had mixed responses across root productivity assessment methods. Both chronic and seasonal drying increased root diameter, which might be associated to support mycorrhizal. The third hypothesis that drying effects on root dynamics, morphology, and symbiotic associations are greater in wetter forests because roots in these forests are less adapted to dry conditions was partially supported. Chronic drying suppressing root productivity at deeper soil layers and increasing mortality in the surface primarily in the wettest site, but other responses were most prominent in other forests. So, the magnitude of the drying effect varied among forests and root characteristics. The prediction that roots in the most fertile forest would be more resilient

to drying was supported, because fertile forests had a lack of responses to chronic drying at some dates and depths and larger deeper root productivity when compared to other sites, but this should be further investigated. The observed differences of responses from experimental and seasonal drying from some of the measured variables also highlight that model predictions based on seasonality may provide different results from what plants experience under chronic drying. A conceptual figure can be found in Figure 3.14.

3.7 Figures

Figure 3.1.

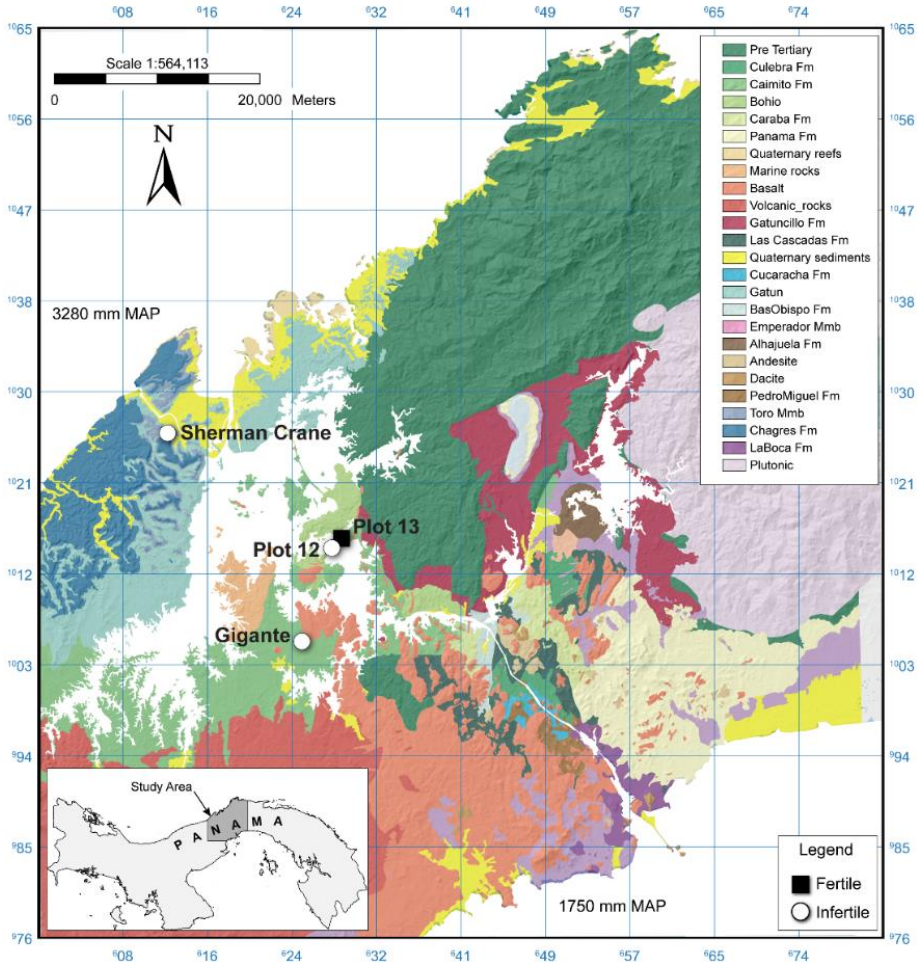

Figure 3.1: The four lowland tropical forest study sites are shown along a rainfall gradient on the Isthmus of Panama. Geological substrates and formations (Fm, shown in different colors) give rise to large variation in soil fertility, which is not correlated with the rainfall gradient. Rainfall increases from 1750 mm mean annual precipitation (MAP) on the Pacific coast to >3200 on the Caribbean coast, with sites for this study ranging from 2350 (Gigante) to 3400 (Sherman Crane). Soil fertility for the study sites is shown as fertile (black squares) or infertile (white circles). Citation: Geología de la República de Panamá, digitalizada del mapa Geológico de Panamá, 1:250,000 preparado por el Ministerio de Comercio e Industrias, Dirección General de Recursos Minerales, año 1990. Ministerio de Comercio e Industrias, Dirección General de Recursos Minerales, año 1990. Site details are presented in Table 3.1.

Figure 3.2.

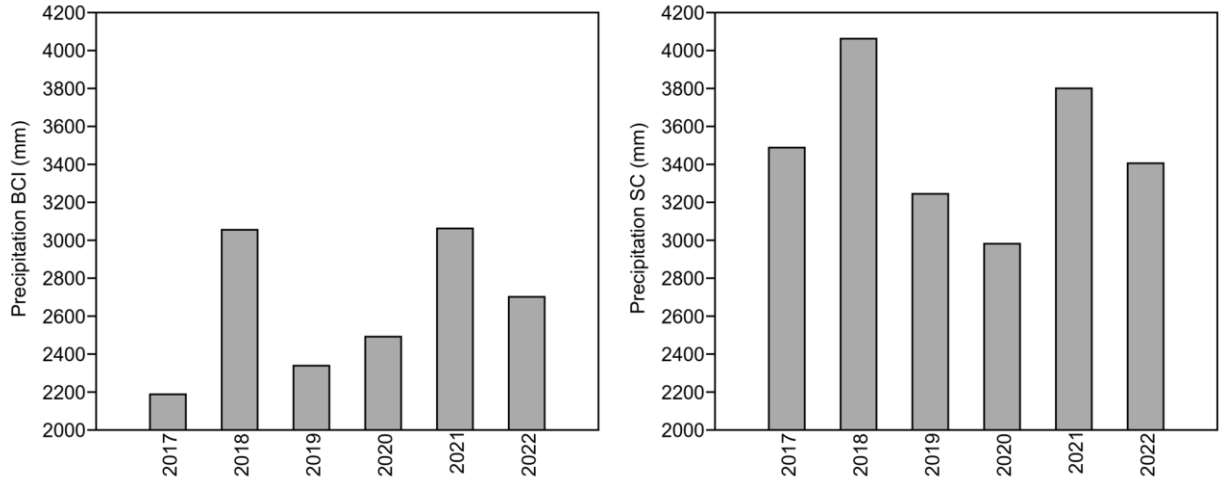

Figure 3.2: Mean annual precipitation in Barro Colorado Island (left) across different years and in Sherman Crane (San Lorenzo, right). The sites GIG, P12 and P13 are near BCI so have similar mean annual precipitations than the figure on the left. The site SC is located in San Lorenzo so have similar mean annual precipitation than the figure on the right. Data from Paton, 2023a and Paton, 2023b.

Figure 3.3.

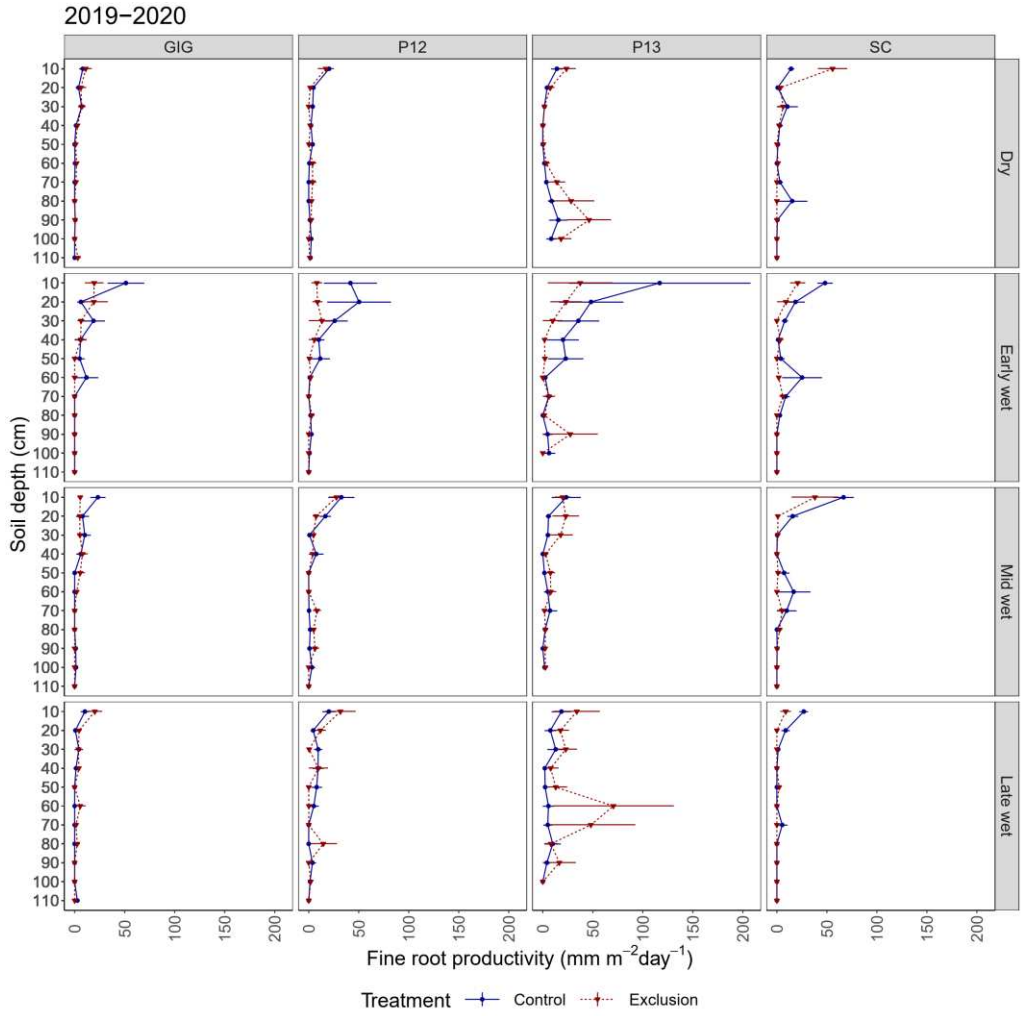

Figure 3.3: Fine root length productivity per minirhizotron window area and day (mm m^{-2} day^{-1}) during the first year of measurement (second year of chronic drying) is presented as the year average by soil depth and across treatments such as throughfall exclusion in red lines and control in blue lines. The different colors represent the different treatments. Data are presented for four different forests (columns) from seasonal tropical forests in Panama varying in mean annual precipitation and fertility. Seasons are presented in rows. Points and error bars represent mean ± standard errors across plots (n=4).

Figure 3.4.

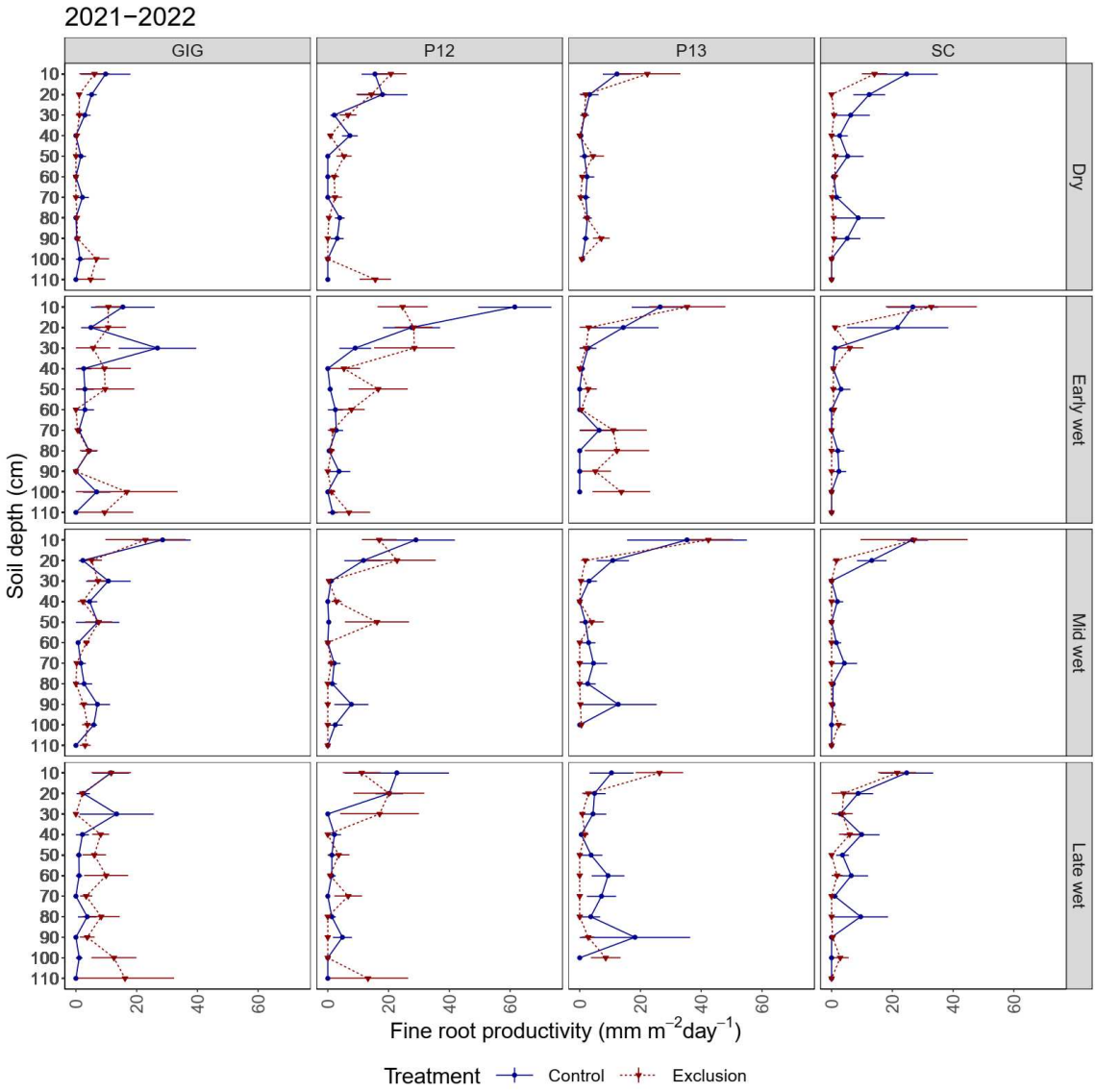

Figure 3.4: Fine root length productivity per minirhizotron window area and day (mm m^{-2} day^{-1}) during the second year of measurement (third year of chronic drying) is presented as the year average by soil depth and across treatments such as throughfall exclusion in red lines and control in blue lines. The different colors represent the different treatments. Data are presented for four different forests (columns) from seasonal tropical forests in Panama varying in mean annual precipitation and fertility. Seasons are presented in rows. Points and error bars represent mean ± standard errors across plots (n=4).

Figure 3.5.

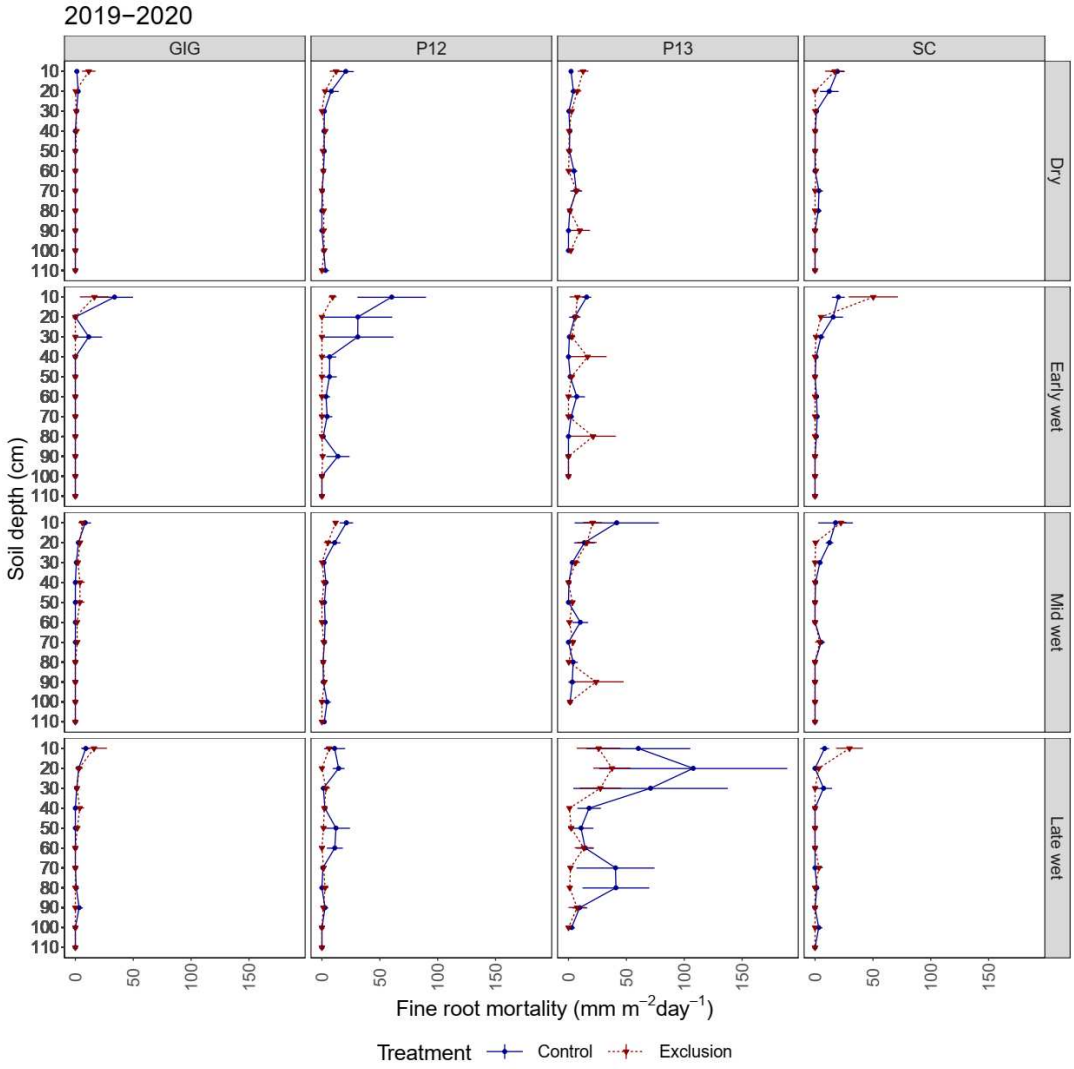

Figure 3.5: Fine root length mortality per minirhizotron window area and day (mm m^{-2} day^{-1}) during the first year of measurement (second year of chronic drying) is presented as the year average by soil depth and across treatments such as throughfall exclusion in red lines and control in blue lines. The different colors represent the different treatments. Data are presented for four different forests (columns) from seasonal tropical forests in Panama varying in mean annual precipitation and fertility. Seasons are presented in rows. Points and error bars represent mean ± standard errors across plots (n=4).

Figure 3.6.

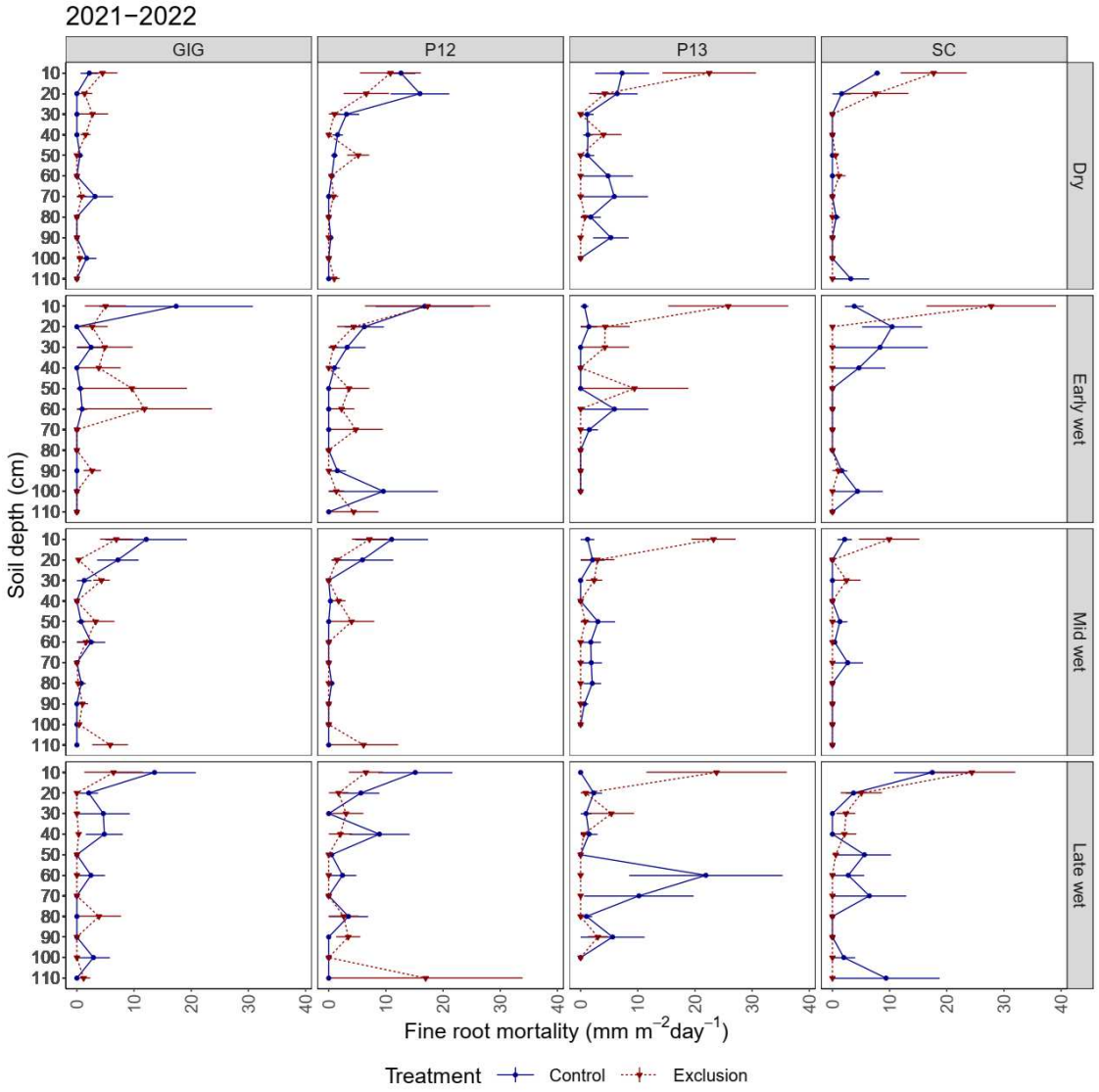

Figure 3.6: Fine root length mortality ("disappearance") per minirhizotron window area and day (mm m^{-2} day^{-1}) during the second year of measurement (third year of chronic drying) is presented as the year average by soil depth and across treatments such as throughfall exclusion in red lines and control in blue lines. The different colors represent the different treatments. Data are presented for four different forests (columns) from seasonal tropical forests in Panama varying in mean annual precipitation and fertility. Seasons are presented in rows. Points and error bars represent mean ± standard errors across plots (n=4).

Figure 3.7.

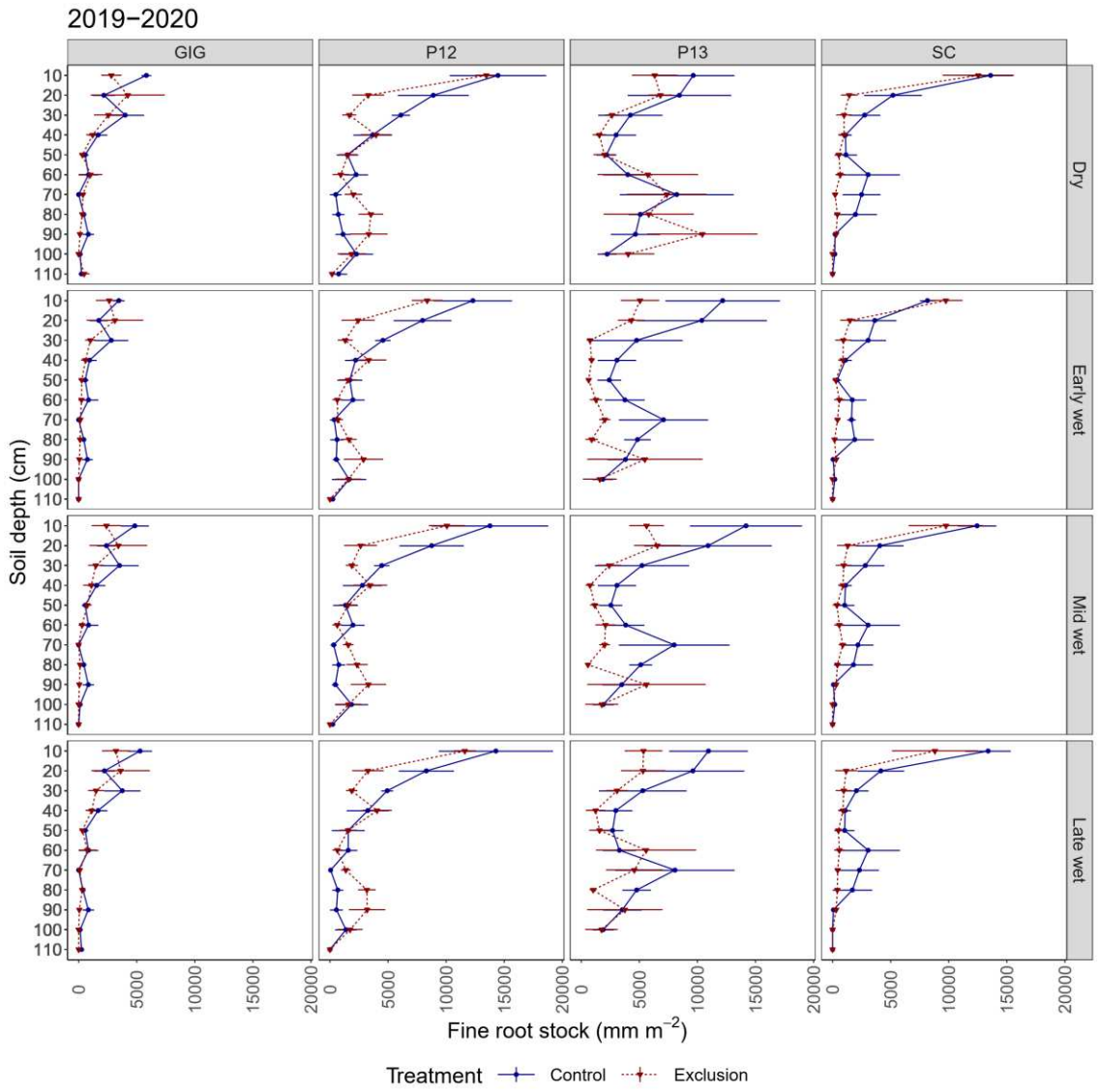

Figure 3.7: Fine root length stock per minirhizotron window area and day (mm m^{-2}) during the first year of measurement (second year of chronic drying) is presented as the year average by soil depth and across treatments such as throughfall exclusion in red lines and control in blue lines. The different colors represent the different treatments. Data are presented for four different forests (columns) from seasonal tropical forests in Panama varying in mean annual precipitation and fertility. Seasons are presented in rows. Points and error bars represent mean ± standard errors across plots (n=4).

Figure 3.8.

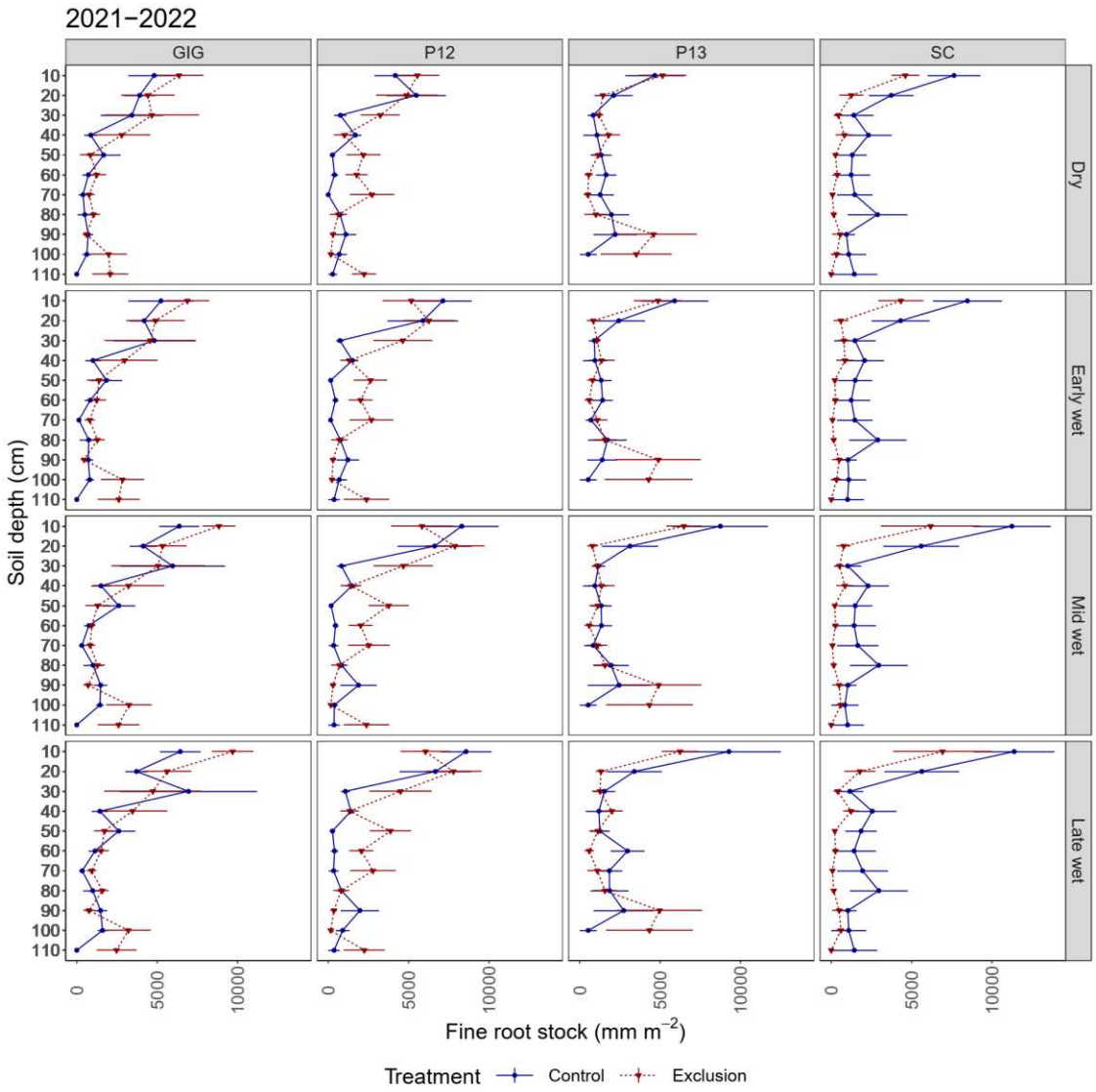

Figure 3.8: Fine root length peak stock per minirhizotron window area (mm m^{-2}) is presented. as the year average by soil depth and across treatments such as throughfall exclusion in red lines and control in blue lines. The different colors also represent the different years of measurement (2019-2020 and 2021-2022). Data are presented for four different forests (columns) from seasonal tropical forests in Panama varying in mean annual precipitation and fertility. Seasons are presented in rows. Points and error bars represent mean ± standard errors across plots (n=4).

Figure 3.9.

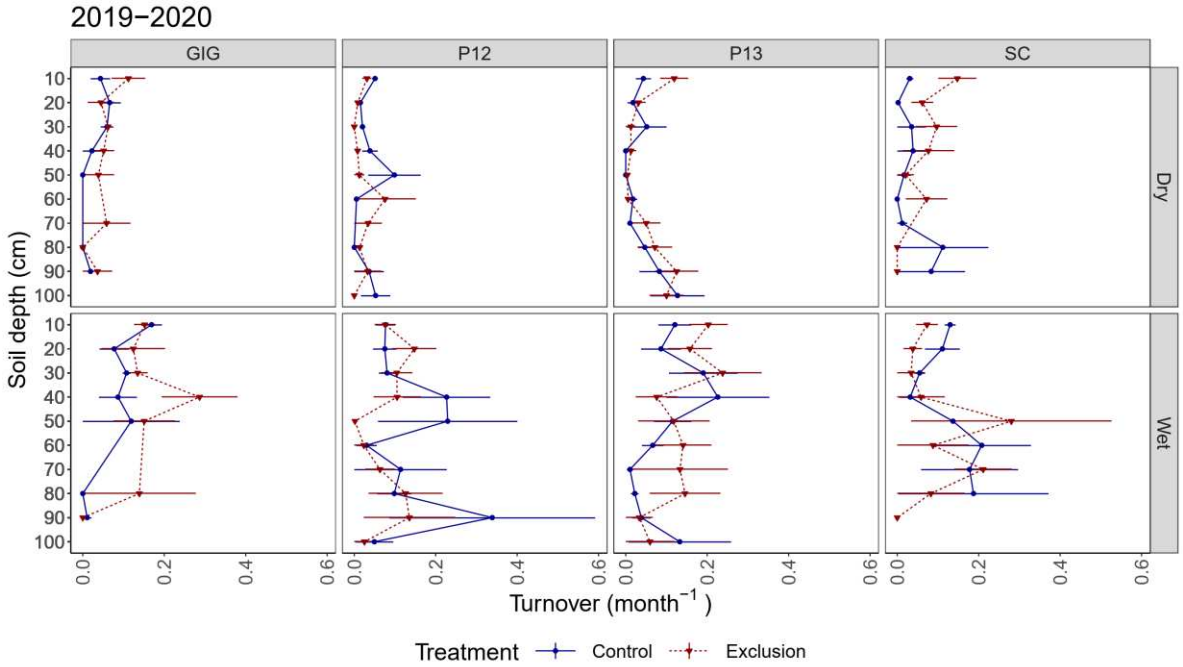

Figure 3.9: Fine root turnover averaged by month (month^{-1}) during the first year of measurement (second year of chronic drying) for each season, by soil depth, treatments such as throughfall exclusion in red and control in blue and years using minirhizotron method. The different colors also represent the different treatments. Data are presented for four different forests (columns) from seasonal tropical forests in Panama varying in mean annual precipitation and fertility. Seasons are presented in rows. Points and error bars represent mean ± standard errors across plots (n=4).

Figure 3.10.

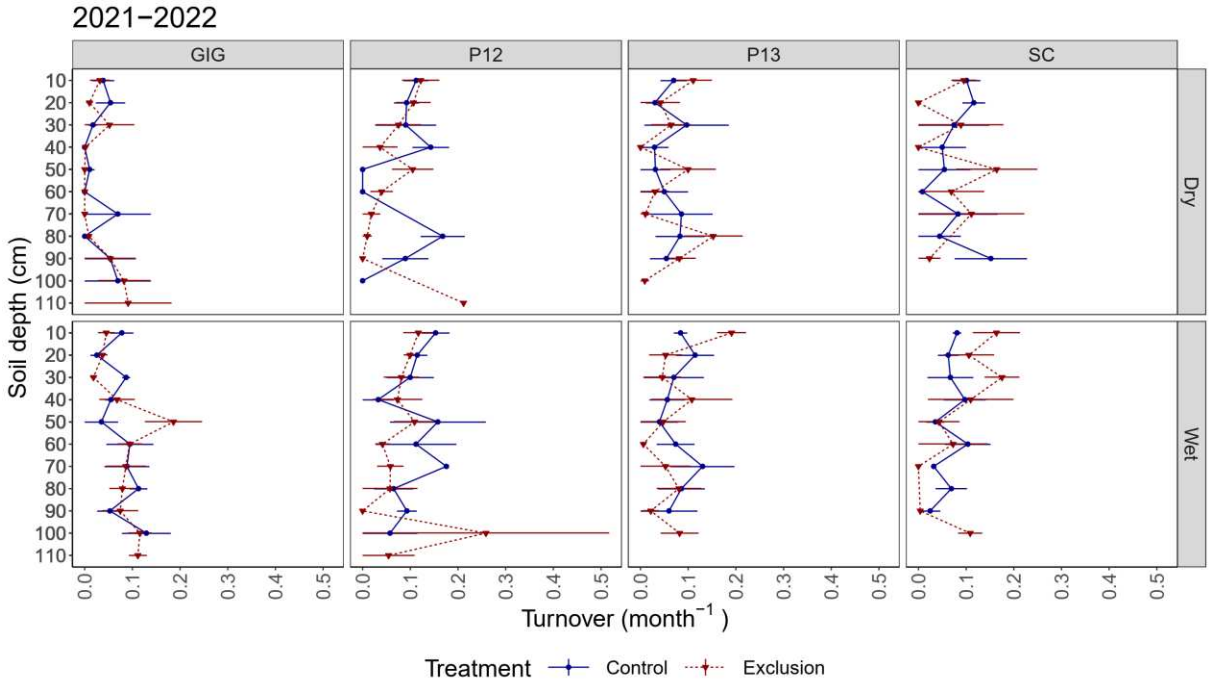

Figure 3.10: Fine root turnover averaged by month (month^{-1}) during the second year of measurement (third year of chronic drying) for each season, by soil depth, treatments such as throughfall exclusion in red and control in blue and years using minirhizotron method. The different colors also represent the different treatments. Data are presented for four different forests (columns) from seasonal tropical forests in Panama varying in mean annual precipitation and fertility. Seasons are presented in rows. Points and error bars represent mean ± standard errors across plots (n=4).

Figure 3.11.

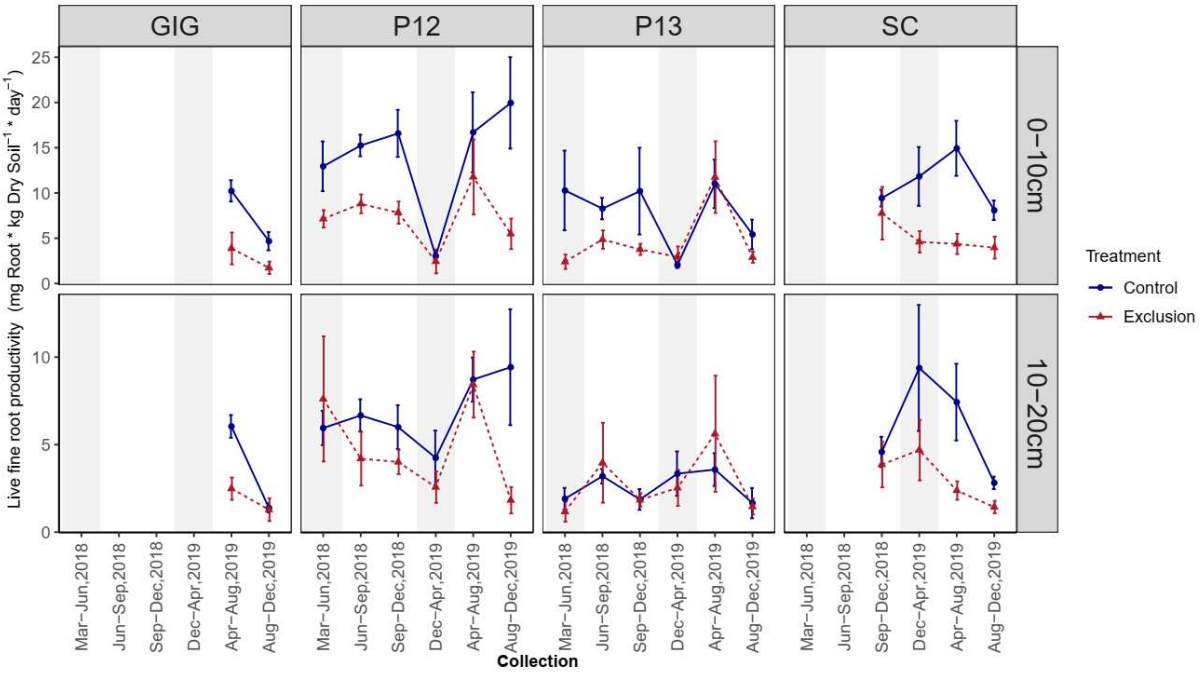

Figure 3.11: Live fine root biomass productivity (mg root * kg dry soil^{-1} * day^{-1}) from ingrowth core method. Data is presented over time with 3-4 months periods collections, soil depth and across treatments such as throughfall exclusion in red lines and control in blue lines. Data are presented for four different forests from seasonal tropical forests in Panama varying in mean annual precipitation and fertility. Points and error bars represent mean ± standard errors across plots (n=4). Gray shading represents dry season.

Figure 3.12.

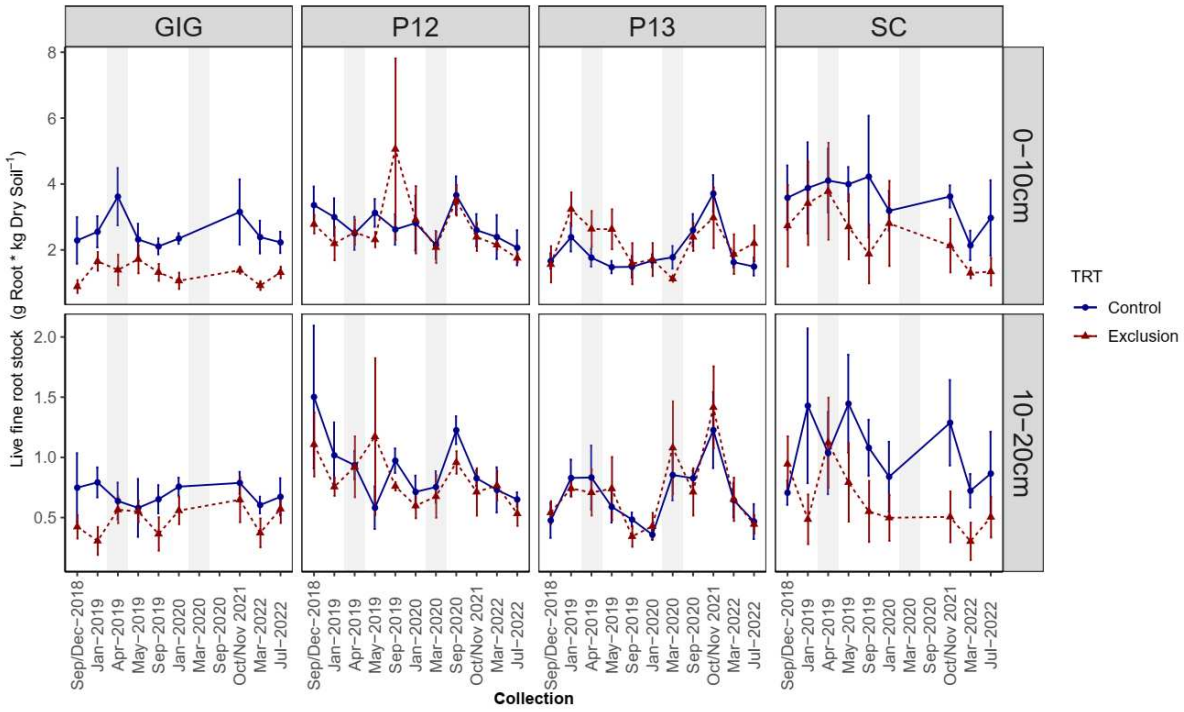

Figure 3.12: Live fine root stocks biomass (g root * kg dry soil^{-1}) from sequential coring method. Data is presented over time (collection months and years), soil depth and across treatments such as throughfall exclusion in red lines and control in blue lines. Data are presented for four different forests from seasonal tropical forests in Panama varying in mean annual precipitation and fertility. Points and error bars represent mean ± standard errors across plots (n=4). Gray shading represents dry season.

Figure 3.13.

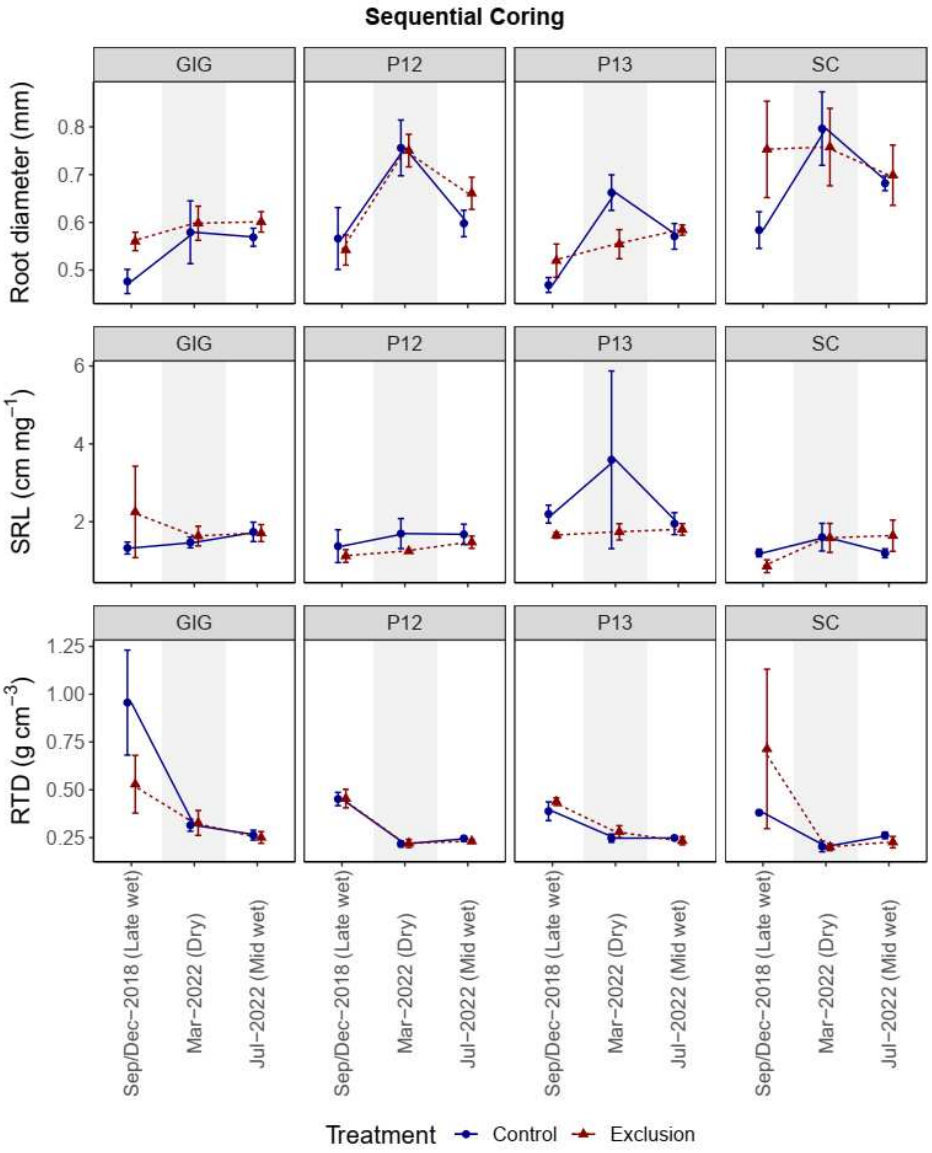

Figure 3.13: Live fine root morphology from sequential coring method. Top: Root diameter (mm); Middle: Specific root length (cm mg^{-1}); Bottom: Root tissue density (g cm^{-3}). Data is presented over time (3 different collection dates) and across treatments such as throughfall exclusion in red lines and control in blue lines. Data are presented for four different forests from seasonal tropical forests in Panama varying in mean annual precipitation and fertility. Data was averaged across 0-10 and 10-20 cm depth since depth was not a significant factor. Points and error bars represent mean ± standard errors across plots (n=4). Gray shading represents dry season.

Figure 3.14.

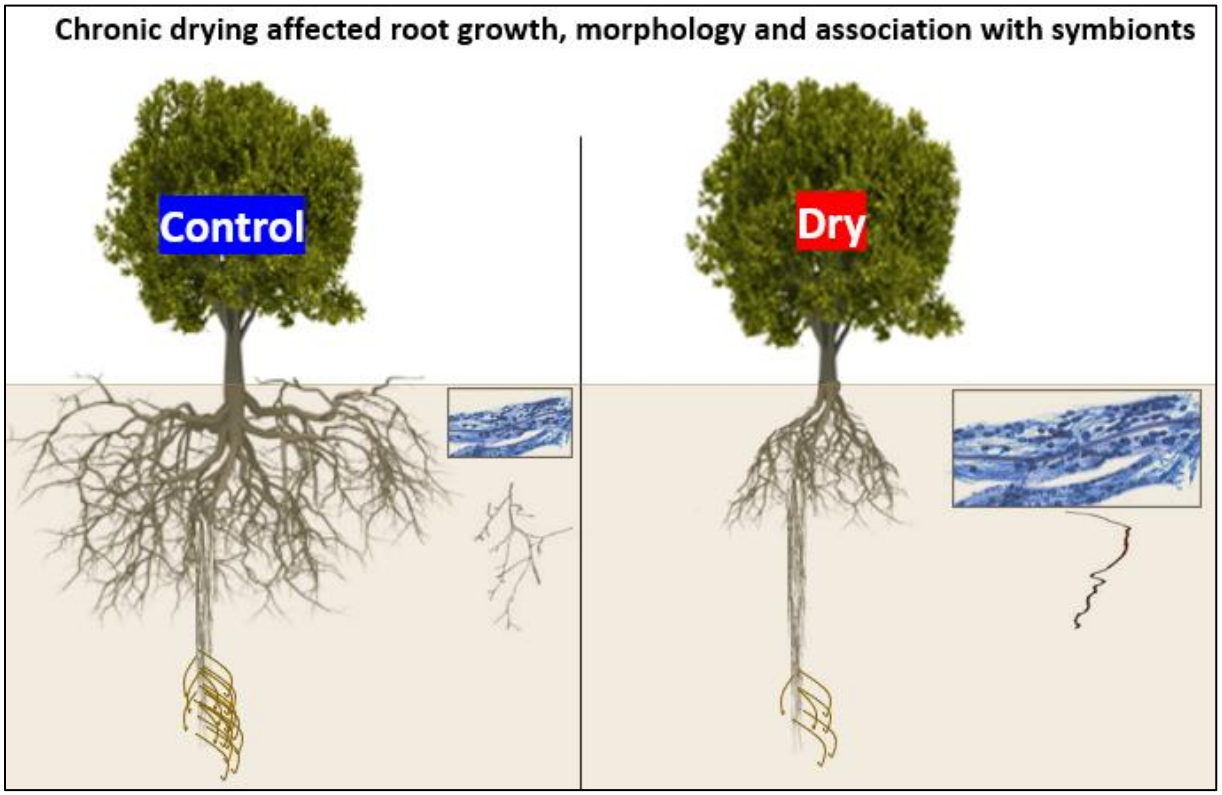

Figure 3.14: Conceptual figure for chapter 3. This chapter uncovered novel complexities in root responses to drying across different tropical forests, extending our previous understanding that plants alter their morphology to explore larger soil volumes to compensate for reduced growth and biomass. We now demonstrate that chronic drying not only decreases root growth and biomass but can increases arbuscular mycorrhizal fungi (AMF) colonization and alters root morphology in a way (larger diameter) that appear to predominantly support AMF functions rather than aiding plants in soil volume exploration by themselves. Additionally, root productivity and stocks were observed to be larger at deeper soil layers during the dry season, likely for water uptake. However, the suppression of these roots under chronic drying conditions may increase plant vulnerability. The study also indicates that fertile forests may possess some resilience to drying, as evidenced by their larger productivity at deeper soil layers, which could be beneficial under drying conditions and did not show responses to chronic drying at some dates at the soil surface. The observed decrease in root stocks and productivity with drying might suggest a potential reduction in carbon inputs to the soil in tropical forests. Conversely, an increase in AMF colonization associated with drying could potentially enhance carbon inputs to the soil. These impacts on soil carbon storage warrant further investigation. The first hypothesis that **chronic and seasonal drying decrease root production and stocks at the soil surface and increase these at depth where soil moisture is greater** was partially supported. In support of the hypothesis, chronic drying generally decreased root productivity and stocks at surface. Also in support, seasonal drying decreased productivity (except in the wettest site), but seasonal drying did not change root stocks as hypothesized. Also contrary to the hypothesis, chronic drying decreased productivity and stocks at deeper soil layers, whereas seasonal drying increased deep root productivity and stocks. The second hypothesis that

chronic and seasonal drying lead to changes in root morphology and symbiotic associations, with root shifting toward greater resource acquisition traits was partially supported. Chronic drying increased mycorrhizal colonization, but seasonal drying decreased it. Chronic drying did not increase SRL and seasonal drying had mixed responses across root productivity assessment methods. Both chronic and seasonal drying increased root diameter, which might be associated to support mycorrhizal. The third hypothesis that **drying effects on root dynamics, morphology, and symbiotic associations are greater in wetter forests because roots in these forests are less adapted to dry conditions** was partially supported. Chronic drying suppressing root productivity at deeper soil layers and increasing mortality in the surface primarily in the wettest site, but other responses were most prominent in other forests. So, the magnitude of the drying effect varied among forests and root characteristics. The prediction that **roots in the most fertile forest would be more resilient to drying** was supported, because fertile forests had a lack of responses to chronic drying at some dates and depths and larger deeper root productivity when compared to other sites, but this should be further investigated.

3.8 Tables

Table 3.1. Site characteristics are given for the four tropical forests used in this study (Cusack *et al.*, 2018).

Variable	Site			
	GIG	P12	P13	SC
Latitude North	9.09918	9.17936	9.18788	9.28087
Longitude East	-79.854	-79.83	-79.821	-79.975
Soil order	Oxisol	Ultisol	Alfisol	Oxisol
Fertility	Infertile	Infertile	Fertile	Infertile
MAP (mm)	2350	2600	2600	3421
Profile Clay% 1.0m	86.129	52.298	49.228	78.217
Above ground biomass (Mg /ha) >10cm dbh	201.8	212.8	260.2	304.9
SOC to 1 m kg/m2	19	19	12	13
Total N to 1 m kg/m2	2.01	1.45	1.01	1
Total P to 1 m g/m2	152.95	241.66	204.13	233.59
resin-extractable P to 1 m AEM Pi gP/m2	0.25	0.33	1.58	0.15
DOC to 1 m g/m2	318.32	267.33	65.32	375.3
Total Extractable Bases to 1 m kg/m2	1.37	0.63	5.29	0.22

Table 3.2: Methods summary. Root ingrowth core, sequential coring and minirhizotron installation, sample collections dates, number of collections and number of samples at four different forests in the PARCHED experiment in Panama. Each site has 8 plots with 5 ingrowth cores, 3 sequential coring and 1 minirhizotron tube per plot for each sample collection. Ingrowth cores and sequential coring have 2 depths per core and minirhizotron have 230 images per tube.

Method	Collections	P12	P13	SC	GIG
Ingrowth core	Installation	Feb, 2018	Feb, 2018	Sep, 2018	Jan, 2019
	First collection	Jun, 2018	Jun, 2018	Dec, 2018	Apr, 2019
	Number of collections	6	6	4	2
	Last collection	Dec, 2019	Dec, 2019	Dec, 2019	Jan, 2020
	Number of samples	480	480	320	160
Sequential coring	First collection	Sep, 2018	Sep, 2018	Sep, 2018	Dec, 2018
	Number of collections	12	12	10	10
	Last collection	Jul, 2022	Jul, 2022	Jul, 2022	Jul, 2022
	Number of samples	576	576	480	480
Minirhizotron	Installation	Sep, 2017	Dec, 2017	Feb, 2018	Oct, 2018
	First collection	Feb, 2019	Feb, 2019	Feb, 2019	Feb, 2019
	Number of collections	32	32	32	33
	Last collection	Oct, 2022	Oct, 2022	Oct, 2022	Oct, 2022
	Number of images	58880	58880	58880	60720
Throughfall experiment installation end date		Jun, 2018	May, 2018	Jul, 2018	Dec, 2018

Table 3.3: Arbuscular mycorrhizal fungi (AMF) colonization (%) in fine roots during the wet season across different soil depths and treatments in four forests: GIG, P12, P13, and SC. Control treatment refers to natural conditions without throughfall exclusion, while Exclusion treatment indicates the experimental drying condition. Values represent mean ± standard error across plots (n = 4).

Depth	Treatment	AMF colonization (%) - wet season			
		GIG	P12	P13	SC
0-10cm	Control	32.15 ± 3.78	32.22 ± 3.81	33.82 ± 3.64	33.76 ± 3.68
0-10cm	Exclusion	37.13 ± 2.66	32.05 ± 8.51	42.94 ± 10.73	28.67 ± 7.58
10-20cm	Control	20.99 ± 2.15	23.21 ± 3.64	20.90 ± 1.42	28.67 ± 2.87
10-20cm	Exclusion	26.06 ± 11.02	28.85 ± 10.16	19.32 ± 7.30	33.20 ± 12.25

LITERATURE CITED

Allen K, Dupuy JM, Gei MG, Hulshof C, Medvigy D, Pizano C, Salgado-Negret B, Smith CM, Trierweiler A, Van Bloem SJ, et al. 2017. Will seasonally dry tropical forests be sensitive or resistant to future changes in rainfall regimes? *Environmental Research Letters* 12(2): 15.

Andrade JL, Meinzer FC, Goldstein G, Schnitzer SA. 2005. Water uptake and transport in lianas and co-occurring trees of a seasonally dry tropical forest. *Trees-Structure and Function* 19(3): 282-289.

Artaxo P, Hansson HC, Machado LAT, Rizzo LV. 2022. Tropical forests are crucial in regulating the climate on Earth. *PLOS Climate* 1(8).

Auge RM, Toler HD, Saxton AM. 2016. Mycorrhizal Stimulation of Leaf Gas Exchange in Relation to Root Colonization, Shoot Size, Leaf Phosphorus and Nitrogen: A Quantitative Analysis of the Literature Using Meta-Regression. *Front Plant Sci* 7: 1084.

Barros V, Melo A, Santos M, Nogueira L, Frosi G, Santos MG. 2020. Different resource-use strategies of invasive and native woody species from a seasonally dry tropical forest under drought stress and recovery. *Plant Physiology and Biochemistry* 147: 181-190.

Beard KH, Vogt KA, Vogt DJ, Scatena FN, Covich AP, Sigurdardottir R, Siccama TG, Crowl TA. 2005. Structural and functional responses of a subtropical forest to 10 years of hurricanes and droughts. *Ecological Monographs* 75(3): 345-361.

Bonal D, Burban B, Stahl C, Wagner F, Herault B. 2016. The response of tropical rainforests to drought-lessons from recent research and future prospects. *Ann For Sci* 73: 27-44.

Brodribb TJ, Powers J, Cochard H, Choat B. 2020. Hanging by a thread? Forests and drought. *Science* 368(6488): 261-+.

Brundrett MC. 2002. Coevolution of roots and mycorrhizas of land plants. *New Phytologist* 154(2): 275-304.

Cabugao KG, Yaffar D, Stenson N, Childs J, Phillips J, Mayes MA, Yang X, Weston DJ, Norby RJ. 2021. Bringing function to structure: Root–soil interactions shaping phosphatase activity throughout a soil profile in Puerto Rico. *Ecology and Evolution* 11(3): 1150-1164.

Cao K-f. 2000. Water relations and gas exchange of tropical saplings during a prolonged drought in a Bornean heath forest, with reference to root architecture. *Journal of Tropical Ecology* 16(1): 101-116.

Cavelier J, Wright SJ, Santamaría J. 1999. Effects of irrigation on litterfall, fine root biomass and production in a semideciduous lowland forest in Panama. *Plant and Soil* 211(2): 207-213.

Chacon SS, Cusack DF, Khurram A, Bill M, Dietterich LH, Bouskill NJ. 2023. Divergent responses of soil microorganisms to throughfall exclusion across tropical forest soils driven by soil fertility and climate history. *Soil Biology and Biochemistry* 177.

Chadwick R, Good P, Martin G, Rowell DP. 2015. Large rainfall changes consistently projected over substantial areas of tropical land. *Nature Climate Change* 6(2): 177-181.

Comas LH, Becker SR, Cruz VV, Byrne PF, Dierig DA. 2013. Root traits contributing to plant productivity under drought. *Frontiers in Plant Science* 4: 16.

Cordeiro AL, Norby RJ, Andersen KM, Valverde-Barrantes O, Fuchslueger L, Oblitas E, Hartley IP, Iversen CM, Gonçalves NB, Takeshi B, et al. 2020. Fine-root dynamics vary with soil

depth and precipitation in a low-nutrient tropical forest in the Central Amazonia. *Plant-Environment Interactions* 1(1): 3-16.

Crowther TW, van den Hoogen J, Wan J, Mayes MA, Keiser AD, Mo L, Averill C, Maynard DS. 2019. The global soil community and its influence on biogeochemistry. *Science* 365(6455).

Cusack D, Karpman J, Ashdown D, Cao Q, Ciochina M, Halterman S, Lydon S, Neupane A. 2016. Global change effects on humid tropical forests: Evidence for biogeochemical and biodiversity shifts at an ecosystem scale. *Reviews of Geophysics* 54(3): 523-610.

Cusack DF, Addo-Danso SD, Agee EA, Andersen KM, Arnaud M, Batterman SA, Brearley FQ, Ciochina MI, Cordeiro AL, Dallstream C, et al. 2021. Tradeoffs and Synergies in Tropical Forest Root Traits and Dynamics for Nutrient and Water Acquisition: Field and Modeling Advances. *Frontiers in Forests and Global Change* 4.

Cusack DF, Ashdown D, Dietterich LH, Neupane A, Ciochina M, Turner BL. 2019. Seasonal changes in soil respiration linked to soil moisture and phosphorus availability along a tropical rainfall gradient. *Biogeochemistry* 145(3): 235-254.

Cusack DF, Dietterich L, Sulman BN. 2023. Soil Respiration Responses to Throughfall Exclusion Are Decoupled From Changes in Soil Moisture for Four Tropical Forests, Suggesting Processes for Ecosystem Models. *Global Biogeochemical Cycles* 37: e2022GB007473.

Cusack DF, Markesteijn L, Condit R, Lewis OT, Turner BL. 2018. Soil carbon stocks across tropical forests of Panama regulated by base cation effects on fine roots. *Biogeochemistry* 137(1-2): 253-266.

Cusack DF, Turner BL. 2020. Fine Root and Soil Organic Carbon Depth Distributions are Inversely Related Across Fertility and Rainfall Gradients in Lowland Tropical Forests. *Ecosystems* 24(5): 1075-1092.

da Costa AC, Galbraith D, Almeida S, Portela BT, da Costa M, Silva Junior Jde A, Braga AP, de Goncalves PH, de Oliveira AA, Fisher R, et al. 2010. Effect of 7 yr of experimental drought on vegetation dynamics and biomass storage of an eastern Amazonian rainforest. *New Phytol* 187(3): 579-591.

Das S, Sarkar S. 2024. Arbuscular mycorrhizal fungal contribution towards plant resilience to drought conditions. *Front Fungal Biol* 5: 1355999.

Davidson EA, Ishida FY, Nepstad DC. 2004. Effects of an experimental drought on soil emissions of carbon dioxide, methane, nitrous oxide, and nitric oxide in a moist tropical forest. *Global Change Biology* 10(5): 718-730.

Deng Q, Zhang D, Han X, Chu G, Zhang Q, Hui D. 2018. Changing rainfall frequency rather than drought rapidly alters annual soil respiration in a tropical forest. *Soil Biology and Biochemistry* 121: 8-15.

Dietterich LH, Bouskill NJ, Brown M, Castro B, Chacon SS, Colburn L, Cordeiro AL, Garcia EH, Gordon AA, Gordon E, et al. 2022. Effects of experimental and seasonal drying on soil microbial biomass and nutrient cycling in four lowland tropical forests. *Biogeochemistry* 161(2): 227-250.

Espeleta JF, Clark DA. 2007. Multi-scale variation in fine-root biomass in a tropical rain forest: A seven-year study. *Ecological Monographs* 77(3): 377-404.

Fan Y, Miguez-Macho G, Jobbagy EG, Jackson RB, Otero-Casal C. 2017. Hydrologic regulation of plant rooting depth. *Proceedings of the National Academy of Sciences of the United States of America* 114(40): 10572-10577.

Field CB, Behrenfeld MJ, Randerson JT, Falkowski P. 1998. Primary production of the biosphere: Integrating terrestrial and oceanic components. *Science* 281(5374): 237-240.

Giovannetti M, Mosse B. 1980. An Evaluation of Techniques for Measuring Vesicular Arbuscular Mycorrhizal Infection in Roots. *New Phytologist* 84(3): 489-500.

Green IJ, Dawson LA, Proctor J, Duff EI, Elston DA. 2005. Fine root dynamics in a tropical rain forest is influenced by rainfall. *Plant and Soil* 276(1-2): 23-32.

INVAM ICoVAMF. 2023. Staining of Mycorrhizal Roots.

Jackson RB, Canadell J, Ehleringer JR, Mooney HA, Sala OE, Schulze ED. 1996. A global analysis of root distributions for terrestrial biomes. *Oecologia* 108(3): 389-411.

Jobbagy EG, Jackson RB. 2000. The vertical distribution of soil organic carbon and its relation to climate and vegetation. *Ecological Applications* 10(2): 423-436.

Johnson MG, Tingey DT, Phillips DL, Storm MJ. 2001. Advancing fine root research with minirhizotrons. *Environmental and Experimental Botany* 45(3): 263-289.

Kharin VV, Zwiers FW, Zhang X, Hegerl GC. 2007. Changes in temperature and precipitation extremes in the IPCC ensemble of global coupled model simulations. *Journal of Climate* 20(8): 1419-1444.

Kong D, Ma C, Zhang Q, Li L, Chen X, Zeng H, Guo D. 2014. Leading dimensions in absorptive root trait variation across 96 subtropical forest species. *New Phytol* 203(3): 863-872.

Koske RE, Gemma JN. 1989. A modified procedure for staining roots to detect VA mycorrhizas. *Mycological Research* 92(4): 486-488.

Kuyper TW, Jansa J. 2023. Arbuscular mycorrhiza: advances and retreats in our understanding of the ecological functioning of the mother of all root symbioses. *Plant and Soil*: 48.

Magrin GO, Marengo JA, Boulanger J-P, Buckeridge MS, Castellanos E, Poveda G, Scarano FR, Vicuna S 2014. Central and South America. In: Barros VR, C.B. Field, D.J. Dokken, M.D. Mastrandrea, K.J. Mach, T.E. Bilir, M. Chatterjee, K.L. Ebi, Y.O. Estrada, R.C. Genova, B.Girma, E.S. Kissel, A.N. Levy, S. MacCracken, P.R. Mastrandrea, and L.L. White ed. *Climate Change 2014: Impacts, Adaptation, and Vulnerability. Part B: Regional Aspects. Contribution of Working Group II to the Fifth Assessment Report on the Intergovernmental Panel on Climate Change*. Cambridge, United Kingdom and New York, NY, USA: Cambridge University Press, 1499-1566.

Markesteijn L, Poorter L. 2009. Seedling root morphology and biomass allocation of 62 tropical tree species in relation to drought- and shade-tolerance. *Journal of Ecology* 97(2): 311-325.

McCormack ML, Dickie IA, Eissenstat DM, Fahey TJ, Fernandez CW, Guo D, Helmisaari H-S, Hobbie EA, Iversen CM, Jackson RB, et al. 2015. Redefining fine roots improves understanding of below-ground contributions to terrestrial biosphere processes. *New Phytologist* 207(3): 505-518.

Meinzer FC, Andrade JL, Goldstein G, Holbrook NM, Cavelier J, Wright SJ. 1999. Partitioning of soil water among canopy trees in a seasonally dry tropical forest. *Oecologia* 121(3): 293-301.

Metcalfe DB, Meir P, Aragao L, da Costa ACL, Braga AP, Goncalves PHL, Silva JD, de Almeida SS, Dawson LA, Malhi Y, et al. 2008. The effects of water availability on root growth and morphology in an Amazon rainforest. *Plant and Soil* 311(1-2): 189-199.

Metcalfe DB, Williams M, Aragao L, da Costa ACL, de Almeida SS, Braga AP, Goncalves PHL, Silva JD. 2007. A method for extracting plant roots from soil which facilitates rapid sample processing without compromising measurement accuracy. *New Phytologist* 174(3): 697-703.

Moser G, Schuldt B, Hertel D, Horna V, Coners H, Barus H, Leuschner C. 2014. Replicated throughfall exclusion experiment in an Indonesian perhumid rainforest: wood production,

litter fall and fine root growth under simulated drought. *Global Change Biology* 20(5): 1481-1497.
Nepstad DC. 2002. The effects of partial throughfall exclusion on canopy processes, aboveground production, and biogeochemistry of an Amazon forest. *Journal of Geophysical Research* 107(D20).
Nepstad DC, Decarvalho CR, Davidson EA, Jipp PH, Lefebvre PA, Negreiros GH, Dasilva ED, Stone TA, Trumbore SE, Vieira S. 1994. The role of deep roots in the hydrological and carbon cycles of Amazonian forests and pastures. *Nature* 372(6507): 666-669.
Norby RJ, Ledford J, Reilly CD, Miller NE, O'Neill EG. 2004. Fine-root production dominates response of a deciduous forest to atmospheric CO2 enrichment. *Proceedings of the National Academy of Sciences of the United States of America* 101(26): 9689-9693.
Oliveira RS, Dawson TE, Burgess SSO, Nepstad DC. 2005. Hydraulic redistribution in three Amazonian trees. *Oecologia* 145(3): 354-363.
Oliveira RS, Eller CB, Barros FV, Hirota M, Brum M, Bittencourt P. 2021. Linking plant hydraulics and the fast-slow continuum to understand resilience to drought in tropical ecosystems. *New Phytol* 230(3): 904-923.
Paton S. 2023a. Meteorological and hydrological summary for Barro Colorado Island. *Smithsonian Tropical Research Institute*: 42.
Paton S 2023b. Meteorological and hydrological summary for the San Lorenzo/Fort Sherman canopy crane: Panama: Smithsonian Tropical Research Institute. Retrieved from https ….
Rasse DP, Rumpel C, Dignac MF. 2005. Is soil carbon mostly root carbon? Mechanisms for a specific stabilisation. *Plant and Soil* 269(1-2): 341-356.
Rodtassana C, Tanner EVJ. 2018. Litter removal in a tropical rain forest reduces fine root biomass and production but litter addition has few effects. *Ecology* 99(3): 735-742.
Santiago LS, Mulkey SS. 2005. Leaf productivity along a precipitation gradient in lowland Panama: patterns from leaf to ecosystem. *Trees-Structure and Function* 19(3): 349-356.
Sciumbata M, Wenina YEM, Mbemba M, Dargie GC, Baird AJ, Morris PJ, Ifo SA, Aerts R, Lewis SL. 2023. First estimates of fine root production in tropical peat swamp and terra firme forests of the central Congo Basin. *Scientific Reports* 13(1): 12315.
Tao S, Chave J, Frison PL, Le Toan T, Ciais P, Fang J, Wigneron JP, Santoro M, Yang H, Li X, et al. 2022. Increasing and widespread vulnerability of intact tropical rainforests to repeated droughts. *Proc Natl Acad Sci U S A* 119(37): e2116626119.
Taylor JP, Wilson B, Mills MS, Burns RG. 2002. Comparison of microbial numbers and enzymatic activities in surface soils and subsoils using various techniques. *Soil Biology & Biochemistry* 34(3): 387-401.
Valdes M, Asbjornsen H, Gomez-Cardenas M, Juarez M, Vogt KA. 2006. Drought effects on fine-root and ectomycorrhizal-root biomass in managed Pinus oaxacana Mirov stands in Oaxaca, Mexico. *Mycorrhiza* 16(2): 117-124.
Valverde-Barrantes OJ, Horning AL, Smemo KA, Blackwood CB. 2016. Phylogenetically structured traits in root systems influence arbuscular mycorrhizal colonization in woody angiosperms. *Plant and Soil* 404(1-2): 1-12.
Vargas Gutiérrez G, Pérez-Aviles D, Raczka N, Pereira-Arias D, Tijerín-Triviño J, Pereira-Arias LD, Medvigy D, Waring BG, Morrisey E, Brzostek E, et al. 2023. Throughfall exclusion and fertilization effects on tropical dry forest tree plantations, a large-scale experiment. *Biogeosciences* 20(11): 2143-2160.

Wright SJ, Cornejo FH. 1990. Seasonal drought and the timing of flowering and leaf fall in a Neotropical forest. *Reproductive Ecology*.

Yaffar D, Norby RJ. 2020. A historical and comparative review of 50 years of root data collection in Puerto RicoPalabras Clave. *Biotropica* 52(3): 563-576.

Yavitt JB, Wright SJ. 2001. Drought and irrigation effects on fine root dynamics in a tropical moist forest, Panama. *Biotropica* 33(3): 421-434.

Zhou L, Liu Y, Zhang Y, Sha L, Song Q, Zhou W, Balasubramanian D, Palingamoorthy G, Gao J, Lin Y, et al. 2019. Soil respiration after six years of continuous drought stress in the tropical rainforest in Southwest China. *Soil Biology & Biochemistry* 138.

CHAPTER 4: DRYING EFFECTS ON TROPICAL TREE SEEDLING CARBON AND NUTRIENT DYNAMICS ARE MEDIATED BY SOIL FERTILITY AND MYCORRHIZAL ASSOCIATION

4.1 Summary

Tropical forests have the largest plant productivity on Earth, which will likely be sensitive to regional shifts in rainfall and drying trends. Seedling development can be particularly sensitive to drought, since small root systems have limited capacity to explore for deeper soil water. Drought effects in tropical seedling might be ameliorated by associations with arbuscular mycorrhizal fungal (AMF) and by high soil fertility, which can improve growth and nutrient status. To explore this, we conducted a greenhouse experiment with tropical tree seedlings in a factorial drying, soil fertility, AMF inoculation over 4 months. We tested the hypotheses: H1) Drying decreases tropical seedling growth, but AMF inoculation and high soil fertility mitigate these effects by supporting water and nutrient acquisition; H2) Improved seedling growth with AMF and high soil fertility under drying is related to traits that maximize soil resource acquisition and minimize moisture loss, such as high specific root length (SRL) with low specific leaf area (SLA); H3) Drying suppresses root organic exudates to soils as plants prioritize water rather than nutrient acquisition, but low soil fertility supports relative increases in root exudates. Plants were grown in a $^{13}CO_2$–labeled headspace and given an initial ^{15}N-labeled fertilizer. After four-month plants were moved to ambient air to observe ^{13}C dilution of plant tissues over one week. Overall, drying decreased plant biomass across plant tissues, but this was mediated by larger positive effects of high soil fertility and AMF inoculation on plant growth. At the end of the experiment, uptake of ambient CO_2 was allocated most rapidly to leaves, and this new C was allocated to roots fastest under dry

conditions. Leaf and root traits responded to all treatments, with AMF in particular promoting smaller SLA, SRL, leaf and root %N, and promoting larger root diameter, root tissue density, and photosynthetic capacity. These AMF effects were generally largest under fertile conditions, with drying mainly promoting larger root diameter. A large portion of the initial dose of ^{15}N was retained in plants (>60%), primarily in leaves, with a positive effect of AMF. Finally, drying increased leached C in the end of the experiment as did soil fertility, whereas AMF suppressed it. Overall, this study indicates that AMF can have a large positive effect on tropical seedling growth under drought, via changes in morphological traits, plant nutrient retention, and reduced C expenditure in root exudates. This study offers insight to how tropical forest seedlings might respond to drought across site-scale environmental variation.

4.2 Introduction

Tropical forests, which contain 25 – 40% of the world's terrestrial carbon (C) stocks (Field *et al.*, 1998; Jobbagy & Jackson, 2000), are facing atmospheric drying in many regions (Kharin *et al.*, 2007; Magrin *et al.*, 2014). Across a large body of tropical field and greenhouse studies, drying appears to negatively affect tropical plant growth, reduced ecosystem C storage in plants and soils, and reduce biodiversity (Cusack *et al.*, 2016). Large-scale studies in the Amazon showed that drying increased large tree mortality (da Costa *et al.*, 2010), decreased root production, and changed leaf and root morphological traits (Metcalfe *et al.*, 2008). The capacity for tropical tree species to adapt to drying is poorly understood at the species-scale, and might vary spatially depending on other ecosystem characteristics like moisture levels, soil fertility, and symbiotic associations.

Drying represents a fundamental reduction in soil resources, and is thus expected to shift plant biomass allocation. The optimal partitioning frameworks suggests that plants strategically allocate biomass above versus belowground to access the scarcest resources (Bloom *et al.*, 1985). Accordingly, drought has tended to increase community-scale tropical forest biomass toward roots across studies (Cusack *et al.*, 2021). Understanding finer-scale species- and trait- responses and adaptations to drying generally requires greenhouse research because of the size and complexity of tropical forests. Greenhouse studies have reported decreased total plant biomass and growth rates in response to drying, including increased root:shoot ratios (i.e. root mass fraction) for seedling species from Ghana (Amissah *et al.*, 2015), Hawaii (Barton & Shiels, 2020), and China (Asefa *et al.*, 2022), as well as increased root:leaf area for Australian seedlings (Thomas *et al.*, 2000). One study with Hawaiian species did not find changes in root:shoot ratios with drying (Barton & Shiels, 2020), and seedlings from Seychelles found no change in this ratio but overall reduced growth with drought (Schumacher *et al.*, 2008). Thus, most tropical seedling studies have found reduced growth and increased belowground biomass allocation with drying, with some variation among studies likely related to the extent of drying, the availability of other resources, and species-specific differences in flexibility.

Environmental characteristics, such as soil fertility and the availability of root symbionts, can help ameliorate the negative effects of drought. Photosynthetic rates which are important as the control point over C entering the plant, and plant growth have been shown to decrease under drought stress (Yang *et al.,* 2021). However, these effects can be diminished when plants are exposed to symbiotic relationships and fertility. For example, a meta-analysis showed that plants had greater drought resistance when their roots were associated with arbuscular mycorrhizal fungi (AMF), with increased plant photosynthetic rates (Auge et al., 2016). Other recent reviews indicate

that AMF can also increase nutrient uptake rates and nutrient use efficiency in crops (Tang et al., 2022), which in turn can improve plants' drought tolerance (Cheng *et al.,* 2021). Also, photosynthetic capacity appears to be regulated not only by climate, but also by soil fertility (Smith *et al.,* 2019) which can have an impact on drought tolerance. Thus, individual species' drought tolerance can shift depending on soil fertility and AMF.

In addition to the shifts in biomass allocation, plants can respond to drying with changes in biomass structure, morphology, and dynamics. Plant traits, such as tissue density and area per weight, are important to plant functions aboveground (Lerdau et al., 2023) and belowground (Laliberté, 2017; Freschet et al., 2021). Recent advances in root ecology suggest that plants allocate biomass to roots with different rooting depths, morphologies, and nutrient content depending on the nature of resource limitation (e.g., moisture or different nutrients) (Cusack *et al.*, 2021). For example, tropical trees have increased specific root length (SRL, cm mg^{-1}) in response to experimental drought (Metcalfe et al., 2008). Plant allocation to tissues with different traits or symbiotic associations has been represented as tradeoff frameworks. For example, the "leaf economic spectrum" describes a tradeoff in leaves with fast turnover and high nutrient content ("fast" strategy) versus slower turnover, lower nutrient content ("slow" strategy) (Wright *et al.*, 2004; Reich, 2014; Diaz *et al.*, 2016). For belowground, the "root economic space" has added a second axis to this framework (Bergmann *et al.*, 2020), including a "do it yourself" root growth strategy, versus an "outsourcing" mycorrhizal association strategy for resource acquisition. For roots, the first fast vs. slow axis has been associated with high root N content versus high root tissue density (RTD). Thus, plant allocation to different structures and symbioses belowground may depend on the availability of mycorrhizal symbionts, and soil fertility. We suggest that these tradeoffs have a particular importance under low moisture conditions, when plants benefit most

from an outsourcing, symbiotic strategy, and where higher fertility can support root specialization for water acquisition.

Changes in plant growth with drought can have downstream effects on soil C storage and cycling. First, root biomass turnover is likely the primary contributor of new C to mineral soils (Rasse *et al.*, 2005), with strong relationships between root biomass and soil C stocks across diverse tropical forests (Cusack *et al.*, 2018) and as presented in chapter 2. Second, root exudates of low molecular weight organic compounds can be an important flux of C, representing up to 10% of global NPP, into soils (Chari *et al.*, 2024). Third, root associations with fungi, such as AMF, that increase fungal hyphae in soil, can also contribute to soil C storage when hyphae turn over (Wang *et al.*, 2023). For example, AMF decreased root exudates by one tree species in a canopy-scale greenhouse drought (Biosphere 2) (Hildebrand *et al.*, 2023), while soil infertility tends to increase root exudation rates to promote nutrient mineralization across a broad range of studies (Dakora & Phillips, 2002). Thus, factors that change plant biomass allocation belowground, such as drought, or that moderate the negative effects of drought, such as nutrients and AMF, can ultimately influence the transfer of plant C into soils.

We conducted a greenhouse experiment to assess drought effects on a relatively abundant Neotropical tree seedling species, comparing interacting effects of soil fertility and AMF inoculation. We used a whole-plant approach to link changes in biomass allocation with above-belowground coordination in trait responses. We measured whole-plant C and nutrient dynamics (e.g., biomass, root:shoot ratios, photosynthetic rates), plant traits (e.g. specific leaf area [SLA, $cm^2\ g^{-1}$], SRL), and transfer of plant C into soils (e.g., root leachate, extractable soil C) to address the following hypotheses: H1) Drying decreases tropical seedling growth, but AMF inoculation and high soil fertility mitigate these effects by supporting water and nutrient acquisition; H2)

Improved seedling growth with AMF inoculation and high soil fertility under drying is related to traits that maximize soil resource acquisition and minimize moisture loss, such as high SRL with low SLA; H3) Drying suppresses root organic exudates to soils as plants prioritize water rather than nutrient acquisition, but high soil fertility supports relative increases in root exudates.

4.3 Methods

Experiment design

We conducted an experiment using a relatively abundant Neotropical tree species, *Tabebuia rosea,* grown in pots in a $^{13}CO_2$-enriched continuous labeling chamber described in Soong et al. (2014) for 4 months at Colorado State University, followed by an 8-day ^{13}C-dilution period when plants were transferred to ambient atmosphere. We assessed treatment effects of drying, fertility and AMF inoculation on measurements of plant growth, photosynthate allocation, plant traits, and C and nutrients in plant tissues, soil leachate and soil extractions.

The experiment was a full factorial design with 8 treatments including the following variables: moisture level (wet or dry), soil fertility (high-fertility and low-fertility) and AMF or no AMF (n = 10 seedlings per treatment, 80 seedlings total), with treatment details below. We used 40 pots with two seedlings each inside the chamber, arranged in a stratified design around fans and air inlet/outlet in case of temperature or humidity gradients within the chamber (Figure SI 3.1). We also grew seven pots with two seedlings each outside the chamber, receiving high fertility with both moisture and AMF inoculation treatments to produce control tissues without isotopic labels (Table SI 3.1).

Seedling and Pot Preparation

Seeds of *Tabebuia rosea* (acquired from Sheffield's Seeds, Locke, NY, USA) were soaked overnight and then planted in a 50:50 vl. mixture of sand and ceramic clay in trays. When seedlings had their first true leaves the most robust individuals were transferred into 15 L pots containing the same soil matrix. Prior to planting, pots filled with the soil matrix was repeatedly rinsed and leached with water until leachate contained dissolved organic C (DOC) levels near our detection limits (see below), such that we could assess C accumulation in the soils at the end of the experiment. The pots were prepared with one tension lysimeter each, and all pots contained a nylon 37-µm mesh bag of 25 cm x 7 cm to trap AMF biomass while excluding fine roots (roots < 2mm diameter, and with roots typically not grow < 45 µm diameter). The lysimeter and mesh bag effectively divided each pot into two compartments, such that the two seedlings in each pot were somewhat independent and were observed at the end of the experiment to have minimal root entanglement. Seedling heights when all pots were planted and put into the ^{13}C labeling chamber ranged from 1.3 to 5 cm (03/06/2020 = Day 0). Seedling height was measured from the ground level to the leaf base of the first fully expanded leaf. We counted the initial number of leaves per seedling and fertilized the pots on the same day they were transplanted prior to closing all pots into the sealed continuous labeling chamber.

Growth Chamber

The chamber was made with acrylic walls 1.2 m x 2.4 m x 3.6 m in size. A computerized IRGA control system kept CO_2 concentrations between 360 and 400 ppm during the experiment. The temperature and humidity monitoring system connected to the air conditioner and dehumidifier kept the temperature at 79 – 83 °F, and the humidity at 70 – 90%. The chamber was

outfitted with an irrigation system and pots had leachate tubes coming out of the chamber to deliver and collect water from pots without opening the chamber. Each pot was equipped with a drip irrigation ring that was connected to a pump outside the chamber to tap water. Pot leachate samples were collected from the tension lysimeters connected to collectors outside the chamber via tubing though the chamber walls. To prevent air leakage and maintain chamber integrity, all entry points for irrigation and leachate samples were sealed with silicone. CO_2 delivery was achieved through a system utilizing two CO_2 gas tanks with different ^{13}C enrichment levels. A diaphragm pump continuously circulated chamber air through an Infrared Gas Analyzer (IRGA), allowing for real-time monitoring and adjustment of CO_2 concentrations. The chamber was sealed on 03/12/2020 and opened on 06/30/2020. We measured chamber CO_2 regularly on a Δ V Advantage IRMS, coupled to a Gas Bench II (Thermo Fisher Scientific). More information about the labeling chamber can be found in Soong et al (2014).

Application of Isotopic Labels

We used a two-isotope labeling approach, using headspaces enriched in $^{13}CO_2$, and adding a ^{15}N-enriched fertilizer to all of the pots at the beginning of the experiment.

The labeling chamber was maintained at ~425 CO_2 ppm headspace (Figure SI 3.2) using enriched ^{13}C–CO_2 and kept at 3.27 ± 0.13 atom% ^{13}C (ambient atmosphere $\delta^{13}C$-CO_2 is -8‰). Plants were maintained in the sealed chamber after the initial germination period until the harvest period, at which time the CO_2 label was turned off and plants were exposed to ambient CO_2 still inside the chamber for one week until harvested, stratifying harvest dates across treatments, so that each block had a different time period of exposure to ambient CO_2 before harvesting. This time series was then used to assess uptake of ambient CO_2, incorporation into biomass, and rates of

allocation to different plant tissues.

We added a ^{15}N label (7 atom% made from $K^{15}NO_3$ 60 atom% ^{15}N) in the first two fertilization applications to all the pots to track retention rates of N over the course of the experiment. We used different addition levels for the fertile and infertile treatments. At the beginning of the experiment on 03/06/2020 we added 300 ml Hoagland solution to each pot for the fertile treatment, and 60 ml of Hoagland solution + 240 ml of DI water for the infertile treatment (i.e. 20% of nutrients added to infertile vs. fertile, suspended in the same quantity of water). The Hoagland solution contained 1M of $CaCl_2*2H_2O$, $MgSO_4*7H_2O$, $NaH_2PO_4*H_2O$ and labeled N ($K^{15}NO_3$); and also 0.04M, 0.008M, 0.008M, 0.0003M and 0.0003M of H_3BO_3, $MnSO_4*4H_2O$, $ZnSO_4*7H_2O$, $CuSO_4*5H_2O$ and MoO_3 respectively. Chemicals are all ACS, reagent grade and did not contain C. Then, we added 60 ml of the same ^{15}N labeled Hoagland solution concentration to all pots (fertile and infertile) for a second dose on the day the pots were placed inside the chamber before it was sealed (03/12/2020). The different levels of fertilization for the treatments over the first two additions results in 3x more ^{15}N added to fertile pots compared with infertile pots as an initial label.

Treatments

For the mycorrhizal treatment, we added 15 ml of AMF inoculum to holes from 0 – 5 cm at the surface of each pot prior to planting the seedlings, and we added a sterile inoculum to control pots. The live inoculum included *Claroideoglomus etunicatum*, *Rhizophagus clarus* and *Rhizophagus intraradices* AMF species (obtained from the International Culture Collection of (Vesicular) Arbuscular Mycorrhizal Fungi (INVAM) at West Virginia University).

For the moisture treatment, all pots started at 100% field capacity (FC) using initial tests

of total weight at soil saturation with no leakage. Plants were initially irrigated approximately weekly to maintain the wet treatment between 70 – 80% FC, and the dry treatment between 30 – 50% FC. Specifically, when the dry treatment reached 30% of FC, we irrigated to increase it to 50% FC to simulate infrequent rain events and then let the soil dry again to 30%. All the field capacity calculations were based on preliminary evaporation tests conducted inside and outside the chamber to test evaporation rates per day on plant-free pots. After 11 weeks in the chamber, the dry treatment did not show reduced height growth based on visual assessment, so we implemented an extended dry down, during which the dry treatment pots were not irrigated for 15 days, until leaves showed signs of turgor loss (drooping). At this point, pots from the dry treatment reached 15% FC. Then 120 ml of water was added so plants would not die and exudates could be collected. Then we kept FC between 10 – 35%. The dry treatment was then irrigated one last time (300 ml) on the first day of harvesting since plants started to wilt and we couldn`t get stomatal conductance.

For the first fertilization, only the ^{15}N-enriched solution was used for all pots (see above), but all following fertilization delivered through the chamber irrigation system was not ^{15}N-enriched. High fertility pots received the same amount of nutrients found in 300 ml of Hoagland solution per week for the first month after pots were placed inside the chamber using the irrigation system, and this was increased to the same amount of nutrients found in 350 ml, 400 ml and 450 ml of Hoagland solution on months 2, 3 and 4 respectively to account for greater nutrient requirements as the plants got bigger. For low-fertility pots, no additional fertilizer was added for 4 weeks, and then 20% of the high-fertility levels were added on weeks 5, 7 and 13, because some leaves began to show yellowing.

Leachate Collections for DOC and Total Dissolved Nitrogen (TDN)

Leachates samples were collected from the tension lysimeters connected to collectors outside the chamber as described above. Leachates samples were collected every two weeks from 03/16/2020 (Day 10) to 05/18/2020 (Day 80) from 44 pots (40 inside and 4 outside the chamber fitted with lysimeters), and then weekly from 06/01/20 (Day 94)) to 06/30/20 (Day 123), for a total of 11 leachates samples collections over the ~4-month experiment. Prior to collections, plants were first irrigated at the levels indicated above, then allowed to sit for 8 – 12 hours (overnight when possible) to provide a long enough time for roots to interact with soil water, produce organic exudates, and take up nutrients. After this period, lysimeters were placed on tension using a vacuum hand pump (Soil Moisture Equipment Corp.) and left for up to 24 hours, collecting leachates into clean Falcon tubes and Nalgene bottles. Approximately 20 mL was collected from each pot at each collection event, and then frozen until further analysis. This design yielded 484 leachates samples over four months.

Harvest Measurements

Harvesting occurred over eight days from July 2 – 9, 2020, after the headspace ^{13}C-CO_2 label was shut off on July 2 and the chamber was ventilated. Pots were selected to harvest each day in a stratified design across treatments, to allow observation of uptake of atmospheric CO_2 over the eight-day post-chamber period (i.e., replicate pots per treatment were harvested both early and later during the sampling week). This approach allowed us to observe uptake and allocation of atmosphere CO_2 to plant biomass, since the ambient CO_2 was depleted in ^{13}C relative to the growth chamber headspace. Immediately before harvesting each plant, leaf photosynthetic rates, total photosynthetic flux, maximum carboxylation rate (Vcmax), and maximum electron transport

rate (Jmax) were measured (details below). Then, during harvest individual seedlings were sampled for total root, leaf, and stem biomass. We also measured: number of leaves attached to the stem, number of cotyledons, leaf color-status, root and shoot height, number of compound leaves, number of fallen leaves, and number of nodes. Following harvest, we measured leaf and root morphological traits, and content of C, N, $d^{13}C$ and $d^{15}N$ content. We also measured total and extractable C and nutrient from soils in pots at three depths. In total, we measured ~40 seedling growth, photosynthetic, and morphological characteristics, and nutrient content of plants and soils. All harvesting details are given below.

Leaf-level Gas Exchange

We used a Li-Cor gas analyzer system (LI-6400, LI-COR Inc., Lincoln, NE, USA) to measure leaf gas exchange of light-saturated CO_2 assimilation, using a photosynthetic rate versus intercellular CO_2 concentration (A–Ci) response curves (n = 454), and the one-point method for instantaneous photosynthetic rate (n = 1901) on all 80 seedlings from our experiment. We did the measurements on 5-6 leaves per pot including old, mature, and young leaves. For the A-Ci response curves, we measured one mature leaf per pot. For the one-point method we measured from 2 – 3 leaves per plant across leaf ages. Leaf age was determined by height up the stem, with older leaves near the base and new leaves flushing near the apex. For each leaf we measured gas exchange 9 to 11 times for the one-point method. The measurements were taken from 6 am to 9:30 am immediately preceding harvesting of each plant. We set temperature in the leaf chamber to 26 ^oC, humidity to 60 – 70 %, and light to 1500 mmol m^{-2} s^{-1} for one-point measurements. For the A-Ci curves, we used internal CO_2 concentration (Ci) values in the following order: 400, 50, 100, 150, 250, 500, 700, 1000, 1500, 2250, 400 ppm. For one-point measurements, we used Ci values

of 400 ppm. We estimated the Vcmax and Jmax from the A-Ci curves using the *plantecophys* package in R; these parameters reflect the capacity of the leaf's enzymatic machinery to fix CO_2 and the electron supply for photosynthesis, respectively.

Soil Extractable DOC, TDN, and Mineral Nutrients

We separated soils from seedling A and seedling B per pot into different categories: soils from the surface (0 – 15 cm), deeper soils (15 – 30 cm) and soils within the AMF mesh sleaves (no root ingrowth was observed). Soils were then immediately extracted for soluble DOC, TDN, phosphate, nitrate+nitrite and ammonium analyses. For extractions, we weighed from 55 to 65 g of fresh, homogenized, soil for each sample into a 125 ml plastic bottle and added 97 to 103 ml of DI water. We shook samples for 1 h at 110 rpm and then filtered them through pre-rinsed Whatman No. 1 filters, collected into falcon tubes, and froze for until chemical analyses (see below). We also measured gravimetric soil moisture.

Plant Processing and Morphological Traits

After harvesting, roots were gently washed with tap water through a 0.25 mm mesh size sieve. Roots were then separated into root orders 1-2, 3, 4 and 5, with order 1 being root tips and progressing back toward the main stem at order 5. This approach is more likely to capture the different functions observed among fine root orders than the traditionally method of classifying fine roots as ≤ 2 mm in diameter (McCormack *et al.*, 2015). For simplification of some analyses root orders were then classified as absorptive (root order 1-2 and 3) versus transportive (root order 4 and 5). The four categories of root order were then scanned separately for each individual seedling (80 seedlings) using a Microtek ScanMaker 9800XL plus at 1200 dpi to assess

morphological traits. Some plants had a large quantity of roots that did not fit on the scanner screen, and some individual samples required up to 21 scans to encompass all roots, resulting in 405 total images.

Leaf area was measured on fresh leaves with an automated leaf area meter (LI-3100C; Li-Cor, Lincoln, NE, USA) for each of the individual leaves per plant.

After scanning, all plant tissues were dried in a gravity convection oven (Fisher Scientific) at 60°C until weight stabilized (at least 48 hours). Total root, stem, and leaf dry weight were then measured on a 2-place balance. Belowground:aboveground biomass ratio was calculated by dividing total root biomass by leaf + stem biomass and root:shoot biomass ratio was calculated by dividing root biomass by leaf biomass. Leaf morphological traits were calculated using leaf scans and biomass measures, including specific leaf area (SLA, cm^2/g) and total leaf area (cm^2).

Root scans were analyzed using WinRHIZO (WinRHIZO Regular, Regent Instruments, Canada) to determine root length, area, volume and diameter. Then, using information from scans together with biomass weights, root morphological traits per root order were calculated, including: total root length (cm), root tissue density (RTD, g/cm^3), specific root length (SRL, cm/mg), average diameter per order (mm), and total root length (cm). For some whole-plant analyses morphological traits such as SRL, RTD, fine root diameter, and nutrient content were averaged across root orders per plant, whereas growth traits such as root length and biomass were summed (see below).

Liquid chemical analyses

Soil extracts and leachate from lysimeters were analyzed DOC, TDN, and mineral nutrient concentrations at Colorado State University, EcoCore Facility. Liquid TOC and TDN

concentrations were measured on a Shimadzu TOC analyzer. Dissolved phosphate, ammonium and nitrate + nitrite were analyzed on a Alpkem Flow Solution IV Automated wet chemistry system (O.I. Analytical, College Station TX).

For final soil extraction samples, we analyzed TOC and TDN in a total of 176 samples for surface soils and deep soils (pot side A and B) including pots inside and outside of the chamber (44 pots) and 16 soil samples from root exclusion mesh (2 per treatment only for pots inside the chamber – only one mesh per pot available). We also analyzed 80 samples for surface and deep soils from pots inside the chamber (only for pot side A) for phosphate, ammonium and nitrate + nitrite. For soil extraction samples, we calculated C extracted divided per dry soil mass at the end of the experiment.

For the pot leachate time series samples collected over the course of the experiment, we analyzed in total 154 samples for TOC and TDN from 4 different collections spread across the course of the experiment (Day 21: 3/27/2020; Day 67: 5/5/2020, Day 82: 5/20/2020; Day 118 6/25/2020), and 39 samples for phosphate, ammonium and nitrate + nitrite together from one collection (Day 21: 3/27/2020) as above. We used measured concentrations to calculate C and nutrient fluxes into soil water (leachate) by multiplying the concentrations by the volume of water added through the irrigation system on the previous day (ml). Similar calculations were conducted for TDN, ammonium, nitrate + nitrite, and phosphate to assess nutrient retention in plants after addition via irrigation, and the measure final nutrient extraction levels. We were unable to collect leachates from one treatment (Wet+Fertile+With AMF) on the final collection date (6/25/2020). For soil leachates samples, we also calculated leached DOC and TDN divided per absorptive root biomass (g) from orders 1, 2 and 3 at the end of the experiment.

Solid Chemical and Isotopic Analyses

Plant tissues and soils were analyzed for total C and N content and isotopes. We ground all leaves separately by age per sample (young, mature and old), and root orders per sample in a Wiley mill. For chemical analyses, root orders 1-2 were combined with order 3 to produce enough material for analyses, with these three orders typically considered absorptive roots. Root orders 4 and 5 were ground and analyzed separately. Stem, root material (orders 1-3, 4 and 5), and leaves (mature) from each seedling were packed into tin capsules (0.68 to 1.59 mg tissue per sample), and then analyzed for %C, %N, ^{13}C and ^{15}N atom% on a PDZ Europa ANCA-GSL elemental analyzer interfaced to a PDZ Europa 20-20 isotope ratio mass spectrometer (Sercon Ltd., Cheshire, UK) at University of California – Davis Stable Isotope Facility. Every tenth sample was analyzed in duplicate for quality control, and if nutrient content varied >5% between samples these were re-analyzed.

Soils from pots were air dried and 147.52 to 148.45 mg were packed into tin capsules similarly to plant tissues to analyze %C, %N, ^{13}C and ^{15}N. We initially tested 18 surface soil samples for treatments with the largest plant growth (fertile and with AMF) to determine if we could detect C and ^{13}C. Soil C levels were very low and near detection limits, so we did not analyze the full set of samples considering that smaller plant would likely produce soil C below detection limits. In total, we measured 582 samples across all tissues and soils.

^{15}N Retention in Plant Tissues

To calculate the ^{15}N retention in each seedling across tissues we compared fine ^{15}N content to initial fertilization additions. In order to obtain the mass of ^{15}N in plants, we first calculated the N content for each tissue type for every seedling by multiplying the biomass of each tissue by its

%N. Then, we calculated this N mass by the corresponding ^{15}N atom%. Subsequently, we determined the ^{15}N retention for each tissue type and the total biomass of each seedling as a percentage of the initial ^{15}N added to each plant. The initial ^{15}N was calculated based on the volume of Hoagland solution used, the mass of $K^{15}NO_3$, and its molecular weight. The infertile treatment pots each received 1,132 µg ^{15}N, while the fertile treatment pots received 3,396 µg ^{15}N, and we estimated that each of the two seedling per pot accessed half of this amount. This calculation provided a %N-retention value for each seedling tissue at the end of the experiment.

Statistical analyses

We used Principal Component Analysis (PCA) and cluster analyses to assess overall patterns in the large data set of plant characteristics. All variables were scaled and centered prior to this analysis. Initial PCA were run using all measured variables. Then a targeted PCA was run using only plant characteristics. The variables used in this final PCA were: root morphology (SRL, RTD and root diameter) for root order separately, below/aboveground biomass ratios, plant chemistry (%N and %C), total plant biomass, and specific leaf area. Cluster analysis and multiple analysis of variance (MANOVA) with post hoc Hotelling's T-squared test were used to characterize the main patterns of separation among treatments. Then, we conducted an effect size analysis (mean Cohen's d values with standard errors) to determine the positive or negative main effects of drying, fertility, and AMF inoculation on each measured variable.

To assess treatment effects on seedling growth, photosynthesis, morphology, chemistry, soil extractions, and pot leachate, we used three-way analysis of variance (ANOVA) including main treatment effects of drying, fertility, and AMF inoculation. These analyses included additional predictive factors, including root order, leaf age, soil depth/location and also

interactions. Seedlings served as replicates (n=10 seedlings per treatment). For time series soil leachate data, we used repeated measures MANOVA to assess effects of time.

To assess the dilution of plant tissue ^{13}C over the post-chamber period, we calculated slopes of change in tissue $\delta\ ^{13}C$ over the 8 days for leaves, root orders 1-3, root order 4, and root order 5. We also calculated intercepts to determine $\delta\ ^{13}C$ of each tissue at time = 0 (when chamber was turned off). We then compared intercepts and slopes across plant tissue types and treatments, using main effects rather than treatment combination (wet/dry, fertile/infertile, AMF/no-AMF) in ANOVA. For example, replicates for the wet treatment were: wet+fertile+AMF, wet+fertile, wet+infertile+AMF and wet+infertile (n = 4). We conducted post-hoc Tukey HSD means separation tests to compare slopes and intercepts among significant effects. Then, to assess rates of allocation of new C from leaves to roots, we calculated slopes of $\delta\ ^{13}C$ in leaf tissue (y axis) versus in roots (x axis) using paired collections for each plant. We assessed main treatment effects and root order as predictors of these allocation slopes using ANOVA.

Statistical assumptions of normal distribution and homogeneity of variances across groups of each type of data were verified through Shapiro-Wilk and Levene's tests respectively, and diagnostic plots. Log transformations were applied when normality assumptions were not met. Variables that were log transformed are identified in statistical output tables. Outliers, most common in root trait data, were identified using the Interquartile Range (IQR) method and we excluded two from a total of 80 samples, which were for RTD from root order 1-2 that had extremely larger outliers, likely from recording error. For post hoc tests following all significant ANOVA and MANOVA we used Tukey HSD tests or pairwise comparisons. All analyses were conducted using R version 4.3.0 or JMP 17.0. Significance was set a $p < 0.05$ unless otherwise noted, and data are presented as mean ± standard error (s.e.). All raw data is shown in table SI 3.1.

4.4 Results

Overall Plant Responses to Drying, Fertility, and AMF Inoculation

Moisture, fertility, and AMF inoculation had broad-scale effects on plants and soils, with the largest and most numerous positive effect sizes resulting from fertility and AMF inoculation, and smaller and more mixed effect sizes from moisture (Figure 4.1).

Overall, plant responses sorted primarily by fertility and AMF inoculation in PCA and cluster analysis, and the separation by moisture was most apparent when combined with high fertility and AMF inoculation (Figure 4.2, Figure SI 3.3, Figure SI 3.4, Table SI 3.2, Table SI 3.3). The first two PCA axes explained 31.41% and 18.04% of the overall variation, respectively, with PC3 explaining an additional 9.54% (Figure 4.2A, Table SI 3.2). On PC1, fine root diameter was most strongly weighted against SRL, SLA, root %N and leaf %N (Figure 4.2A, Table SI 3.2). On PC2, below:aboveground biomass ratios were weighted against total plant biomass. On PC3, RTD was weighted against root %C.

In the additional PCA analysis with all plant and soil responses combined, there was a similar separation of treatments, with most axes explained by root or plant biomass characteristics (Figure SI 3.4A, Table SI 3.4). The Pearson correlation matrix with bivariate relationships illustrates some of the tradeoffs indicated on the first PCA axes (Figure SI 3.5).

Plant Growth, Photosynthesis & Carbon Allocation Patterns

Moisture, fertility, and AMF inoculation all promoted increased plant growth and influenced biomass allocation patterns over the course of the experiment, whereas only fertility and AMF inoculation were related to measure of photosynthesis at the end of the experiment, with

numerous interactions, including alleviating drying effects (details below).

Total Plant Biomass and shoot height

Total plant biomass ranged from 0.84 to 21 g, and final shoot height from 7.1 to 35 cm. Moisture, fertility, and AMF inoculation, plus the fertility*AMF interaction, were significant effects for predicting total plant biomass, for tissue types separately (Figure 4.3A, Table SI 3.5), and for shoot height (Table SI 3.5, Table 4.1). Post hoc tests revealed that high moisture, high fertility, and AMF inoculation increased total plant biomass, for each tissue type, and shoot height. AMF inoculation and fertility together resulted in the largest increases in biomass and shoot height in the interaction also alleviating drying effects supporting the first hypothesis (Table 4.1, Table SI 3.6).

Total Root Length

Total plant root length summed across all root orders ranged from 599.8 to 1989.9 21 cm. AMF inoculation was the only significant effect on total root length summed across all root orders per individual (Figure SI 3.6A). Post hoc tests revealed that AMF inoculation increased total root length. For root length by root orders separately, moisture, fertility, AMF, root order, fertility*root order, AMF*root order, and fertility*AMF were significant predictors (Table SI 3.5, Table 4.1). Further tests showed that root length increased from root order 5 < 4 < 1-2 < 3. Also, moisture, fertility and AMF inoculation generally increased root length. Most effects were for root length of 4^{th} order roots (Table SI 3.5, Table 4.1).

Total Leaf Area

Total leaf area ranged from 41.6 to 1124.3 cm^2 across all data. Fertility, AMF inoculation, and fertility*AMF and moisture*fertility*AMF interactions were significant effects for total leaf area (Figure SI 3.6B, Table SI 3.5, Table 4.1). Post hoc tests revealed that high fertility and AMF inoculation promoted greater total leaf area. The three-way interaction is illustrated in the fertile treatment, where absence of AMF led to larger leaf area in the wet treatment, but not in the dry treatment (Table 4.1).

Total Photosynthetic C Flux Per Plant

Total photosynthetic C flux per plant ranged from 0.006 to 0.63 µmol/s across all plants. Fertility, AMF inoculation, and the fertility*AMF interaction were significant effects for predicting the total photosynthetic C flux per plant at the end of the experiment (i.e., photosynthesis scaled up using leaf area, Figure 4.3B, Table SI 3.5, Table 4.2). Post hoc tests revealed that fertility and AMF inoculation increased photosynthesis, and AMF inoculation led to the largest increases in final photosynthetic C flux per plant in fertile conditions, illustrating the interaction (Figure 4.3B, Table SI 3.6).

Instantaneous Photosynthesis Rate

Instantaneous photosynthesis rate ranged from 0.18 to 9.13 µmol/m^2/s across all data. Similar to total photosynthetic fluxes, AMF inoculation, fertility, leaf age, and the fertility*AMF interaction were significant effects for instantaneous photosynthetic rates per leaf area measured at the end of the experiment (Figure SI 3.7, Table 4.2). AMF inoculation increased this rate, while fertility decreased it. Plants with no AMF in fertile conditions had the lowest photosynthetic rates,

illustrating the interaction (Table 4.2). Young leaves typically had the highest photosynthetic rates, and old leaves had the lowest (Figure SI 3.8, Table SI 3.1).

Vcmax and Jmax

AMF inoculation and the fertility*AMF interaction were significant effects for Vcmax and Jmax (Figure SI 3.8, Table 4.2). Post hoc tests showed increases in both parameters with AMF, with the largest increases in fertile conditions, and the lowest values in fertile conditions without AMF compared to all infertile conditions (Table 4.2).

Biomass Allocation

Belowground/aboveground biomass ratio ranged from 0.17 to 1.09 across all data. Fertility and the moisture*fertility*AMF interaction were significant predictors of below:aboveground biomass ratios and root:leaf biomass ratios (Figure SI 3.9 Table SI 3.5, Table 4.1). Post hoc tests revealed that infertile soils had higher ratios compared to fertile soils, with the root:leaf ratio typically >1 in infertile soils (Figure SI 3.7). The highest ratios were in infertile, wet conditions without AMF, while the lowest ratios were in fertile, wet conditions without AMF, illustrating the interaction and also the dominant influence of fertility on these ratios.

Real-time allocation of C to plant tissues

Assessing changes in plant tissue $\delta\ ^{13}C$ over the 8-day post-chamber period showed that leaf, shoot and root tissues generally declined its $\delta\ ^{13}C$, indicating uptake of ambient CO_2 (less enriched in $\delta\ ^{13}C$ than the label used in the chamber), and incorporation of ambient CO_2 into biomass on this time-scale (Figure SI 3.10). Assessing differences in these slopes among

treatments and plant tissues, moisture and tissue had significant effects, with marginal effects of fertility ($p = 0.09$) and AMF ($p = 0.1$), and no interactions. Comparing the slopes of dilution over time, the shallowest rate of change in $\delta^{13}C$ over time was for fine roots orders 1-3 ($\delta^{13}C$ -27.5 ± 9.7 ‰/day), and the fastest rate of change was for leaves ($\delta^{13}C$ -52.7 ± 12.3 ‰/day) and shoots ($\delta^{13}C$ -56.9 ± 12 ‰/day) (Table 4.3, Table SI 3.8). Comparing treatments, rates of change over time were significantly faster for the dry ($\delta^{13}C$ -63.7 ± 7.7 ‰/day) versus wet ($\delta^{13}C$ -22.8 ± 3.4 ‰/day) treatment across plant tissues, and marginally faster in infertile ($\delta^{13}C$ -49.8 ± 8.3 ‰/day) versus fertile ($\delta^{13}C$ -36.7 ± 6.5 ‰/day) treatments ($p = 0.1$).

We assessed the slopes of $\delta^{13}C$ of leaves versus paired $\delta^{13}C$ of roots within each plant to further explore the allocation patterns of C from leaves to roots over the post-chamber 8-day period. There was no effect of root order, so we used average root values to create these relationships. Moisture was the only significant effect on ^{13}C leaf versus ^{13}C root slopes, such that there was a positive relationship for ^{13}C leaf versus ^{13}C root dilution in dry treatments, but no relationship in wet treatments (Figure 4.4), with average slopes across dry treatments of 0.57 ± 0.1 leaf‰/root‰, and across wet treatments of 0.24 ± 0.07 leaf‰/root‰ ($n = 4$ replicate slopes per main effect) (Table 3, Table SI 3.8). That is, in dry treatments, as leaves declined in $\delta^{13}C$ over the post-treatment period, some of this new C was apparently allocated quickly to roots leading to also declines in root $\delta^{13}C$. In contrast, dilution of leaves and roots in the wet treatment appeared to proceed independently, which could be related to the relatively slow rate of change in the wet treatment over time (see above).

We assessed the intercepts of the regressions for $\delta^{13}C$ of plant tissues versus time as an indication of the amount of enriched C across plant tissues (i.e. intercept = t0, or $\delta^{13}C$ content of each tissue on the day the atmospheric label was turned off). There were significant effects of plant

tissue type, AMF, marginally significant effect of moisture, and interactions with tissue type in predicting plant tissue $\delta^{13}C$ at the end of the labeling experiment (Table 4.3, Table SI 3.8). Leaves ($\delta^{13}C$ 2219 ± 23 ‰) had the highest $\delta^{13}C$ at the end of the labeling experiment, followed by shoots and higher order roots, with the lowest $\delta^{13}C$ in fine roots orders 1-3 ($\delta^{13}C$ 2099 ± 25 ‰). Thus, leaves were most similar to the $^{13}CO_2$ in the chamber headspace, while the newest roots had less enriched tissues. Assessing treatment effects and interactions with tissues, the most consistent effect was that plants with AMF had significantly more ^{13}C enriched root and shoot tissues compared with the no-AMF treatment, but leaves didn't have differences in enrichment in treatments without AMF versus with AMF. Drying tended to increase ^{13}C enrichment across tissues, but the effect was not always significant.

Plant Morphology & Chemistry

Moisture, soil fertility, and AMF inoculation had effects on both leaf and root morphology, with numerous interactions (details below). Overall, the high moisture treatment had smaller SLA, lower SRL and larger root diameter, but these effects were moderated by fertility and AMF.

Specific Leaf Area

Specific leaf area ranged from 103.4 to 476.2 cm^2/g across all data. Fertility, AMF inoculation, moisture*AMF and fertility*AMF were significant effects for SLA (Figure 4.5A, Table 4.4). Post hoc tests revealed that soil fertility increased SLA and AMF inoculation decreased it. Drier conditions had generally higher SLA, but this was most pronounced when AMF was present, illustrating the interaction. Also, the absence of AMF combined with high fertility led to the largest SLA, regardless of moisture (Figure 4.5A, Table SI 3.6).

Specific Root Length

Specific root length ranged from 0.02 to 16.52 cm/mg across all data. Moisture, fertility, AMF inoculation, root order, moisture*AMF, fertility*root order, and AMF*root order were significant effects for SRL (Figure 4.5C, Table SI 3.5, Table 4.4, Figure SI 3.11). Post hoc tests revealed that moisture, fertility and AMF inoculation decreased SRL. SRL decreased as root order increased. AMF had the strongest negative effect on SRL affecting all root orders. Fertility and AMF affected decreased SRL only in larger root orders (Figure 4.5C), and drying tended to decrease SRL for root order 5 (Figure 4.5C, Figure SI 3.11). AMF increased SRL in dry treatments more than in wet treatments, illustrating the interaction (Table 4.4).

Root Diameter

Root diameter ranged from 0.26 to 4.2 mm across all data. Moisture, fertility, AMF inoculation, root order, moisture*AMF, fertility*AMF, moisture*root order, fertility*root order, and fertility*AMF*root order were significant effects for root diameter (Figure 4.5E, Table SI 3.5). Post hoc tests showed that moisture, fertility, and AMF inoculation all led to larger root diameter. AMF inoculation in wet, fertile treatments had the largest root diameter within each root order, with overall larger diameter for higher root orders (Figure SI 3.12, Table 4.4). The smallest diameters were typically in dry, infertile treatments across orders.

Root Tissue Density

Total plant biomass ranged from 0.05 to 1.58 cm^2/mg. Fertility, AMF inoculation, root order, fertility*AMF, fertility*root order, AMF*root order, and fertility*AMF*root order

interactions were significant effects for RTD (Table SI 3.5). Post hoc tests revealed that RTD increased with AMF inoculation in particular, and was somewhat higher in infertile treatments (Figure 4.5F). The positive effect of AMF on RTD was strongest in infertile conditions for lower root orders (1-3) (Figure SI 3.13, Table 4.4).

Carbon and Nitrogen Content in Plant Tissues

Root %N ranged from 0.44 to 3.16 %. Fertility, AMF inoculation, root order, moisture*fertility, moisture*AMF, and moisture*fertility*AMF*order were significant effects in the analysis of %N in roots (Figure SI 3.14, Table SI 3.5, Table 4.6). Post hoc tests revealed that root %N increased with high fertility and decreased with AMF presence across root orders (Figure 4.5D, Figure SI 3.14). Root %N also decreased as root order increased (Figure SI 3.14). Root %N was greatest in the wet, fertile treatment with no AMF.

Leaves %N ranged from 0.86 to 4.85 %. Leaves %N responded to treatments similarly, with a larger effect of fertility and more consistent declines in %N with AMF inoculation across moisture treatments (Figure 4.5B, Table 4.6, Table SI 3.5).

Shoot %N ranged from 0.15 to 2.35 %. Fertility and AMF inoculation were similarly significant effects in the analysis of %N in shoots, without interactions, with fertility increasing shoot %N and AMF decreasing it (Table 4.6, Table SI 3.5).

Root %C ranged from 36.4 to 61.9 %. Root order and the fertility*root order interaction were significant for predicting %C in roots (Table SI 3.5). There was higher %C in lower versus higher root orders, and higher root %C under infertile versus fertile conditions (Figure SI 3.16, Table 4.6).

Leaves %C ranged from 40.7 to 51.2 % and shoot %C from 32.8 to 63.2 %. There was no

significant effect of treatments on shoot %C and only a marginally significant effect of fertility on leaf %C (Table 4.6, Table SI 3.5).

Root C/N ratio ranged from 17.6 to 100.1. Fertility, AMF inoculation, root order, moisture*AMF, fertility*AMF, AMF*order, and moisture*fertility*AMF were significant effects for root C:N ratios (Table SI 3.5). High fertility decreased root C:N ratio, while AMF inoculation increased root C:N ratio, particularly for higher root orders (4 and 5) (Table 4.6).

Leaves C/N ratio ranged from 9.4 to 50.8. Moisture, fertility, AMF inoculation, moisture*fertility, moisture*AMF, and fertility*AMF significantly affected the C:N ratios of leaves (Table SI 3.5). Fertility decreased leaf C:N ratios, while AMF inoculation and moisture increased leaf C:N ratio. AMF inoculation and moisture availability interacted differently under high fertility (Table 4.6).

Shoots C/N ratio ranged from 20.8 to 277.2. Fertility and AMF inoculation significantly affected the C/N ratio of shoots, with post hoc tests revealing that fertility decreased C/N ratio while AMF inoculation increased it (Table SI 3.5, Table 4.6).

Proportion of $\delta^{15}N$ Retention in Plant Tissues

The proportion of plant $\delta^{15}N$ retention is the percentage of $\delta^{15}N$ that was retained in plants, instead of leaching in the beginning of the experiment. Across all plant tissues, it ranged from 12 to 100%. Fertility, AMF inoculation, plant tissue type, fertility*AMF, fertility*plant tissue, AMF*plant tissue and water*fertility*AMF*plant tissue were significant effects for predicting the percent retention of ^{15}N added at the beginning of the experiment (Table SI 3.5). Post hoc tests revealed that both fertility and AMF inoculation increased ^{15}N retention. Also, retention was larger in leaf tissues, followed by root order 1-3, root order 5, shoots, and finally root order 4 (Figure

4.6).

Subsequent tests for each plant tissue separately revealed that for root order 1-3, the only significant predictor of ^{15}N retention was AMF inoculation (Table SI 3.5), which increased retention. For leaves, both fertility and AMF inoculation were significant predictors of ^{15}N retention, both increasing retentions. For the whole plant, shoots and root order 4, AMF inoculation, fertility and fertility*AMF were significant predictors of ^{15}N retention, with the largest retention in the fertility + AMF treatment (Figure 4.6). For root order 5, moisture, AMF inoculation, fertility, fertility*AMF and moisture*fertility were significant predictors of ^{15}N retention. Post hoc tests revealed that moisture decreased ^{15}N retention in this largest root order, while AMF inoculation and fertility increased retention (Figure 4.6).

Leached Dissolved Organic Carbon, Total Dissolved Nitrogen, and Nutrients

Across our time series of leachate collections, high fertility generally increased DOC and TDN fluxes from pots, whereas AMF inoculation decreased both. High moisture increased DOC in the beginning of the experiment, while drying increased DOC in the end. High moisture and fertility also decreased the C:N ratio of leachate from pots, whereas AMF tended to increase this ratio.

Leached DOC

Moisture, fertility, AMF inoculation, time, and moisture*time were significant effects in the repeated measures analysis of total leached DOC at each time point (mg, scaled up according to irrigation water added the day before) (Figure 4.7, Table SI 3.5, Table 4.7). Post hoc tests revealed that moisture and fertility increased leached DOC overall, while AMF inoculation

decreased DOC leaching. Leached DOC also generally increased with time. The interaction occurred because initially, drying decreased leached DOC (Days 21 [3/27] and 67 [5/5]), but this trend reversed toward the end of the experiment (Day 118 [6/25]), when dry treatments had more leached DOC (Table SI 3.6).

Fertility and AMF inoculation were significant effects in the analysis of the time series of leachate DOC concentrations (mg/L) without interactions (Table SI 3.5). Post hoc tests revealed that fertility increased leachate DOC concentrations, and AMF decreased it across all dates (Table 4.7). There was no time effect on leachate DOC concentrations.

For the final time point, fertility was the only significant main effect for leached DOC per absorptive root biomass (mg C/g absorptive root) (Figure SI 3.17A, Table 4.7). Post hoc tests revealed that fertility increased leached DOC per absorptive root biomass and AMF marginally decreased.

Leached TDN

Moisture, fertility, fertility*AMF inoculation, moisture*time, fertility*time, and AMF*time interactions were significant effects in the analysis of total leached TDN (mg, scaled up according to irrigation water added to pots the day before, Figure SI 3.18, Table SI 3.5, Table 4.7). Post hoc tests revealed that moisture and fertility both increased leached TDN, and leached TDN was largest in high moisture during the first part of the experiment (Days 21 [3/27] and 67 [5/5]). AMF inoculation decreased leached TDN only for the last collection date (Day 118 [6/25]).

Similarly, moisture, fertility, fertility*AMF inoculation, fertility*time, and AMF*time interactions were significant effects in the analysis of the time series of leached TDN concentration (mg/L) (Table SI 3.5, Table 4.7). Moisture and fertility both increased leached TDN

concentrations, while AMF decreased leached TDN only for the last collection date (Day 118 [6/25]).

For the final time point, fertility and AMF inoculation were significant effects for leached TDN per absorptive root biomass (mg N/g absorptive root, Figure SI 3.17B, Table 4.7). High fertility increased leached TDN per absorptive root biomass, while AMF inoculation decreased it.

Leachate C:N Ratios

Moisture, fertility, fertility*AMF inoculation and AMF*time interactions were significant effects in the time series of leachate C:N ratios (Table SI 3.5, Table 4.7). Post hoc tests revealed that high moisture and fertility both decreased leachate C:N ratios, and AMF increased leachate C:N ratios on the last date of collection (6/25). There was no overall time effect on leachate C/N ratio.

Leached Mineral Nutrients

Overall, drying decreased total leached phosphate, and increased phosphate concentrations in leachate when AMF was absent. Fertilization decreased total leached phosphate and phosphate concentrations. High fertility also increased leachate nitrate+nitrite concentrations, particularly when AMF were present.

Specifically, moisture, fertility, and moisture*fertility were significant effects for predicting leached phosphate (mg, scaled up using irrigation water volume added the day before) (Table SI 3.5) on Day 21 of the experiment, but there were no significant effects for leached ammonium (mg) or nitrate+nitrite (mg) (Table SI 3.5, Figure SI 3.19). Post hoc tests revealed that moisture increased total leached phosphate while fertility decreased it. The leached phosphate was

lowest in dry conditions independent of fertility, intermediate in wet-fertile treatments, and highest in wet-infertile treatments (Table 4.7, Figure SI 3.19).

For the leachate phosphate concentrations (mg/L), fertility, and moisture*AMF were significant effects (Table SI 3.5). Post hoc tests revealed that fertility decreased leachate phosphate concentrations. The interaction between moisture and AMF occurred because drying increased phosphate concentration when AMF was absent (Table 4.7). There were no significant effects for predicting ammonium concentration (mg/L) (Table SI 3.5, Figure SI 3.19). Fertility and fertility*AMF were significant effects for nitrate+nitrite concentration (mg/L) (Table SI 3.5). Post hoc tests revealed that high fertility increased nitrate+nitrite concentration and the largest concentration was observed in the presence of high fertility and AMF.

Soil Extractable DOC, TDN, and Nutrients

At the end of the experiment, soil extractable DOC and TDN were greatest in the soil surface. Moisture tended to increase extractable DOC, while fertility decreased extractable DOC and increased extractable TDN. AMF inoculation decreased extractable TDN, with details as follows.

Fertility and soil location were significant effects for extractable DOC (mg C/kg dry soil), without interactions (Figure SI 3.20A, Table SI 3.5, Table 8). Post hoc tests revealed that fertility decreased extractable DOC, with the least extractable DOC in soils within the root exclusion mesh, intermediate in deep soil, and largest in surface soils, suggesting accumulation of DOC near the surface. Moisture had a marginal positive effect on extractable DOC ($p = 0.09$) (Table SI 3.6).

Fertility, AMF inoculation, soil location, fertility*AMF, fertility*soil location, and AMF*soil location interactions were significant effects for extractable TDN (mg N/kg dry soil)

(Figure SI 3.20B, Table SI 3.5, Table 4.8). Post hoc tests revealed that high fertility increased extractable TDN, while AMF inoculation decreased it. Extractable TDN was least in deeper soil, intermediate within the root exclusion mesh, and largest at surface soil. The largest levels of extractable TDN were in fertile conditions without AMF, followed by fertile conditions with AMF, and then in infertile conditions.

Fertility, AMF inoculation, soil location, and fertility*AMF were significant effects for predicting soil extractable DOC:TDN ratios (Table SI 3.5, Table 4.8). Post hoc tests revealed that fertility decreased soil extractable DOC:TDN ratios, and AMF increased them. The extractable DOC:TDN ratios were smallest at surface, intermediate within the root exclusion mesh, and largest at deeper soil. Soil extractable DOC:TDN ratios were largest overall in infertile treatments with AMF.

Fertility, AMF inoculation, and soil location were significant effects for predicting soil extractable nitrate + nitrite (mg nutrient/kg dry soil) without interactions (Figure SI 3.21, Table SI 3.5, Table 4.8). Post hoc tests revealed that fertility increased and AMF inoculation decreased extractable nitrate+nitrite. Extractable nitrate+nitrite levels were smallest in deeper soil, intermediate within the root exclusion mesh, and largest at surface soil. There were no significant predictors of soil extractable ammonium (mg nutrient/kg dry soil) (Figure SI 3.21, Table SI 3.5, Table 4.8).

Fertility, soil location, and fertility*soil location were significant effects for soil extractable phosphate (mg nutrient/kg dry soil) (Figure SI 3.21, Table SI 3.5, Table 4.8). Post hoc tests revealed that fertility increased extractable phosphate, and there was the least extractable phosphate in deeper soil, and most in surface soil and within the root exclusion mesh.

Final Soil C, N, and Moisture

At the end of the experiment a subset of 16 surface soils were analyzed for total nutrient content, including wet+fertile+AMF and dry+fertile+AMF treatments to maximize plant growth and likelihood of transfer of plant tissues into soils. In these initial analyses there was no differences in total soil %C, %N, C:N ratio, ^{13}C or ^{15}N between the treatments, and levels were very low (e.g., < 0.05% C or N, Figure SI 3.22, Table SI 3.5, Table SI 3.9), such that we decided not to analyze other treatments with smaller plants.

Final gravimetric soil moisture (g water/g dry soil) was measured at harvest, and AMF inoculation, fertility, soil location, moisture*fertility, AMF*fertility, and fertility*soil location were significant effects (Table SI 3.5). Post hoc tests revealed that both fertility and AMF inoculation decreased soil moisture. However, the moisture treatment itself did not have consistent effects on final soil moisture, despite the lower irrigation level and the prolonged drought near the middle of the experiment that results in plant wilting (see Methods). By the end of the experiment, drying treatment plants were smaller, so water use was likely greatly reduced, resulting in underutilization of water. The smallest soil moisture was in surface soil, followed by deep soil and then within root exclusion mesh (Table 4.8).

4.5 Discussion

Flexibility in Tropical Seedling Growth and Traits with Changing Resources

This study illustrates the flexibility of a tropical seedling growth, C and N allocation, morphology, and nutrient use under changing resource conditions. The PCA and cluster analyses illustrate the flexibility of different plant characteristics with different changes in resources. For

example, PC1 showed an apparent tradeoff between fine root diameter vs. SRL, SLA, and %N in leaves, stems, and roots, but these traits responded differently to the three main treatments and their interactions. In particular, high moisture, fertility, and AMF all promoted larger plant biomass, larger root diameter, and lower SRL, especially in larger root orders, but other plant traits had varying responses to the three treatments. Specifically: high moisture promoted larger C/N ratio in leaves and lower percentage of $\delta^{15}N$ retention in larger root orders; high fertility promoted higher SLA, lower below/aboveground biomass ratio, higher plant %N and percentage of retention of ^{15}N in proportion of the amount added, smaller C/N ratios, and higher plant photosynthesis; AMF inoculation promoted higher RTD, lower SLA, lower SRL, lower %N and larger C/N ratios across most plant tissues, larger $\delta^{15}N$ retention in plant tissues, and higher plant photosynthesis.

Thus, the main traits to respond uniformly to the treatments were biomass, root diameter, and SRL, with high resource conditions promoting larger biomass and diameter, and smaller SRL. Larger fine root diameter could serve several functions under higher resource conditions. Larger diameter in the presence of AMF may serve to optimize the root habitat via larger cortex area for AMF to colonize, as shown in subtropical and temperate ecosystems (Brundrett, 2002; Kong *et al.*, 2014; Valverde-Barrantes *et al.*, 2016). Larger root diameters can also facilitate transport of water and nutrients under higher resource conditions (El Amrani, 2023). Thinner, longer roots with lower tissue density have high SRL, which is thought to help absorb more nutrients and water per biomass invested (Ostonen *et al.*, 2007; Freschet *et al.*, 2021), and with less metabolic costs (El Amrani, 2023), making larger SRL a common adaptation to resource scarcity. In our experiment, lower resource conditions promoted smaller diameter and larger SRL roots (i.e., longer and thinner), indicating that plants optimized biomass investment belowground to structures specialized for resource acquisition. Interestingly, while AMF were associated with lower SRL

roots, they also promoted larger total root length, which can promote larger soil exploration in addition to the hyphae per se. Aside from biomass, fine root diameter, and SRL, other plant characteristics were variable in their flexibility depending on the nature of resource change.

Drying Effects on Seedling Growth

Overall, drought as a main effect shifted key aspects of seedling growth and development, although effects were not a large or broadly distributed across seedling characteristics as the effects of fertility and AMF.

First, drying reduced overall seedling plant growth, with similar effects across plant tissues. Second, although drying only had a complex interacting effect on belowground/aboveground ratios (i.e., biomass allocation), drying was the main significant effect predicting the rate of ^{13}C-dilution for all plant tissues over the post-chamber period, with a marginal effect of fertility, such that dry and infertile plant tissues were diluted more quickly by fixed atmospheric CO_2 relative to their biomass over time. Drying was also the only main effect on the relationship between leaf versus root ^{13}C-dilution during our post-chamber period. The positive relationship between leaf and root ^{13}C dilution in drying treatments but not in wet treatments illustrated active allocation of newly fixed C to both leaves and roots in the dry-treatment seedlings. In contrast, the flat line for leaf versus root ^{13}C in the wet treatment indicates little dilution in leaves, but active dilution of roots.

There are explanations for these drying effects on real-time C uptake and allocation. First, the plants grown in wet conditions, particularly with nutrients and AMF, were larger, and thus had a larger stock of ^{13}C-enriched biomass to dilute during the post-chamber phase. However, these

plants also had higher final photosynthesis flux per plant, so it is not clear that dilution should have been slower just because of larger biomass. Also, these larger high moisture plants showed active dilution in roots, which had approximately the same biomass as leaves in these plants (root:leaf ratios ~1). It is also possible that these plants respired more of the current photosynthates. Alternatively, the more stressed dry (and infertile) plants could have retained more of the CO_2 fixed as sugars and starches to be distributed throughout the plant, rather than releasing these via respiration. On average, 67% of the CO_2 fixed by the leaves can be allocated to starch production, but this proportion varies greatly depending on growing conditions (Livingston & Medes, 1947). There could also be a difference in the use of stored versus fresh C across the treatments. For example, stored C compounds can support fine root growth in broadleaved species (Gaudinski *et al.*, 2009) and leaves growth in in oaks (Vizoso *et al.*, 2008), whereas more recently fixed C is often used for active metabolism, such as respiration (Epron *et al.*, 2012). The larger wet plants had more biomass to dilute, and likely had more stored C to support new growth in leaves, which did not dilute over the 8-day period. In contrast, the smaller, more stressed dry plants were clearly actively using newly fixed C for both leaf and fine root growth over this period.

Third, as noted above, drying influenced some plant morphological and nutrient characteristics, with drying decreasing root diameter, increasing SRL, decreasing leaf C/N, and increasing ^{15}N retention for older fine roots (5^{th} order). The lower leaf C/N and higher ^{15}N retention in older roots are likely indicative of less N leaching in the drying treatments, since excess moisture can promote nutrient leaching particularly when root systems are small, such as observed in an irrigation experiment with young avocado trees (Kiggundu *et al.*, 2011). Also, these responses could be a consequence of that these tissues (mature leaves and older roots) were formed when the labeled N was applied Relatedly, drying also shifted C and N leaching, with less total leached

DOC early in the experiment, less leached TDN throughout, and increased leached DOC, but suppressed soil extractable DOC at the end of the experiment. The less leaching of TDN may be related to larger uptake of N in the dry treatments such as indicated by the higher ^{15}N retention supporting the lower leaf C/N.

Somewhat surprisingly, drying as a main effect did not lead to broader changes in seedling characteristics, such as photosynthetic capacity, other leaf and root morphological traits, or general plant nutrient content and stoichiometry. Nonetheless, drying effects were substantial in some cases, which can shed light on how this tropical tree species might respond to climatic drying or droughts.

Drying Effects on Seedlings Moderated by Soil Fertility and AMF Inoculation

In general, drought had the fewer and weaker main effects on seedling growth and physiology compared to fertility and AMF effects. However, there were many instances of significant interactions of drought with these other main effects, indicating the strong mediating effects of fertility and AMF on seedling growth. Specifically, drought had significant interacting effects on: total leaf area (3-way), below/aboveground ratio (3-way), root/leaf ratio (3-way), SLA (with AMF), SRA (with AMF), root C/N (3-way), leaf C/N (3-way), and leached total phosphate (with AMF). In the interactions with AMF, drought typically had an effect except in the presence of AMF. For example, drying increased SLA, but the AMF inoculation greatly muted this effect, driving SLA down. Drying increased phosphate leaching fluxes, except when AMF were present, presumably because AMF promoted retention of nutrients (see below). The three-way interactions were more complex, such as drying alone increased belowground/aboveground and root/leaf ratios in fertile conditions, but addition of AMF reversed this trend. Clearly, the presence of AMF, and

the abundance of soil nutrients, can have a large influence on how seedling characteristics respond to drying.

AMF Effects on Drought Resistance

Our results suggest that AMF were the most important factor promoting plant growth, final photosynthesis flux per plant, photosynthetic rates, and shifts in morphology, and that AMF effects were greatest under high fertility. For example, the largest plant growth was in wet conditions with high soil fertility and AMF, and this was followed closely by plant growth in dry conditions with high soil fertility and AMF supporting out first hypothesis, with much lower growth when AMF were not present across other conditions. A review of >200 studies on AMF effects on plant water balances, AMF generally improved growth, yield and survival in dry treatments through increased access to water, often also associated with increases in plant P (Augé, 2001). Two recent reviews summarize mechanisms by which AMF can increase plant drought resilience, including fungal water absorption and transport, root morphological modifications, increased leaf enzyme and photosynthetic activity, antioxidant defenses, and osmotic adjustments (Kuyper & Jansa, 2023; Das & Sarkar, 2024). A recent greenhouse study with tree species from karst ecosystems in China found that AMF inoculation had a positive effect on plant biomass and growth under dry conditions (Zhang *et al.*, 2019). We also observed that AMF increased SRL in dry treatments more than in wet treatments which aligns with a previous controlled study showing that AMF improved drought tolerance of tea plants by changes in root architecture and hormones (Liu *et al.*, 2023).

Fertility Effects on Drought Resistance

Fertility alone can also mediate the effects of drought on plants. Plants in low moisture

soils in our experiment had positive growth effects with high fertility, although these were not as large as the AMF effects. Fertility can promote drought resistance in plants when they accumulate nutrient reserves, as reviewed in Grossnickle and MacDonald (2017). In agricultural settings, high fertility mitigated seedlings drought stress by increasing plant biomass and photosynthetic rates in tomato (Ahanger *et al.*, 2021), and increasing plant biomass in maize (Studer *et al.*, 2017). Under infertile conditions, plants in our study had overall less growth but larger belowground/aboveground and root:leaf ratios. This follows patterns from a broad meta-analysis across ecosystems assessing nutrient effects on biomass allocation (Poorter *et al.*, 2012). A study of maize seedlings found that fertilization decreased the root:shoot ratio only in well-watered treatment, with no effect in dry treatments (Studer *et al.*, 2017). Our study did not find the interaction with drying.

For plant inputs of C to soils in the end of the experiment, when C fluxes to soil were larger, fertility greatly increased leached DOC, exacerbating positive drying effects on increasing leached DOC toward the end of the experiment, with the largest leaching of DOC in fertile, dry treatments. The greater leachate in high fertility soils could be related to larger root biomass overall, exposing more root surface area for exudation or leaching, however fertile treatments had higher leachable DOC even per gram of root biomass for the final time point. Typically, infertility has been associated with more root C exudation, such as in a review across the Amazon Basin, where plants in infertile, low-P soils had larger fluxes of root exudation compared with high-fertility soils (Reichert *et al.*, 2022), presumably as a strategy to promote microbial activity and nutrient mineralization in the rhizosphere. It is not clear why high fertility promoted DOC leaching in our experiment, except that perhaps photosynthetic production surpassed biomass growth demands in these plants (Prescott, 2022). The higher DOC leaching from dryer soils in the end of the

experiment could indicate a stress response or a reduced microbial respiration of the exuded DOC, following a positive drought effect on *Quercus ilex* root C exudation in a different greenhouse experiment, and a positive effect on aspen root exudation under drought, cold, and shade (Karst *et al.*, 2017). Also, larger SRL, as found in our low-resource treatments (drying), has been found to be positively related to root C exudation (Jiang *et al.*, 2022). Thus, high fertility seems to have exacerbated a positive drying effect on leachable DOC in our study, which might reflect root exudates, but the mechanisms behind the fertility effect are not entirely clear.

These leaching trends are in contrast with soil extractable DOC at the end of the experiment, which was significantly lower in fertile treatments and tended to be lower in dryer treatments. The high soil extractable DOC in infertile soils might indicate an accumulation of root exudates or turnover, with this measure more indicative of cumulative effects that the leaching data which gave 24-hour snap shots.

Interacting Effects of AMF and Soil Fertility on Seedling Characteristics

In our study, some of the largest positive effect on plant growth and photosynthesis were with high fertility and AMF inoculation applied together, whereas as each added to drought alone typically had smaller effects. For example, positive AMF effects on growth and plant traits were largest in the presence of high fertility, also pointing toward the role of AMF in helping plants acquire and retain nutrients. We saw positive effects of combined AMF and fertility, which were often nearly as large in dry compared with wet treatments. That is, AMF plus nutrients helped plant growth nearly overcome negative effects of drying. These data suggest that the primary role of AMF in this study was in relation to improving plant nutrition and nutrient retention, rather than AMF effects on hydration. This helps explain why the AMF effects were so large in fertile

treatments (when they could acquire nutrients for their hosts), and much smaller in infertile treatments. Nonetheless, even in infertile treatments, the presence of AMF increased plant growth at higher moisture, suggesting that they also play a role in plant hydration, although in this case it was much smaller than for plant nutrition.

Similar to our study, drought inhibited growth and development of *Alhagi sparsifolia* seedlings in a greenhouse experiment in China, but when these seedlings were inoculated with AMF and fertilized with N there was a large plant growth height and biomass, high N content and photosynthetic capacity even under drought (Aili *et al.*, 2023). A greenhouse experiment in Malaysia with *Acacia mangium* also showed that high fertility combined with AMF led to more plant biomass across tissue types and taller shoot heigh compared with each factor added alone (Jeyanny *et al.*, 2011).

Fertility is very well known to increase photosynthesis, especially because N is a critical element in chlorophyll production (Evans, 1989; Evans, 2013), and we saw expected increases in final photosynthesis flux per plant, and plant tissue %N with high fertility in our experiment. However, the strong positive effects on photosynthetic capacity were dependent on the presence of AMF. AMF inoculation similarly increased photosynthetic capacity in a greenhouse experiment with *Ipomoea carnea* (Amaya-Carpio *et al.*, 2009), and *Zea mays* under drought stress (Zhu *et al.*, 2012). A meta-analysis indicated that positive effects of AMF on photosynthetic rates are likely related to improving host nutrition (Auge *et al.*, 2016). At the same time, AMF can consume up to 20% of plant-fixed C, as shown in a $^{14}CO_2$ labeling experiment with *Cucumis sativus* (Jakobsen & Rosendahl, 1990), which can also promote plants with AMF symbionts to increase photosynthetic rates and reduce storage of photosynthate, as shown in a greenhouse experiment also with *Cucumis sativus* (Gavito et al., 2019). The positive effect of AMF on host nutrition, when there are nutrients

available, explains why we saw large interacting effects of fertility and AMF on photosynthetic rates.

Fertility was associated with larger SLA, which increases light capture per biomass investment in leaves (Westoby *et al.*, 2000). However, the smaller SLA (thicker leaves) with AMF inoculation in our study was actually associated with higher final photosynthesis flux per plant, photosynthesis rate, Jmax and Vcmax, possibly because of higher chlorophyll content per unit area in these smaller SLA leaves (Marenco *et al.*, 2009), which is supported by the higher leaf %N in the AMF treatments.

AMF Promotes Plant Retention of Nutrients and Reduces Leaching Losses

Our data point toward improved plant nutrient retention in the presence of AMF, including reduced leaching losses of TDN, mineral N, and phosphate, reduced extractable TDN and nitrate+nitrite, as well as higher plant tissue %N and ^{15}N retention. Similar to our results, a greenhouse experiment in Japan showed that AMF colonization reduced plant N losses, while increasing leaf chlorophyll content and plant dry mass (Sarkar *et al.*, 2015). AMF and fertility also increased retention of the ^{15}N label added at the beginning of the experiment. The decreased leached N in AMF inoculation treatments suggest that AMF fungi was increasing plant N retention (Smith & Read, 2008). Our observation is aligned with other experiments showing that AMF can significantly reduce plant nutrient losses (Bender *et al.*, 2015; He *et al.*, 2021).

Treatment Effects on Plant $\delta^{13}C$

The differences in plant tissue $\delta^{13}C$ when the labeling chamber was turned off (i.e., t=0 for post-incubation dilution) most likely resulted from C isotope fractionation through plant

metabolism, and transportation with the most depleted $\delta^{13}C$ in the youngest fine roots (orders 1-3) (Farquhar *et al.*, 1989). Our results follow other ^{13}C labeling experiments differences in tissues. For example: wheat at the elongation stage also had the highest $\delta^{13}C$ values in leaves followed by stems (Sun *et al.*, 2019); wheat, pea and vetch labeled plants had higher $\delta^{13}C$ values in shoots versus roots (Tahir *et al.*, 2018); *Ceiba pentandra* trees had higher $\delta^{13}C$ values in leaves, followed by stems, and then roots (Mannerheim *et al.*, 2020).

An interesting aspect of this data is the significant effect of AMF and moisture treatments on the differences in $\delta^{13}C$ across tissues, with AMF promoting relatively ^{13}C-enriched root and shoot tissues, with no changes on leaves $\delta^{13}C$, compared with the no-AMF treatment. Also, drying tended to increase ^{13}C enrichment across tissues. Greater leaf $\delta^{13}C$ enrichment is typical of higher water use efficiency (WUE), in which the isotope discrimination for $\delta^{13}C$ is relatively low, leading to an enriched $\delta^{13}C$ in plant matter, which can occur under drought-stressed conditions if plants are C-starved (Farquhar & Richards, 1984; Farquhar *et al.*, 1989; Sanket J. More, 2020). Thus, our results indicate that drought increased WUE at the leaf scale. Effects of AMF on changes in plant $\delta^{13}C$, leading the relatively ^{13}C-enriched tissues downstream of leaves could result from the transfer of C from plants to AMF through roots, which might preferentially transfer lighter C compounds, retaining the heavier ^{13}C in the plant tissues.

Patterns Across Plant Tissues

We observed some differences in treatment effects among plant tissues. For example, we also saw larger ^{15}N retention in the leaf tissues versus roots and shoots, suggesting strategic allocation of N to leaves during the early stages of plant growth. For root traits, diameter, RTD and C/N ratio generally increased with root order (i.e. from younger to older roots), and root length, SRL, %C,

and %N decreased with root order. Across reviews, smaller root orders typically have smaller diameter, higher %N, greater AMF colonization rates, supporting their greater importance for soil exploration and resource acquisition compared with larger order roots (Guo *et al.*, 2008; McCormack *et al.*, 2015). Higher root orders typically have higher diameter, higher RTD, and are mainly involved in the transport and storage of nutrients (Rewald *et al.*, 2011; McCormack *et al.*, 2015) which is also aligns with our study.

We also observed interactions of root orders with treatments for SRL, root diameter, RTD, C%, N% and C:N ratio, such that in many cases not all root orders responded. Generally larger root orders (older) responded to more treatments. This may suggest that older roots had more time being exposed to treatments which may be the reason why they responded more.

4.6 Conclusion

Our results show that the *Tabebuia rosea* tropical seedling is able to adapt its growth, photosynthesis, leaf and root traits, and nutrient economies in response to drought. Our novel ^{13}C-dillution data showed a fundamental difference in C allocation for drought versus high moisture seedlings, with rapid allocation of newly fixed C to both leaves and roots under drought. For many metrics, the effects of drought were strongly mediated by soil fertility and AMF inoculation, to the extent that these effects were often larger than the drought effects alone. AMF in particular greatly improved plant nutrient retention, photosynthetic rates, and overall growth, while also influencing leaf and root traits. The first hypothesis that drying decreases tropical seedling growth, but AMF inoculation and high soil fertility mitigate these effects by supporting water and nutrient acquisition was supported by the data in this study and was likely related to the larger retention of nutrients when AMF and fertility were present. The second hypothesis that improved seedling

growth with AMF inoculation and high soil fertility under drying is related to traits that maximize soil resource acquisition and minimize moisture loss, such as high SRL with low SLA was partially supported. Contrary to expectations, the larger plant growth in the dry treatment with AMF inoculation and high soil fertility was associated with lower SRL, but in agreement with the hypothesis this treatment combination had lower SLA, indicating that plants were outsourcing soil exploration and minimizing moisture loss. The third hypothesis that drying suppresses root organic exudates to soils as plants prioritize water rather than nutrient acquisition, but low soil fertility supports relative increases in root exudates was partially supported. In agreement with the hypothesis, drying suppressed leached DOC in soil extractions, and in leachates in the beginning of the experiment, but this reversed in the end of the experiment when drying increased leached DOC, potentially because of a reduced microbial respiration of the exuded DOC or a stress response which should be further investigated. There was no interaction of drying and fertility, so low soil fertility does not promote increased root exudates under drying. These results can have implications for how tropical tree seedlings may respond to increased chronic drying and drought across landscape-scale gradients in soil fertility and soil symbionts, but further experiments should be conducted with other species. The strong interacting effects of fertility and AMF inoculation could also be useful in tropical forest restoration efforts under a changing climate. A conceptual figure and a shorter summary of hypotheses and a few results related to the hypotheses can be found in Figure 4.8.

4.7 Figures

Figure 4.1.

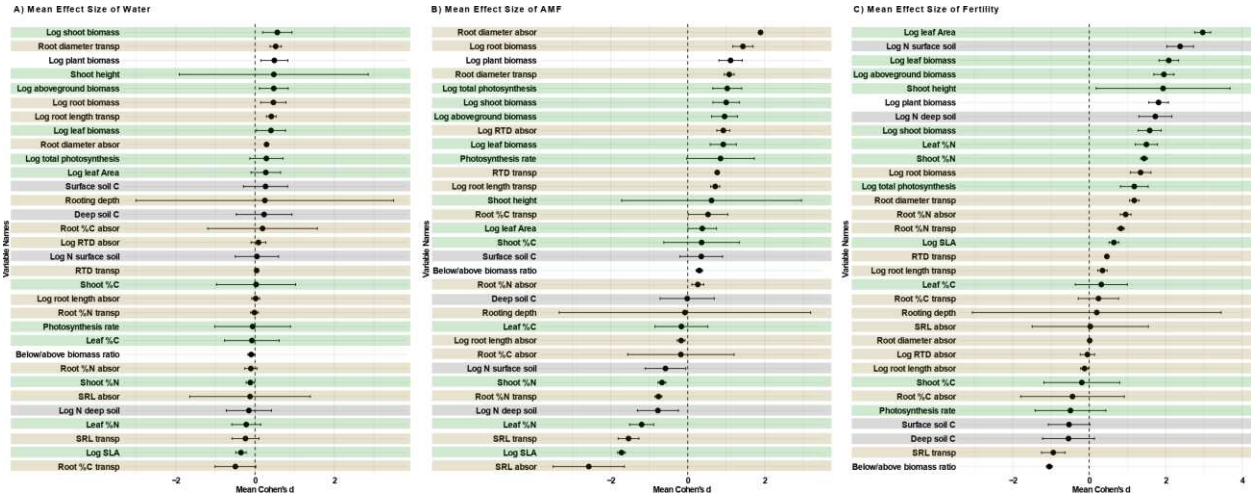

Figure 4.1: Mean Cohen's d values and standard errors for each numerical variable between treatments were calculated, providing insights into the effect sizes of each treatment on these variables. Mean effect size of how different variables respond to moisture availability (A), Arbuscular Mycorrhizal Fungi presence (B) and Fertility (C). Variables on the right side of zero increased with the treatment and variables on the left side decreased. Variables with green background represent aboveground traits, variables with brown background represent belowground traits, variables with gray background represent soil extraction chemistry and variables with no background represent whole plant characteristics.

Figure 4.2.

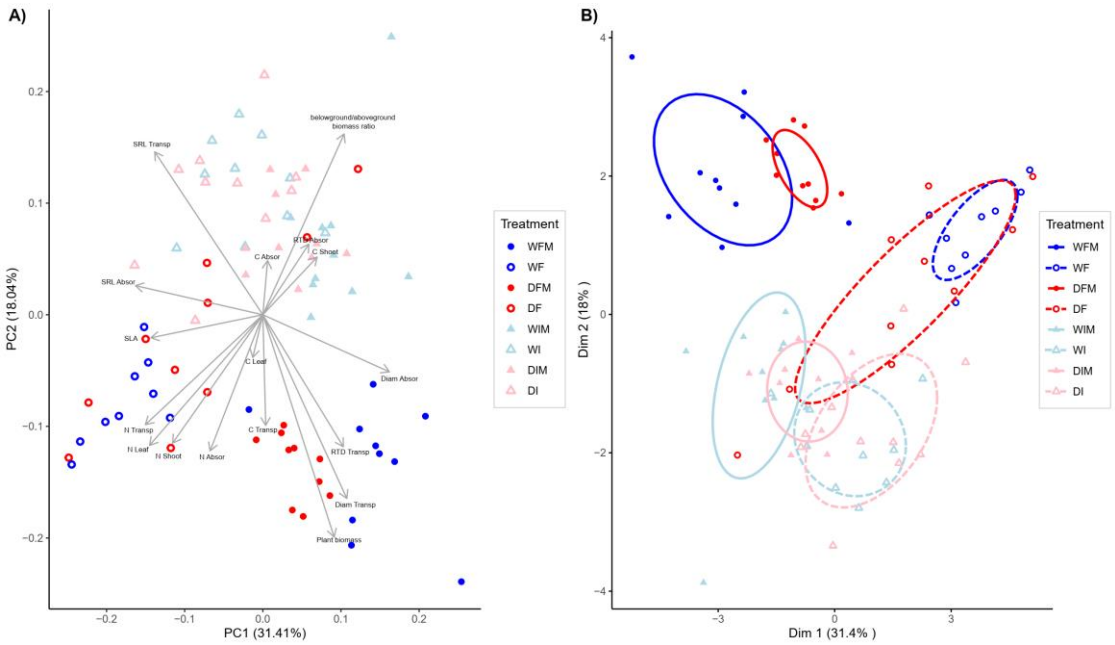

Figure 4.2: Tradeoffs in aboveground and belowground plant traits are shown for different treatments using PCA analyses and clusters. Traits evaluated were: Root morphology (SRL, RTD and root diameter) and chemistry (N and C) traits for absorptive and transportive roots separately, below/aboveground biomass ratio, total plant biomass, and specific leaf area. Root morphology from absorptive roots was considered as the roots from orders 1-2 and from transportive roots as the average among order 3, 4 and 5. For root chemistry, absorptive roots were the ones averaged across orders 1-2 and 3, and transportive roots were averaged across orders 4 and 5. All figures show different clusters for the same data where it presents how plant traits together are affected by different treatments. Principal Coordinates Analysis (PCoA) and k-means clustering analyses were conducted using the scaled data to assess separation of variables among treatments. A) Shows PCA results (traits names are shown in the figure) and B) shows different clusters for the same data where it presents how all these variables together are affected by different treatments. Principal Coordinates Analysis (PCoA) and k-means clustering analyses were conducted using the scaled data to assess separation of variables among treatments. The Euclidean-based approach was used and the data was segregated into distinct clusters using k-means clustering with k = 8. W=Wet, D=Dry, F=Fertile, I=Infertile, M= Mycorrhizal presence.

Figure 4.3.

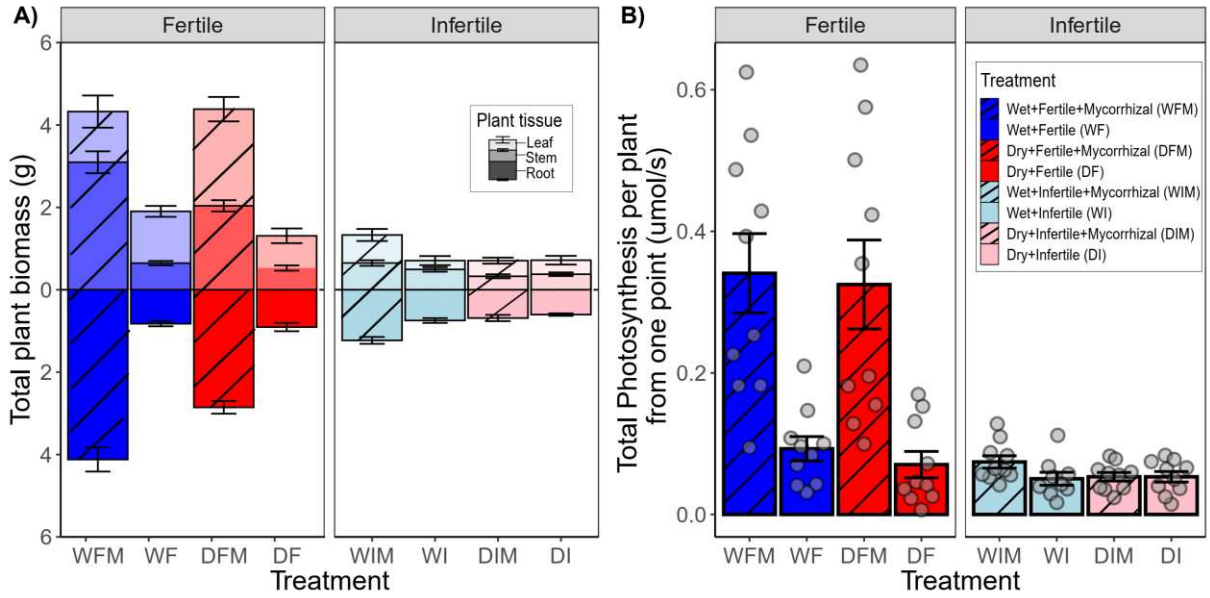

Figure 4.3: Plant biomass and photosynthesis collected in the end of the experiment across different treatments. Data are mean ± SE (n = 10). The division in the middle of the figure shows fertile treatments on the left and infertile treatments on the right. Blue and red colors represent wet and dry treatment respectively and patterns are added when AMF is present. A) Total plant biomass (g) from different plant organs and B) Final photosynthetic flux per plant (µmol CO_2 per plant/second) obtained by multiplying photosynthesis rates from one-point method and total leaves area per plant.

Figure 4.4.

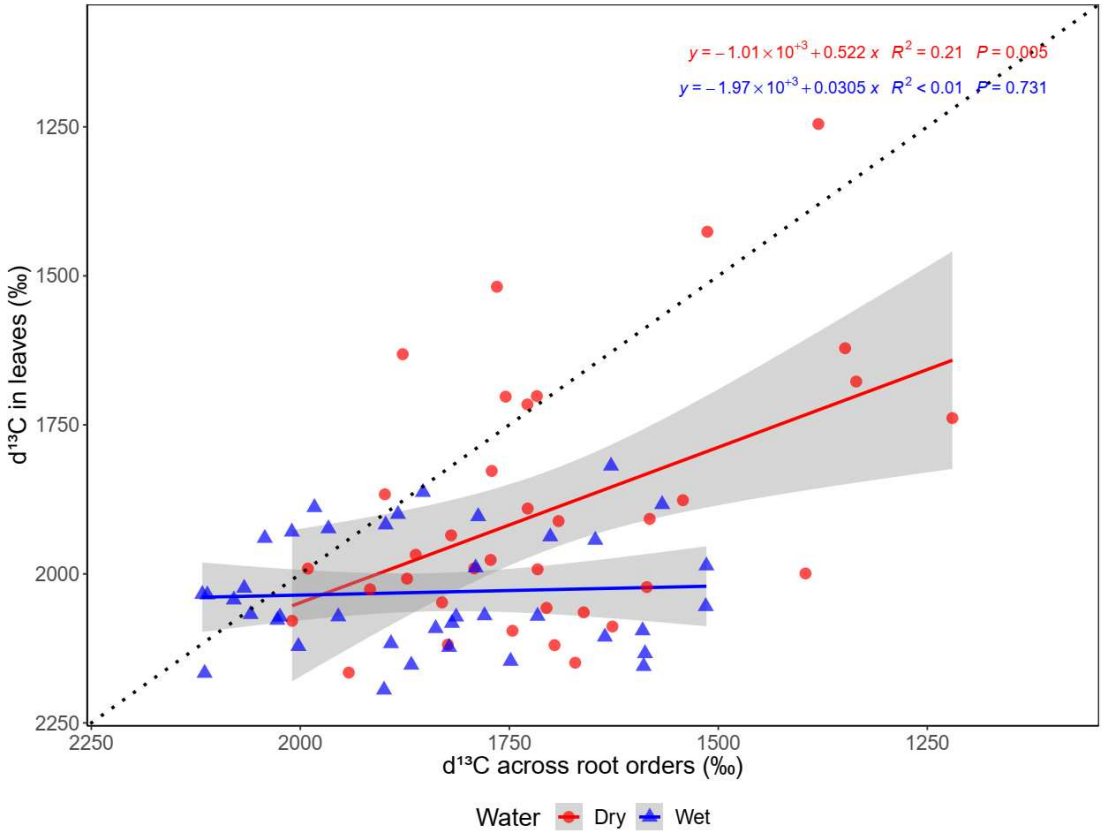

Figure 4.4: Regression of δ ^{13}C (‰) of leaves versus roots under dry and wet conditions. This figure presents the ^{13}C content of plant tissues during an 8-day period of plant harvest, in which plants, after being exposed to larger ^{13}C/^{12}C ratio (inside the labeling chamber), got exposed with atmospheric carbon with larger ^{12}C/^{13}C ratio (when tanks were turned off). δ ^{13}C from roots was averaged across root orders. Axis varies from larger to smaller δ ^{13}C to indicate dilution of δ ^{13}C as new lighter C is being assimilated. Positive slopes indicate a decrease in ^{13}C in roots generally corresponds to a decrease in leaves indicating dilution for leaves and roots. The black dashed 1:1 line represents a slope = 1 which would indicate equivalent decrease in ^{13}C (dilution) in both leaves and roots, suggesting a uniform new carbon (lighter) allocation. The data indicate that dry conditions tend to increase the slopes, suggesting a more balanced increase in δ ^{13}C in roots and leaves. In wet treatments, the slope closer to 0 represent minimal increases in leaf ^{13}C relative to root δ ^{13}C, implying that as roots accumulate more ^{12}C (diluting δ ^{13}C), leaves exhibit negligible changes in δ ^{13}C dilution, suggesting that plants may be prioritizing new carbon for roots growth over leaves.

Figure 4.5.

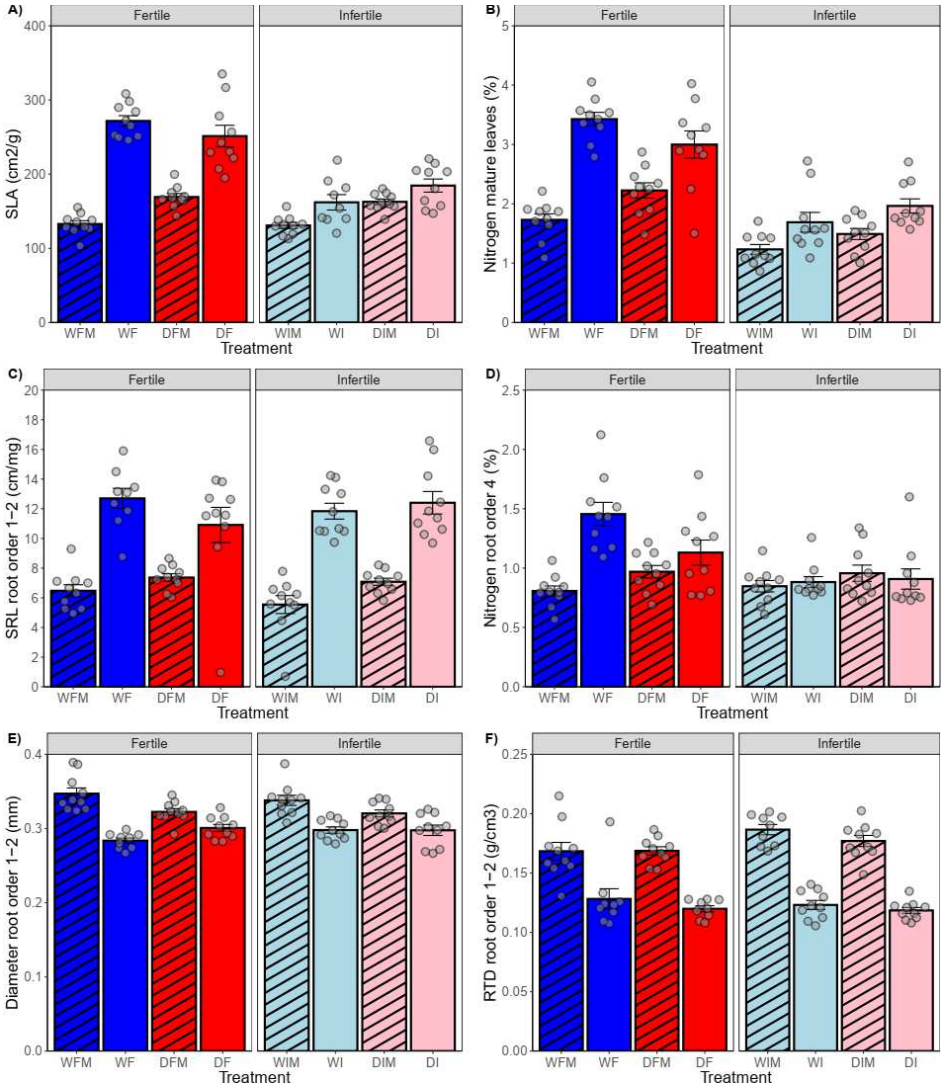

Figure 4.5: Plant morphological traits collected in the end of the experiment across different treatments. Data are mean ± SE (n = 10). The division in the middle of the figure shows fertile treatments on the left and infertile treatments on the right. Blue and red colors represent wet and dry treatment respectively and patterns are added when AMF is present. W=Wet, D=Dry, F=Fertile, I=Infertile, M= Mycorrhizal presence. A) Specific leaf area of leaves (cm^2/g); B) Nitrogen from mature leaves (%); C) Specific root length (cm/mg) of roots from order 1-2; D) Nitrogen from root order 4 (%); E) Diameter (mm) of root order1-2 and F) Root tissue density of root order 1-2 (g/cm3). These were variables important in tradeoffs of morphological plant traits (Figure 4.2).

Figure 4.6.

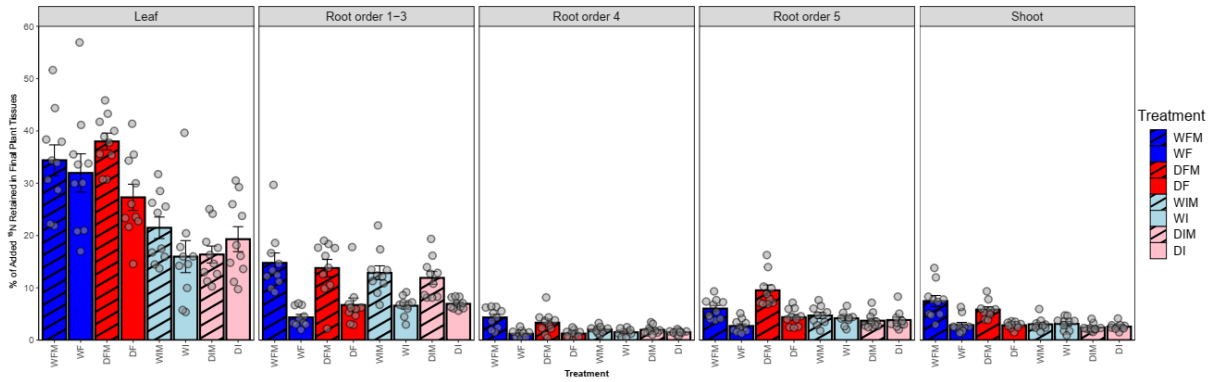

Figure 4.6: ^{15}N retention (%) across different treatments and plant tissues. Data are mean ± SE (n = 10). Blue and red colors represent wet and dry treatment respectively and patterns are added when AMF is present. W=Wet, D=Dry, F=Fertile, I=Infertile, M= Mycorrhizal presence. We determined the ^{15}N retention for each tissue type based on the total biomass of each seedling as a percentage of the initial ^{15}N addition for each plant.

Figure 4.7.

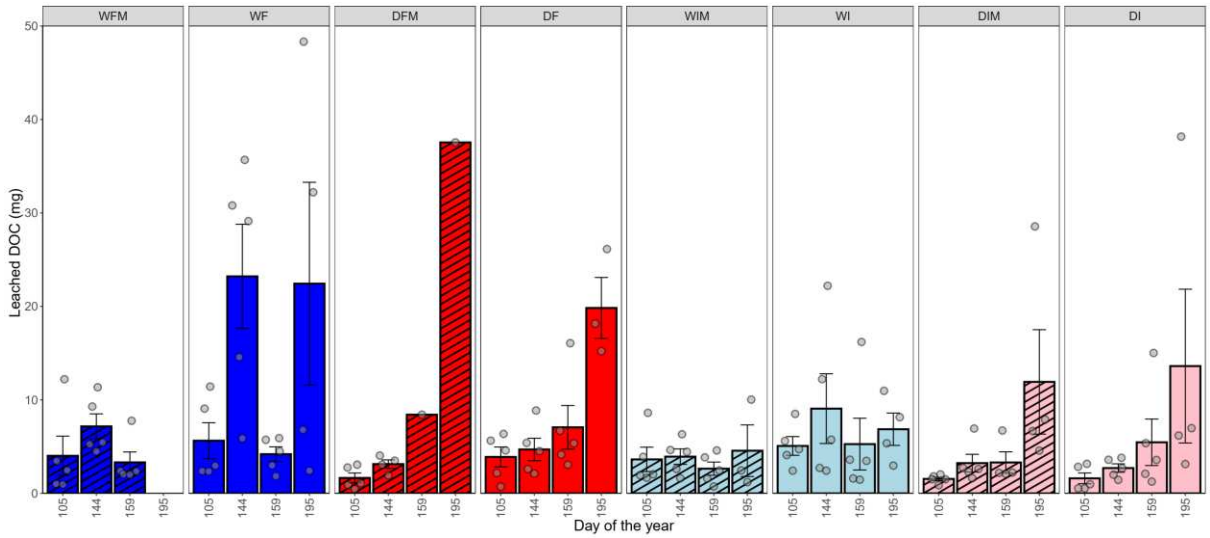

Figure 4.7: Leached DOC collected during the experiment across different dates and different treatments. The total amount of carbon was calculated by multiplying the concentration by the water added through irrigation before hands (se methods). Data are mean ± SE (n = 5). Note: On certain dates, fewer than 5 samples were collected due to the inability to obtain exudates from some pots by the experiment's conclusion. The four panels in the left show fertile treatments and the last four panels on the right show infertile treatments. Blue and red colors represent wet and dry treatment respectively and patterns are added when AMF is present. W=Wet, D=Dry, F=Fertile, I=Infertile, M= Mycorrhizal presence.

Figure 4.8.

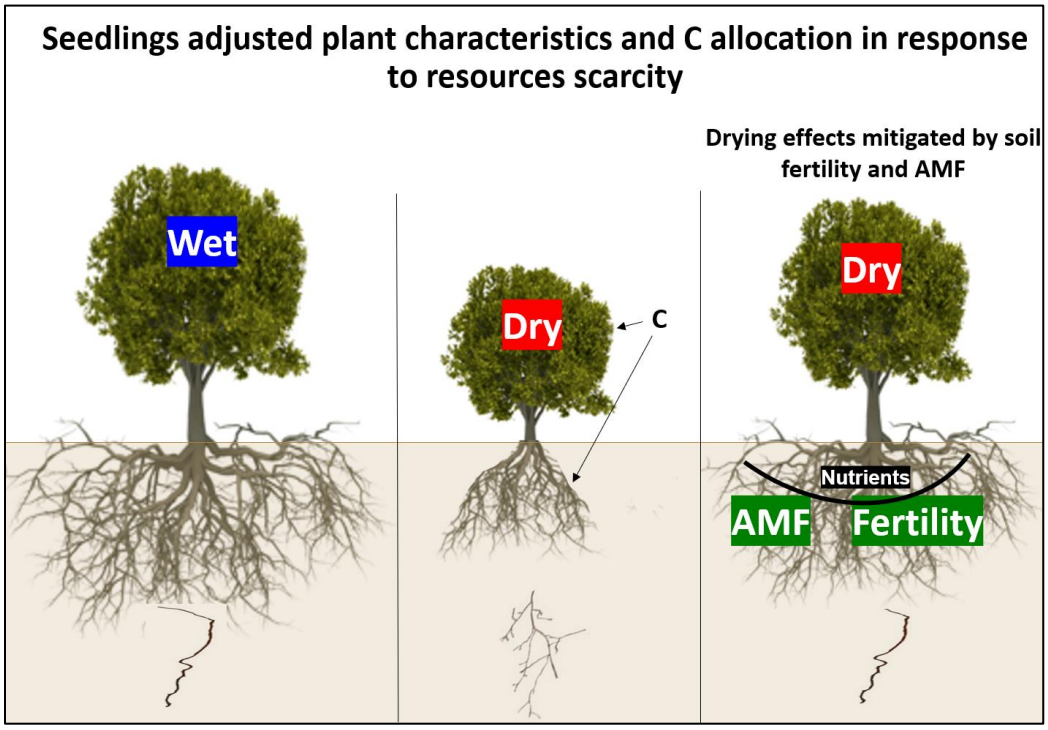

Figure 4.8: Conceptual figure for chapter 4. This chapter showed that the effects of drying conditions included lower plant growth, with new carbon being allocated to both leaves and roots in the end of the experiment differently from wet treatments where most of the new C was allocated to roots. Additionally, there was a reduction in root diameter coupled with an increase in specific root length (SRL). The negative impacts of drying were mitigated by soil fertility and the presence of arbuscular mycorrhizal fungi (AMF). One possible mechanism behind this mitigation may be related to enhanced uptake of water and nutrients facilitated by AMF. The first hypothesis that **drying decreases tropical seedling growth, but AMF inoculation and high soil fertility mitigate these effects by supporting water and nutrient acquisition** was supported by the data in this study and was likely related to the larger retention of nutrients when AMF and fertility were present. The second hypothesis that **improved seedling growth with AMF inoculation and high soil fertility under drying is related to traits that maximize soil resource acquisition and minimize moisture loss, such as high SRL with low SLA** was partially supported. Contrary to expectations, the larger plant growth in the dry treatment with AMF inoculation and high soil fertility was associated with lower SRL, but in agreement with the hypothesis this treatment combination had lower SLA, indicating that plants were outsourcing soil exploration and minimizing moisture loss. The third hypothesis that **drying suppresses root organic exudates to soils as plants prioritize water rather than nutrient acquisition, but low soil fertility supports relative increases in root exudates** was partially supported. In agreement with the hypothesis, drying suppressed leached DOC in soil extractions, and in leachates in the beginning of the experiment, but this reversed in the end of the experiment when drying increased leached DOC, potentially because of a reduced microbial respiration of the exuded DOC or a stress response which should be further investigated. There was no interaction of drying and fertility, so low soil fertility do not promote increased root exudates under drying.

4.8 Tables

Table 4.1: Summary of Plant Growth Metrics. This table presents the mean values and standard errors (Mean + SE) for plant growth variables, categorized by the moisture levels (Wet, Dry), soil fertility (Fertile, Infertile), and mycorrhizal fungi presence (Mycorrhizal, No Mycorrhizal). DF= dry, fertile; DFM = dry, fertile, with mycorrhiza; DI = dry, infertile; DIM = dry, infertile, with mycorrhiza; WF = wet, fertile; WFM = wet, fertile, with mycorrhiza; WI = wet, infertile; WIM = wet, infertile, with mycorrhiza.

Variable	Mean ± SE	Treatment							
		DF	DFM	DI	DIM	WF	WFM	WI	WIM
Total leaf area (cm2)	Mean	329.69	738.89	136.50	113.77	520.10	642.40	129.75	172.19
	SE	46.75	50.96	24.46	11.02	42.76	66.73	21.77	18.42
Total leaves biomass (g)	Mean	1.31	4.38	0.72	0.71	1.90	4.87	0.71	1.33
	SE	0.18	0.30	0.11	0.07	0.13	0.48	0.11	0.15
Shoot biomass (g)	Mean	0.53	2.04	0.38	0.33	0.65	3.40	0.49	0.65
	SE	0.06	0.14	0.04	0.05	0.05	0.38	0.05	0.07
Total roots biomass (g)	Mean	0.91	2.85	0.60	0.69	0.82	4.45	0.75	1.23
	SE	0.10	0.15	0.03	0.08	0.06	0.42	0.06	0.08
Total plant biomass (g)	Mean	2.74	9.28	1.70	1.72	3.37	12.72	1.95	3.21
	SE	0.30	0.54	0.17	0.18	0.23	1.14	0.21	0.27
Root order 1 2 biomass (g)	Mean	0.20	0.60	0.09	0.11	0.10	0.89	0.09	0.24
	SE	0.05	0.06	0.01	0.02	0.01	0.15	0.02	0.04
Root order 3 biomass (g)	Mean	0.19	0.57	0.16	0.22	0.18	0.92	0.20	0.33
	SE	0.02	0.05	0.01	0.02	0.02	0.13	0.02	0.02
Root order 4 biomass (g)	Mean	0.11	0.38	0.08	0.10	0.13	0.93	0.09	0.17
	SE	0.02	0.04	0.01	0.02	0.02	0.13	0.01	0.02
Root order 5 biomass (g)	Mean	0.45	1.22	0.27	0.26	0.41	1.71	0.35	0.48
	SE	0.06	0.07	0.03	0.04	0.03	0.14	0.03	0.08
Total roots biomass (g)	Mean	0.91	2.85	0.60	0.69	0.82	4.45	0.75	1.23
	SE	0.10	0.15	0.03	0.08	0.06	0.42	0.06	0.08
Shoot height (cm)	Mean	15.13	22.81	11.95	10.69	18.17	24.14	13.29	14.21
	SE	0.85	0.80	1.01	0.78	0.50	1.57	0.88	0.58
Rooting depth (cm)	Mean	37.18	40.70	38.18	37.62	41.46	40.95	40.41	36.86
	SE	1.83	2.48	2.95	2.45	2.09	1.74	2.74	2.43
Below:above biomass ratio	Mean	0.54	0.45	0.61	0.68	0.32	0.57	0.67	0.66
	SE	0.07	0.02	0.06	0.04	0.01	0.06	0.05	0.06
Length Root order 1-2 (cm)	Mean	398.17	337.79	367.64	402.70	389.41	372.60	399.43	363.61
	SE	35.14	16.59	21.21	23.73	32.06	28.84	26.43	21.32
Length Root order 3 (cm)	Mean	469.50	500.05	492.00	546.66	510.10	551.12	501.31	527.06
	SE	39.60	15.26	32.91	30.62	31.55	33.67	28.75	22.78
Length Root order 4 (cm)	Mean	167.44	332.84	183.57	192.57	237.33	473.75	196.34	226.70
	SE	35.80	50.94	24.39	23.69	45.99	60.19	34.11	20.63
Length Root order 5 (cm)	Mean	53.56	62.85	48.95	40.00	52.69	55.80	41.59	50.98
	SE	6.96	6.56	8.78	2.38	4.02	8.35	3.49	6.30

Table 4.2: Summary of Photosynthetic Responses. This table presents the mean values and standard errors (Mean + SE) for plant photosynthesis variables, categorized by the moisture levels (Wet, Dry), soil fertility (Fertile, Infertile), and mycorrhizal fungi presence (Mycorrhizal, No Mycorrhizal). DF= dry, fertile; DFM = dry, fertile, with mycorrhiza; DI = dry, infertile; DIM = dry, infertile, with mycorrhiza; WF = wet, fertile; WFM = wet, fertile, with mycorrhiza; WI = wet, infertile; WIM = wet, infertile, with mycorrhiza.

Variable	Mean ± SE	Treatment							
		DF	DFM	DI	DIM	WF	WFM	WI	WIM
Photosynthesis rate (young leaf) (µmol CO_2/m2/s)	Mean	1.90	4.26	4.56	4.92	1.63	6.00	3.22	4.91
	SE	0.41	0.69	0.89	0.82	0.24	0.90	0.35	0.66
Photosynthesis rate (mature leaf) (µmol CO_2/m2/s)	Mean	2.31	4.47	4.81	5.05	1.70	4.36	4.14	4.06
	SE	0.59	1.61	0.97	0.66	0.42	1.53	0.57	0.70
Photosynthesis rate (old leaf) (µmol CO_2/m2/s)	Mean	1.52	4.18	3.02	3.01	1.36	2.30	2.61	3.86
	SE	0.34	0.93	0.45	0.43	0.27	0.53	0.44	0.40
Photosynthesis rate (averaged young and mature leaves) (µmol CO_2/m2/s)	Mean	2.08	4.36	4.79	4.87	1.74	5.37	3.63	4.52
	SE	0.36	0.79	0.79	0.54	0.28	0.76	0.20	0.50
Final photosynthesis flux per plant (µmol CO_2/plant/s)	Mean	0.07	0.32	0.05	0.05	0.09	0.34	0.05	0.07
	SE	0.02	0.06	0.01	0.01	0.02	0.06	0.01	0.01

Table 4.3. Slopes and intercepts from regression analysis of $\delta^{13}C$ (‰) isotope composition in plant tissues over an 8-day period when plants were exposed to atmospheric lighter CO_2 (larger $^{12}C/^{13}C$ ratio) after growing inside a chamber with smaller $^{12}C/^{13}C$ ratio for ~4 months. The table presents intercepts and slopes derived from linear regression models, showing the dynamics of $\delta^{13}C$ in leaf, different root orders, and shoot tissues over time (X = day of harvesting; Y = plant tissue). It also presents intercepts and slopes derived from linear regression models showing the dynamics of $\delta^{13}C$ in leaves (Y axis) versus $\delta^{13}C$ in roots (X axis) from different root orders. DF= dry, fertile; DFM = dry, fertile, with mycorrhiza; DI = dry, infertile; DIM = dry, infertile, with mycorrhiza; WF = wet, fertile; WFM = wet, fertile, with mycorrhiza; WI = wet, infertile; WIM = wet, infertile, with mycorrhiza. DF= dry, fertile; DFM = dry, fertile, with mycorrhiza; DI = dry, infertile; DIM = dry, infertile, with mycorrhiza; WF = wet, fertile; WFM = wet, fertile, with mycorrhiza; WI = wet, infertile; WIM = wet, infertile, with mycorrhiza.

Regression	Treatment							
	DF	DFM	DI	DIM	WF	WFM	WI	WIM
Intercept x = day harvesting y= δ13C leaf	2331.8	2325.1	2454.6	1995.7	2272.2	2045.1	2158.3	2167.5
Slope x = day harvesting y= δ13C leaf	-80.8	-71.2	-113.6	-54.0	-37.8	-4.0	-26.7	-33.3
Intercept x = day harvest y= δ13C Root O1-3	1525.1	1978.6	1789.8	2010.0	1499.3	1999.3	1450.7	2027.5
Slope x = day harvest y= δ13C Root O1-3	-14.14	-35.44	-46.63	-75.47	-3.16	-2.95	2.58	-44.42
Intercept x = day harvest y= δ13C Root O4	1952.3	2155.7	1922.5	2461.2	1947.3	2006.7	1780.4	2153.5
Slope x = day of harvest y= δ13C Root O4	-51.7	-67.1	-50.3	-141.1	-31.1	7.6	-22.6	-39.6
Intercept x = day harvest y= δ13C Root O5	1846.1	2069.6	1754.8	2177.5	2065.9	2225.9	2047.9	2128.5
Slope x = day harvest y= δ13C Root O5	-20.59	-44.30	3.28	-67.34	-31.59	-20.44	-29.39	-27.36
Intercept x = day harvest y= δ13C shoot	1995.6	2371.6	2083.7	2239.6	1986.5	2188.8	1841.7	2086.2
Slope x = day harvest y= δ13C shoot	-65.9	-101.2	-72.4	-103.1	-31.9	-25.4	-14.8	-40.2
Intercept x = δ13C Root 1-3 / y= δ13C leaf	1755.7	209.7	-338.9	742.6	2009.1	1292.6	1725.9	996.3
Slope x = δ13C Root 1-3 / y= δ13C leaf	0.10	0.99	1.43	0.60	0.08	0.37	0.20	0.55
Intercept x = δ13C Root 4 / y = δ13C leaf	1322.8	1318.1	618.2	1346.9	2154.2	1164.7	2063.7	1827.2
Slope x = δ13C Root 4 / y = δ13C leaf	0.34	0.37	0.76	0.20	-0.01	0.42	-0.03	0.08
Intercept x = δ13C Root 5 / y = δ13C leaf	1224.3	916.4	1701.0	-72.7	2006.3	1186.3	651.8	1834.4
Slope x = δ13C Root 5 / y = δ13C leaf	0.39	0.58	0.10	0.98	0.06	0.40	0.72	0.07

Table 4.4: Summary of Morphological Traits. This table presents the mean values and standard errors (Mean + SE) for plant morphology variables, categorized by the moisture levels (Wet, Dry), soil fertility (Fertile, Infertile), and mycorrhizal fungi presence (Mycorrhizal, No Mycorrhizal). DF= dry, fertile; DFM = dry, fertile, with mycorrhiza; DI = dry, infertile; DIM = dry, infertile, with mycorrhiza; WF = wet, fertile; WFM = wet, fertile, with mycorrhiza; WI = wet, infertile; WIM = wet, infertile, with mycorrhiza.

Variable	Mean ± SE	Treatment							
		DF	DFM	DI	DIM	WF	WFM	WI	WIM
SLA (cm2/g)	Mean	251.3	169.1	184.6	162.6	271.7	132.8	193.4	130.8
	SE	14.5	4.69	8.83	3.79	7.08	4.47	32.77	4.01
Diameter Root order 1-2 (mm)	Mean	0.30	0.32	0.30	0.32	0.28	0.35	0.30	0.34
	SE	0.00	0.00	0.01	0.00	0.00	0.01	0.00	0.01
SRL Root order 1-2 (cm/mg)	Mean	10.91	7.36	12.40	7.08	12.70	6.47	11.84	5.54
	SE	1.18	0.26	0.76	0.24	0.68	0.41	0.53	0.61
SRA Root order 1-2 (cm2/mg)	Mean	1.02	0.74	1.15	0.71	1.13	0.70	1.10	0.58
	SE	0.11	0.02	0.04	0.02	0.06	0.03	0.04	0.06
RTD Root order 1-2 (g/cm3)	Mean	0.24	0.17	0.12	0.18	0.13	0.17	0.12	0.33
	SE	0.12	0.00	0.00	0.00	0.01	0.01	0.00	0.14
Diameter Root order 3 (mm)	Mean	0.46	0.55	0.40	0.41	0.41	0.66	0.41	0.46
	SE	0.02	0.03	0.01	0.01	0.01	0.04	0.01	0.02
SRL Root order 3 (cm/mg)	Mean	4.91	3.14	6.14	4.33	5.29	2.49	5.96	3.88
	SE	0.39	0.24	0.26	0.19	0.23	0.40	0.40	0.17
SRA Root order 3 (cm2/mg)	Mean	0.69	0.52	0.77	0.56	0.68	0.49	0.76	0.55
	SE	0.02	0.03	0.02	0.02	0.03	0.06	0.05	0.01
RTD Root order 3 (g/cm3)	Mean	0.13	0.15	0.13	0.18	0.15	0.14	0.13	0.17
	SE	0.01	0.01	0.00	0.01	0.01	0.01	0.01	0.01
Diameter Root order 4 (mm)	Mean	0.92	1.06	0.76	0.73	0.86	1.33	0.72	0.91
	SE	0.07	0.09	0.05	0.04	0.04	0.07	0.03	0.05
SRL Root order 4 (cm/mg)	Mean	1.59	0.97	2.27	2.20	1.84	0.68	2.27	1.47
	SE	0.24	0.12	0.21	0.24	0.17	0.17	0.23	0.16
SRA Root order 4 (cm2/mg)	Mean	0.42	0.30	0.52	0.48	0.49	0.26	0.50	0.40
	SE	0.04	0.02	0.03	0.03	0.03	0.05	0.03	0.03
RTD Root order 4 (g/cm3)	Mean	0.11	0.14	0.11	0.12	0.10	0.14	0.12	0.11
	SE	0.01	0.01	0.01	0.01	0.01	0.01	0.01	0.00
Diameter Root order 5 (mm)	Mean	1.98	2.90	1.85	1.91	2.25	3.50	2.08	2.33
	SE	0.08	0.16	0.13	0.13	0.10	0.16	0.10	0.22
SRL Root order 5 (cm/mg)	Mean	0.13	0.05	0.19	0.18	0.13	0.04	0.12	0.13
	SE	0.01	0.01	0.03	0.02	0.01	0.01	0.01	0.02
SRA Root order 5 (cm2/mg)	Mean	0.08	0.04	0.10	0.10	0.09	0.04	0.08	0.08
	SE	0.01	0.00	0.01	0.01	0.00	0.01	0.01	0.01
RTD Root order 5 (g/cm3)	Mean	0.27	0.34	0.23	0.22	0.21	0.37	0.27	0.24
	SE	0.02	0.03	0.02	0.01	0.01	0.03	0.03	0.03

Table 4.5: Summary of Isotopic Composition. This table presents the mean values and standard errors (Mean + SE) for isotopic variables in plants, categorized by the moisture levels (Wet, Dry), soil fertility (Fertile, Infertile), and mycorrhizal fungi presence (Mycorrhizal, No Mycorrhizal). DF= dry, fertile; DFM = dry, fertile, with mycorrhiza; DI = dry, infertile; DIM = dry, infertile, with mycorrhiza; WF = wet, fertile; WFM = wet, fertile, with mycorrhiza; WI = wet, infertile; WIM = wet, infertile, with mycorrhiza.

Variable	Mean ± SE	Treatment							
		DF	DFM	DI	DIM	WF	WFM	WI	WIM
^{15}N Mature Leaf (at-%)	Mean	1.5	0.7	0.8	1.0	0.8	0.7	0.8	0.8
	SE	0.3	0.0	0.1	0.2	0.1	0.0	0.1	0.1
δ ^{15}N-Air Mature Leaf (‰)	Mean	3077.9	882.0	1284.1	1706.1	1286.6	980.9	1093.2	1150.2
	SE	734.5	84.0	187.4	430.4	189.6	98.0	144.0	151.7
^{15}N Root order 1-3 (at-%)	Mean	2.0	1.1	1.2	1.2	1.3	1.0	1.0	0.8
	SE	0.2	0.1	0.1	0.1	0.1	0.1	0.1	0.1
δ ^{15}N-Air Root order 1-3 (‰)	Mean	4583.3	2051.1	2310.8	2374.0	2462.2	1621.5	1789.0	1177.0
	SE	567.5	147.7	190.8	360.2	259.1	189.9	183.9	148.5
^{15}N Root order 4 (at-%)	Mean	2.0	1.5	1.2	1.5	1.1	1.0	1.0	0.8
	SE	0.2	0.1	0.1	0.3	0.1	0.1	0.1	0.1
δ ^{15}N-Air Root order 4 (‰)	Mean	4508.7	3145.0	2432.9	3082.4	2028.9	1784.0	1829.4	1307.7
	SE	696.5	394.2	327.0	721.6	283.0	234.0	212.6	180.2
^{15}N Root order 5 (at-%)	Mean	2.3	1.6	1.2	1.4	1.1	0.9	1.1	0.9
	SE	0.3	0.1	0.1	0.2	0.1	0.1	0.1	0.1
δ ^{15}N-Air Root order 5 (‰)	Mean	5421.2	3483.3	2209.4	2882.9	2107.1	1593.8	2056.2	1401.1
	SE	881.1	268.3	261.5	460.5	369.1	213.6	305.9	189.5
^{15}N Shoot (at-%)	Mean	1.4	0.7	0.9	1.1	0.9	0.7	0.7	0.7
	SE	0.2	0.0	0.1	0.1	0.1	0.0	0.0	0.0
δ ^{15}N-Air Shoot (‰)	Mean	2773.4	966.0	1480.2	2094.2	1348.6	928.1	980.0	973.0
	SE	560.7	75.7	158.3	306.7	209.0	100.8	134.9	102.9

Table 4.6: Summary of Chemical Properties. This table presents the mean values and standard errors (Mean + SE) for plant chemistry variables, categorized by the moisture levels (Wet, Dry), soil fertility (Fertile, Infertile), and mycorrhizal fungi presence (Mycorrhizal, No Mycorrhizal). DF= dry, fertile; DFM = dry, fertile, with mycorrhiza; DI = dry, infertile; DIM = dry, infertile, with mycorrhiza; WF = wet, fertile; WFM = wet, fertile, with mycorrhiza; WI = wet, infertile; WIM = wet, infertile, with mycorrhiza.

Variable	Mean ± SE	Treatment							
		DF	DFM	DI	DIM	WF	WFM	WI	WIM
C percent Mature Leaf (%)	Mean	45.70	45.37	45.47	45.66	45.65	46.27	45.65	44.17
	SE	0.31	0.78	0.27	0.60	0.23	0.31	0.65	0.21
N percent Mature Leaf (%)	Mean	3.00	2.23	1.96	1.49	3.43	1.73	1.69	1.23
	SE	0.23	0.13	0.12	0.09	0.11	0.10	0.17	0.08
C/N ratio Mature Leaf	Mean	16.46	21.01	23.78	31.72	13.45	27.72	29.03	37.19
	SE	1.85	1.29	1.17	1.99	0.45	1.91	2.36	2.31
C percent Root order 1-3 (%)	Mean	45.51	46.49	47.66	46.58	47.23	45.12	47.71	48.10
	SE	0.59	0.41	0.68	1.38	1.77	1.03	0.30	0.64
N percent Root order 1-3 (%)	Mean	1.66	1.89	1.35	1.75	2.06	1.53	1.26	1.59
	SE	0.06	0.09	0.05	0.07	0.14	0.08	0.06	0.05
C/N ratio Root order 1-3	Mean	27.72	25.45	35.70	26.89	23.29	30.07	38.65	30.43
	SE	1.25	1.84	1.17	0.92	0.85	1.28	2.05	0.66
C percent Root order 4 (%)	Mean	44.82	45.20	45.87	45.83	44.12	46.09	45.06	45.65
	SE	0.49	0.61	0.66	0.49	0.74	0.23	0.31	0.28
N percent Root order 4 (%)	Mean	1.13	0.97	0.91	0.96	1.46	0.81	0.88	0.85
	SE	0.11	0.05	0.09	0.07	0.10	0.04	0.05	0.05
C/N ratio Root order 4	Mean	42.56	48.07	53.04	49.84	31.40	58.54	51.97	55.40
	SE	3.59	3.07	3.11	3.12	1.94	3.23	1.98	3.09
C percent Root order 5 (%)	Mean	45.59	47.30	44.23	45.34	44.71	44.81	44.28	44.09
	SE	0.26	1.00	0.52	0.37	0.29	0.54	0.57	0.88
N percent Root order 5 (%)	Mean	0.85	0.78	0.72	0.64	1.01	0.66	0.63	0.68
	SE	0.05	0.04	0.07	0.03	0.07	0.04	0.03	0.04
C/N ratio Root order 5	Mean	55.94	61.55	66.29	72.45	46.42	70.23	71.54	66.12
	SE	3.84	2.40	5.54	3.40	3.65	4.31	3.19	3.60
C percent Shoot (%)	Mean	41.75	43.08	41.94	43.49	42.01	42.70	43.38	42.66
	SE	1.09	0.62	1.12	0.31	0.69	0.56	0.34	0.38
N percent Shoot (%)	Mean	0.81	0.68	0.46	0.43	0.86	0.53	0.52	0.39
	SE	0.10	0.03	0.03	0.04	0.08	0.03	0.06	0.04
C/N ratio Shoot	Mean	59.48	64.08	94.26	116.49	52.44	84.21	93.14	120.54
	SE	7.80	2.36	5.04	18.61	4.84	5.95	10.54	13.08

Table 4.7: Summary of Leachate Dynamics. This table presents the mean values and standard errors (Mean + SE) for leachate variables from the plant growth medium, categorized by the moisture levels (Wet, Dry), soil fertility (Fertile, Infertile), and mycorrhizal fungi presence (Mycorrhizal, No Mycorrhizal). DF= dry, fertile; DFM = dry, fertile, with mycorrhiza; DI = dry, infertile; DIM = dry, infertile, with mycorrhiza; WF = wet, fertile; WFM = wet, fertile, with mycorrhiza; WI = wet, infertile; WIM = wet, infertile, with mycorrhiza.

Variable	Mean ± SE	Treatment							
		DF	DFM	DI	DIM	WF	WFM	WI	WIM
Leached DOC - collection 2 (mg)	Mean	3.90	1.65	1.61	1.55	5.64	4.02	5.07	3.63
	SE	0.71	0.35	0.38	0.13	1.28	1.40	0.67	0.87
Leached TDN - collection 2 (mg)	Mean	0.10	0.38	0.08	0.03	0.35	0.70	0.15	0.13
	SE	0.02	0.11	0.02	0.00	0.08	0.24	0.04	0.02
Leachates C/N ratio - collection 2	Mean	77.31	12.46	24.70	68.13	54.64	24.60	46.15	36.31
	SE	25.04	3.95	7.83	10.94	20.51	11.69	9.01	8.59
Leached phosphate - collection 2 (mg)	Mean	0.07	0.06	0.08	0.07	0.12	0.12	0.15	0.16
	SE	0.00	0.00	0.00	0.00	0.00	0.00	0.01	0.01
Leached Nitrate + Nitrite - collection 2 (mg)	Mean	0.23	0.59	0.26	0.04	0.38	0.70	0.33	0.55
	SE	0.06	0.09	0.07	0.01	0.06	0.20	0.05	0.18
Leached Ammonium - collection 2 (mg)	Mean	0.01	0.00	0.00	0.00	0.00	0.01	0.00	0.00
	SE	0.01	0.00	0.00	0.00	0.00	0.00	0.00	0.00
Leached DOC per Absorptive root biomass - collection 2 (mg /g)	Mean	5.79	0.75	3.99	2.82	13.08	1.35	9.32	3.60
	SE	1.15	0.13	1.17	0.42	3.45	0.41	0.84	0.94
Leached TDN per Absorptive root biomass - collection 2 (mg /g)	Mean	0.14	0.22	0.20	0.05	0.54	0.20	0.32	0.12
	SE	0.03	0.08	0.04	0.01	0.16	0.06	0.09	0.02
Leached phosphate per Absorptive root biomass - collection 2 (mg /g)	Mean	0.10	0.03	0.19	0.13	0.22	0.04	0.30	0.15
	SE	0.01	0.00	0.02	0.01	0.01	0.00	0.04	0.01
Leached Nitrate + Nitrite per Absorptive root biomass - collection 2 (mg /g)	Mean	0.33	0.29	0.70	0.06	0.63	0.21	0.68	0.50
	SE	0.08	0.05	0.24	0.02	0.11	0.05	0.12	0.17
Leached Ammonium per Absorptive root biomass - collection 2 (mg /g)	Mean	0.01	0.00	0.00	0.00	0.01	0.00	0.01	0.00
	SE	0.01	0.00	0.00	0.00	0.00	0.00	0.00	0.00
Leached DOC - collection 5 (mg)	Mean	4.70	3.13	2.71	3.24	23.21	7.17	9.06	3.93
	SE	0.80	0.29	0.30	0.63	3.72	0.89	2.49	0.55

Leached TDN - collection 5 (mg)	Mean	0.11	0.10	0.05	0.08	0.21	1.52	0.50	0.31
	SE	0.05	0.03	0.01	0.04	0.03	0.42	0.17	0.08
Leachates C/N ratio - collection 5	Mean	116.94	47.62	74.86	152.89	118.93	22.04	65.69	22.42
	SE	20.80	9.29	12.99	40.98	20.55	7.69	25.43	5.32
Leached DOC per Absorptive root biomass - collection 5 (mg /g)	Mean	6.54	1.32	5.91	5.53	52.92	2.20	15.85	3.86
	SE	0.99	0.12	0.43	1.09	6.66	0.21	4.13	0.64
Leached N per Absorptive root biomass - collection 5 (mg /g)	Mean	0.24	0.04	0.14	0.11	0.40	0.51	1.07	0.28
	SE	0.13	0.01	0.05	0.05	0.07	0.16	0.40	0.07
Leached DOC - collection 6 (mg)	Mean	7.07	8.42	5.46	3.31	4.19	3.32	5.27	2.64
	SE	1.55	0.00	1.66	0.75	0.52	0.74	1.85	0.47
Leached TDN - collection 6 (mg)	Mean	0.30	0.18	0.17	0.16	0.69	0.81	0.36	0.15
	SE	0.07	0.00	0.03	0.05	0.13	0.22	0.11	0.04
Leachates C/N ratio - collection 6	Mean	32.32	47.74	35.45	41.80	9.77	9.85	23.78	37.62
	SE	5.44	0.00	6.15	10.68	2.66	3.66	5.55	10.34
Leached DOC per Absorptive root biomass - collection 6 (mg /g)	Mean	9.63	4.03	12.47	5.93	9.23	1.06	11.11	2.64
	SE	1.51	0.00	3.39	1.45	1.17	0.22	4.38	0.54
Leached TDN per Absorptive root biomass - collection 6 (mg /g)	Mean	0.52	0.08	0.39	0.27	1.16	0.27	0.63	0.13
	SE	0.18	0.00	0.07	0.09	0.27	0.08	0.15	0.03
Leached DOC - collection 10 (mg)	Mean	19.83	37.55	13.62	11.92	22.43	NA	6.86	4.56
	SE	2.06	0.00	5.38	3.66	7.10	NA	1.13	1.74
Leached N - collection 10 (mg)	Mean	1.85	0.11	0.89	0.17	3.83	NA	0.49	0.03
	SE	0.45	0.00	0.27	0.06	1.41	NA	0.15	0.01
Leachates C/N ratio - collection 10	Mean	23.51	331.51	72.84	137.85	57.11	NA	43.79	146.07
	SE	10.73	0.00	43.20	38.29	31.10	NA	20.74	32.81
Leached DOC per Absorptive root biomass - collection 10 (mg /g)	Mean	27.44	15.54	39.63	20.94	59.88	NA	11.72	4.20
	SE	3.78	0.00	18.52	6.41	17.89	NA	1.19	1.72
Leached TDN per Absorptive root biomass - collection 10 (mg /g)	Mean	2.43	0.05	1.91	0.24	3.46	NA	0.87	0.03
	SE	0.58	0.00	0.54	0.07	1.41	NA	0.20	0.01

Table 4.8: Summary of Soil Nutrient Extraction. This table presents the mean values and standard errors (Mean + SE) for soil extraction variables, categorized by the moisture levels (Wet, Dry), soil fertility (Fertile, Infertile), and mycorrhizal fungi presence (Mycorrhizal, No Mycorrhizal). DF= dry, fertile; DFM = dry, fertile, with mycorrhiza; DI = dry, infertile; DIM = dry, infertile, with mycorrhiza; WF = wet, fertile; WFM = wet, fertile, with mycorrhiza; WI = wet, infertile; WIM = wet, infertile, with mycorrhiza.

Variable	Mean ± SE	Treatment							
		DF	DFM	DI	DIM	WF	WFM	WI	WIM
Soil moisture - Soil Surface (g water/g dry soil)	Mean	0.14	0.11	0.16	0.17	0.13	0.10	0.16	0.15
	SE	0.01	0.00	0.01	0.01	0.00	0.00	0.00	0.01
Extractable DOC - Soil Surface (mg nutrient/kg dry soil)	Mean	1.89	2.40	2.38	3.14	2.11	2.66	3.09	3.11
	SE	0.24	0.30	0.46	0.45	0.37	0.40	0.35	0.46
Extractable TDN - Soil Surface (mg nutrient/kg dry soil)	Mean	23.02	17.22	3.55	1.90	27.20	13.85	4.29	2.24
	SE	3.68	2.32	0.42	0.35	2.11	2.54	0.49	0.34
Extractable phosphate - Soil Surface (mg nutrient/kg dry soil)	Mean	1.53	2.10	1.24	1.04	1.87	1.38	1.14	1.00
	SE	0.21	0.19	0.11	0.05	0.29	0.17	0.06	0.04
Extractable Nitrate + Nitrite - Soil Surface (mg nutrient/kg dry soil)	Mean	17.70	16.22	6.82	5.34	22.72	14.12	15.64	5.71
	SE	1.98	1.74	3.54	4.13	1.37	2.31	8.12	2.56
Extractable Ammonium - Soil Surface (mg nutrient/kg dry soil)	Mean	0.10	0.09	0.08	0.08	0.09	0.09	0.10	0.11
	SE	0.01	0.02	0.02	0.01	0.01	0.02	0.01	0.01
Soil moisture - Soil Deep (g water/g dry soil)	Mean	0.17	0.11	0.23	0.22	0.16	0.10	0.24	0.24
	SE	0.01	0.00	0.01	0.02	0.01	0.00	0.01	0.01
Extractable DOC - Soil Deep (mg nutrient/kg dry soil)	Mean	1.31	1.91	2.38	3.05	2.44	1.92	3.20	2.43
	SE	0.26	0.46	0.35	0.46	0.83	0.39	0.50	0.41
Extractable TDN - Soil Deep (mg nutrient/kg dry soil)	Mean	8.50	5.31	1.21	1.08	10.19	2.50	1.75	0.48
	SE	2.23	1.48	0.12	0.34	1.33	0.78	0.66	0.04
Extractable phosphate - Soil Deep (mg nutrient/kg dry soil)	Mean	0.91	0.84	1.15	1.12	0.95	0.94	1.21	1.15

	SE	0.08	0.06	0.05	0.07	0.15	0.07	0.06	0.06
Extractable Nitrate + Nitrite - Soil Deep (mg nutrient/kg dry soil)	Mean	8.95	3.31	2.32	4.30	9.77	5.20	4.26	0.27
	SE	2.80	0.67	1.42	3.21	1.79	3.38	1.92	0.09
Extractable Ammonium - Soil Deep (mg nutrient/kg dry soil)	Mean	0.10	0.08	0.10	0.11	0.11	0.10	0.11	0.10
	SE	0.01	0.01	0.01	0.02	0.02	0.01	0.01	0.01
Soil moisture - Root exclusion mesh (g water/g dry soil)	Mean	0.20	0.14	0.24	0.22	0.16	0.13	0.25	0.26
	SE	0.00	0.00	0.01	0.02	0.00	0.00	0.01	0.01
Extractable DOC - Root exclusion mesh (mg nutrient/kg dry soil)	Mean	1.57	1.50	1.33	0.81	0.53	2.16	1.98	3.22
	SE	0.61	0.19	0.08	0.14	0.24	0.62	0.36	0.23
Extractable TDN - Root exclusion mesh (mg nutrient/kg dry soil)	Mean	15.20	4.99	2.47	0.24	20.24	3.64	11.82	2.97
	SE	4.24	1.26	1.00	0.13	2.68	0.90	4.44	1.16
Extractable phosphate - Root exclusion mesh (mg nutrient/kg dry soil)	Mean	3.14	0.76	1.20	1.06	1.78	1.86	1.38	1.23
	SE	2.42	0.10	0.14	0.01	0.81	1.06	0.12	0.06
Extractable Nitrate + Nitrite - Root exclusion mesh (mg nutrient/kg dry soil)	Mean	15.00	5.33	4.49	0.33	19.04	3.87	16.60	0.85
	SE	7.42	2.31	0.20	0.01	3.46	1.55	13.76	0.52
Extractable Ammonium - Root exclusion mesh (mg nutrient/kg dry soil)	Mean	0.12	0.09	0.12	0.09	0.09	0.06	0.09	0.07
	SE	0.00	0.01	0.03	0.00	0.00	0.01	0.01	0.00

LITERATURE CITED

Ahanger MA, Qi M, Huang Z, Xu X, Begum N, Qin C, Zhang C, Ahmad N, Mustafa NS, Ashraf M, et al. 2021. Improving growth and photosynthetic performance of drought stressed tomato by application of nano-organic fertilizer involves up-regulation of nitrogen, antioxidant and osmolyte metabolism. *Ecotoxicol Environ Saf* 216: 112195.

Aili Y, Chen X, Gao W, Wang H, Dawuti M, Ma X. 2023. Response of Alhagi sparsifolia Seedlings to AMF Inoculation and Nitrogen Addition under Drought Stress. *Atmosphere* 14(3).

Amaya-Carpio L, Davies FT, Fox T, He C. 2009. Arbuscular mycorrhizal fungi and organic fertilizer influence photosynthesis, root phosphatase activity, nutrition, and growth of Ipomoea carnea ssp fistulosa. *Photosynthetica* 47(1): 1-10.

Amissah L, Mohren GMJ, Kyereh B, Poorter L. 2015. The Effects of Drought and Shade on the Performance, Morphology and Physiology of Ghanaian Tree Species. *Plos One* 10(4): 22.

Asefa M, Worthy SJ, Cao M, Song XY, Lozano YM, Yang J. 2022. Above- and below-ground plant traits are not consistent in response to drought and competition treatments. *Annals of Botany* 130(7): 939-950.

Augé RM. 2001. Water relations, drought and vesicular-arbuscular mycorrhizal symbiosis. *Mycorrhiza* 11(1): 3-42.

Auge RM, Toler HD, Saxton AM. 2016. Mycorrhizal Stimulation of Leaf Gas Exchange in Relation to Root Colonization, Shoot Size, Leaf Phosphorus and Nitrogen: A Quantitative Analysis of the Literature Using Meta-Regression. *Front Plant Sci* 7: 1084.

Barton K, Shiels A. 2020. Additive and non-additive responses of seedlings to simulated herbivory and drought data. *Dryad*.

Bender SF, Conen F, Van der Heijden MGA. 2015. Mycorrhizal effects on nutrient cycling, nutrient leaching and N2O production in experimental grassland. *Soil Biology and Biochemistry* 80: 283-292.

Bergmann J, Weigelt A, van der Plas F, Laughlin DC, Kuyper TW, Guerrero-Ramirez N, Valverde-Barrantes OJ, Bruelheide H, Freschet GT, Iversen CM, et al. 2020. The fungal collaboration gradient dominates the root economics space in plants. *Science Advances* 6(27): eaba3756.

Bloom AJ, Chapin FS, Mooney HA. 1985. Resource limitation in plants - an economic analogy. *Annual Review of Ecology and Systematics* 16: 363-392.

Brundrett MC. 2002. Coevolution of roots and mycorrhizas of land plants. *New Phytologist* 154(2): 275-304.

Chari NR, Tumber-Dávila SJ, Phillips RP, Bauerle TL, Brunn M, Hafner BD, Klein T, Obersteiner S, Reay MK, Ullah S, et al. 2024. The global root exudate carbon flux. *bioRxiv*

Cheng S, Zou YN, Kuca K, Hashem A, Allah EFA, Wu QS. 2021. Elucidating the Mechanisms Underlying Enhanced Drought Tolerance in Plants Mediated by Arbuscular Mycorrhizal Fungi. *Frontiers in Microbiology* 12.

Cusack D, Markesteijn L, Condit R, Lewis O, Turner B. 2018. Soil carbon stocks in tropical forests of Panama regulated by base cation effects on fine roots. *Biogeochemistry* 137(1-2): 253-266.

Cusack DF, Addo-Danso SD, Agee EA, Andersen KM, Arnaud M, Batterman SA, Brearley FQ, Ciochina MI, Cordeiro AL, Dallstream C, et al. 2021. Tradeoffs and Synergies in Tropical

Forest Root Traits and Dynamics for Nutrient and Water Acquisition: Field and Modeling Advances. *Frontiers in Forests and Global Change* 4: 704469.

Cusack DF, Karpman J, Ashdown D, Cao Q, Ciochina M, Halterman S, Lydon S, Neupane A. 2016. Global change effects on humid tropical forests: Evidence for biogeochemical and biodiversity shifts at an ecosystem scale. *Reviews of Geophysics* 54(3): 523-610.

da Costa AC, Galbraith D, Almeida S, Portela BT, da Costa M, Silva Junior Jde A, Braga AP, de Goncalves PH, de Oliveira AA, Fisher R, et al. 2010. Effect of 7 yr of experimental drought on vegetation dynamics and biomass storage of an eastern Amazonian rainforest. *New Phytol* 187(3): 579-591.

Dakora FD, Phillips DA. 2002. Root exudates as mediators of mineral acquisition in low-nutrient environments. *Plant and Soil* 245(1): 35-47.

Das S, Sarkar S. 2024. Arbuscular mycorrhizal fungal contribution towards plant resilience to drought conditions. *Front Fungal Biol* 5: 1355999.

Diaz S, Kattge J, Cornelissen JH, Wright IJ, Lavorel S, Dray S, Reu B, Kleyer M, Wirth C, Prentice IC, et al. 2016. The global spectrum of plant form and function. *Nature* 529(7585): 167-171.

El Amrani B. 2023. Exploring the importance of root architecture plasticity in plant adaptation to environmental constraints. *Plant Species Biology* 38(5): 234-244.

Epron D, Bahn M, Derrien D, Lattanzi FA, Pumpanen J, Gessler A, Hogberg P, Maillard P, Dannoura M, Gerant D, et al. 2012. Pulse-labelling trees to study carbon allocation dynamics: a review of methods, current knowledge and future prospects. *Tree Physiol* 32(6): 776-798.

Evans JR. 1989. Photosynthesis and nitrogen relationships in leaves of c-3 plants. *Oecologia* 78(1): 9-19.

Evans JR. 2013. Improving photosynthesis. *Plant Physiol* 162(4): 1780-1793.

Farquhar GD, Ehleringer JR, Hubick KT. 1989. Carbon Isotope Discrimination and Photosynthesis. *Annual Review of Plant Biology* 40(Volume 40, 1989): 503-537.

Farquhar GD, Richards RA. 1984. Isotopic Composition of Plant Carbon Correlates With Water-Use Efficiency of Wheat Genotypes. *Functional Plant Biology* 11(6).

Field CB, Behrenfeld MJ, Randerson JT, Falkowski P. 1998. Primary production of the biosphere: Integrating terrestrial and oceanic components. *Science* 281(5374): 237-240.

Freschet GT, Roumet C, Comas LH, Weemstra M, Bengough AG, Rewald B, Bardgett RD, De Deyn GB, Johnson D, Klimesova J, et al. 2021. Root traits as drivers of plant and ecosystem functioning: current understanding, pitfalls and future research needs. *New Phytol* 232(3): 1123-1158.

Gaudinski JB, Torn MS, Riley WJ, Swanston C, Trumbore SE, Joslin JD, Majdi H, Dawson TE, Hanson PJ. 2009. Use of stored carbon reserves in growth of temperate tree roots and leaf buds: analyses using radiocarbon measurements and modeling. *Global Change Biology* 15(4): 992-1014.

Gavito ME, Jakobsen I, Mikkelsen TN, Mora F. 2019. Direct evidence for modulation of photosynthesis by an arbuscular mycorrhiza-induced carbon sink strength. *New Phytologist* 223(2): 896-907.

Grossnickle SC, MacDonald JE. 2017. Why seedlings grow: influence of plant attributes. *New Forests* 49(1): 1-34.

Guo D, Xia M, Wei X, Chang W, Liu Y, Wang Z. 2008. Anatomical traits associated with absorption and mycorrhizal colonization are linked to root branch order in twenty-three Chinese temperate tree species. *New Phytologist* 180(3): 673-683.

He Y, Yang R, Lei G, Li M, Li T, Zhan F, Li Y. 2021. Arbuscular mycorrhizal fungus–induced decrease in phosphorus loss due to leaching in red soils under simulated heavy rainfall. *Journal of Soils and Sediments* 21(2): 881-889.

Hildebrand GA, Honeker LK, Freire-Zapata V, Ayala-Ortiz C, Rajakaruna S, Fudyma J, Daber LE, AminiTabrizi R, Chu RL, Toyoda J, et al. 2023. Uncovering the dominant role of root metabolism in shaping rhizosphere metabolome under drought in tropical rainforest plants. *Science of the Total Environment* 899.

Jakobsen I, Rosendahl L. 1990. Carbon flow into soil and external hyphae from roots of mycorrhizal cucumber plants. *New Phytologist* 115(1): 77-83.

Jeyanny V, Lee SS, Rasidah KW. 2011. Effects of arbuscular mycorrhizal inoculation and fertilisation on the growth of acacia mangium seedlings. *Journal of Tropical Forest Science* 23(4): 404-409.

Jiang Z, Thakur MP, Liu RQ, Zhou GY, Zhou LY, Fu YL, Zhang PP, He YH, Shao JJ, Gao J, et al. 2022. Soil P availability and mycorrhizal type determine root exudation in sub-tropical forests. *Soil Biology & Biochemistry* 171.

Jobbagy EG, Jackson RB. 2000. The vertical distribution of soil organic carbon and its relation to climate and vegetation. *Ecological Applications* 10(2): 423-436.

Karst J, Gaster J, Wiley E, Landhausser SM. 2017. Stress differentially causes roots of tree seedlings to exude carbon. *Tree Physiol* 37(2): 154-164.

Kharin VV, Zwiers FW, Zhang X, Hegerl GC. 2007. Changes in temperature and precipitation extremes in the IPCC ensemble of global coupled model simulations. *Journal of Climate* 20(8): 1419-1444.

Kiggundu N, Migliaccio KW, Schaffer B, Li Y, Crane JH. 2011. Water savings, nutrient leaching, and fruit yield in a young avocado orchard as affected by irrigation and nutrient management. *Irrigation Science* 30(4): 275-286.

Kong D, Ma C, Zhang Q, Li L, Chen X, Zeng H, Guo D. 2014. Leading dimensions in absorptive root trait variation across 96 subtropical forest species. *New Phytol* 203(3): 863-872.

Kuyper TW, Jansa J. 2023. Arbuscular mycorrhiza: advances and retreats in our understanding of the ecological functioning of the mother of all root symbioses. *Plant and Soil*: 48.

Laliberté E. 2017. Below-ground frontiers in trait-based plant ecology. *New Phytologist* 213(4): 1597-1603.

Lerdau MT, Monson RK, Ehleringer JR. 2023. The carbon balance of plants: economics, optimization, and trait spectra in a historical perspective. *Oecologia* 203(3-4): 297-310.

Liu C-Y, Hao Y, Wu X-L, Dai F-J, Abd-Allah EF, Wu Q-S, Liu S-R. 2023. Arbuscular mycorrhizal fungi improve drought tolerance of tea plants via modulating root architecture and hormones. *Plant Growth Regulation* 102(1): 13-22.

Livingston LG, Medes G. 1947. The Biosynthesis of C13 Compounds. *Journal of General Physiology* 31(1): 75-88.

Magrin GO, Marengo JA, Boulanger J-P, Buckeridge MS, Castellanos E, Poveda G, Scarano FR, Vicuna S 2014. Central and South America. In: Barros VR, C.B. Field, D.J. Dokken, M.D. Mastrandrea, K.J. Mach, T.E. Bilir, M. Chatterjee, K.L. Ebi, Y.O. Estrada, R.C. Genova, B.Girma, E.S. Kissel, A.N. Levy, S. MacCracken, P.R. Mastrandrea, and L.L. White ed. *Climate Change 2014: Impacts, Adaptation, and Vulnerability. Part B: Regional Aspects.*

Contribution of Working Group II to the Fifth Assessment Report on the Intergovernmental Panel on Climate Change. Cambridge, United Kingdom and New York, NY, USA: Cambridge University Press, 1499-1566.

Mannerheim N, Blessing CH, Oren I, Grunzweig JM, Bachofen C, Buchmann N. 2020. Carbon allocation to the root system of tropical tree Ceiba pentandra using 13C pulse labelling in an aeroponic facility. *Tree Physiol* 40(3): 350-366.

Marenco RA, Antezana-Vera SA, Nascimento HCS. 2009. Relationship between specific leaf area, leaf thickness, leaf water content and SPAD-502 readings in six Amazonian tree species. *Photosynthetica* 47(2): 184-190.

McCormack ML, Dickie IA, Eissenstat DM, Fahey TJ, Fernandez CW, Guo D, Helmisaari H-S, Hobbie EA, Iversen CM, Jackson RB, et al. 2015. Redefining fine roots improves understanding of below-ground contributions to terrestrial biosphere processes. *New Phytologist* 207(3): 505-518.

Metcalfe DB, Meir P, Aragao L, da Costa ACL, Braga AP, Goncalves PHL, Silva JD, de Almeida SS, Dawson LA, Malhi Y, et al. 2008. The effects of water availability on root growth and morphology in an Amazon rainforest. *Plant and Soil* 311(1-2): 189-199.

Ostonen I, Püttsepp Ü, Biel C, Alberton O, Bakker MR, Lõhmus K, Majdi H, Metcalfe D, Olsthoorn AFM, Pronk A, et al. 2007. Specific root length as an indicator of environmental change. *Plant Biosystems* 141(3): 426-442.

Poorter H, Niklas KJ, Reich PB, Oleksyn J, Poot P, Mommer L. 2012. Biomass allocation to leaves, stems and roots: meta-analyses of interspecific variation and environmental control. *New Phytologist* 193(1): 30-50.

Prescott CE. 2022. Sinks for plant surplus carbon explain several ecological phenomena. *Plant and Soil* 476(1-2): 689-698.

Rasse DP, Rumpel C, Dignac MF. 2005. Is soil carbon mostly root carbon? Mechanisms for a specific stabilisation. *Plant and Soil* 269(1-2): 341-356.

Reich PB. 2014. The world-wide 'fast-slow' plant economics spectrum: a traits manifesto. *Journal of Ecology* 102(2): 275-301.

Reichert T, Rammig A, Fuchslueger L, Lugli LF, Quesada CA, Fleischer K. 2022. Plant phosphorus-use and -acquisition strategies in Amazonia. *New Phytologist* 234(4): 1126-1143.

Rewald B, Ephrath JE, Rachmilevitch S. 2011. A root is a root is a root? Water uptake rates of Citrus root orders. *Plant Cell and Environment* 34(1): 33-42.

Sanket J. More VR, Saravanan Raju. 2020. *Climate Change and Crop Stress - Chapter 17 - Carbon isotope discrimination studies in plants for abiotic stress*. Academic Press.

Sarkar A, Asaeda T, Wang QY, Rashid MH. 2015. Arbuscular mycorrhizal influences on growth, nutrient uptake, and use efficiency of Miscanthus sacchariflorus growing on nutrient-deficient river bank soil. *Flora* 212: 46-54.

Schumacher E, Kueffer C, Tobler M, Gmuer V, Edwards PJ, Dietz H. 2008. Influence of drought and shade on seedling growth of native and invasive trees in the Seychelles. *Biotropica* 40(5): 543-549.

Smith SE, Read DJ. 2008. *Mycorrhizal Symbiosis*: Academic Press.

Smith NG, Keenan TF, Colin Prentice I, Wang H, Wright IJ, Niinemets Ü, Crous KY, Domingues TF, Guerrieri R, Yoko Ishida F, et al. 2019. Global photosynthetic capacity is optimized to the environment. *Ecology Letters* 22(3): 506-517.

Studer C, Hu Y, Schmidhalter U. 2017. Interactive Effects of N-, P- and K-Nutrition and Drought Stress on the Development of Maize Seedlings. *Agriculture* 7(11).

Sun Z, Wu S, Zhu B, Zhang Y, Bol R, Chen Q, Meng F. 2019. Variation of (13)C and (15)N enrichments in different plant components of labeled winter wheat (Triticum aestivum L.). *Peerj* 7: e7738.

Tahir MM, Recous S, Aita C, Pfeifer IC, Chaves B, Giacomini SJ. 2018. Field 13C Pulse Labeling of Pea, Wheat, and Vetch Plants for Subsequent Root and Shoot Decomposition Studies. *Revista Brasileira De Ciencia Do Solo* 42(0).

Tang H, Hassan MU, Feng L, Nawaz M, Shah AN, Qari SH, Liu Y, Miao J. 2022. The Critical Role of Arbuscular Mycorrhizal Fungi to Improve Drought Tolerance and Nitrogen Use Efficiency in Crops. *Front Plant Sci* 13: 919166.

Thomas DS, Eamus D, Shanahan S. 2000. Influence of season, drought and xylem ABA on stomatal responses to leaf-to-air vapour pressure difference of trees of the Australian wet-dry tropics. *Australian Journal of Botany* 48(2).

Valverde-Barrantes OJ, Horning AL, Smemo KA, Blackwood CB. 2016. Phylogenetically structured traits in root systems influence arbuscular mycorrhizal colonization in woody angiosperms. *Plant and Soil* 404(1-2): 1-12.

Vizoso S, Gerant D, Guehl JM, Joffre R, Chalot M, Gross P, Maillard P. 2008. Do elevation of CO(2) concentration and nitrogen fertilization alter storage and remobilization of carbon and nitrogen in pedunculate oak saplings? *Tree Physiol* 28(11): 1729-1739.

Wang YJ, He XH, Meng LL, Zou YN, Wu QS. 2023. Extraradical Mycorrhizal Hyphae Promote Soil Carbon Sequestration through Difficultly Extractable Glomalin-Related Soil Protein in Response to Soil Water Stress. *Microb Ecol* 86(2): 1023-1034.

Westoby M, Warton D, Reich PB. 2000. The Time Value of Leaf Area. *The American Naturalist* 155(5): 649-656.

Wright IJ, Reich PB, Westoby M, Ackerly DD, Baruch Z, Bongers F, Cavender-Bares J, Chapin T, Cornelissen JH, Diemer M, et al. 2004. The worldwide leaf economics spectrum. *Nature* 428(6985): 821-827.

Yang X, Lu M, Wang Y, Wang Y, Liu Z, Chen S. 2021. Response Mechanism of Plants to Drought Stress. *Horticulturae* 7(3).

Zhang ZF, Zhang JC, Xu GP, Zhou LW, Li YQ. 2019. Arbuscular mycorrhizal fungi improve the growth and drought tolerance of Zenia insignis seedlings under drought stress. *New Forests* 50(4): 593-604.

Zhu XC, Song FB, Liu SQ, Liu TD, Zhou X. 2012. Arbuscular mycorrhizae improves photosynthesis and water status of Zea mays L. under drought stress. *Plant, Soil and Environment* 58(4): 186-191.

CHAPTER 5: TROPIROOT 1.0 – DATABASE OF TROPICAL ROOT CHARACTERISTICS ACROSS ENVIRONMENTS[2]

5.1 Summary

TropiRoot 1.0 database is a compilation of root data from tropical regions. I led this initiative which was a collaborative effort among the TropiRoot trait Initiative, the Fine-Root Ecology Database (FRED), the Global Root Trait (GRooT) database, Colorado State University (CSU), and the Smithsonian Tropical Research Institute (STRI). Tropical ecosystems are usually not very well represented in global databases, especially belowground data. Therefore, TropiRoot 1.0 database contributes to an extensive compilation of root traits from tropical regions worldwide, which offers a tool for evaluating ecological hypotheses within the tropics and also in comparison with other global biomes. The database covers root traits affected by global change drivers and natural gradients, with data from over 25 countries across continents at both species and community level. This database increases the available data for tropical roots, with more than 8000 rows of data collected from 106 new sources. This includes information on root biomass, morphology, dynamics, and chemistry, among other traits. We believe that this data will be of great interest to the scientific community.

[2] Cordeiro, A.L et al. 2024. TropiRoot 1.0 – Database of tropical root characteristics across environments. Manuscript under review by Ecology.

5.2 Introduction

Tropical ecosystems contain the world's largest biodiversity of vascular plants. Yet, our understanding of tropical functional diversity and its contribution to global diversity patterns is constrained by data availability. This discrepancy underscores an urgent need to bridge data gaps by incorporating comprehensive tropical root data into global datasets. Here, we provide a database of tropical root characteristics. This new database, TropiRoot 1.0, will be instrumental in evaluating an array of hypotheses pertaining to root functional ecology and plant biogeography, both within the tropics and relative to other global biomes. The data compilation was conducted by the TropiRoot trait Initiative, in partnership with the Fine-Root Ecology Database (FRED) and the Global Root Trait (GRooT) database, Colorado State University (CSU) and the Smithsonian Tropical Research Institute (STRI). Literature search and data extraction were conducted between 2020 - 2024. Literature was identified using Web of Science, Scopus and complemented using the expert knowledge of member of TropiRoot. To provide broad environmental and geographical distributions, literature searches included root characteristics (traits) across global change drivers, natural gradients, and from different continents. We adopted FRED standardized data columns and streamlined the format to enhance the accessibility for data extraction across various user groups. This optimized framework was achieved through strategic additions and eliminations of columns chosen by members of Tropiroot group, resulting in a smaller, yet comprehensive datasheet. To make the database compatible with other global root trait initiatives, root characteristics identification was standardized following the codes provided by FRED. I personally led this initiative by creating the datasheet to compile the data, compiling each extracted paper to the database, extracting data myself, helping students and collaborators to extract and check data,

answering questions about data extraction process, contacting manuscript authors to request data, teaching collaborators on how to enter the data, writing the manuscript and the user guide such as is similar to FRED, but with details from Tropiroot and submitting the database. These efforts culminated in data extracted from 106 new sources, resulting in more than 8000 rows of data (either species or community data). Most of the data in TropiRoot 1.0 includes root characteristics such as root biomass, morphology, root dynamics, mass fraction, architecture, anatomy, physiology and root chemistry. This initiative represents a 30% increase of the currently available data for tropical roots in FRED. TropiRoot 1.0, contains root characteristics from 25 different countries where seven are located in Asia, six in South America, five in Central America and the Caribbean, four in Africa, two in North America, and 1 in Oceania. Due to the volume of data, when ancillary data was available, including soil data, these data was either extracted and included in the database or their availability was recorded in an additional column. Multiple contributors checked the entries for outliers during the collation process to ensure data quality. For text-based observations, we examined all cells to ensure that their content relates to their specific categories. For numerical observations, we ordered each numerical value from least to greatest and plotted the values, checking apparent outliers against the data in their respective sources and correcting or removing incorrect or impossible values. Some data contain root characteristics in different columns presented in different units, including originally published units. By filling a gap from global databases, TropiRoot 1.0 expands our knowledge of otherwise so far underrepresented regions, and our ability to assess global trends. This advancement can be used to improve tropical forest representation in vegetation models.

5.3 Database compilation

Data acquisition

The data compilation was conducted by myelf, the TropiRoot trait Initiative (TropiRoot; https://tropiroottrait.github.io/TropiRootTrait/index.html), in partnership with the Fine-Root Ecology Database (FRED) and the Global Root Trait (GRooT) database, Colorado State University (CSU) and the Smithsonian Tropical Research Institute (STRI). Literature search and data extraction were conducted between 2020 - 2024. Literature was identified using Web of Science, Scopus and complemented using the expert knowledge of member of TropiRoot. To provide broad environmental and geographical distributions, literature searches included root traits across global change drivers, natural gradients, and from different continents. Our methodology involved adopting FRED's standardized data columns while streamlining the format to enhance accessibility across various user groups. This optimized framework was achieved through strategic additions and eliminations, resulting in a distilled yet comprehensive datasheet with columns available in FRED and other columns added. The TropiRoot group selected scientific papers for data extraction and inclusion in their database, guided by a range of themes that align with their research interests. We applied standardized procedures and identified ~830 papers in multiple languages (English, Spanish, and Portuguese), which report results from the field, pot experiments, laboratory-based or modeling studies of roots that were conducted in tropical latitudes with a few sources from subtropical latitudes from 1978 to 2021. From these, we meticulously acquired data from the original papers or authors from 106 sources, encompassing a diverse range of root traits either from species or community level. This corresponds to one-third of sources already present in the FRED database (317 papers). We used the WebPlotDigitizer (Rohatgi 2024) online tool to

extract data from figures when they were not available in supplemental material or tables. Our workflow adopted FRED's standardized data columns with some adaptations. Our current database now contains over 8000 lines of data derived from these 106 sources. It is important to note that a single paper can contribute multiple data entries to our analysis. This is due to the methodology of capturing multiple traits (such as specific root length (SRL), diameter, etc.) from the same site, plot, or treatment, each documented in separate columns within our database. Due to the volume of data, when ancillary data was available, including soil data, these data was either extracted and included in the database or their availability was recorded in an additional column. Multiple contributors checked the entries for outliers during the collation process to ensure data quality. This database can also contain the same trait with different units in different columns in order to match with the row data from the original publication, so conversions still need to be made to transfer information across databases. The TropiRoot 1.0 database focused on fine roots (traditionally defined as roots less than 2 mm in diameter), as coarse roots are studied using different methodologies, often at different scales, and have different traits and trait interpretations. However, it accepts data collected from roots of all diameters and contains observations of coarse roots. Also, although most of the sources are from tropical regions, this database contains some subtropical studies. The sources included in the database are described in Table 5.4 and the complete database is in Table SI 4.1– Appendix 4.

Trait and Site Data

Data was acquired from publicly available data sources presented in column D of the database. While we used numbers presented in tables or in article text whenever possible, much data was only available in graphic form. We extracted data from graphs using the WebPlotDigitizer

online tool.

The quality of all observations was checked prior to the publication of TropiRoot 1.0 as follows: For text-based observations, we examined all cells to ensure that their content relates to their specific categories. For numerical observations, we ordered each numerical value from least to greatest and plotted the values, checking apparent outliers against the data in their respective sources and correcting or removing incorrect or impossible values. For statistical metrics (e.g. sample size, standard error, standard deviation), we checked them to ensure that each accompanied a main value. Some statistical metrics were not provided by contributors; thus, they need to be used carefully.

Derived Locations

Coordinate values were set, in order of priority, as (1) the single latitude/longitude point location reported in the original data source, (2) the minimum and maximum latitudes and longitudes reported in the original data source, or (3) an estimated latitude and longitude based on the description of the sampling location reported in the original data source and using Google Earth to obtain an approximate location. When necessary, latitude/longitude data were converted to decimal degrees using the following website: https://www.gps-coordinates.net/gps-coordinates-converter

Do-It-Yourself FRED Data Entry

We encourage the broader scientific community to contribute published and unpublished data to databases. TropiRoot 1.0 has no established funding support, so we encourage the scientific community to contribute data to FRED (http://roots.ornl.gov). The FRED team has written a series

of guidelines to help facilitate this, which can be found at http://roots.ornl.gov/DIY. If you don't have time to enter in this format, you can contact the TropiRoot team to help you enter data in a shortened version of FRED.

5.4 Data Use Guidelines

Data users are expected to follow professional scientific norms of citing and referencing inputs to their research. This does not preclude data users from contacting data contributors for collaboration purposes. Data users do not need to contact the TropiRoot team to use the data - it is freely available.

Tips for Using TropiRoot 1.0

TropiRoot 1.0 does not have a User Interface, so the complete datasheet needs to be downloaded and columns filtered by the user as the user sees fit. Note that there will be multiple columns for the same root trait, in some cases because the same traits may have different units. It is the responsibility of the user to convert the units from the specific traits to be used.

Data File Description for TropiRoot 1.0

The full TropiRoot_Database_1.0.csv is a Microsoft Excel spreadsheet (.CSV) file with over 8,000 observations of root traits from over 100 documented data sources (Figure 5.1, Table SI 4.1 – Appendix 4.). Associated statistical metric observations (Table 5.3) and ancillary data observations regarding associated site, vegetation, edaphic, and climatic conditions are more numerous. For example, ancillary data may repeat for all rows reported at the same geographic location.

5.5 Data File Organization

TropiRoot 1.0 Header Rows:

The TropiRoot_Database_1.0.csv (Table SI 4.1 – Appendix 4) is structured with seven header rows, mirroring the format used in the FRED database. Table 5.1 provides a detailed description of these headers in their sequential order. It is important to highlight that this version includes two additional headers beyond those found in FRED. While the column names and definitions generally align with those in FRED, deviations occur with specific root traits or newly introduced columns, which bear unique names. For columns that correspond directly to FRED, a unique column ID is assigned for ease of reference. However, it should be noted that certain traits may lack a column ID, a situation arising when contributors are unable to identify an equivalent column ID in FRED, despite its potential existence.

No Data and NA Values:

Cells with no data appear as blank cells or "NA" in the database. It's important to distinguish that cells marked with "NA" denote instances where information was searched but could not be located, whereas blank cells may also signify data that was not entered. In certain scenarios, these blank cells imply that the information was not verified in the original data source, though it may still exist within the original data source.

The Following Generalizations and Abbreviations Have Been Used in FRED and are also used in TropiRoot 1.0:

- 'Root mass' refers to root dry mass unless otherwise stated (e.g., 'root fresh mass').
- Each trait or ancillary data value is the mean of collected data unless otherwise stated.

- The word ‘root’ in a trait name or description refers to the part specified in the ‘belowground part’ column (Column ID F00055) and, therefore may refer to coarse roots, fine roots, or the total root system, but also to belowground stem, rhizome, or other belowground non-root entities.

See Table 5.2 for Statistical Metrics used in TropiRoot 1.0 (copied from FRED 3.0) and for column identification.

See Table 5.3 for Abbreviations used for units in TropiRoot 1.0 (copied from FRED 3.0) and in the Data Dictionary.

Disclaimer of Liability

The TropiRoot team, along with the referenced FRED database and any associated parties or employees, disclaims all warranties, both explicit and implicit, and does not assume any legal liability or responsibility for the precision, completeness, or practical utility of any disclosed information, tools, products, or processes. Furthermore, it is important to acknowledge that the database was collaboratively produced by multiple contributors and is an independent entity, not directly associated with FRED. Despite rigorous data verification against individual sources by a secondary reviewer, inconsistencies or errors may still be present. Unlike FRED, TropiRoot 1.0 offers a more compact dataset, which excludes some information that may be available in the original source and allows for a greater degree of flexibility and subjectivity in certain columns, particularly within ancillary data where interpretations may vary among contributors. For instance, the methods section endeavors to accurately reflect the methodologies as described in the original sources, resulting in a diverse array of entries.

Contact Us

For queries, report mistakes and suggestions, please contact: TropiRoottrait@gmail.com

Data Dictionary for TropiRoot 1.0:

Column ID (same as in FRED) is the unique and unchanging identifier for the root trait, associated statistical metric, ancillary data observation, or descriptive field listed in Column names (same as in FRED). Units / Format and Description for the respective column follow.

Note that the complete Description (Definition from FRED/TropiRoot) is included in the TropiRoot_Database_1.0.csv file (Table SI 4.1 – Appendix 4).

In the TropiRoot database, similar types of ancillary data are grouped under common prefixes, such as 'Notes_', 'Data_', 'Plant taxonomy_', etc., with 'Notes_' typically encompassing descriptive ancillary data. Starting from column AU, all root traits are named according to the terminologies used in their original sources. Additionally, a unique column ID linking to the corresponding FRED column ID is provided in line 6 for each trait. It's important to note that even when a trait shares a column ID with FRED, the units of measurement may differ, as this database retains the original units from the source material. If a trait is assigned a column ID, it signifies that its data can be integrated into FRED, albeit with careful unit conversion as necessary. Traits not found in FRED are explicitly marked as "NOT IN FRED" on line 6, and those requiring unit conversion are highlighted in red with "NEED TO CONVERT" in line 5, underscoring the importance of meticulous attention to unit conversions.

A note about some data values: we used WebPlotDigitizer, a point-and-click online tool, to extract data from graphs and charts. Data derived from it are presented with more decimal places than in the original data in some cases. However, this does not necessarily correspond to the

number of significant figures in the source data; the additional decimal places should be treated with caution.

5.6 Figures

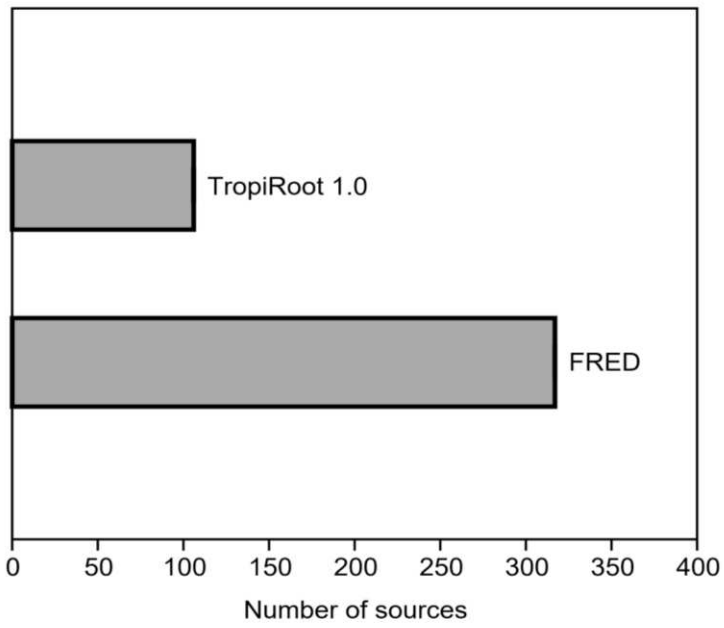

Figure 5.1: Number of sources in the Fine Root Ecological Database (FRED) and TropiRoot 1.0 database. This new database added ~30 % of new data from tropical root traits.

5.7 Tables

Table 5.1. Header rows (i.e., the first 5 rows) are descriptive and do not have unique row IDs; these rows come with each download of the TropiRoot 1.0 database.

Header position	Header name	Example	Description
1st	Column names (same as in FRED)	Root N content	Name of root trait or ancillary data type selected by FRED curators.
2nd	Units	mg/g	Units of data in column.
3rd	Definition from FRED/TropiRoot	Mass of nitrogen per root mass for sampled roots.	Definition of root trait or ancillary data type, as in the Data Dictionary of this document.
4th	Column ID (same as in FRED)	F00261 (F00001 to F01474)	Unique identifier for column. If the column is moved, renamed, or otherwise changed in future versions, Column ID remains the same.
5th	Name in TRY or TropiRoot explanation	Root nitrogen content per dry mass	The name of root trait or ancillary data type in the TRY database (www.try-db.org) if applicable.

Table 5.2. Statistical metrics and definitions associated with many traits or ancillary data types.

Statistical term	Definition
n	Sample size: number of observations for specified parameter
SE	Standard error of specified parameter; SD/(√n) for specified parameter
SD	Standard deviation of specified parameter
Median	Value below which 50% of observed data for specified parameter falls
Upper quartile	Value below which 75% of observed data for specified parameter falls
Lower quartile	Value below which 25% of observed data for specified parameter falls
95th percentile	Value below which 95% of observed data for specified parameter falls
5th percentile	Value below which 5% of observed data for specified parameter falls
95 percent confidence margin	Size of interval that has a 95% certainty of including the true mean.
Min	Minimum value observed for specified parameter
Max	Maximum value observed for specified parameter
Modal	Value for specified parameter that occurs most in the data set
Upper bound	If data are presented for pre-defined interval, the upper bound of that interval
Lower bound	If data are presented for a pre-defined interval, the lower bound of that interval

Table 5.3. Abbreviations used for units in TropiRoot 1.0 (copied from FRED 3.0). Note that some items that are commonly presented as superscripts (e.g., cm^2) or subscripts (e.g., CO_2) will appear in TropiRoot 1.0 without this special formatting (e.g. cm2 and CO2, respectively). Similarly, the abbreviation "u" is used for micro- instead of the commonly used "µ". This was done to avoid the use of special text characters in the database which may not be compatible with some software or analyses.

Abbreviation	Stands for
branch	Root branch
cm	Centimeters
cm^2	Square centimeters
cm^3	Cubic centimeters
cmolc	Centimoles of charge
d	Days
degrees_C	Degrees Celsius
FW	Fresh weight
g	Grams
g_C	Grams root carbon
h	Hours
ha	Hectares (square hectometers)
kg	Kilograms
km	Kilometers
L	Liters
m	Meters
m^2	Square meters
m^3	Cubic meters
mg	Milligrams
Mg	Megagrams (metric tons)
min	Minutes
ml	Milliliters
mm	Millimeters
mm^2	Square millimeters
µm	Micrometers
$µm^2$	Square micrometers
mmol	Millimoles
µmol	Micromoles
mmolc	Millimoles of charge
mo	Months
MPa	Megapascals
mV	Millivolts
ng	Nanograms
nmol	Nanomoles
-cbar	Negative centibars
per_mil	Thousandths
pmol	Picomoles
s	Seconds
µg	Micrograms
µm	Micrometers
µmol	Micromoles
yr	Years

Table 5.4: References from data added to TropiRoot 1.0

#	Reference / source / PI
2	Apgaua, Deborah M. G., Tng, David Y. P., Forbes, Samantha J., Ishida, Yoko F., Vogado, ra O., Cernusak, Lucas A. and Laurance, Susan G. W. (2019) Elevated temperature and CO2 cause differential growth stimulation and drought survival responses in eucalypt species from contrasting habitats. Tree Physiology 39, 1806-1820
3	Asbjornsen, Heidi & Vogt, Kristiina & Ashton, Mark. (2004). Synergistic responses of oak, pine and shrub seedlings to edge environments and drought in a fragmented tropical highland oak forest, Oaxaca, Mexico. Forest Ecology and Management. 192. 313-334. 10.1016/j.foreco.2004.01.035.
4	Barton, Kasey and Shiels, Aaron. (2020) Additive and non-additive responses of seedlings to simulated herbivory and drought data. Dryad
5	Campo, J. and Merino, A. (2016) Variations in soil carbon sequestration and their determinants along a precipitation gradient in seasonally dry tropical forest ecosystems. Global Change Biology 22, 1942-1956
6	Chacon, Noemi, Dezzeo, Nelda, Rangel, Maiella and Flores, Saul. (2008) Seasol changes in soil phosphorus dymics andRoot mass along a flooded tropical forest gradient in the lower Orinoco river, Venezuela. Biogeochemistry 87, 157-168
7	Cao, K. (2000). Water Relations and Gas Exchange of Tropical Saplings during a Prolonged Drought in a Bornean Heath Forest, with Reference to Root Architecture. Journal of Tropical Ecology, 16(1), 101-116.
8	Nomura, Naofumi & Kikuzawa, Kihachiro. (2003). Productive phenology of tropical montane forests: Fertilization experiments along a moisture gradient. Ecological Research. 18. 573 - 586. 10.1046/j.1440-1703.2003.00579.x.
9	O'Brien, M., Leuzinger, S., Philipson, C. et al. Drought survival of tropical tree seedlings enhanced by non-structural carbohydrate levels. Nature Clim Change 4, 710–714 (2014). https://doi.org/10.1038/nclimate2281
10	Poungparn, Sasitorn, Komiyama, Akira, Umnouysin, Suthathip, Rodtassa, Chadtip, Sangtiean, Tanuwong, Maknual, Chatree, Pravinvongvuthi, Tamai, Suchewaboripont, Vilanee and Kato, Shogo. (2020) Ten-Year Estimation of Net Primary Productivity in a Mangrove Forest under a Tropical Monsoon Climate in Eastern Thailand: Significance of the Temperature Environment in the Dry Season. Forests 11
11	Schumacher, Eva, Kueffer, Christoph, Tobler, Monika, Gmuer, Veronika, Edwards, Peter J. and Dietz, Hansjoerg. (2008) Influence of drought and shade on seedling growth of tive and invasive trees in the Seychelles. Biotropica 40, 543-549
12	Tang, Songbo, Xu, Yimin, Lin, Yongbiao, Hou, Enqing, Shen, Weijun, Wang, Jun and Kuang, Yuanwen. (2018) Seasonal drought may alter N availability but not water use efficiency of domint trees in a subtropical forest. Global Ecology and Conservation 16

13	Valdés, M., Asbjornsen, H., Gómez-Cárdenas, M. et al. Drought effects on fine-Root and ectomycorrhizal-Root biomass in managed Pinus oaxacana Mirov stands in Oaxaca, Mexico. Mycorrhiza 16, 117–124 (2006). https://doi.org/10.1007/s00572-005-0022-9
14	Wang, Guiling, Alo, Clement, Mei, Rui and Sun, Shanshan. (2011) Droughts, hydraulic redistribution, and their impact on vegetation composition in the Amazon forest. Plant Ecology 212, 663-673
15	Zhou, Liguo, Liu, Yuntong, Zhang, Yiping, Sha, Liqing, Song, Qinghai, Zhou, Wenjun, Balasubramanian, D., Palingamoorthy, Gmoorthy, Gao, Jinbo, Lin, Youxing, Li, Jing, Zhou, Ruiwu, Myo, Sai Tay Zar, Tang, Xianhui, Zhang, Jin, Zhang, Peng, Wang, Shusen and Grace, John. (2019) Soil respiration after six years of continuous drought stress in the tropical rainforest in Southwest Chi. Soil Biology & Biochemistry 138
16	Doughty, Christopher E., Malhi, Yadvinder, Araujo-Murakami, Alejandro, Metcalfe, Daniel B., Silva-Espejo, Javier E., Arroyo, Luzmila, Heredia, Juan P., Pardo-Toledo, Erwin, Mendizabal, Luz M., Rojas-Landivar, Victor D., Vega-Martinez, Meison, Flores-Valencia, Marcio, Sibler-Rivero, Rebeca, Moreno-Vare, Luzmarina, Viscarra, Laura Jessica, Chuviru-Castro, Tamara, Osinaga-Becerra, Marilin and Ledezma, Roxana. (2014) Allocation tradeoffs dominate the response of tropical forest growth to seasonal and interannual drought. Ecology 95, 2192-2201
17	Tyree, M. T., Engelbrecht, B. M. J., Vargas, G. and Kursar, T. A. (2003) Desiccation tolerance of five tropical seedlings in Panama. Relationship to a field assessment of drought performance. Plant Physiology 132, 1439-1447
18	Wolfe, B. (2017) Retention of stored water enables tropical tree saplings to survive extreme drought conditions. Tree Physiology, 37 (469-480). doi: 10.1093/treephys/tpx001
19	Cusack, D.F., Markesteijn, L., Condit, R. et al. Soil carbon stocks across tropical forests of Panama regulated by base cation effects on Fine Roots. Biogeochemistry 137, 253–266 (2018). https://doi.org/10.1007/s10533-017-0416-8
20	Roa-Fuentes, L.L., Campo, J. & Parra-Tabla, V. Plant Biomass Allocation across a Precipitation Gradient: An Approach to Seasonally Dry Tropical Forest at Yucatán, Mexico. Ecosystems 15, 1234–1244 (2012). https://doi.org/10.1007/s10021-012-9578-3
21	Schappe, Tyler & Albornoz, Felipe & Turner, Benjamin & Neat, Abbey & Condit, Richard & Jones, F.. (2017). The role of soil chemistry and plant neighbourhoods in structuring fungal communities in three Panamanian rainforests. Journal of Ecology. 105. 569-579. 10.1111/1365-2745.12752.
22	Cusack, D.F., Ashdown, D., Dietterich, L.H. et al. Seasonal changes in soil respiration linked to soil moisture and phosphorus availability along a tropical rainfall gradient. Biogeochemistry 145, 235–254 (2019). https://doi.org/10.1007/s10533-019-00602-4
23	Shibata, M., Sugihara, S., Mvondo-Zé, A., Araki, S., & Funakawa, S. (2017). Nitrogen flux patterns through Oxisols and Ultisols in tropical forests of Cameroon, Central Africa. Soil Science and Plant Nutrition, 63, 306 - 317.
24	Brum, Mauro, Vadeboncoeur, Matthew A., Ivanov, Valeriy, Asbjornsen, Heidi, Saleska, Scott, Alves, Luciana F., Penha, Deliane, Dias, Jadson D., Aragao, Luiz E. O. C., Barros, Fernanda, Bittencourt, Paulo, Pereira, Luciano and Oliveira, Rafael S. (2019) Hydrological niche segregation defines forest structure and drought tolerance strategies in a seasonal Amazon forest. Journal of Ecology 107, 318-333

25	Davidson, E. A., Ishida, F. Y. and Nepstad, D. C. (2004) Effects of an experimental drought on soil emissions of carbon dioxide, methane, nitrous oxide, and nitric oxide in a moist tropical forest. Global Change Biology 10, 718-730
26	Deng, Q., Zhang, D., Han, X., Chu, G., Zhang, Q., & Hui, D. (2018). Changing rainfall frequency rather than Drought rapidly ALTERS ANNUAL soil respiration in a tropical forest. Soil Biology and Biochemistry, 121, 8-15. doi:10.1016/j.soilbio.2018.02.023
27	Moser G, Schuldt B, Hertel D, Horna V, Coners H, Barus, H, Leuschner, C. 2014. Replicated throughfall exclusion experiment in an Indonesian perhumid rainforest: wood production, litter fall and fine root growth under simulated drought. Global Change Biology 20:1481-1497.
28	Belk E.L., Markewitz, D., Rasmussen, T.C., Cvalho, E.J.M, Nepstad, D.C., and Davidson, E.A. (2007). Modeling the effects of throughfall reduction on soil water content in a Brazilian Oxisol under a moist tropical forest. Water Resources Research, 43.
29	Deines Jillian M., Hellmann Jessica J., Curran Timothy J. (2011) Traits associated with drought survival in three Australian tropical rainforest seedlings. Australian Journal of Botany 59, 621-629.
30	Metcalfe, D. B., P. Meir, L. E. O. C. Aragão, Y. Malhi, A. C. L. da Costa, A. Braga, P. H. L. Gonçalves, J. deAthaydes, S. S. deAlmeida, and M. Williams (2007), Factors controlling spatio-temporal variation in carbon dioxide efflux from surface litter, roots, and soil organic matter at four rain forest sites in the eastern Amazon, J. Geophys. Res., 112, G04001.
31	Barros V, Melo A, Santos M, Nogueira L, Frosi G. 2020. Different resource-use strategies of invasive and native woody species from a seasonally dry tropical forest under drought stress and recovery. Plant Physiology and Biochemistry 147 (181–190).
32	Yamada T, Suzuki E, Yamakura T, Tan S. 2005. Tap-root depth of tropical seedlings in relation to species-specific edaphic preferences. Journal of Tropical Ecology 21: 155-160.
33	Sierra Cornejo, N., Hertel, D., Becker, J. N., Hemp, A., & Leuschner, C. (2020). Biomass, Morphology, and Dynamics of the Fine Root System Across a 3,000-M Elevation Gradient on Mt. Kilimanjaro. Frontiers in Plant Science, 11, 13.
34	Torres, J. R., Barba, E., & Choix, F. J. (2019). Production and biomass of mangrove roots in relation to hydroperiod and physico-chemical properties of sediment and water in the Mecoacan Lagoon, Gulf of Mexico. Wetlands Ecology and Management, 27(2–3), 427–442. https://doi.org/10.1007/s11273-019-09669-0
35	Wen Z, Zheng H, Smith JR, Zhao H, Liu L, Ouyang Z. 2019. Functional diversity overrides community-weighted mean traits in linking land-use intensity to hydrological ecosystem services. Science of the Total Environment 682:583-590.
36	Worku, A., Fetene, M., Zewdie, S., & Assefa, Y. 2019. Fine root Biomass of Erica trimera (Engl.) along an altitudinal gradient on Bale Montains, Ethiopia. International Journal of Research -GRANTHAALAYAH, 7(9), 230-245.
37	Xiao, R., Bai, J., Zhang, H., Gao, H., Liu, X., & Wilkes, A. (2011). Changes of P, Ca, Al and Fe contents in fringe marshes along a pedogenic chronosequence in the Pearl River estuary, South China. Continental Shelf Research, 31(6), 739-747.
38	Guilbeault-Mayers, X., Turner, B.L., & Laliberte, E. (2020). Greater root phosphatase activity of tropical trees at low phosphorus despite strong variation among species. Ecology, 101(8).

39	Okada, K., Aiba, S., & Kitayama, K. (2017). Influence of temperature and soil nitrogen and phosphorus availabilities on fine-Root productivity in tropical rainforests on Mount Kinabulu, Borneo. Ecological Research, 32: 145-156. DOI 10.1007/s11284-016-1425-0
40	Poorter, L., & Hayashida-Oliver, Y. (2000). Effects of seasonal drought on gap and understorey seedlings in a Bolivian Moist Forest. Journal of Tropical Ecology, 16 (4), 481-498.
41	Girardin, C. A. J., Aragao, Leoc, Malhi, Y., Huasco, W. H., Metcalfe, D. B., Durand, L., Mamani, M., Silva-Espejo, J. E. and Whittaker, R. J. (2013) Fine Root dynamics along an elevational gradient in tropical Amazonian and Andean forests. Global Biogeochemical Cycles 27, 252-264
42	Brum, M., Teodoro, G.S., Abrahao, A., & Oliveira, R.S. (2017). Coordination of rooting depth and leaf hydraulic traits defines drought-related strategies in the campos rupestres, a tropical montane biodiversity hotspot. Plant Soil. DOI 10.1007/s11104-017-3330-x
43	Markewitz, D., Devine, S., Davidson, E.A., Brando, P., & Nepstad, D.C. (2010). Soil moisture depletion under simulated drought in the Amazon: impacts on deep root uptake. New Physiologist, 187(3).https://doi.org/10.1111/j.1469-8137.2010.03391.x
44	Doughty, C.E., Metcalfe, D.B., Girardin, C.A.J., Amezquita, F.F., Cabrera, D.G.… & Malhi, Y. (2015). Drought impact on forest carbon dynamics and fluxes in Amazonia. Nature, 519:78-82. doi:10.1038/nature14213
45	Ohashi, Mizue, Kume, Tomonori, Yoshifuji, Natsuko, Kho, Lip Khoon, Nakagawa, Michiko and Nakashizuka, Tohru. (2015) The effects of an induced short-term drought period on the spatial variations in soil respiration measured around emergent trees in a typical bornean tropical forest, Malaysia. Plant and Soil 387, 337-349
46	Green, J. J., Dawson, L. A., Proctor, J., Duff, E. I. and Elston, D. A. (2005) Fine root dynamics in a tropical rain forest is influenced by rainfall. Plant and Soil 276, 23-32
47	Anabelle W. Cardoso, Jose A. Medina-Vega, Yadvinder Malhi , Stephen Adu-Bredu, George K.D. Ametsitsi, Gloria Djagbletey, Frank van Langevelde, Elmar Veenendaal & Immaculada Oliveras. 2016. Winners and losers: tropical forest tree seedling survival across a West African forest–savanna transition
48	Sasitorn Poungparn, Thanyalak Charoenphonphakdi, Tanuwong Sangtiean, and Pipat Patanaponpaiboon. (2016) Fine root production in three zones of secondary mangrove forest in eastern Thailand
49	Poorter, L., & Markesteijn, L. (2008). Seedling traits determine drought tolerance of tropical tree species. Biotropica, 40: 321-331. 10.1111/j.1744-7429.2007.00380.x
50	D. C. Nepstad, P. Moutinho, M. B. Dias-Filho, E. Davidson, G. Cardinot, D. Markewitz, R. Figueiredo, N. Vianna, J. Chambers, D. Ray, J. B. Guerreiros, P. Lefebvre, L. Sternberg, M. Moreira, L. Barros, F. Y. Ishida, I. Tohlver, E. Belk, K. Kalif, and K. Schwalbe. (2002) The effects of partial throughfall exclusion on canopy processes, aboveground production, and biogeochemistry of an Amazon forest
51	Miyamoto K, Wagai R, Aiba SI, Nilus R. 2016. Variation in the aboveground stand structure and fine-Root biomass of Bornean heath (kerangas) forests in Relation to altitude and soil nitrogen availability. Trees 30:385-394.

52	Lu, W., Chen, L., Wang, W., Tam, N.F., & Lin, G. (2013). Effects of sea level rise on mangrove Avicennia population growth, colonization and establishment: Evidence from a field survey and greenhouse manipulation experiment. Acta Oecologica, 49: 83-91.
53	Gautam, Tilak Prasad and Mandal, Tej rayan. (2016) Effect of disturbance on biomass, production and carbon dymics in moist tropical forest of eastern Nepal. Forest Ecosystems 3:11
54	Fortunel, C., Ruelle, J., Beauchene, J., Fine, P.V.A., & Baraloto, C. (2014). Wood specific gravity and anatomy of branches and roots in 113 Amazonian rainforest tree species across environmental gradients. New Phytologist, 202: 79-94. 10.1111/nph.12632
55	Edward Castañeda-Moya, Robert R. Twilley, Victor H. Rivera-Monroy, Brian D. Marx, Carlos Coronado-Molina, and Sharon M. L. Ewe. (2011) Patterns of Root Dynamics in Mangrove Forests Along Environmental Gradients in the Florida Coastal Everglades, USA
56	Bebber, D., Brown, N., and Speight, M. (2002). Drought and Root Herbivory in Understorey Parashorea Kurz (Dipterocarpaceae) Seedlings in Borneo. Journal of Tropical Ecology, 18(5), 795-804. https://doi.org/10.1017/s0266467402002511
57	Thomas, D.S., Eamus, D., & Shanahan, S. (2000). Influence of season, drought and xylem ABA on stomatal responses to leaf-to-air vapour pressure difference of trees of the Australian wet-dry tropics. Australian Journal of Botany, 48: 143-151
58	Valverde-Barrantes OJ, Authier L, Schimann H, Baraloto C. Root anatomy helps to reconcile observed root trait syndromes in tropical tree species. Am J Bot. 2021 May;108(5):744-755. doi: 10.1002/ajb2.1659. Epub 2021 May 24. PMID: 34028799.
59	Colón, S. M., and A. E. Lugo. 2006. Recovery of a subtropical dry forest after abandonment of different land uses. Biotropica 38: 354–364.
60	Cuevas E, Brown S, Lugo AE (1991) Above- and belowground organic matter storage and production in a tropical pine plantation and a paired broadleaf secondary forest. Plant Soil 135:257–268. https://doi.org/10.1007/BF00010914
61	Cusack, D. F., Silver, W. L., Torn, M. S., and McDowell, W. H. (2011) Effects of nitrogen additions on above- and belowground carbon dynamics in two tropical forests. Biogeochemistry 104, 203–225.
62	Kangas, P. 1992. Root Regrowth in a Subtropical Wet Forest in Puerto Rico. Biotropica 24: 463–465.
63	McGroddy, M., and W. L. Silver. 2000. Variations in belowground carbon storage and soil CO2 flux rates along a wet tropical climate gradient. Biotropica 32: 614–624.
64	Silver, W. L., and R. K. Miya. 2001. Global patterns in Root decomposition: Comparisons of climate and Litter quality effects. Oecologia 129: 407–419
65	Lima, T. T. S., I. S. Miranda, and S. S. Vasconcelos. 2010. Effects of water and nutrient availability on fine root growth in eastern Amazonian forest regrowth, Brazil. New Phytol. 187: 622–630.
66	Fiala, K., L. Hernández, and P. Holub. 2017. Comparison of vertical distribution of live and dead Fine Root biomass in six types of cuban forests. J. Trop. For. Sci. 29: 275–281.

67	Guevara, R., and I. Romero. 2004. Spatial and temporal abundance of mycelial mats in the soil of a tropical rain forest in Mexico and their effects on the concentration of mineral nutrients in soils and Fine Roots. New Phytol. 163: 361–370.
68	Ibrahim, F., S. Adu-Bredu, S. D. Addo-Danso, A. Duah-Gyamfi, E. A. Manu, and Y. Malhi. 2020. Patterns and controls on fine-Root dynamics along a rainfall gradient in Ghana. Trees - Struct. Funct. 34: 917–929. Available at: https://doi.org/10.1007/s00468-020-01970-3.
69	Adams, F., P. Reddell, M. J. Webb, and W. A. Shipton. 2006. Arbuscular mycorrhizas and ectomycorrhizas on Eucalyptus grandis (Myrtaceae) trees and seedlings in native forests of tropical north-eastern Australia. Aust. J. Bot. 54: 271–281.
70	Addo-Danso, S.D., Defrenne, C.E., McCormack, M.L. et al. Fine-Root morphological trait variation in tropical forest ecosystems: an evidence synthesis. Plant Ecol 221, 1–13 (2020). https://doi.org/10.1007/s11258-019-00986-1
71	Cusack, D. F. and B. L. Turner (2020). "Fine Root and Soil Organic Carbon Depth Distributions are Inversely Related Across Fertility and Rainfall Gradients in Lowland Tropical Forests." Ecosystems in press.
72	Wang, R., Wang, Q., Liu, C., Kou, L., Zhao, N., Xu, Z., ... & He, N. (2018). Changes in trait and phylogenetic diversity of leaves and absorptive roots from tropical to boreal forests. Plant and Soil, 432(1-2), 389-401.
73	Alvarez-Clare, S. and Mack, M.C., 2015. Do foliar, Litter, andRoot nitrogen and phosphorus concentrations reflect nutrient limitation in a lowland tropical wet forest?. PloS one, 10(4), p.e0123796.
74	Burslem, D.F.R.P., Turner, I.M. and Grubb, P.J., 1994. Mineral nutrient status of coastal hill dipterocarp forest and adinandra belukar in Singapore: bioassays of nutrient limitation. Journal of Tropical Ecology, 10(4), pp.579-599.
75	Yokoyama, D., Imai, N., & Kitayama, K. (2017). Effects of nitrogen and phosphorus fertilization on the activities of four different classes of fine-Root and soil phosphatases in Bornean tropical rain forests. Plant and Soil, 416(1), 463-476.
76	Woods, C.L., DeWalt, S.J., Cardelús, C.L. et al. Fertilization influences the nutrient acquisition strategy of a nomadic vine in a lowland tropical forest understory. Plant Soil 431, 389–399 (2018).
77	Pons, T. L., Perreijn, K., Van Kessel, C., & Werger, M. J. (2007). Symbiotic nitrogen fixation in a tropical rainforest: 15N natural abundance measurements supported by experimental isotopic enrichment. New Phytologist, 173(1), 154-167.
78	Fisher, J.B., Malhi, Y., Torres, I.C., Metcalfe, D.B., van de Weg, M.J., Meir, P., Silva-Espejo, J.E. and Huasco, W.H., 2013. Nutrient limitation in rainforests and cloud forests along a 3,000-m elevation gradient in the Peruvian Andes. Oecologia, 172(3), pp.889-902.
79	Gurmesa, G.A., Lu, X., Gundersen, P., Fang, Y., Mao, Q., Hao, C. and Mo, J., 2017. Nitrogen input 15 N signatures are reflected in plant 15 N natural abundances in subtropical forests in China. Biogeosciences, 14(9), pp.2359-2370.

80	DUAN, H.L., LIU, J.X., Deng, Q., CHEN, X.M. and ZHANG, D.Q., 2009. Effects of elevated CO2 and N deposition on plant biomass accumulation and allocation in subtropical forest ecosystems: A mesocosm study. Chinese Journal of Plant Ecology, 33(3), p.570.
81	Lu, X., Mo, J., Gilliam, F.S., Zhou, G. and Fang, Y., 2010. Effects of experimental nitrogen additions on plant diversity in an old-growth tropical forest. Global Change Biology, 16(10), pp.2688-2700.
82	Andersen, K.M., Corre, M.D., Turner, B.L. and Dalling, J.W., 2010. Plant–soil associations in a lower montane tropical forest: physiological acclimation and herbivore-mediated responses to nitrogen addition. Functional Ecology, 24(6), pp.1171-1180.
83	Camenzind, T., Hempel, S., Homeier, J., Horn, S., Velescu, A., Wilcke, W. and Rillig, M.C., 2014. Nitrogen and phosphorus additions impact arbuscular mycorrhizal abundance and molecular diversity in a tropical montane forest. Global Change Biology, 20(12), pp.3646-3659.
83	Camenzind, T., Homeier, J., Dietrich, K., Hempel, S., Hertel, D., Krohn, A., Leuschner, C., Oelmann, Y., Olsson, P.A., Suárez, J.P. and Rillig, M.C., 2016. Opposing effects of nitrogen versus phosphorus additions on mycorrhizal fungal abundance along an elevational gradient in tropical montane forests. Soil Biology and Biochemistry, 94, pp.37-47.
84	Waring, B. G., D. Perez-Aviles, J. G. Murray, and J. S. Powers. 2019. Plant community responses to stand-level nutrient fertilization in a secondary tropical dry forest. Ecology 100(6)
85	Cleveland, C.C. and Townsend, A.R., 2006. Nutrient additions to a tropical rain forest drive substantial soil carbon dioxide losses to the atmosphere. Proceedings of the National Academy of Sciences, 103(27), pp.10316-10321.
87	Gower, S.T. and Vitousek, P.M., 1989. Effects of nutrient amendments on Fine Root biomass in a primary successional forest in Hawai'i. Oecologia, 81(4), pp.566-568.
88	Mo, J., Zhang, W.E.I., Zhu, W., Gundersen, P.E.R., Fang, Y., Li, D. and Wang, H.U.I., 2008. Nitrogen addition reduces soil respiration in a mature tropical forest in southern China. Global Change Biology, 14(2), pp.403-412.
89	Liu, T., Mao, P., Shi, L., Eisenhauer, N., Liu, S., Wang, X., He, X., Wang, Z., Zhang, W., Liu, Z. and Zhou, L., 2020. Forest canopy maintains the soil community composition under elevated nitrogen deposition. Soil Biology and Biochemistry, 143, p.107733.
90	Adamek, M., Corre, M.D. and Hölscher, D., 2011. Responses of Fine Roots to experimental nitrogen addition in a tropical lower montane rain forest, Panama. Journal of Tropical Ecology, 27(1), pp.73-81.
91	Blair, B.C. and Perfecto, I., 2008. Root proliferation and nutrient limitations in a Nicaraguan rain forest. Caribbean Journal of Science, 44(1), pp.36-42.
92	Zhu F, Yoh M, Gilliam FS, Lu X, Mo J (2013) Nutrient Limitation in Three Lowland Tropical Forests in Southern China Receiving High Nitrogen Deposition: Insights from Fine Root Responses to Nutrient Additions. PLoS ONE 8(12): e82661.
93	Cárate-Tandalla, D., Camenzind, T., Leuschner, C. and Homeier, J., 2018. Contrasting species responses to continued nitrogen and phosphorus addition in tropical montane forest tree seedlings. Biotropica, 50(2), pp.234-245.
94	Treseder, K. K., & Vitousek, P. M. (2001). Effects of soil nutrient availability on investment in acquisition of N and P in Hawaiian rain forests. Ecology, 82(4), 946-954

95	Lu, X., Mo, J., Gilliam, F.S., Zhou, G. and Fang, Y., 2010. Effects of experimental nitrogen additions on plant diversity in an old-growth tropical forest. Global Change Biology, 16(10), pp.2688-2700.
96	Gurmesa, G.A., Lu, X., Gundersen, P., Fang, Y., Mao, Q., Hao, C. and Mo, J., 2017. Nitrogen input 15 N signatures are reflected in plant 15 N natural abundances in subtropical forests in China. Biogeosciences, 14(9), pp.2359-2370.
97	Pierick K, Leuschner C, Homeier J. (2021) Topography as a factor driving small-scale variation in tree fine root traits and root functional diversity in a species-rich tropical montane forest. New Phytologist 230, 129-138.
98	Pierick K, Link RM, Leuschner C, Homeier J. (2023) Elevational trends of tree fine root traits in species-rich tropical Andean forests. Oikos e08975.
99	Pierick K, Leuschner C, Link RM, Baez S, Velescu A, Wilcke W, Homeier J (unpublished)
100	Brenes_Arguedas, T., Roddy, A.B., & Kursar, T.A. (2013). Plant traits in relation to the performance and distribution of woody species in wet and dry tropical forest types in Panama. Functional Ecology, 27: 392-402
101	Jimenez, E.M., Penuela-Mora, M.C., Moreno, F., & Sierra, C.A. (2020). Spatial and temporal variation of forest net primary productivity components on contrasting soils northwestern Amazon. Ecosphere, 11. 10.1002/ecs2.3233
102	Campos, J. and Merino, A. (2019). Linking organic P dynamics in tropical dry forests to changes in rainfall regime: Evidences of the Yucatan Peninsula. Forest Ecology and Management 438 (75–85)
103	Andrade, E.M., Rosa, G.Q., Almeida, A.M.M., Da Silva, A.G.R., & Sena, M.G.T. (2020). Rainfall regime on fine root growth in a seasonally dry tropical forest. Revista Caatinga; Mossoró, 33: 458-469. http://dx.doi.org/10.1590/1983-21252020v33n218rc
104	Cordeiro, AL, Norby, RJ, Andersen, KM, et al. Fine-Root dynamics vary with soil depth and precipitation in a low-nutrient tropical forest in the Central Amazonia. Plant-Environment Interactions. 2020; 1: 3–16. https://doi.org/10.1002/pei3.10010
105	Nasto, MK et al. (2019) Nutrient acquisition strategies augment growth in tropical N2-fixing trees in nutrient-poor soil and under elevated CO2. Ecology. 100:e02646
106	Nasto, MK et al. (2017) Nutrient acquisition, soil phosphorus partitioning and competition among trees in a lowland tropical rain forest. New Phytologist. 214:1506-1517

LITERATURE CITED

Guerrero-Ramírez, N. R., Mommer, L., Freschet, G. T., Iversen, C. M., McCormack, M. L., Kattge, J., Poorter, H., van der Plas, F., Bergmann, J., Kuyper, T. W., York, L. M., Bruelheide, H., Laughlin, D. C., Meier, I. C., Roumet, C., Semchenko, M., Sweeney, C. J., van Ruijven, J., Valverde-Barrantes, O. J., Aubin, I., Catford, J. A., Manning, P., Martin, A., Milla, R., Minden, V., Pausas, J. G., Smith, S. W., Soudzilovskaia, N. A., Ammer, C., Butterfield, B., Craine, J., Cornelissen, J. H. C., de Vries, F. T., Isaac, M. E., Kramer, K., König, C., Lamb, E. G., Onipchenko, V. G., Peñuelas, J., Reich, P. B., Rillig, M. C., Sack, L., Shipley, B., Tedersoo, L., Valladares, F., van Bodegom, P., Weigelt, P., Wright, J. P., Weigelt, A. & Schrodt, F. (2020) Global root traits (GRooT) database. *Global Ecology and Biogeography*, 30, 25–37.

Iversen, C. M., McCormack, M. L., Powell, A. S., Blackwood, C. B., Freschet, G. T., Kattge, J., Roumet, C., Stover, D. B., Soudzilovskaia, N. A., Valverde-Barrantes, O. J., van Bodegom, P. M. & Violle, C. (2017) A global Fine-Root Ecology Database to address belowground challenges in plant ecology. *New Phytologist,* 215, 15–26.

Rohatgi, A. (2024) WebPlotDigitizer (Version 4.7). Retrieved from https://automeris.io/WebPlotDigitizer.html

CHAPTER 6: CONCLUSION

This study investigated the responses of root dynamics and characteristics to chronic drying and to seasonal variation across different tropical forests varying in soil fertility and mean annual precipitation (MAP) and across soil depths. The results confirmed that roots are flexible structures that responded to environmental changes, such as experimental and seasonal drying, soil fertility, soil depth and arbuscular mycorrhizal colonization.

Overall, this research demonstrated that chronic drying affected the C cycling by changing patterns on root biomass, dynamics and traits. I also demonstrated that these changes were linked to soil depth, seasonal moisture availability, fertility and root-symbionts interactions. I was also able to show that different tropical forests respond in different manners to disturbance and other environmental factors. Each chapter here provided complementary insights to these dynamics.

The responses of root dynamics and traits to drought revealed that roots are sensitive to drying. The reduced biomass and growth of roots can have important implications on nutrients and water uptake which can in turn affect the whole ecosystem function. These changes are crucial to provide insights on how different tropical forests may respond to a future with increased extreme drought events such as that some forest may be more vulnerable than others.

The role of AMF in improving plant growth under drought conditions provide some mechanisms behind plants resilience to drought which contribute with data to enhance ecosystem models and forest restoration projects. Inoculating seedlings with AMF and ensuring high soil fertility may improve resilience to drought, improving survival and growth rates. Further research with different tropical species will be necessary to determine if these responses are general or species-specific.

The relationship between root traits, such as SRL and biomass with soil C stocks highlights the significant role of not only biomass, but also root form to affect soil C storage. Future studies could focus on root morphological changes at deeper soil layers, longer term exposure to drought, mechanisms on how root morphology, chemistry, and other traits affect C inputs to soils and losses across different tropical soils. Additionally, increased replication and longer-term studies will be crucial for deeper insights on root-soil C relationships.

Future research could also explore the mechanisms driving root morphological changes with depth and their seasonal variations. This research showed seasonal variation of root morphology at the soil surface but measurements at deeper soil layers remain to be studied. Although changes may be smaller at deeper soil layers given this research presented more variation in root characteristics at the soil surface, they could significantly impact water uptake under chronic drying conditions. Long-term and mechanistic studies will be needed to better understand adaptive root responses and their impact on soil processes.

Expanding the geographic scope of research to include a wider range of tropical forest types, including other fertile forests, flooded forests and dry forests could also provide a more comprehensive understanding of how chronic drying can affect root dynamics and characteristics in different forests and their ecological implications. Also, other root traits related to plant hydraulics, physiological traits related to nutrient and water acquisition and specific studies focusing on the mechanisms of transfer of C from roots to soils across different soil depths would be important.

Integrating the patterns found in this study to vegetation models is also a further important step. Current vegetation models lack on root traits and dynamics representation. Therefore, I expect that data from this work (in association with other published data) will be used by modelers

and other researchers to feed models that can predict how different tropical forests may respond to climate change in future scenarios. Further long-term and mechanistic studies designed in association with models needs could further advance our knowledge and help develop effective strategies to understand and predict the future of tropical forest ecosystems.

The findings from this research contribute to current knowledge by demonstrating the rapid shifts of root systems to diverse environmental factors bringing new data that can be used in vegetation models, restoration and conservation strategies. I expect that this work will be used not only by the scientific community, but also have an impact to decision-makers by at least alarming how tropical forests can be vulnerable to drying and how changes in precipitation can alter the important C stocks that have been providing an essential ecosystem service to society. The summary of main topics and conclusion can be found in figure 6.

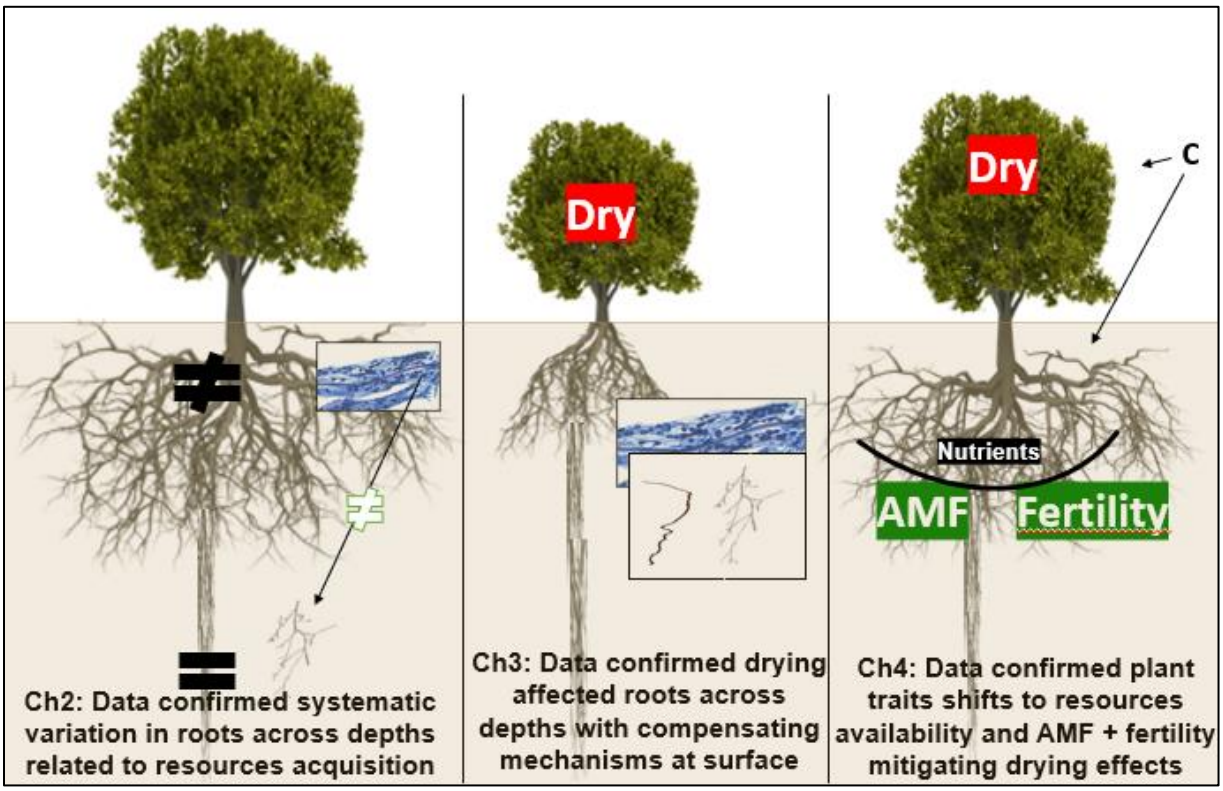

Figure 6.1: Conceptual figure for general conclusions from the dissertation. In chapter 2, I found novel results about how the different tropical forests in situ had similar patterns of root variation with depth. It indicated differences in resources acquisition at the soil surface (likely for nutrients) and at deeper soil layers (likely for water) that are usually less investigated. I also showed a large variation of roots at surface soil across different forests that may influence forest responses to global change factors. In chapter 3, I supported some results across the literature such as drying decreasing root growth at the soil surface. But more novel here were drying decreasing root productivity at deeper soil layers, and changing root morphology and associations with symbionts. All together we observed that drying promoted changes in acquisition strategies and also that fertile forests may respond differently to drying such that these forests may have more resilience because of their lack of biomass responses to chronic drying at the surface across some dates and also larger deep root productivity. In chapter 4, I showed some clear trade-offs in seedlings traits from a greenhouse experiment providing evidence that they are constantly changing in response to the environment. Also, I provided some novel results on the mechanisms, such as nutrient retention, on how mycorrhizal and fertility mitigated some negative effects of drying on plant growth. This aligns with the field study showing some possible resilience in the fertile forests to drying. All these chapters together provided a good understanding on how different forests respond to environmental changes. These impacts on soil C storage, links with root function and possible larger vulnerability of some forests are great topics for future studies.

Supplementary figures

Figure SI 1.1.

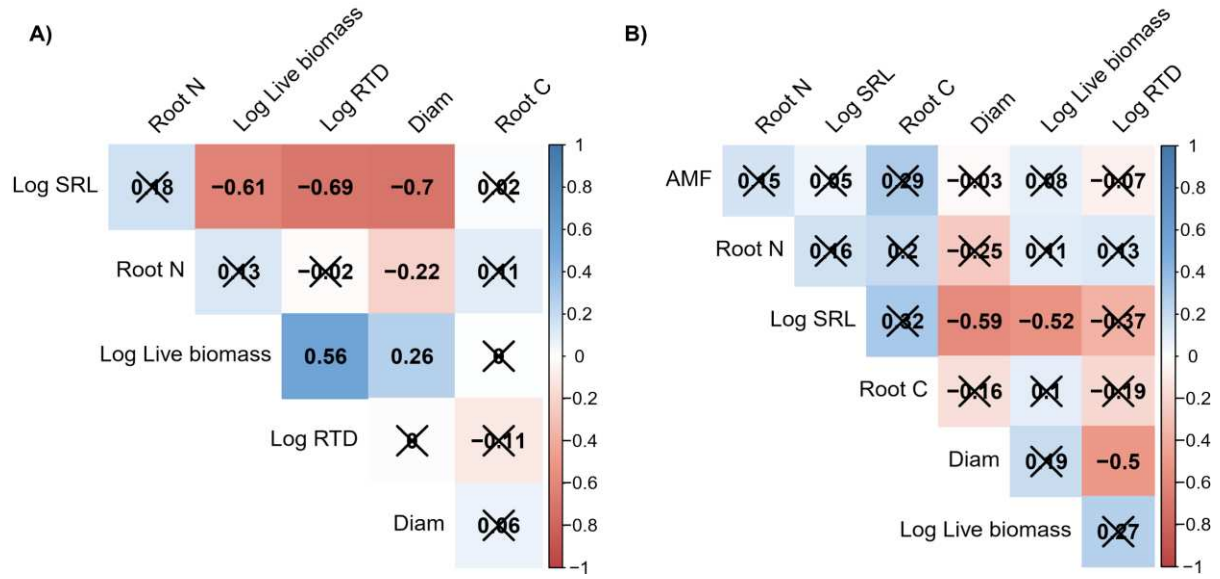

Figure SI 1.1: One – way Pearson correlation values (*r*) are given in each box for all pairs of root characteristics, with non – significant relationships covered by "x". Colors represent a gradient from -1 to 1 with blue boxes showing a positive correlation and red boxes showing a negative correlation. P-values for all correlations are presented in table SI 1.14. A) Results for the whole profile 0 – 1.2 m depths in 10 cm increments. Non-significant P-values using a Bonferroni correction are $p > 0.003$. B) Results for 0 – 20 cm depth in 10 cm increments, including all of the root characteristics in SI 1.1A plus AMF colonization counts. Non-significant P-values using a Bonferroni correction are $p > 0.002$.

Figure SI 1.2.

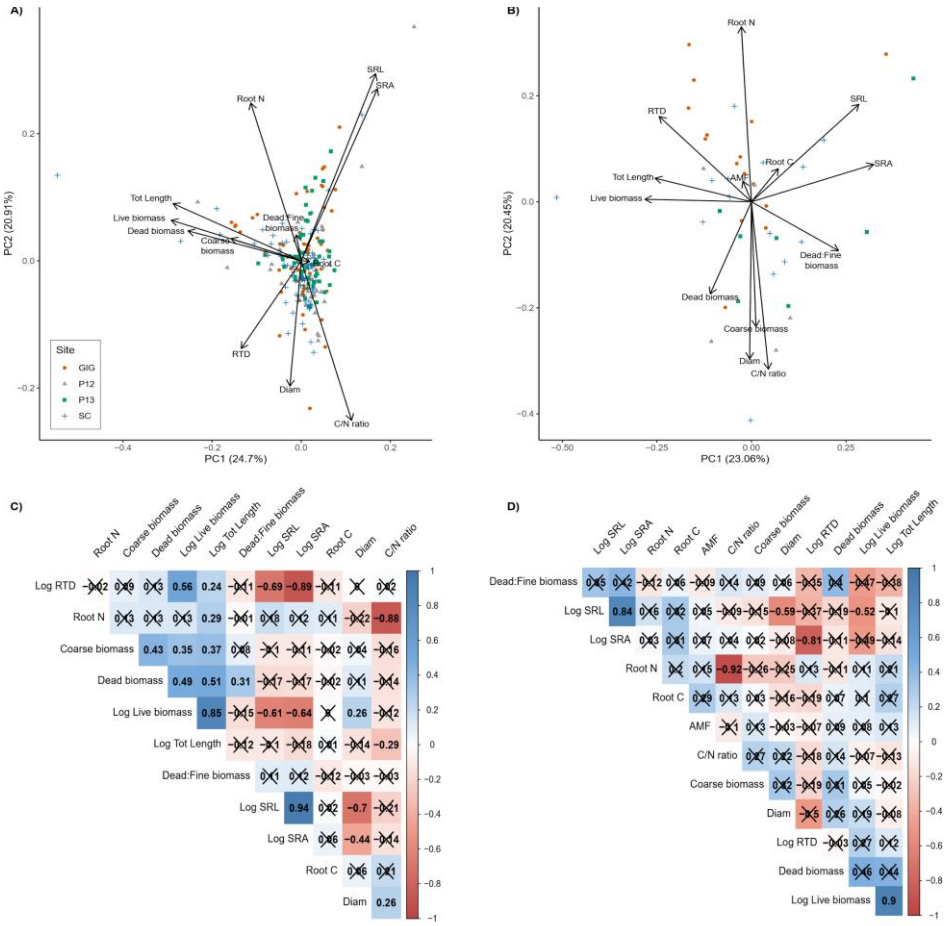

Figure SI 1.2: Tradeoffs in root characteristics are shown for four distinct tropical forests using PCA analyses with all root characteristics measured, including auto – correlated characteristics not shown in the main text. P-values for all correlations are presented in table SI 1.14. A) Shows PCA results 0 – 1.2 m depths using data from 10 cm increments for live fine root biomass, dead fine root biomass, coarse root biomass, dead/ fine root biomass ratio, total fine root length, SRL, SRA, RTD, diameter, root %N, root %C, root C/N ratio. B) Shows a similar PCA 0 – 20 cm depth, including all of the root characteristics in SI 1.2A plus AMF colonization counts. C) One – way Pearson correlation values (*r*) are given in each box for all pairs of root characteristics, with non – significant relationships covered by "x". Colors represent a gradient from -1 to 1 with blue boxes showing a positive correlation and red boxes showing a negative correlation. Pearson correlation plot including all of the root characteristics in SI 2A across different soil depths at 10 cm increments from surface to 1.2 m depth and sites. Non-significant P-values using a Bonferroni correction are $p > 0.0007$. D) One – way Pearson correlation values (*r*) including all of the root characteristics in SI B across different soil depths (0 – 10 and 10 – 20 cm) and sites. Non-significant P-values using a Bonferroni correction are $p > 0.0006$. Crossed cells represent correlations that were not significantly different after applying Bonferroni correction.

Figure SI 1.3.

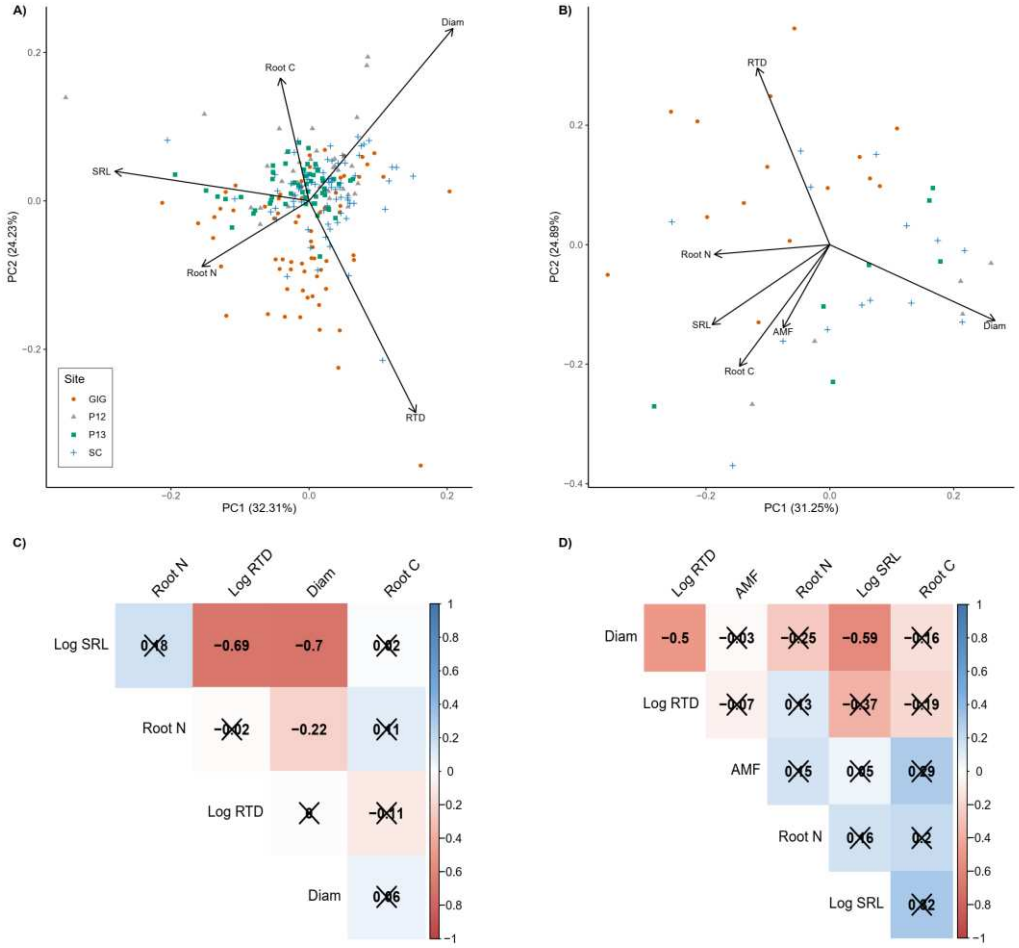

Figure SI 1.3: PCA results are given for root morphology and chemistry, excluding live fine root biomass to assess tradeoffs among these other root characteristics. A) Shows PCA results 0 – 1.2 m depths using data from 10 cm increments for SRL, RTD, diameter, root %N and root %C. B) Shows a similar PCA 0 – 20 cm depth, including all of the root characteristics in SI 1.3A plus AMF colonization counts. C) One – way Pearson correlation values (*r*) are given in each box for all pairs of root characteristics, with non – significant relationships covered by "x". Colors represent a gradient from -1 to 1 with blue boxes showing a positive correlation and red boxes showing a negative correlation. Pearson correlation plot including all of the root characteristics in SI 1.3A across different soil depths at 10 cm increments from surface to 1.2 m depth and sites. Non-significant P-values using a Bonferroni correction are $p > 0.005$. D) One – way Pearson correlation values (*r*) including all of the root characteristics in SI 1.3B across different soil depths (0 – 10 and 10 – 20 cm) and sites. Non-significant P-values using a Bonferroni correction are $p > 0.004$. Crossed cells represent correlations that were not significantly different after applying Bonferroni correction.

Figure SI 1.4.

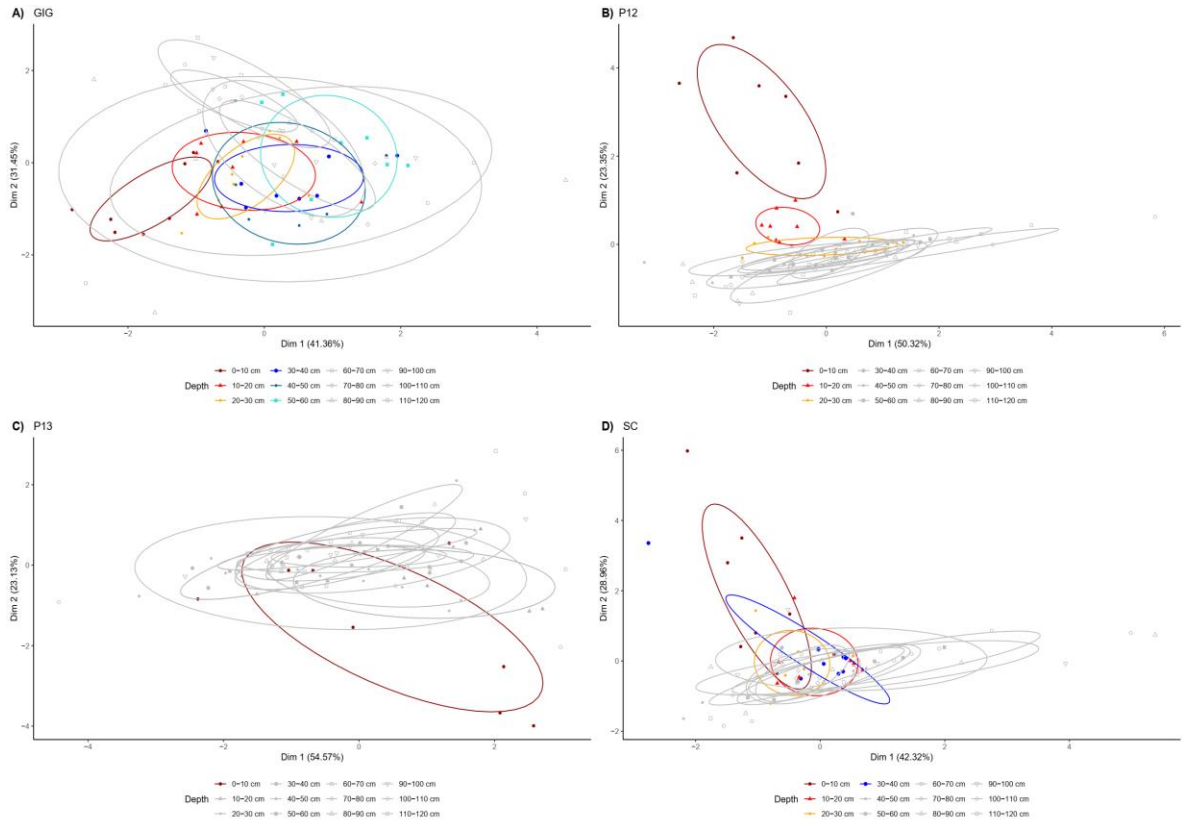

Figure SI 1.4: Cluster analysis for root characteristics is shown separately for the four forest sites. Root data included live fine root biomass, SRL, root diameter, and RTD. Depth separations are shown in different colors. When depths were not significantly different from each other, they were colored in gray (Table SI 1.5). For all sites, surface roots were most different from other depths, with the greatest differences among surface depths at Gigante (GIG). All sites had more similar root characteristics at depth. The percentage of variance explained by the first and second dimensions is shown in the axis labels. The ellipses (confidence level = 0.50) represent the spread of individual samples around the center of each group (n = 8 per depth and site). Cluster analysis involved principal coordinates analysis (PCoA) and k – means clustering on scaled data, using a Euclidean distance metric and selecting k = 12 to divide the data into 12 distinct clusters corresponding to the 12 soil depths.

Figure SI 1.5.

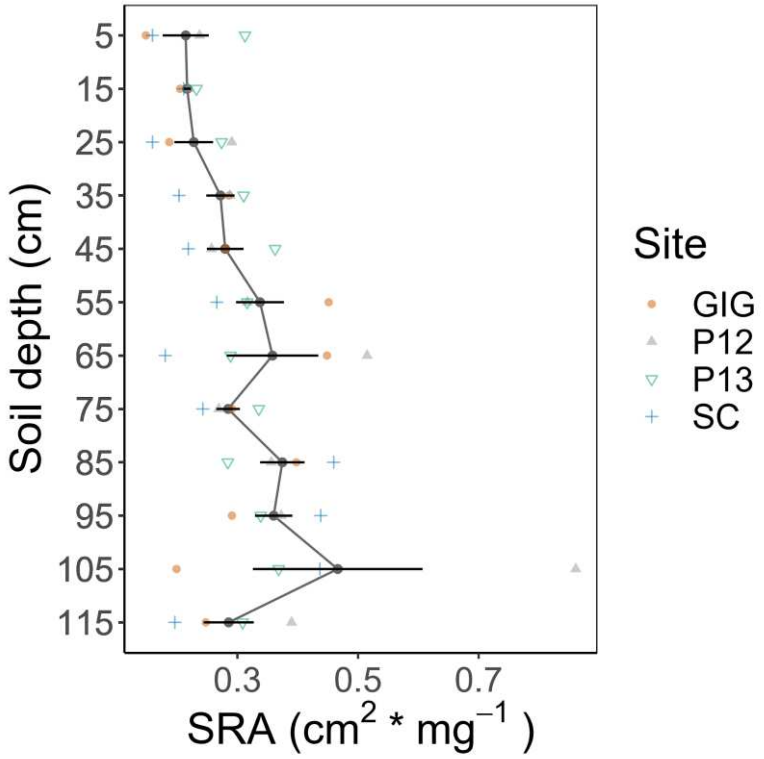

Figure SI 1.5: Specific root area (SRA) is shown by depth across the four sites, illustrating the main effect of depth without a depth*site. Black dots represent Mean ± SE across sites with n = 4 sites for each site and depth. Colored markers represent the average from 8 plots per site for each variable in each site and depth.

Figure SI 1.6.

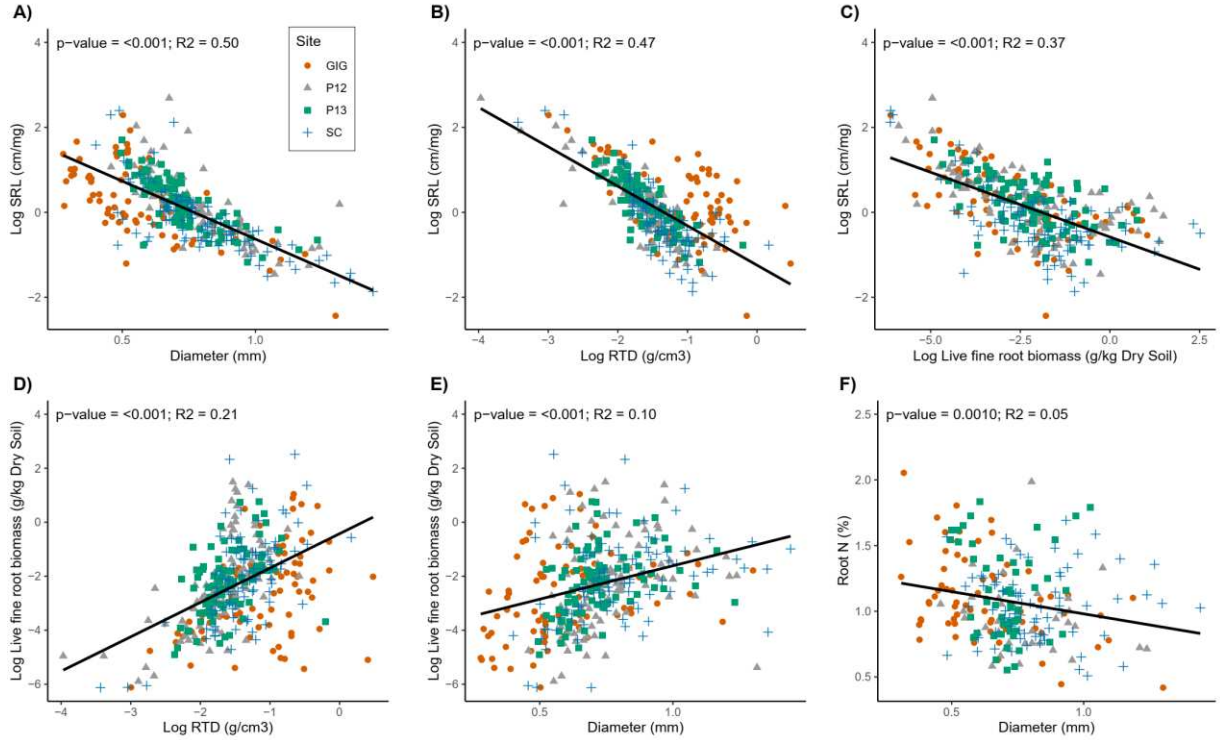

Figure SI 1.6: One – way correlations are given for all root data by 10 cm depth from 0 – 1.2 m (N = 365), with sites in different colors. Only the significant relationships from Figure SI 1.1A are presented. P – values and R^2 are given on each graph.

Figure SI 1.7.

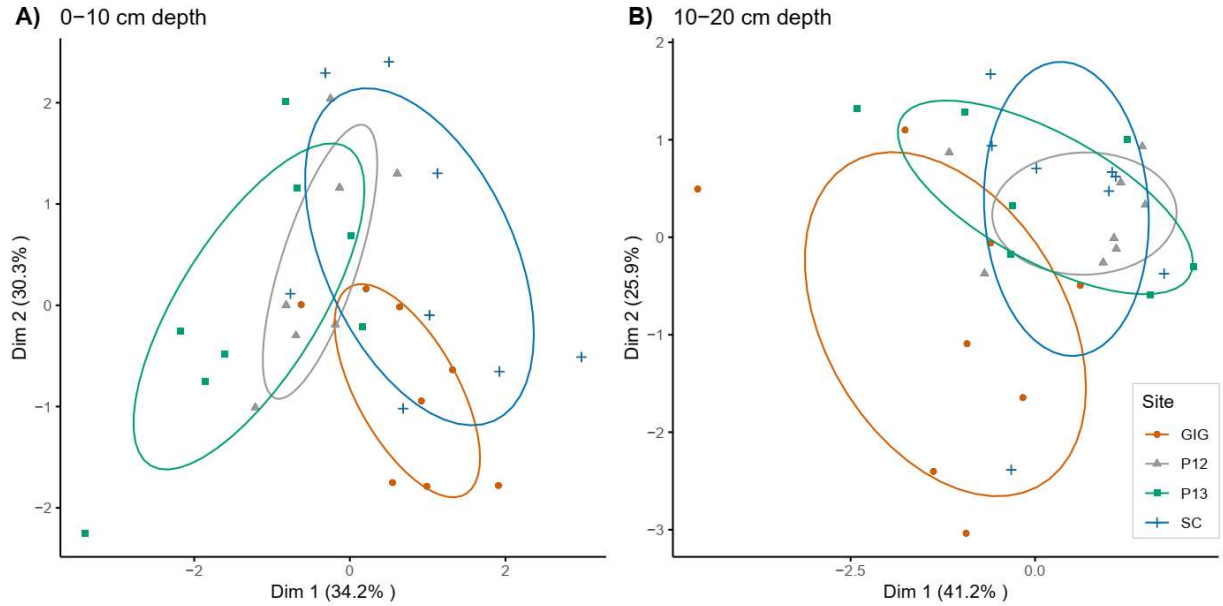

Figure SI 1.7: Cluster analyses is presented for soil depths 0 – 10 and 10 – 20 cm, including AMF colonization rates in addition to variables used in Figure 2.3 (live fine root biomass, specific root length, root diameter, and root tissue density). There was significant site separation for both depths (Table SI 1.7). Sites are shown in different colors. The percentage of variance explained by the first and second dimensions is shown in the axis labels. The ellipses (confidence level = 0.50) represent the spread of individual samples around the center of each group (n = 8 per site). Cluster analysis involved principal coordinates analysis (PCoA) and k – means clustering on scaled data, using a Euclidean distance metric and selecting k = 4 to divide the data into four distinct clusters corresponding to the four forests.

Figure SI 1.8.

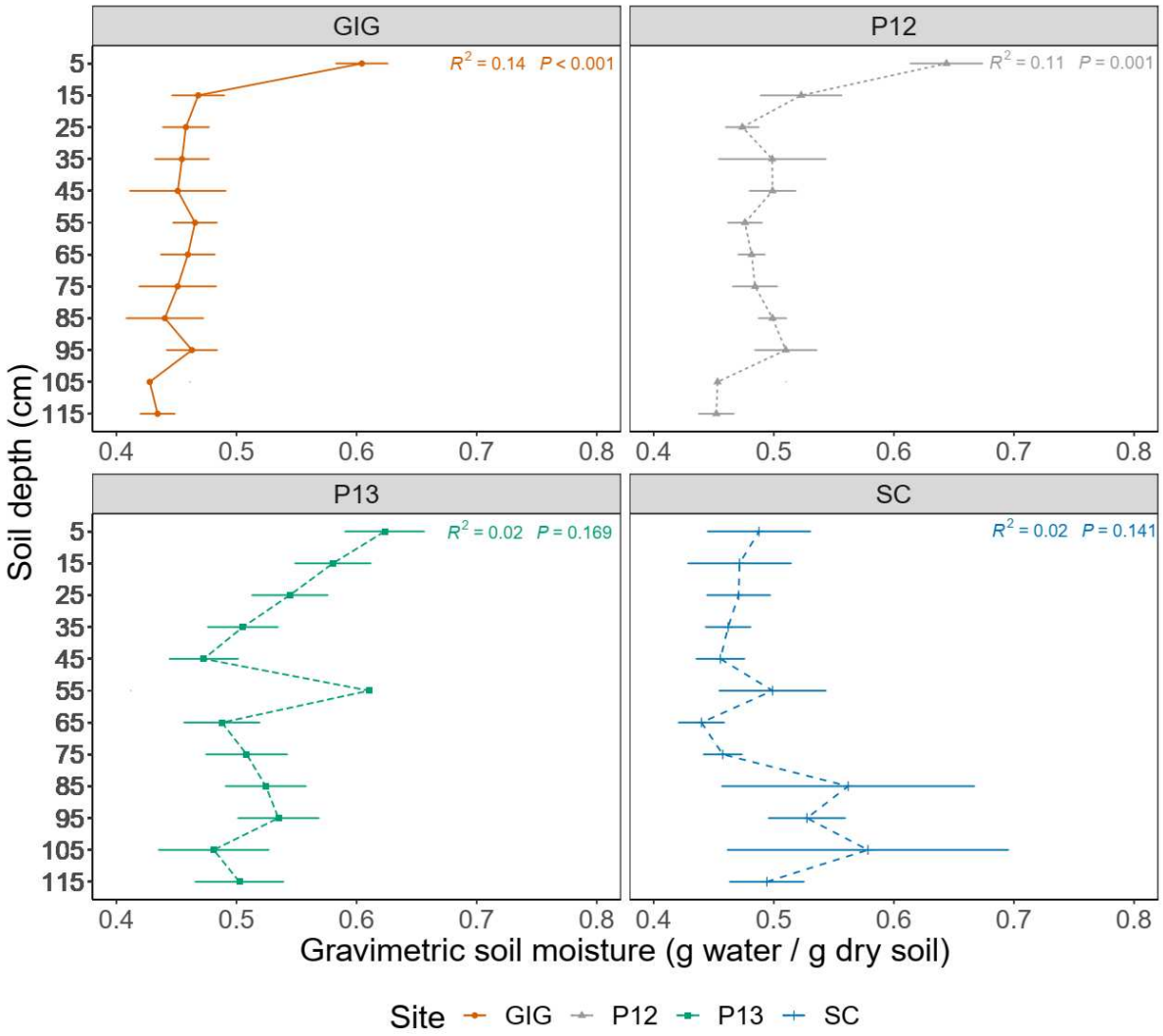

Figure SI 1.8: Gravimetric soil moisture from each soil depth when soils were collected. Soils were collected in September 2017 (P12) – mid wet season, December 2017 (P13) – late wet season, February 2018 (SC) – early dry season after a very wet season, and October 2018 (GIG) – mid wet season. Data is shown by depth and forest site Soil depth is on the y axis and gravimetric soil moisture values are on the x axis, with depth increments presented as midpoints of sampled depth intervals (i.e.: 5 cm for 0 – 10 cm depth). P-values and R^2 are given for regression analyses of depth versus log of gravimetric soil moisture. Colored symbols and bars give mean ± SE for each site and depth (n = 8 plots per site).

List of SI tables:

Table SI 1.1: All raw data for root characteristics across soil depths, plots, and sites are given for four Panamanian forests. AMF colonization rates are available only for 0 – 10 and 10 – 20 cm depths, and root chemistry is available for 4 – 8 plots per depth across sites.

Table SI 1.2: An overview table explains which root characteristics were included in each statistical analysis, and corresponding figures and tables are given.

Table SI 1.3: Results from an initial exploratory PCA are given, which included all root characteristics. Results are for data from the whole soil profile (0 – 1.2 m depth) in 10 cm depth increments, and for the soil surface (0 – 20 cm depth) in 10 cm depth increments including AMF colonization. The final simplified PCA presented in the main text does not include root characteristics auto correlated with the main characteristics of interest.

Table SI 1.4: Results from an exploratory PCA are given, excluding fine root biomass in order to explore tradeoffs only among morphological, chemical, and AMF traits. Results are for data from the whole soil profile (0 – 1.2 m depth) in 10 cm depth increments, and for the soil surface (0 – 20 cm depth) in 10 cm depth increments including AMF colonization.

Table SI 1.5: Results from multivariate post hoc tests are given, using Hotelling's T – squared test for differences indicated in MANOVA. Results are given by depth were significant across all sites. Variables in the final MANOVA included: live fine – root biomass, SRL, diameter, RTD, excluding other characteristics that were auto correlated with these.

Table SI 1.6: Results for post – hoc regressions of each root characteristic are given, separating by site when there was a site*depth interaction. Variables that did not have any effect of depth are not presented here (root %C, dead:total fine root biomass ratio). In each line, '***' is displayed when p – value < 0.001, '**' when p – value < 0.01, '*' when p – value < 0.05. For variables with interaction of site:depth, the significance level with the Bonferroni correction is 0.008 and for variables without interaction, it is 0.01. For variables without interaction of site:depth, all the root characteristics except AMF had a site effect, contributing to the low R^2 values for these regressions with depth. Root %C and dead:total fine root biomass ratio were not included in this table since these variables did not vary with depth.

Table SI 1.7: MANOVA results are given across soil depths using the primary root characteristics.

Table SI 1.8: Exploratory MANOVA results are given across soil depths excluding fine root biomass to explore differences among sites for only morphological traits.

Table SI 1.9: Exploratory MANOVA results are given across soil depths including fine root chemistry, which was not available for all sites and all depths.

Table SI 1.10: Multivariate post hoc test: Hotelling's T – squared test. Post hoc analysis after MANOVA results were significant. Variables included: live fine root biomass, SRL, diameter, RTD.

Table SI 1.11: Results from a forward stepwise model using root characteristics to predict total soil C stocks (g/kg – soil), and extractable DOC (mg C/kg – soil), across depths using soil C data from Cusack & Turner (2021, 0 – 10, 10 – 20, 20 – 50, and 50 – 100 cm, n = 16, with four depths per four sites). Root characteristics tested in the stepwise model were: SRL (cm/mg), RTD (g/cm^3), fine root diameter (mm), live fine root biomass (g/kg dry soil), dead fine root biomass (g/kg dry soil), coarse root biomass (g/kg dry soil), dead:total fine root biomass ratio, root %N, root %C, and soil depth. The table presents to most parsimonious predictive model, with significance levels for each factor selected.

Table SI 1.12: Summed or averaged root characteristics data that were used for stepwise models are given in the same depth increments as used in Cusack & Turner (2021, 0 – 10, 10 – 20, 20 – 50, and 50 – 100 cm). Root biomass variables were summed across the soil profile, while morphology and chemistry were averaged.

Table SI 1.13: Radiocarbon data from fine live roots across four different sites at deeper soil layers (n = 4-5 per site).

Table SI 1.14: P-values for Pearson correlation between root characteristics presented in Figure SI 1.1 and Figure SI 1.2.

Table SI 1.15: Monthly precipitation (mm) in Barro Colorado Island (BCI) and in Sherman Crane (San Lorenzo) in 2017 and 2018. The sites GIG, P12 and P13 are near BCI so have similar monthly precipitation. The site SC is located in San Lorenzo. Data from Paton, 2023a and Paton, 2023b. Data in bold represent soil collection dates. Soils were collected in September 2017 (P12) – mid wet season, December 2017 (P13) – late wet season, February 2018 (SC) – early dry season after a very wet season, and October 2018 (GIG) – mid wet season.

Figure SI 2.1.

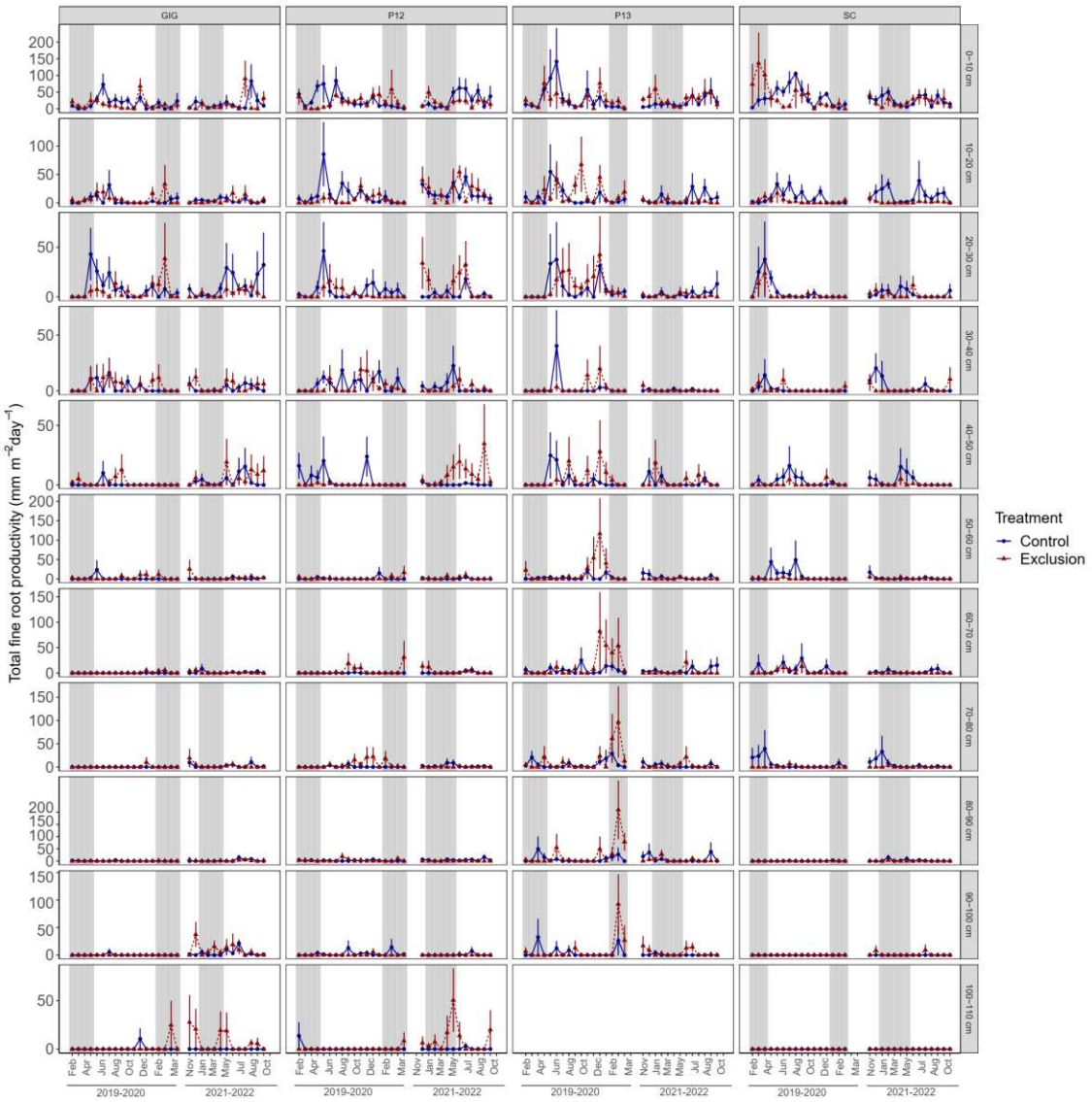

Figure SI 2.1: Fine root length productivity per minirhizotron window area and day (mm m^{-2} day^{-1}) is presented over time (months and years), soil depth and across treatments such as throughfall exclusion in red lines and control in blue lines. Data are presented for four different forests from seasonal tropical forests in Panama varying in mean annual precipitation and fertility. Points and error bars represent mean ± standard errors across plots (n=4). Gray shading represents dry season.

Figure SI 2.2.

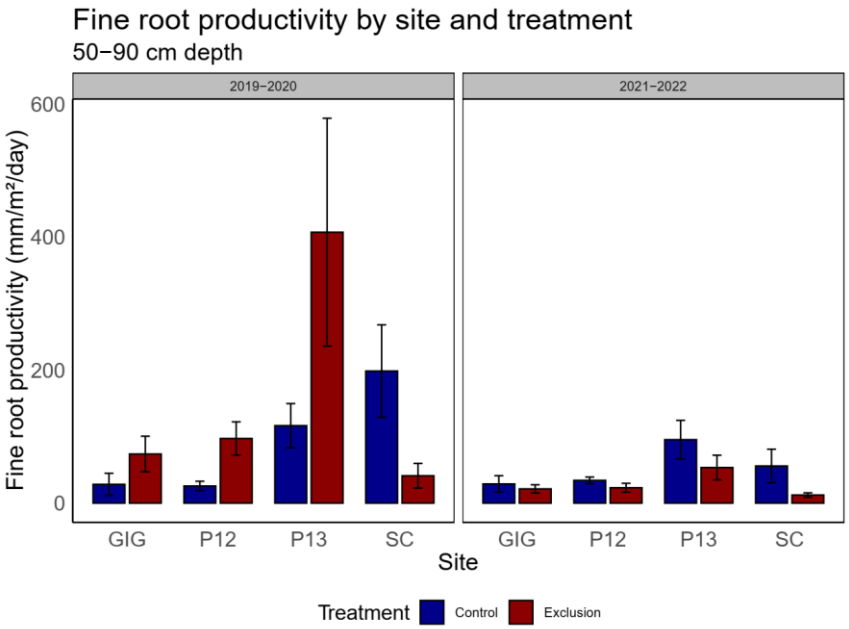

Figure SI 2.2: Fine root productivity at the 50-90 cm depth considering only the positive values. Site, year, treatment*site and treatment*year interactions were significant effects for productivity, such that productivity was larger in the fertile site and smaller in the other sites at this depth. The treatment*site interaction occurred because drying treatment suppressed root productivity driven by the wettest, infertile site (SC) in these deep soils.

Figure SI 2.3.

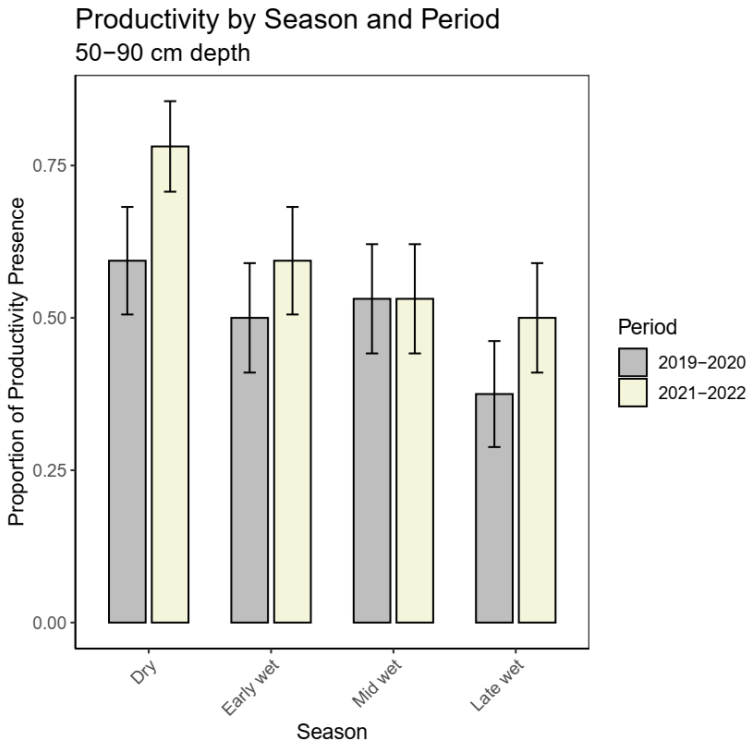

Figure SI 2.3: Proportion of fine root productivity at the 50 – 90 cm depth across seasons and years. Season was the only significant effect in the presence/absence analysis of fine root productivity. Productivity was larger at this depth during the dry season, intermediate during early and mid–wet and smaller during the late wet season, showing an opposite pattern from surface root productivity over seasons. Data are presented for four different forests from seasonal tropical forests in Panama varying in mean annual precipitation and fertility. Bar plots and error bars represent mean ± standard errors across averaged first by site and then for plots (n=4).

Figure SI 2.4.

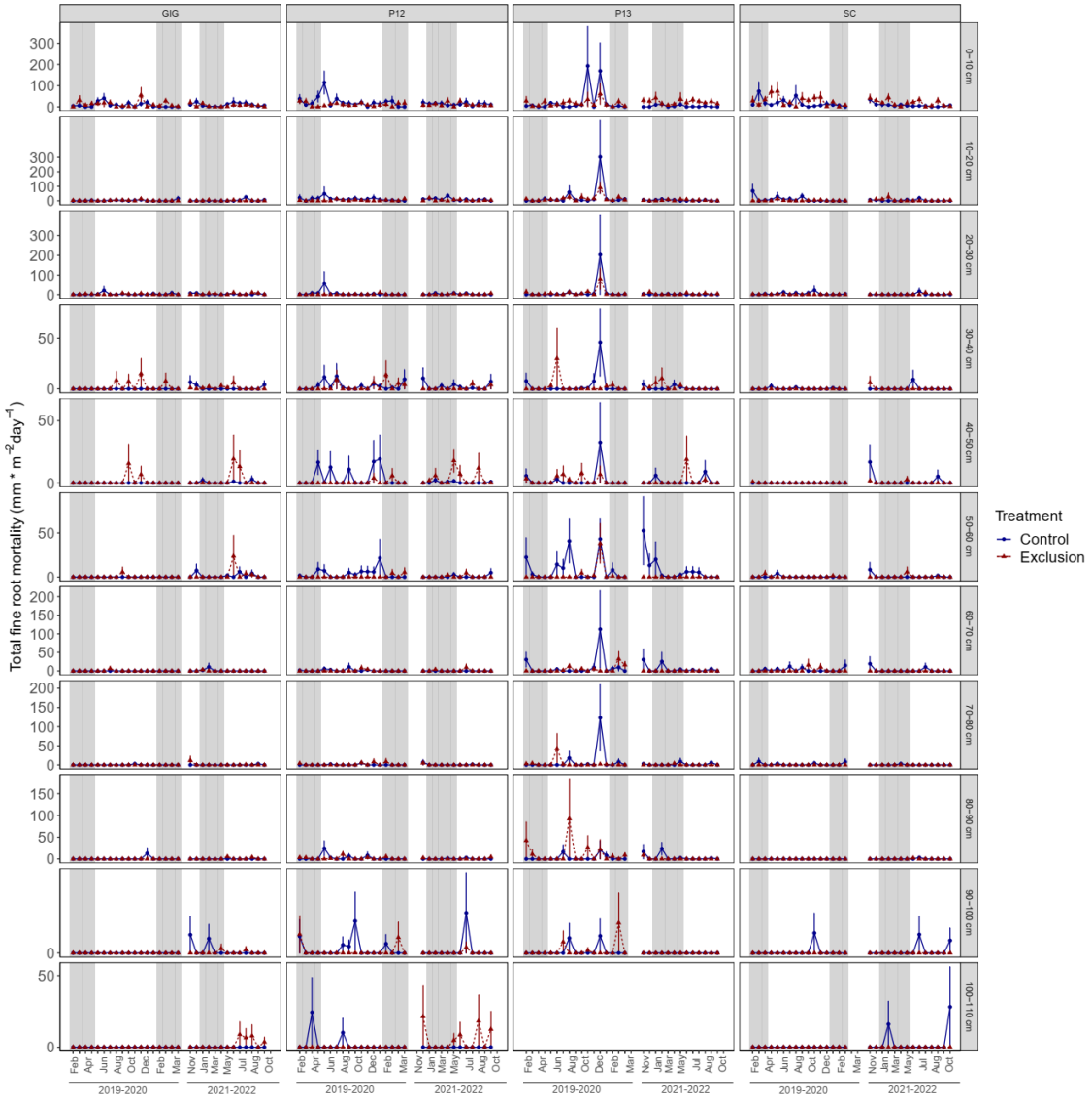

Figure SI 2.4: Fine root length mortality per minirhizotron window area and day (mm m^{-2} day^{-1}) is presented over time (months and years), soil depth and across treatments such as throughfall exclusion in red lines and control in blue lines. Data are presented for four different forests from seasonal tropical forests in Panama varying in mean annual precipitation and fertility. Points and error bars represent mean ± standard errors across plots (n=4). Gray shading represents dry season.

Figure SI 2.5.

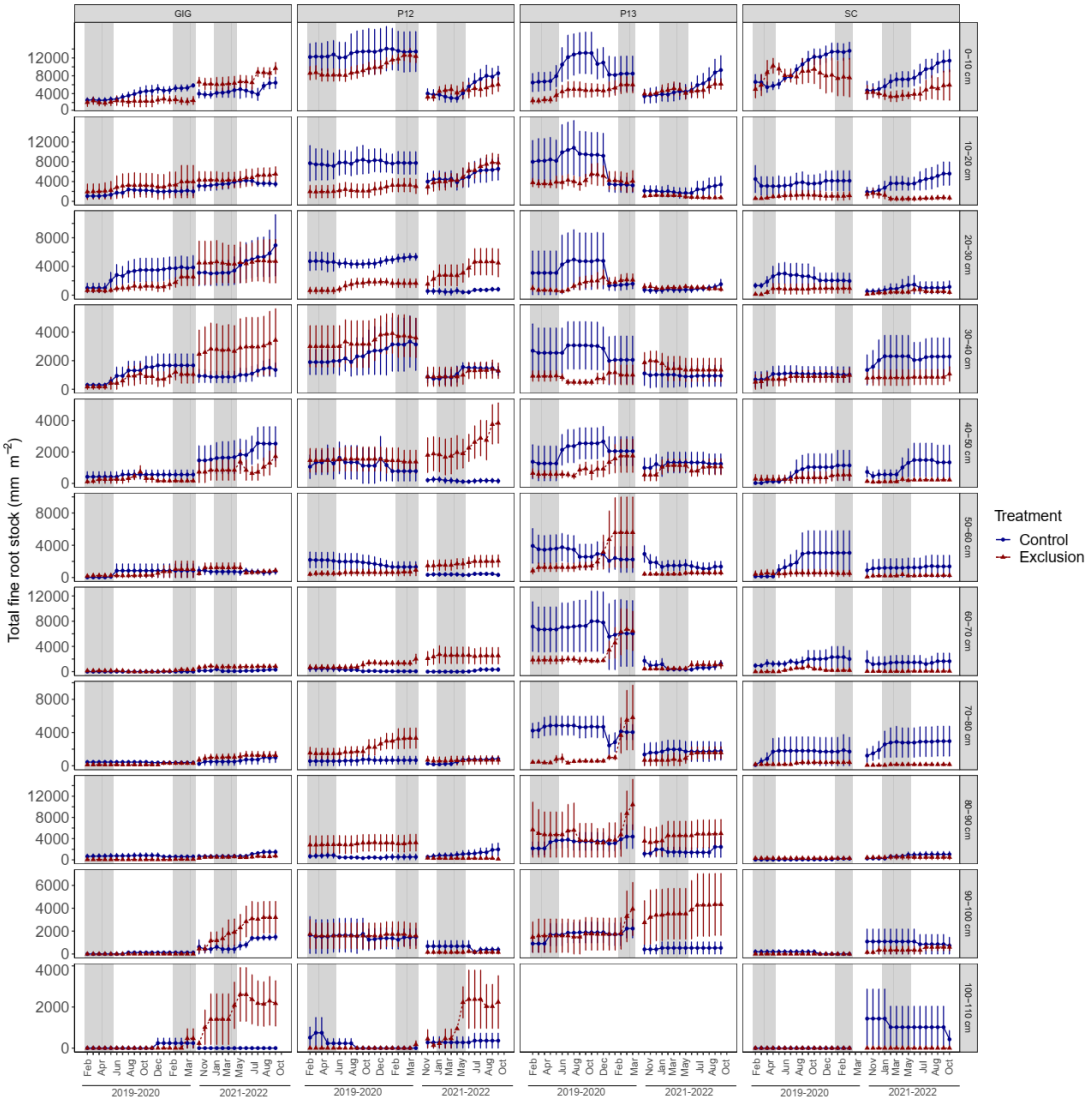

Figure SI 2.5: Fine root length stocks per minirhizotron window area (mm m^{-2}) is presented over time (months and years), soil depth and across treatments such as throughfall exclusion in red lines and control in blue lines. Data are presented for four different forests from seasonal tropical forests in Panama varying in mean annual precipitation and fertility. Points and error bars represent mean ± standard errors across plots (n=4). Gray shading represents dry season.

Figure SI 2.6.

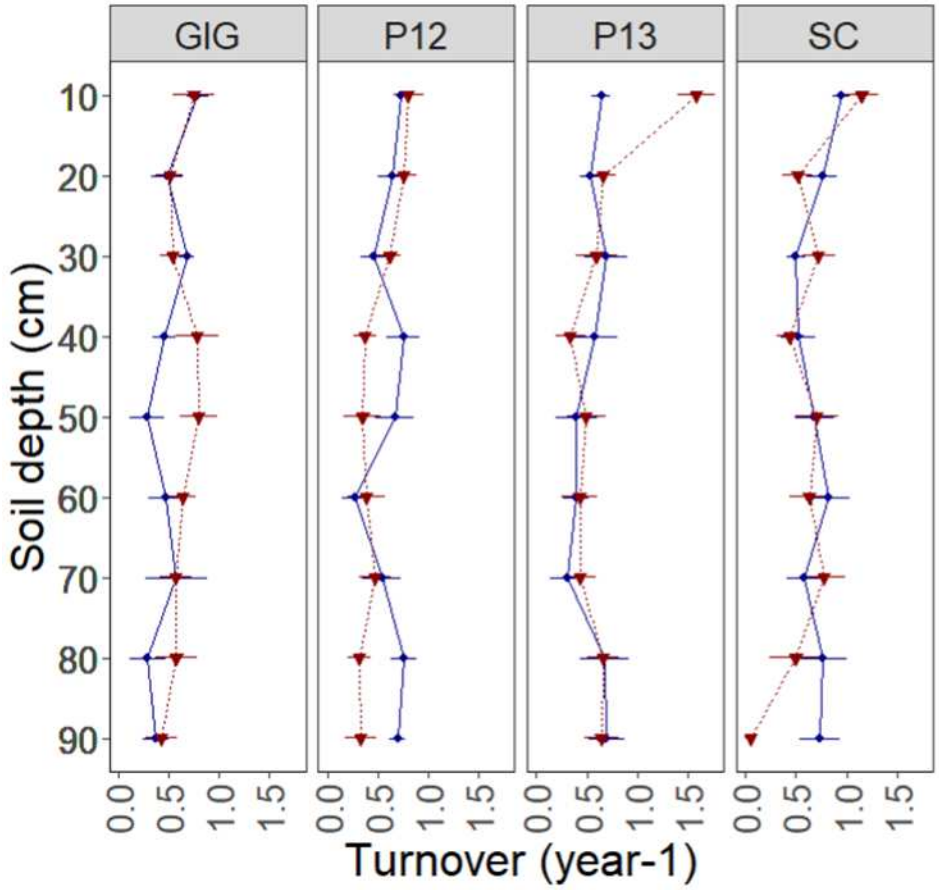

Figure SI 2.6: Annual fine root turnover rates (year^{-1}) by soil depth, treatments such as throughfall exclusion in red and control in blue and years using minirhizotron method. Data was first averaged for the two years of measurements since there was no effect of year on root turnover in the main model. Data are presented for four different forests from seasonal tropical forests in Panama varying in mean annual precipitation and fertility. Points and error bars represent mean ± standard errors across plots (n=4).

Figure SI 2.7.

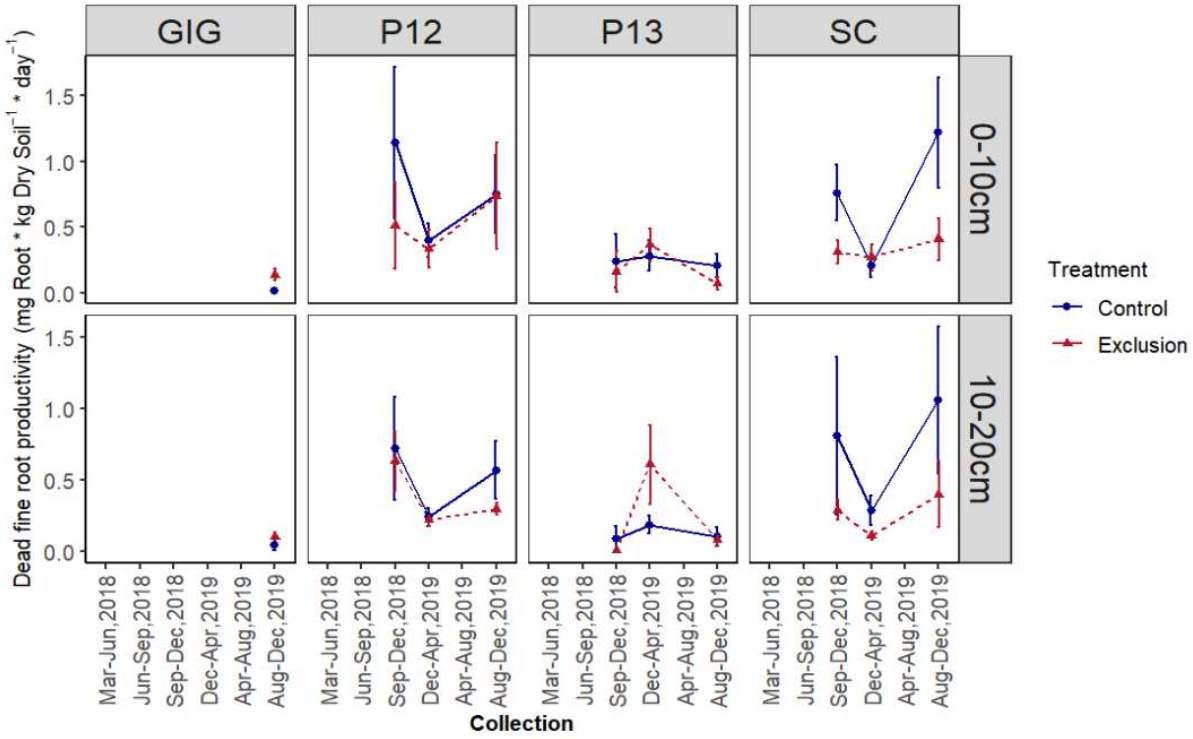

Figure SI 2.7: Dead fine root biomass mortality (mg root * kg dry soil^{-1} * day^{-1}) from ingrowth core method. Data is presented over time with 3-4 months periods collections, soil depth and across treatments such as throughfall exclusion in red lines and control in blue lines. Data are presented for four different forests from seasonal tropical forests in Panama varying in mean annual precipitation and fertility. Points and error bars represent mean ± standard errors across plots (n=4). Gray shading represents dry season.

Figure SI 2.8.

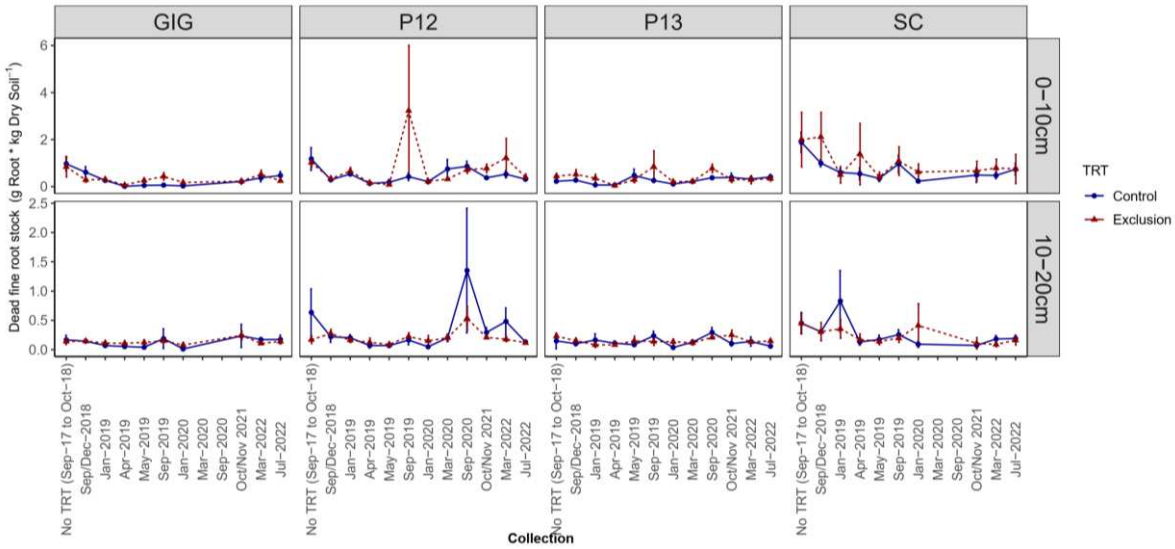

Figure SI 2.8: Dead fine root stocks biomass (g goot * kg dry soil^{-1}) from sequential coring method. Data is presented over time (collection months and years), soil depth and across treatments such as throughfall exclusion in red lines and control in blue lines. Data are presented for four different forests from seasonal tropical forests in Panama varying in mean annual precipitation and fertility. Points and error bars represent mean ± standard errors across plots (n=4). Gray shading represents dry season.

Figure SI 2.9.

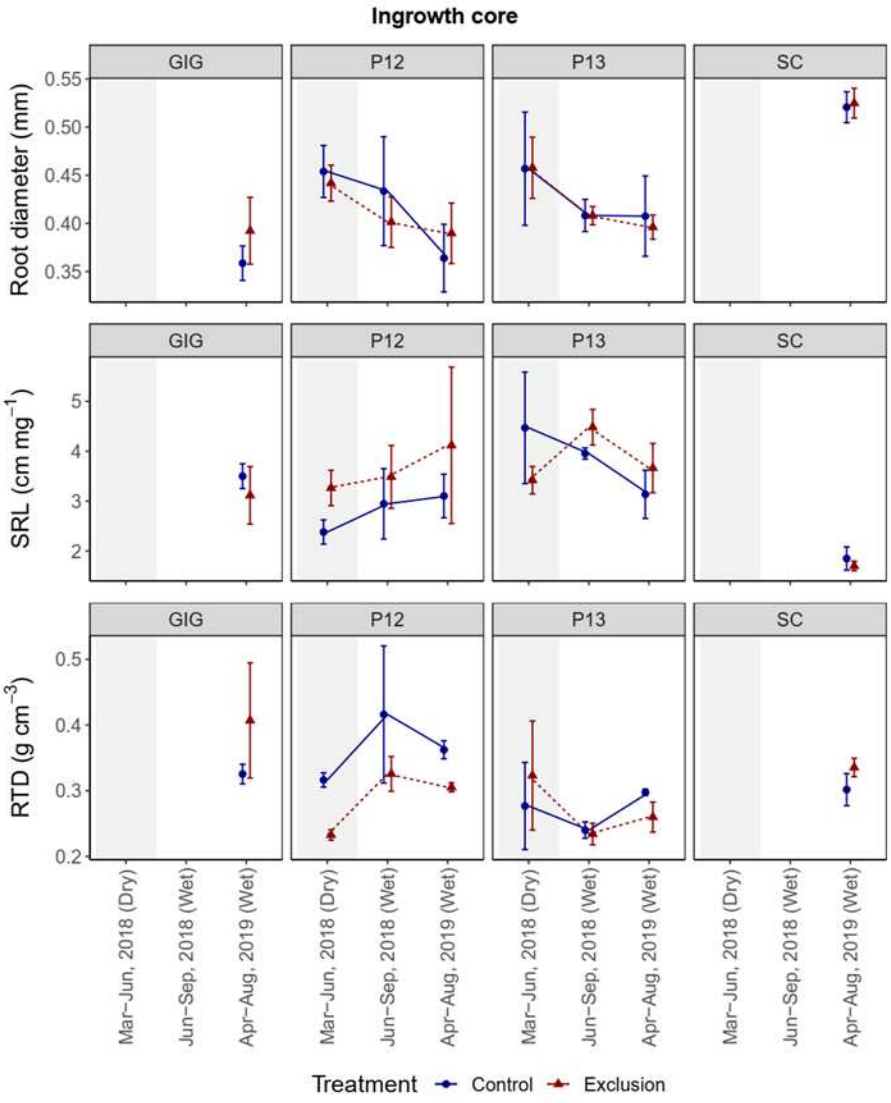

Figure SI 2.9: Live fine root morphology from ingrowth core method. Top: Root diameter (mm); Middle: Specific root length (cm mg^{-1}); Bottom: Root tissue density (g cm^{-3}). Data is presented over time with 3–4-month periods collections and across treatments such as throughfall exclusion in red lines and control in blue lines. Data are presented for four different forests from seasonal tropical forests in Panama varying in mean annual precipitation and fertility. Data was averaged across 0-10 and 10-20 cm depth since depth was not a significant factor. Points and error bars represent mean ± standard errors across plots (n=4). Gray shading represents dry season

Figure SI 2.10.

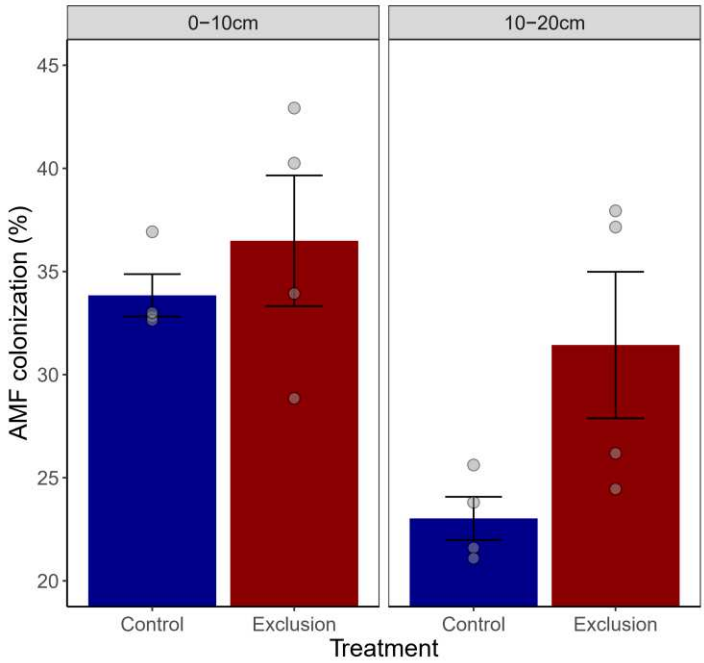

Figure 2.10: AMF colonization to 20 cm depth during the wet season and averaged across sites. The drying treatment generally increased AMF colonization. Data are presented for four different forests from seasonal tropical forests in Panama varying in mean annual precipitation and fertility. Points represent these four different forests. Each point is an average across four plots. Points and error bars represent mean ± standard errors across sites (n=4).

Figure SI 2.11.

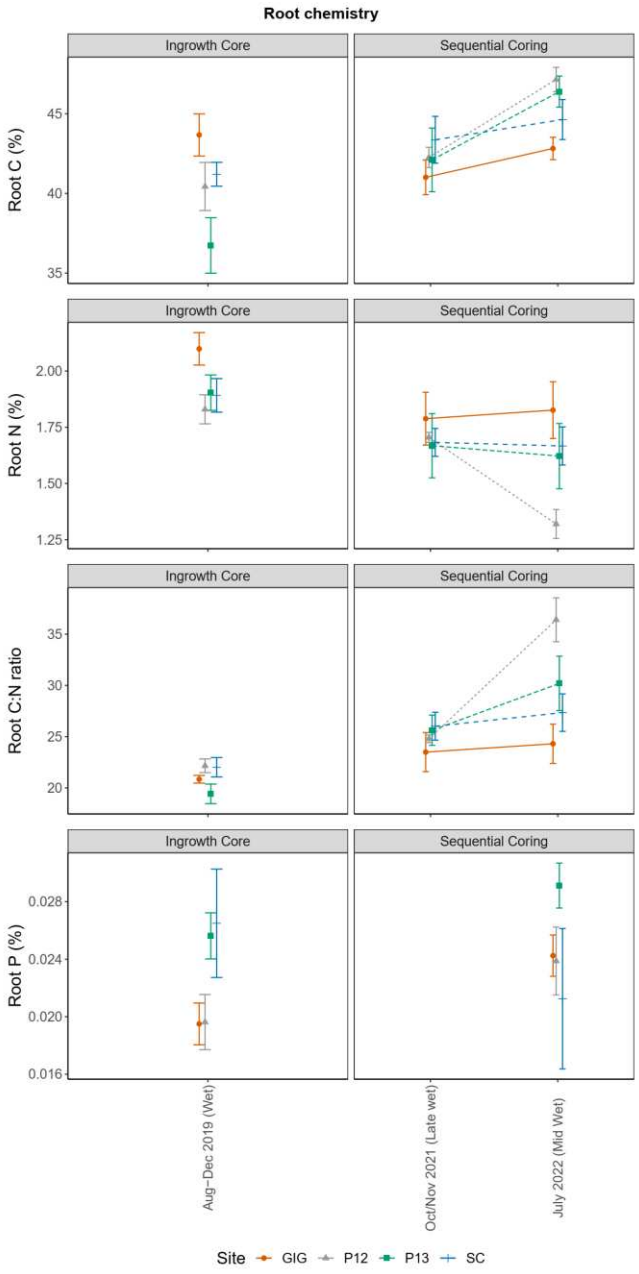

Figure SI 2.11: Live fine root chemistry from ingrowth core and sequential coring method at 0-10 cm depth. Data are presented for four different forests from seasonal tropical forests in Panama varying in mean annual precipitation and fertility and across different collection dates. Colors represent these four different forests. Points and error bars represent mean ± standard errors across plots (n=4).

Supplementary tables

Table SI 2.1: Root dynamics dataset collected using a Rhizosystems minirhizotron camera across different forests, soil depths to 1.2 m and treatments. The data includes raw metrics such as root length and diameter captured within a minirhizotron window area of 8.4mm x 6.3mm (52.92 mm^2). The columns record diverse parameters such as tube number, treatment type, session details, collection dates, seasonal summaries, and geometric measurements related to the tube's position when installed in the field. It also records root length already divided by window area. The forests include: GIG (2350 MAP, infertile, Oxisol), P12 (2600 MAP, infertile, Ultisol), P13 (2600 MAP, fertile, Alfisol), and SC (3421 MAP, infertile, Oxisol).

Table SI 2.2: Ingrowth core data for root biomass and morphology across different forests and treatments. This table summarizes root biomass and morphological characteristics collected using ingrowth cores across four forests, two depths and two treatment conditions. The data presents root biomass, both in terms of dry soil mass and per core volume, and details morphological parameters like root length, diameter, volume, specific root length, specific root area, and root tissue density. Additionally, the table provides environmental conditions such as soil moisture and contextual information like the number of days between ingrowth core installation and collection. The forests include: GIG (2350 MAP, infertile, Oxisol), P12 (2600 MAP, infertile, Ultisol), P13 (2600 MAP, fertile, Alfisol), and SC (3421 MAP, infertile, Oxisol).

Table SI 2.3: Sequential coring data for root biomass and morphology across different forests and treatments. This table summarizes root biomass and morphological characteristics collected using sequential coring method across four forests, two depths and two treatment conditions. The data presents root biomass, both in terms of dry soil mass and per core volume, and details morphological parameters like root length, diameter, volume, specific root length, specific root area, and root tissue density. Additionally, the table provides environmental conditions such as soil moisture and contextual information like the number of days between ingrowth core installation and collection. The forests include: GIG (2350 MAP, infertile, Oxisol), P12 (2600 MAP, infertile, Ultisol), P13 (2600 MAP, fertile, Alfisol), and SC (3421 MAP, infertile, Oxisol).

Table SI 2.4: Data of arbuscular mycorrhizal fungi (AMF) colonization across treatments, depths, forests and seasons. This table presents the proportion of root length colonized by AMF structures for different plots across different forests (GIG, P12, P13, SC), treatments (Control, Exclusion), seasons (Wet, EarlyWet, Dry) and soil depth soil depth (0-10 cm and 10-20 cm), and the corresponding percentage of AMF colonization (%). The forests include: GIG (2350 MAP, infertile, Oxisol), P12 (2600 MAP, infertile, Ultisol), P13 (2600 MAP, fertile, Alfisol), and SC (3421 MAP, infertile, Oxisol).

Table SI 2.5: Fine root chemistry to 10 cm depth, detailing phosphorus (P), carbon (C), nitrogen (N) concentrations, and C:N ratios. The data was collected using ingrowth core and sequential coring methods across different forests, plots, and treatments during specified collection periods. The forests include: GIG (2350 MAP, infertile, Oxisol), P12 (2600 MAP, infertile, Ultisol), P13 (2600 MAP, fertile, Alfisol), and SC (3421 MAP, infertile, Oxisol).

Table SI 2.6: Summary of fine root dynamics collected with the minirhizotron method. Data is presented by period, season, forests and treatment as mean ± standard error across four plots (n = 4). Data represent the average measurements of fine root productivity, mortality, peak root length standing stock (the maximum stock from all the months averaged), and mean length stock from the months measured during each season. Units are in root length (mm) per minirhizotron window area (m2) per day. The forests include: GIG (2350 MAP, infertile, Oxisol), P12 (2600 MAP, infertile, Ultisol), P13 (2600 MAP, fertile, Alfisol), and SC (3421 MAP, infertile, Oxisol).

Table SI 2.7: Annual fine root turnover ($year^{-1}$), productivity, mortality and peak root length across four forests, treatments and depths (0-90 cm). Turnover was calculated as fine root productivity divided by peak root length. The table presents mean values ± standard errors across four plots (n = 4). Data was previously averaged across two different years (2019-2020 and 2021-2022) since years were not found to be a significant factor in the models. The forests include: GIG (2350 MAP, infertile, Oxisol), P12 (2600 MAP, infertile, Ultisol), P13 (2600 MAP, fertile, Alfisol), and SC (3421 MAP, infertile, Oxisol).

Table SI 2.8: Fine root turnover ($month^{-1}$) analysis using minirhizotron methodology. Data are presented by period, season, site, and treatment as mean ± standard error across four plots (n = 4). This table summarizes the average monthly fine root productivity, mortality, and peak length standing stock, where turnover rate is calculated as the productivity divided by the peak standing stock of each season. Values are provided for each depth and treatment, representing root length (mm) per minirhizotron window area (m2) per month. The forests include: GIG (2350 MAP, infertile, Oxisol), P12 (2600 MAP, infertile, Ultisol), P13 (2600 MAP, fertile, Alfisol), and SC (3421 MAP, infertile, Oxisol).

Table SI 2.9: Dynamics of fine root biomass (< 2 mm in diameter) from ingrowth cores across different seasons and treatments. This table displays the productivity and mortality of fine root biomass, measured as milligrams of root per kilogram of dry soil per day, at two soil depths (0-10 cm and 10-20 cm) under control and exclusion treatments and across different forests. Values are reported as mean ± standard error across plots (n = 4). The forests include: GIG (2350 MAP, infertile, Oxisol), P12 (2600 MAP, infertile, Ultisol), P13 (2600 MAP, fertile, Alfisol), and SC (3421 MAP, infertile, Oxisol).

Table SI 2.10: Seasonal variability in fine root biomass from sequential coring method across different forests, treatments and soil depths. Data are reported as mean ± standard error across four plots (n=4) at different seasonal conditions—Dry, Early Wet, Late Wet, and Mid Wet, for multiple forests (GIG, P12, P13, SC) and two depths of 0-10 cm and 10-20 cm. The forests include: GIG (2350 MAP, infertile, Oxisol), P12 (2600 MAP, infertile, Ultisol), P13 (2600 MAP, fertile, Alfisol), and SC (3421 MAP, infertile, Oxisol).

Table SI 2.11: Annual fine root productivity, peak standing stock and turnover calculated as productivity divided by peak standing stock from ingrowth cores and sequential coring. The forests include: GIG (2350 MAP, infertile, Oxisol), P12 (2600 MAP, infertile, Ultisol), P13 (2600 MAP, fertile, Alfisol), and SC (3421 MAP, infertile, Oxisol).

Table SI 2.12: Fine root morphology from the ingrowth core and sequential coring methods. Data

is presented at different forests, depths (01- and 10-20 cm), collection periods and treatments. This table presents mean values ± standard error for root diameter, specific root length, specific root area, and root tissue density. Measurements reflect root traits averaged across four plots (n = 4). The forests include: GIG (2350 MAP, infertile, Oxisol), P12 (2600 MAP, infertile, Ultisol), P13 (2600 MAP, fertile, Alfisol), and SC (3421 MAP, infertile, Oxisol).

Table SI 2.13: Arbuscular mycorrhizal fungi colonization (AMF) (%) across different forests, depths, treatments and seasons when available. Data are reported as mean ± standard error across four plots (n=4). Data for the four forests (GIG, P12, P13, SC) is available for the wet season. The forests include: GIG (2350 MAP, infertile, Oxisol), P12 (2600 MAP, infertile, Ultisol), P13 (2600 MAP, fertile, Alfisol), and SC (3421 MAP, infertile, Oxisol).

Table SI 2.14: Fine root chemistry at 0-10 cm depth across forests, treatments, collection periods and methods. The table presents the concentrations of phosphorus (P), carbon (C), and nitrogen (N), and C:N ratio in fine roots measured using Ingrowth Core and Sequential Coring methods. Results are displayed as mean ± standard error across four plots (n = 4). The forests include: GIG (2350 MAP, infertile, Oxisol), P12 (2600 MAP, infertile, Ultisol), P13 (2600 MAP, fertile, Alfisol), and SC (3421 MAP, infertile, Oxisol).

Table SI 2.15: Model results from minirhizotron analyses. The block on the left represents shows results from repeated measures MANOVA analysis conducted with treatment, forests, session (time - continuous) and depth (continuous) as predictors of fine root dynamics. Because of the amount of zero's, these analyses were conducted with binary data (presence/absence). Since sessions (time) was significant for all the variables, the block in the middle represents post hoc analyses considering treatment, site, depth (when applicable) and season and years (instead of sessions) as predictors. These analyses were conducted only for the whole soil profile and surface roots. For deeper roots, there were still too many zeros in the dataset so we conducted a generalized linear model with presence/absence data and then subsequent analysis considering only the positive values.

Table SI 2.16: ANOVA table with root results from ingrowth core during experiment. The response variables include measurements of fine root productivity, total root length, root mortality, specific root length, root diameter, root tissue density, and root element concentrations (C, N, P, C/N ratio). Data were collected from different soil depths (0-10 cm and 10-20 cm) and analyzed using predictors such as Treatment, Site, Season, Year, and their interactions.

Table SI 2.17: ANOVA table with root results from sequential coring from baseline data and during the experiment for all forests. The response variables include measurements of root biomass, total root length, specific root length (SRL), root diameter, root tissue density (RTD), and root element concentrations (C, N, P, C/N ratio). The data cover measurements from baseline (September 2017 to October 2018) and various experimental collection dates (up to July 2022). Each root parameter was measured at soil depths of 0-10 cm and 10-20 cm, except for element concentrations measured only at 0-10 cm. The predictors include Treatment, Site, Depth, Season, and Year, along with significant interactions.

Table SI 2.18: ANOVA results for fine root turnover. Fine root turnover calculated as ingrowth

core productivity divided by standing crop fine root biomass from sequential coring. Treatment represents throughfall experiment vs control. Forests are indicated in the category column and depth are 0-10 and 10-20 cm. For analyses #2, we excluded two extreme outliers (turnover > 9) from year 2018.

Table SI 2.19: Results of generalized linear model with logistic function analyzing the influence of Treatment, Soil Depth, and Season on the proportion of AMF colonization (%). Coefficients, standard errors, z-values, and p-values are reported for each term.

APPENDIX 3: SUPPLEMENTARY MATERIAL FOR CHAPTER 4

Supplementary figures

Figure SI 3.1.

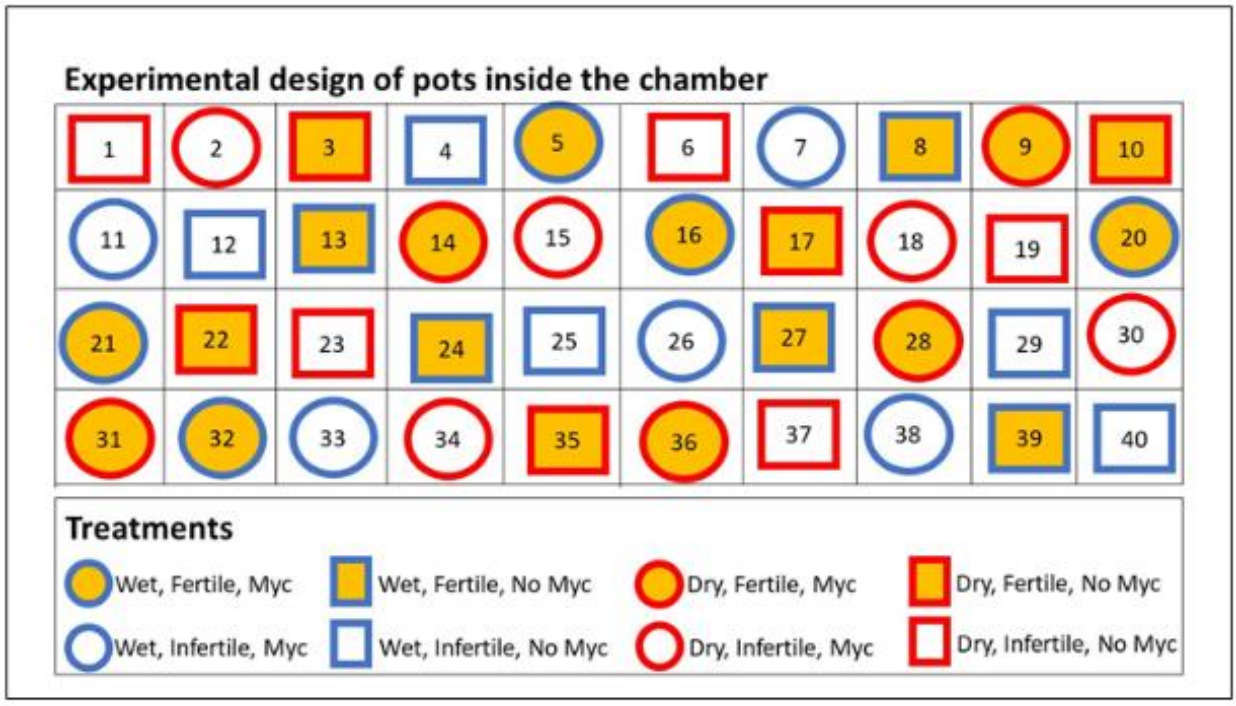

Figure SI 3.1: Experimental design of pots with two seedlings of *Tabebuia rosea* per pot inside the $^{13}CO_2$ continuous labeling chamber.

Figure SI 3.2.

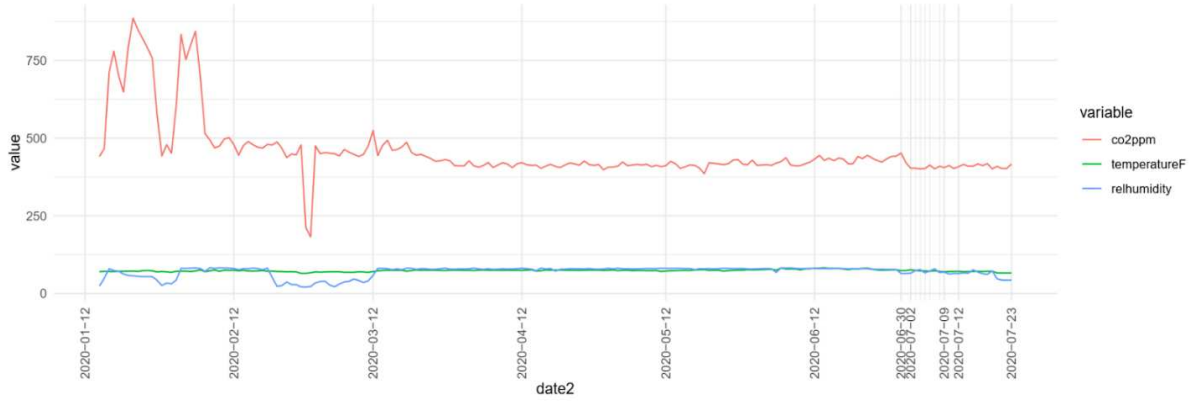

Figure SI 3.2: Temporal variation of environmental conditions within the labeling chamber during the experiment. This figure presents the changes in carbon dioxide concentration (CO_2 ppm), temperature (°F), and relative humidity (%) recorded throughout the duration of the experiment, illustrating the controlled conditions to which the plants were exposed. The chamber was sealed on 03/12/2020 and opened on 06/30/2020.

Figure SI 3.3.

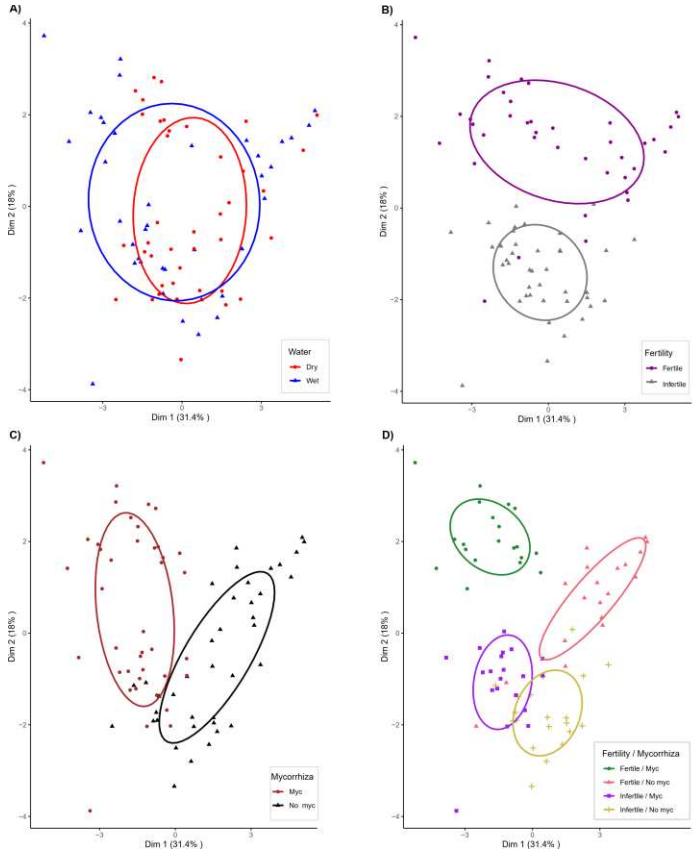

Figure SI 3.3: Tradeoffs in aboveground and belowground plant traits are shown for combinations of treatments varying in Fertility (Fertile vs Infertile), Moisture availability (Wet vs Dry) and Arbuscular Mycorrhizal Fungi association (AMF presence and AMF absence) using PCA analyses. Traits evaluated were: Root morphology (SRL, RTD and root diameter) and chemistry (N and C) traits for absorptive and transportive roots separately, below/aboveground biomass ratio, total plant biomass, and specific leaf area. Root morphology from absorptive roots was considered as the roots from orders 1-2 and from transportive roots as the average among order 3, 4 and 5. For root chemistry, absorptive roots were the ones averaged across orders 1-2 and 3, and transportive roots were averaged across orders 4 and 5. All figures show different clusters for the same data where it presents how plant traits together are affected by different treatments. Principal Coordinates Analysis (PCoA) and k-means clustering analyses were conducted using the scaled data to assess separation of variables among treatments. The Euclidean-based approach was used and the data was segregated into distinct clusters using k-means clustering with k = 2 if only two treatments were being analyzed (1A, 1B, 1C) and k =4 if four treatments were analyzed (1D).

Figure SI 3.4.

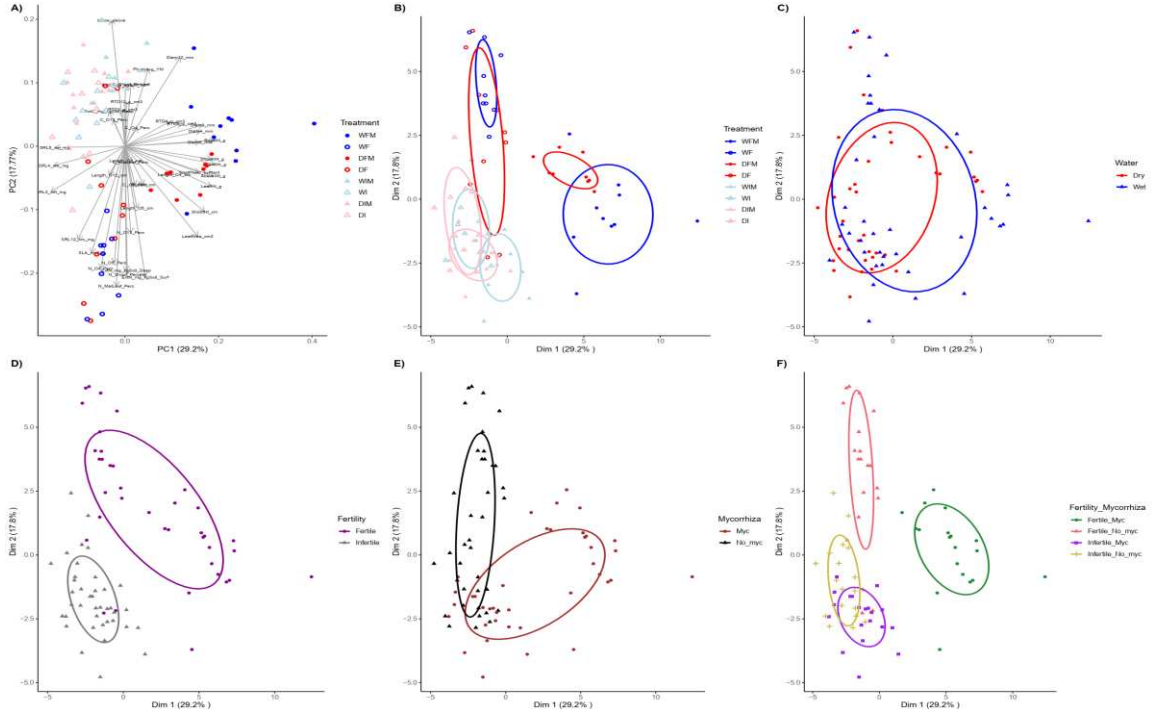

Figure SI 3.4: Tradeoffs in plant traits and plant-environment interactions variables are shown for 8 combinations of treatments varying in Fertility (Fertile vs Infertile), Moisture availability (Wet vs Dry) and Arbuscular Mycorrhizal Fungi association (AMF presence and AMF absence) using PCA analyses. Variables evaluated were: plant biomass from all tissues separately, plant traits (morphology and chemistry from all organs and separating roots in orders), photosynthesis and also soil extraction variables. A) Shows PCA results (traits names are shown in the figure) and B-F) shows different clusters for the same data where it presents how all these variables together are affected by different treatments. Principal Coordinates Analysis (PCoA) and k-means clustering analyses were conducted using the scaled data to assess separation of variables among treatments. The Euclidean-based approach was used and the data was segregated into distinct clusters using k-means clustering with k = 8 if all treatments were analyzed (1B), k = 2 if only two treatments were being analyzed (1C, 1D, 1E) and k =4 if four treatments were analyzed (1F).

Figure SI 3.5.

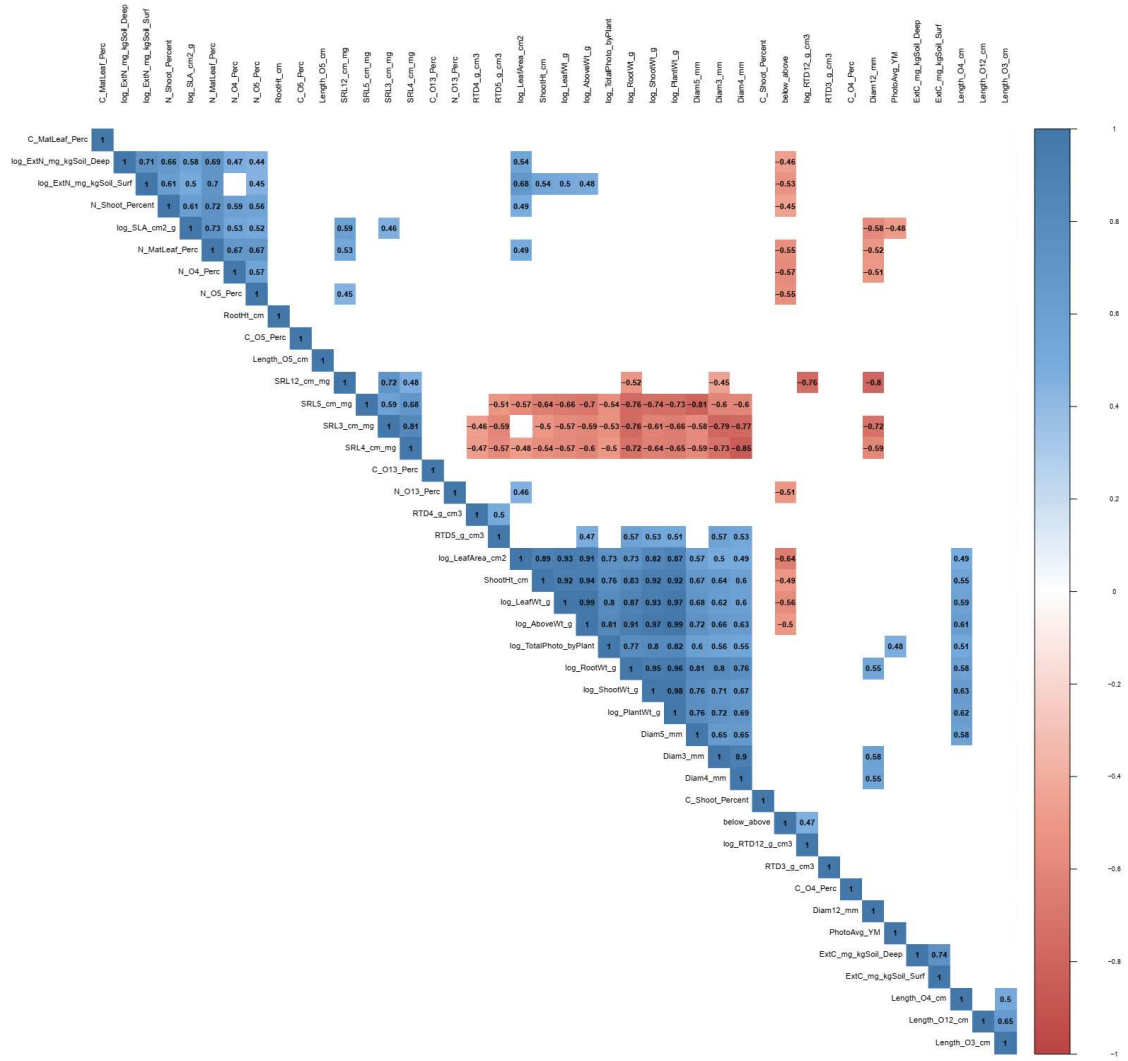

Figure SI 3.5: Pearson correlation plot including all measured variables by plant. Variables are: plant biomass from all tissues separately, plant traits (morphology and chemistry from all organs and separating roots in orders), photosynthesis and also soil extraction variables for surface and deep layer. Blank cells represent correlations that were not significantly different (p-value < 0.05) after applying Bonferroni correction. N = 80 plants (10 per treatment).

Figure SI 3.6.

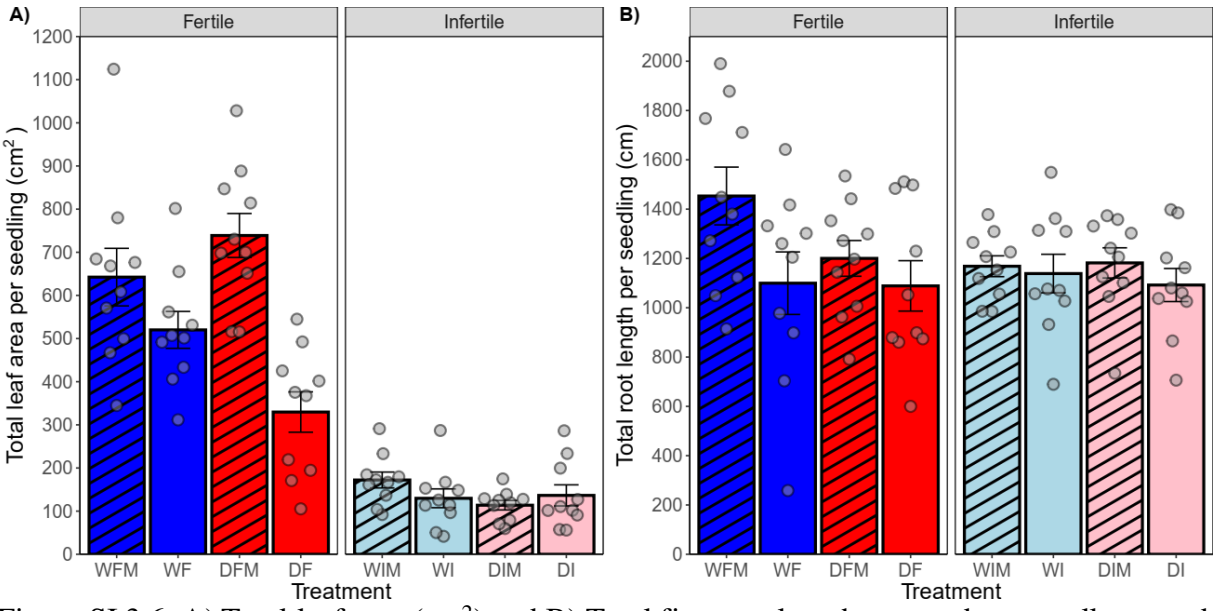

Figure SI 3.6: A) Total leaf area (cm^2) and B) Total fine root length summed across all root orders (cm) across different treatments. Data are mean ± SE (n = 10). The division in the middle of the figure shows fertile treatments on the left and infertile treatments on the right. Blue and red colors represent wet and dry treatment respectively and patterns are added when AMF is present. W=Wet, D=Dry, F=Fertile, I=Infertile, M= Mycorrhizal presence.

Figure SI 3.7.

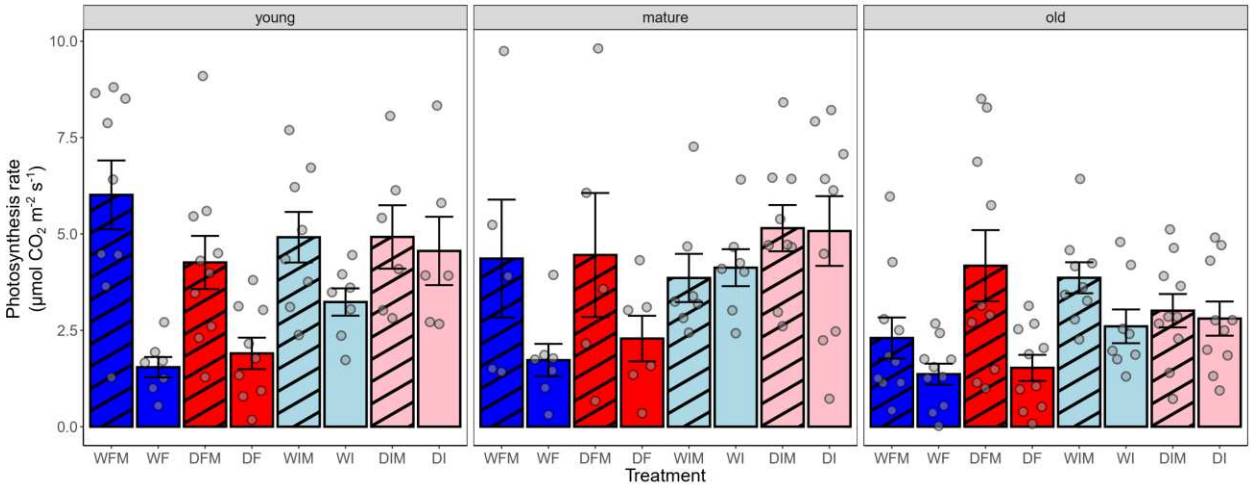

Figure SI 3.7: Photosynthesis rate collected with the one-point method in the end of the experiment across different treatments and leaves age. Pannels show different leaves age. Data are mean ± SE (n = 10). Blue and red colors represent wet and dry treatment respectively and patterns are added when AMF is present. W=Wet, D=Dry, F=Fertile, I=Infertile, M= Mycorrhizal presence.

Figure SI 3.8.

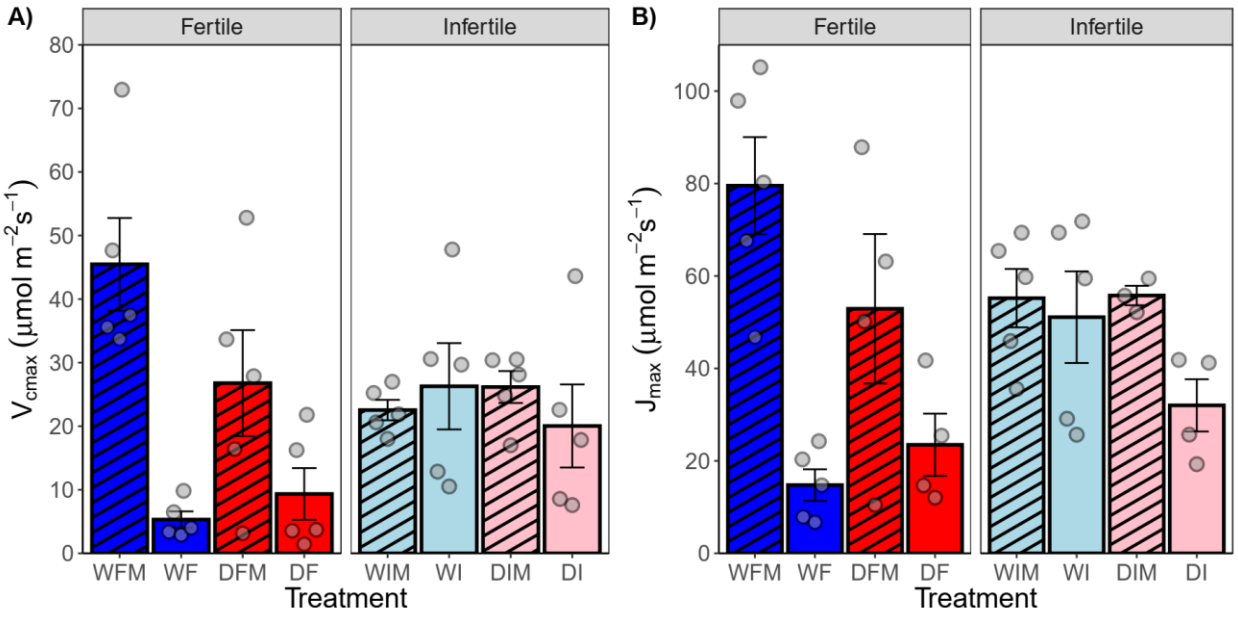

Figure SI 3.8: Photosynthesis dynamics obtained through A-Ci curves across different treatments. Data are mean ± SE (n = 5). The division in the middle of the figure shows fertile treatments on the left and infertile treatments on the right. Blue and red colors represent wet and dry treatment respectively and patterns are added when AMF is present. W=Wet, D=Dry, F=Fertile, I=Infertile, M= Mycorrhizal presence. A) VcMax (maximum rate of carboxylation) and B) JMax (maximum rate of electron transport).

Figure SI 3.9.

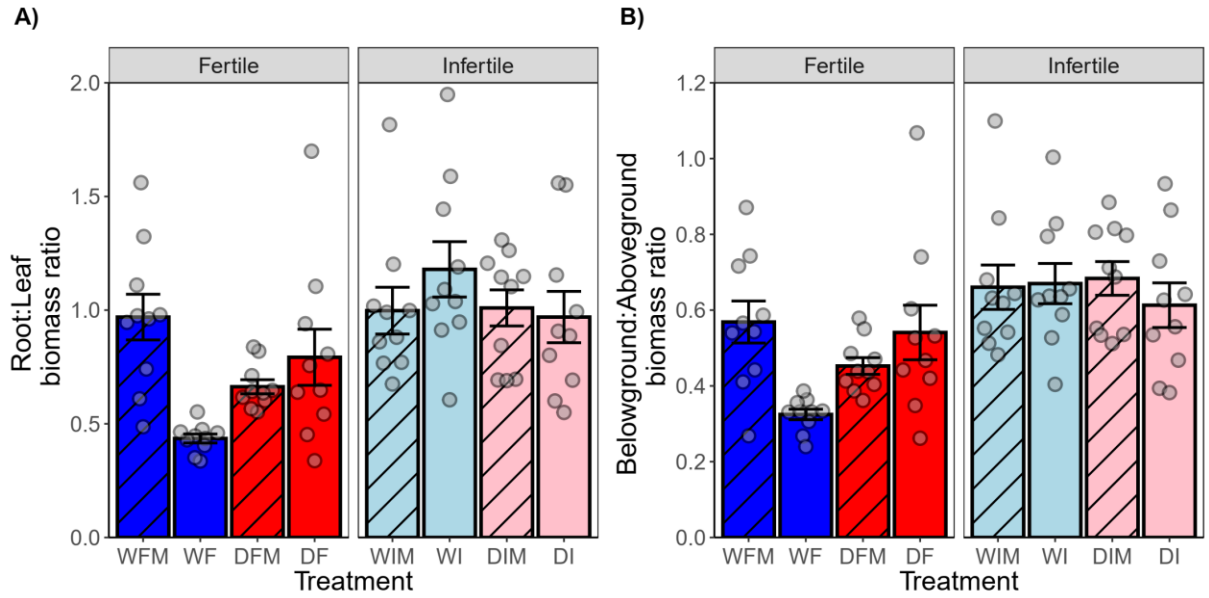

Figure SI 3.9: A) Root: leaf biomass ratio and B) belowground: aboveground biomass ratio across different treatments. Data are mean ± SE (n = 10). The division in the middle of the figure shows fertile treatments on the left and infertile treatments on the right. Blue and red colors represent wet and dry treatment respectively and patterns are added when AMF is present. W=Wet, D=Dry, F=Fertile, I=Infertile, M= Mycorrhizal presence.

Figure SI 3.10.

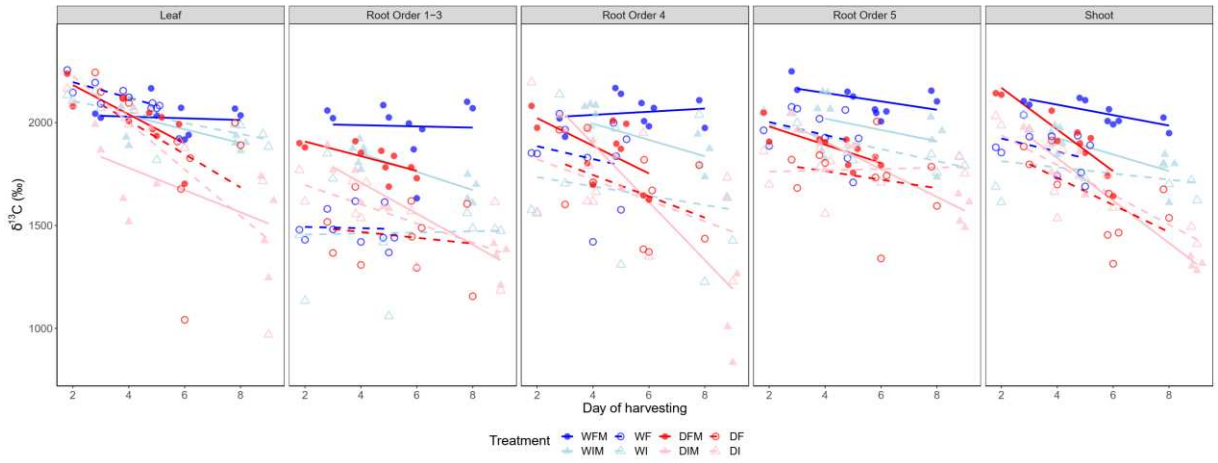

Figure SI 3.10: Temporal dynamics of $\delta^{13}C$ (‰) in different plant tissues during an 8-day post-labeling period when plants were exposed with lighter atmospheric with higher $^{12}C/^{13}C$ ratio. $\delta^{13}C$ decreased with time under varying treatments. This decrease was larger in drying treatments.

Figure SI 3.11.

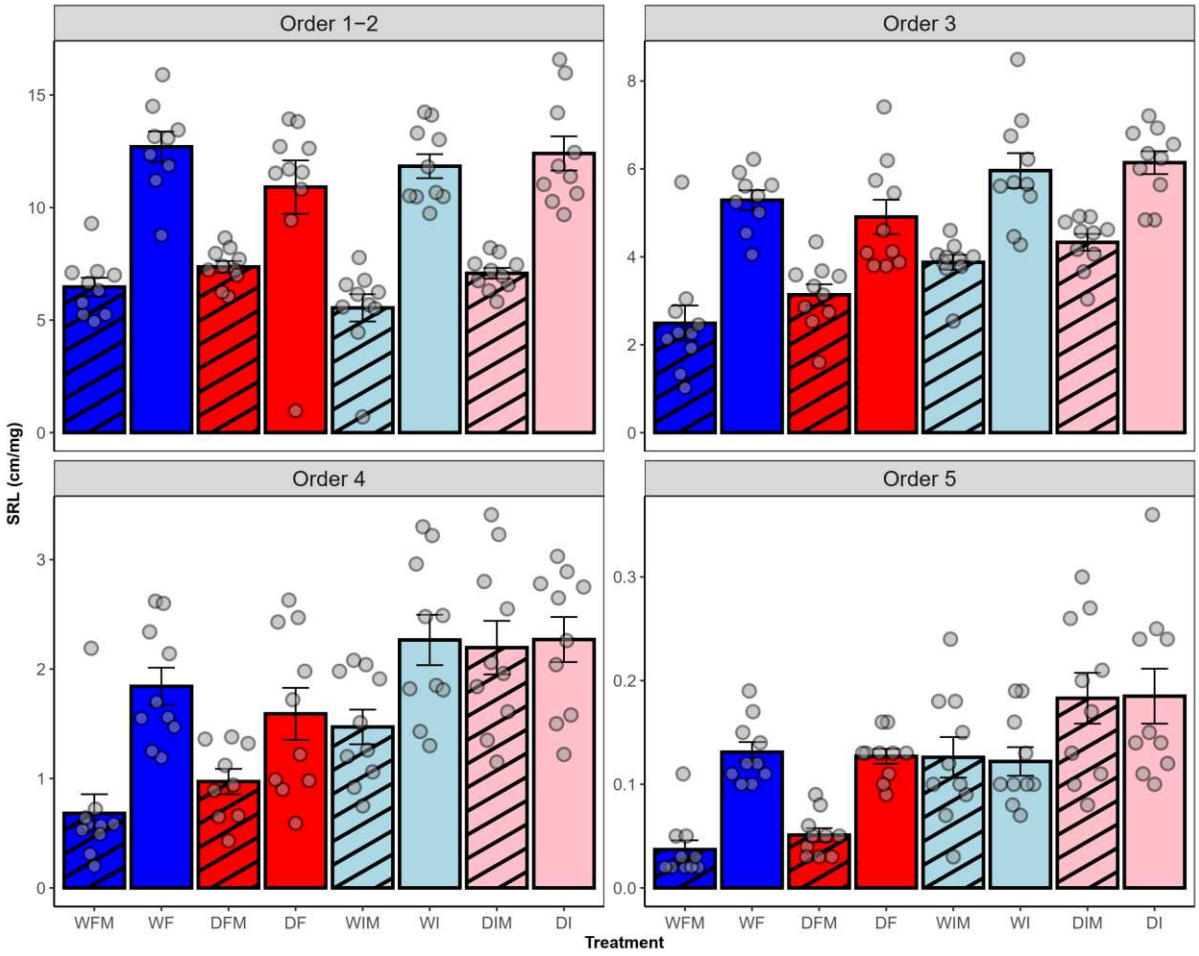

Figure SI 3.11: Specific root length (SRL) collected in the end of the experiment across different treatments. Pannels present different root orders. Data are mean ± SE (n = 10). Blue and red colors represent wet and dry treatment respectively and patterns are added when AMF is present. W=Wet, D=Dry, F=Fertile, I=Infertile, M= Mycorrhizal presence.

Figure SI 3.12.

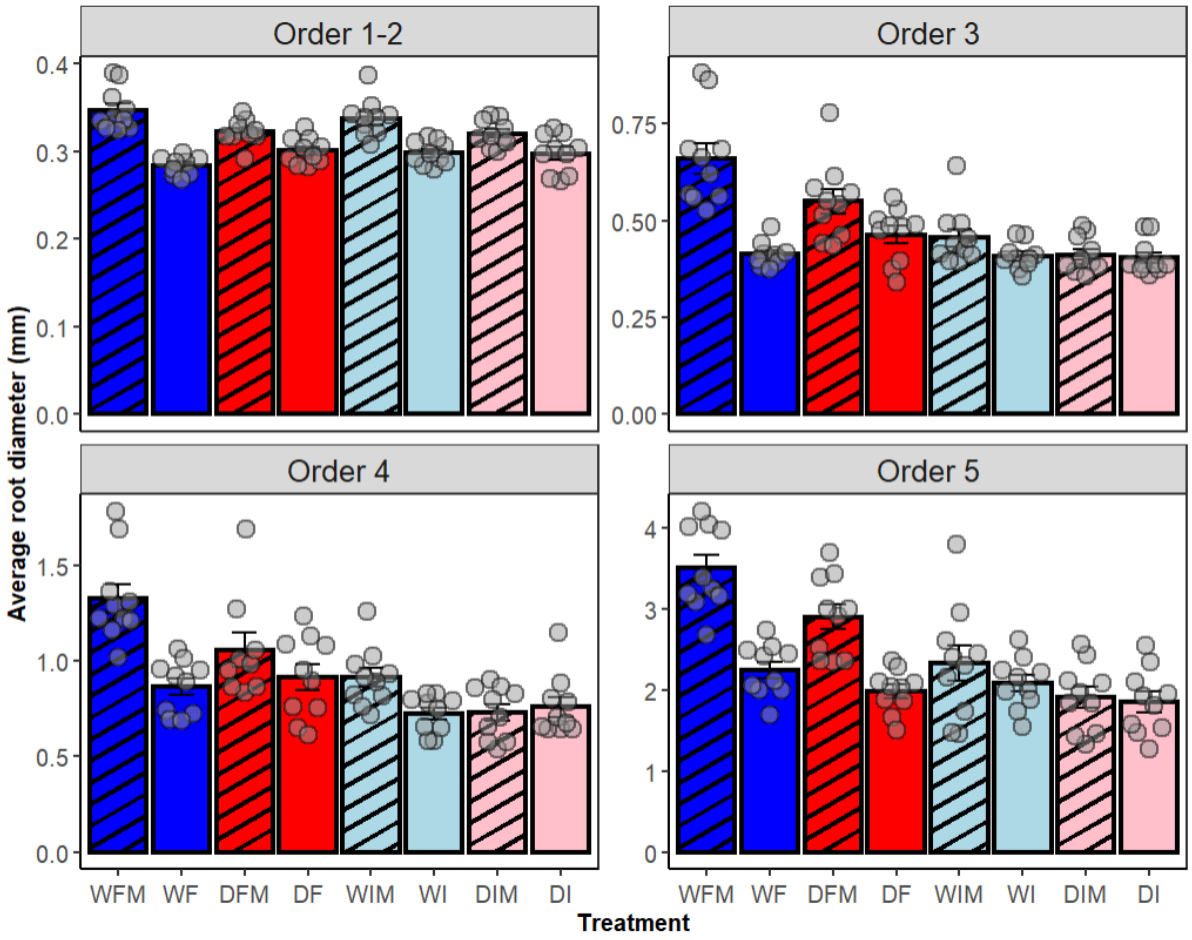

Figure SI 3.12: Root diameter collected in the end of the experiment across different treatments. Pannels present different root orders. Data are mean ± SE (n = 10). Blue and red colors represent wet and dry treatment respectively and patterns are added when AMF is present. W=Wet, D=Dry, F=Fertile, I=Infertile, M= Mycorrhizal presence.

Figure SI 3.13.

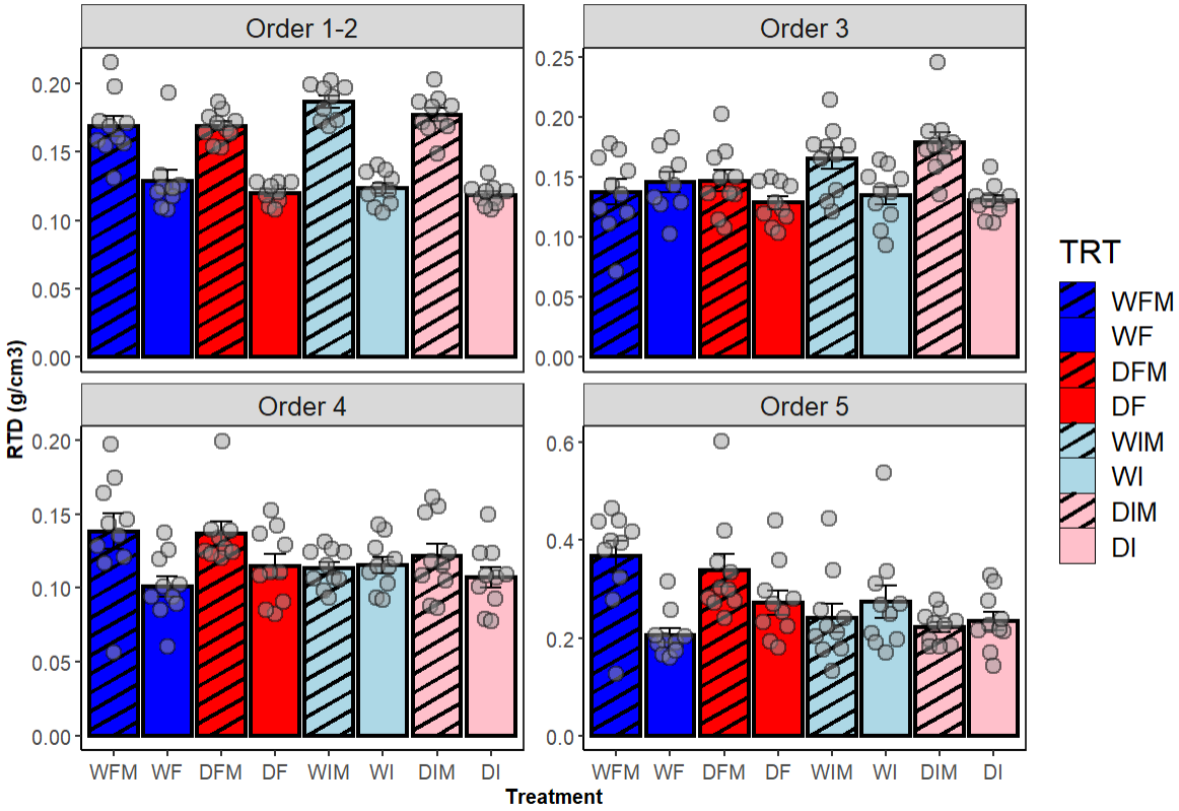

Figure SI 3.13: Root tissue density (RTD) collected in the end of the experiment across different treatments. Pannels present different root orders. Data are mean ± SE (n = 10). Blue and red colors represent wet and dry treatment respectively and patterns are added when AMF is present. W=Wet, D=Dry, F=Fertile, I=Infertile, M= Mycorrhizal presence.

Figure SI 3.14.

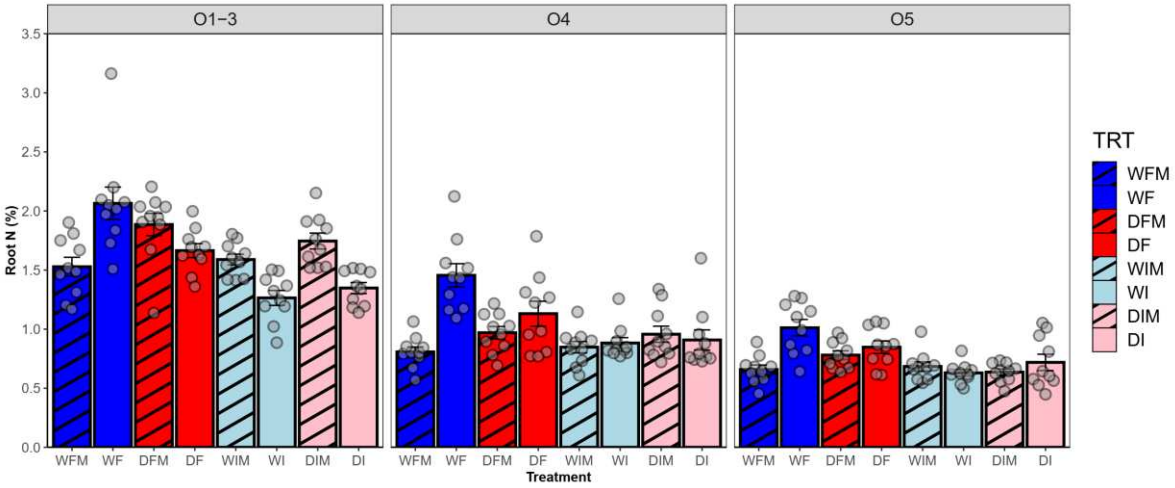

Figure SI 3.14: Root N (%) across different root orders and treatments. Pannels present different root orders. Data are mean ± SE (n = 10). Blue and red colors represent wet and dry treatment respectively and patterns are added when AMF is present. W=Wet, D=Dry, F=Fertile, I=Infertile, M= Mycorrhizal presence.

Figure SI 3.15.

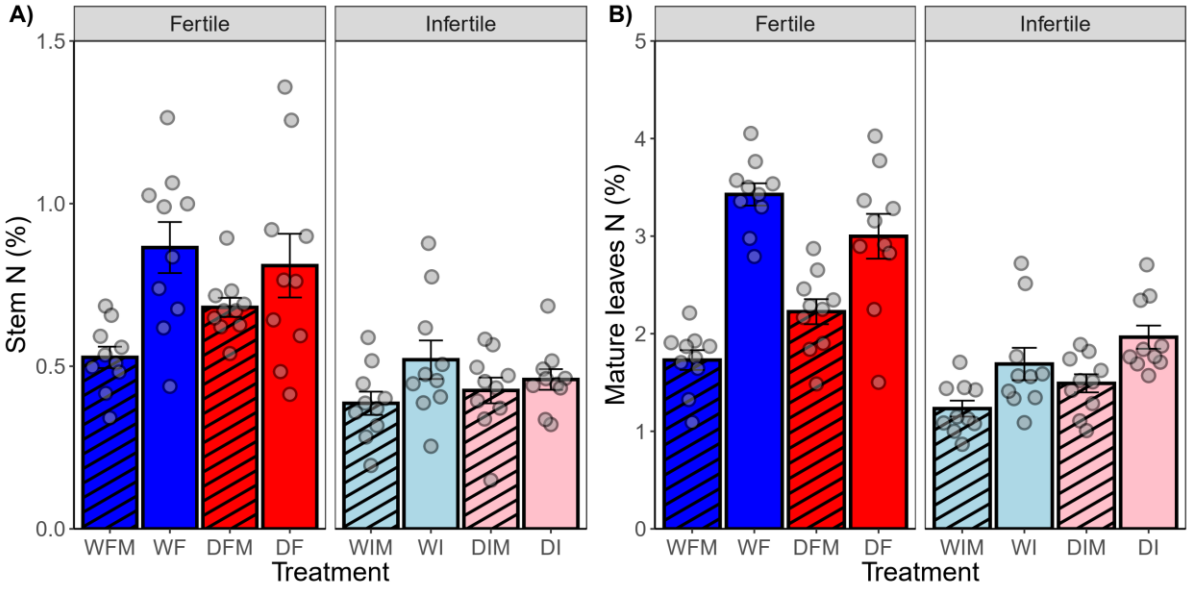

Figure SI 3.15: A) Stem N (%) and B) Mature leaves N (%) across different treatments. Data are mean ± SE (n = 10). The division in the middle of the figure shows fertile treatments on the left and infertile treatments on the right. Blue and red colors represent wet and dry treatment respectively and patterns are added when AMF is present. W=Wet, D=Dry, F=Fertile, I=Infertile, M= Mycorrhizal presence.

Figure SI 3.16.

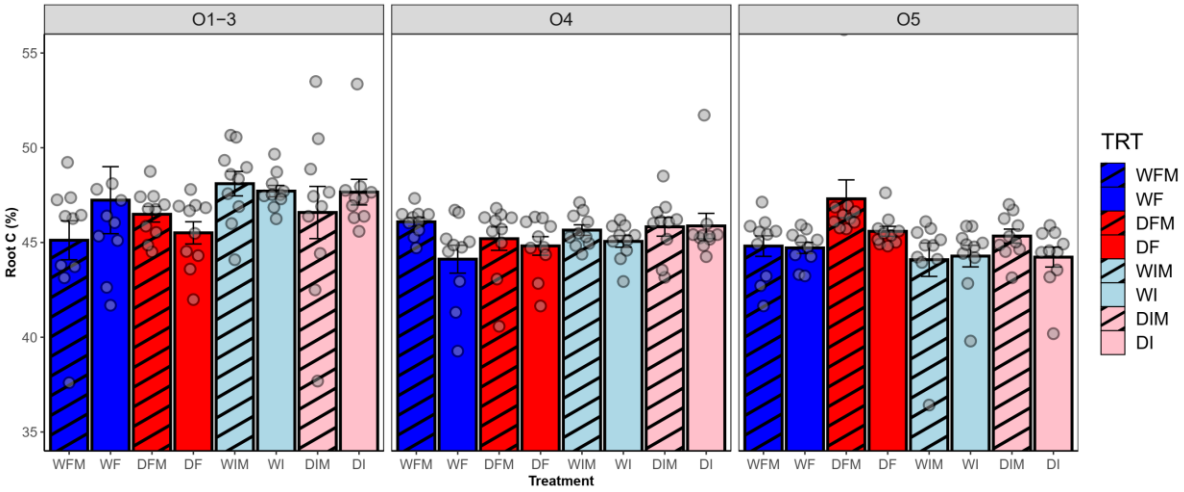

Figure SI 3.16: Root C (%) across different root orders and treatments. Pannels present different root orders. Data are mean ± SE (n = 10). Blue and red colors represent wet and dry treatment respectively and patterns are added when AMF is present. W=Wet, D=Dry, F=Fertile, I=Infertile, M= Mycorrhizal presence.

Figure SI 3.17.

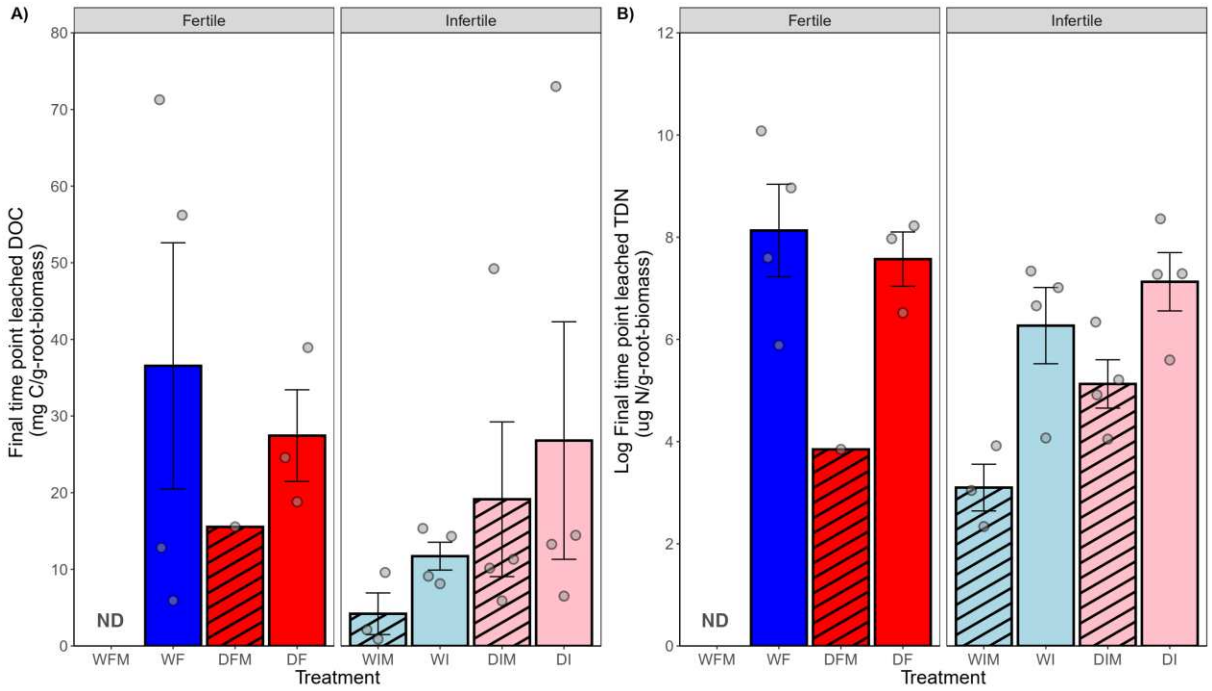

Figure SI 3.17: Final time point leachates per absorptive root biomass. DOC and TDN were measured in the end of the experiment (6/25/2020) as well as root biomass from harvest (July 2020). A) Leached DOC (mg) per absorptive root biomass (g) and B) Log Leached TDN (ug) per absorptive root biomass (g). Leachates were measured across treatments in the end of the experiment. The wet, fertile, with AMF treatment has no data available because it was not possible to collect leachates in this treatment in the last collection date. The division in the middle of the figure shows fertile treatments on the left and infertile treatments on the right. Data are mean ± SE (n = 10). Blue and red colors represent wet and dry treatment respectively and patterns are added when AMF is present. W=Wet, D=Dry, F=Fertile, I=Infertile, M= Mycorrhizal presence.

Figure SI 3.18.

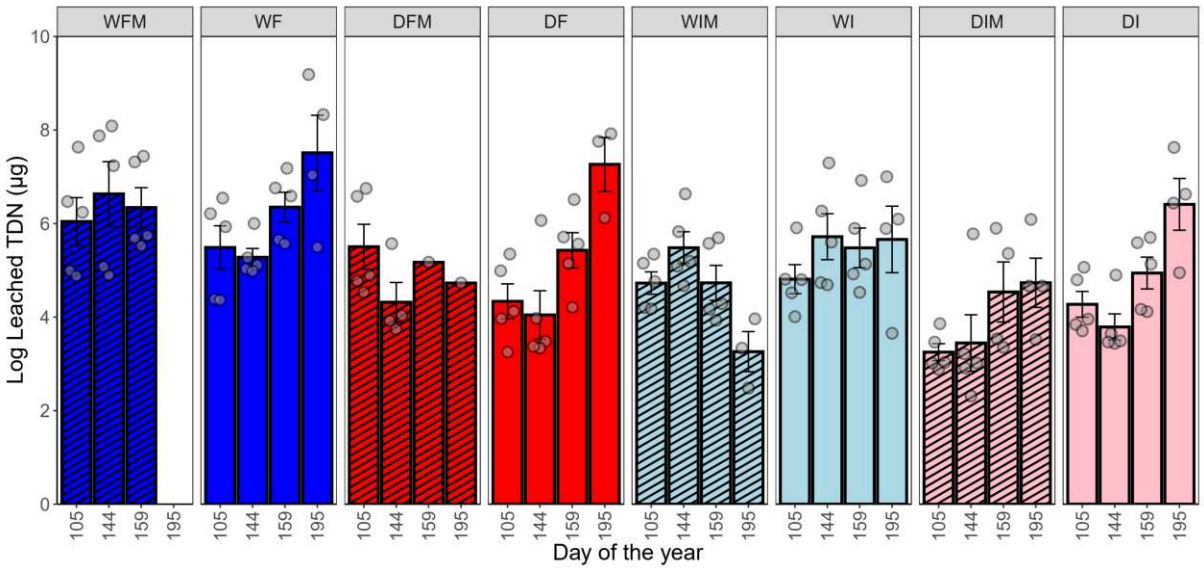

Figure SI 3.18: Log leached TDN (µg) across treatments and time. Pannels present different treatments. Data are mean ± SE (n = 10). Blue and red colors represent wet and dry treatment respectively and patterns are added when AMF is present. W=Wet, D=Dry, F=Fertile, I=Infertile, M= Mycorrhizal presence. We used measured concentrations to calculate leached N by multiplying the concentrations by the volume of water added through the irrigation system on the previous day (ml).

Figure SI 3.19.

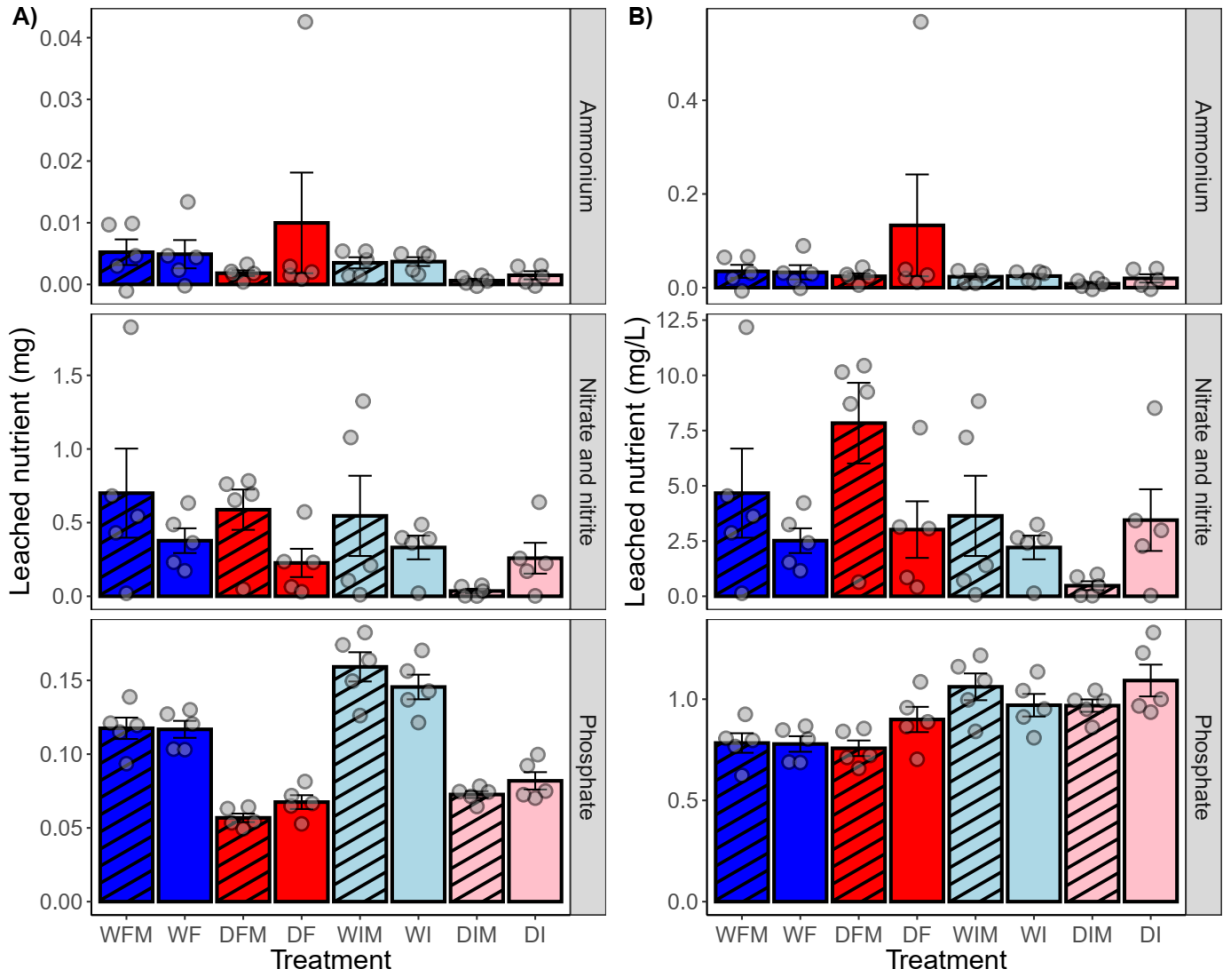

Figure SI 3.19: Total nutrients in leachates ("exudates") across different treatments. Nutrients were measured in the beginning of the experiment (3/27/2020). Pannels present different nutrients measured. Data are mean ± SE (n = 10). Blue and red colors represent wet and dry treatment respectively and patterns are added when AMF is present. W=Wet, D=Dry, F=Fertile, I=Infertile, M= Mycorrhizal presence.

Figure SI 3.20.

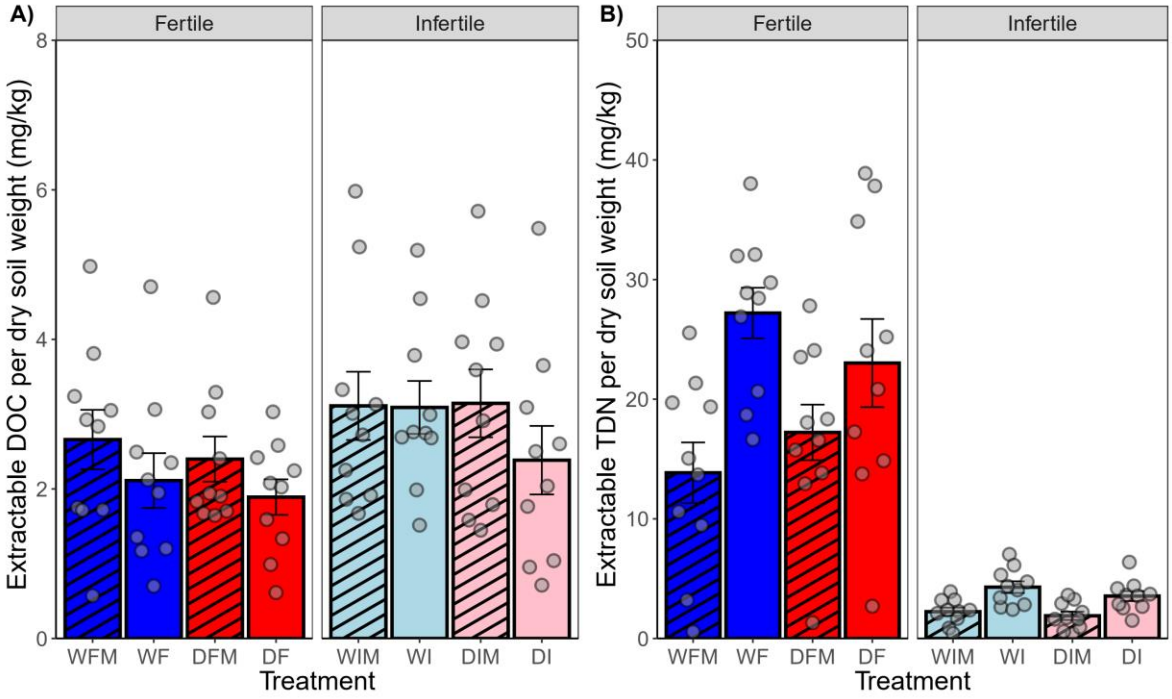

Figure SI 3.20: Chemistry from soil extractions collected at the soil surface during plant harvesting in the end of the experiment across different treatments. A) Extractable dissolved organic carbon (DOC; mg C/ kg dry soil) and B) Extractable total nitrogen (TDN; mg N/ kg dry soil). Data are mean ± SE (n = 10). Blue and red colors represent wet and dry treatment respectively and patterns are added when AMF is present. W=Wet, D=Dry, F=Fertile, I=Infertile, M= Mycorrhizal presence.

Figure SI 3.21.

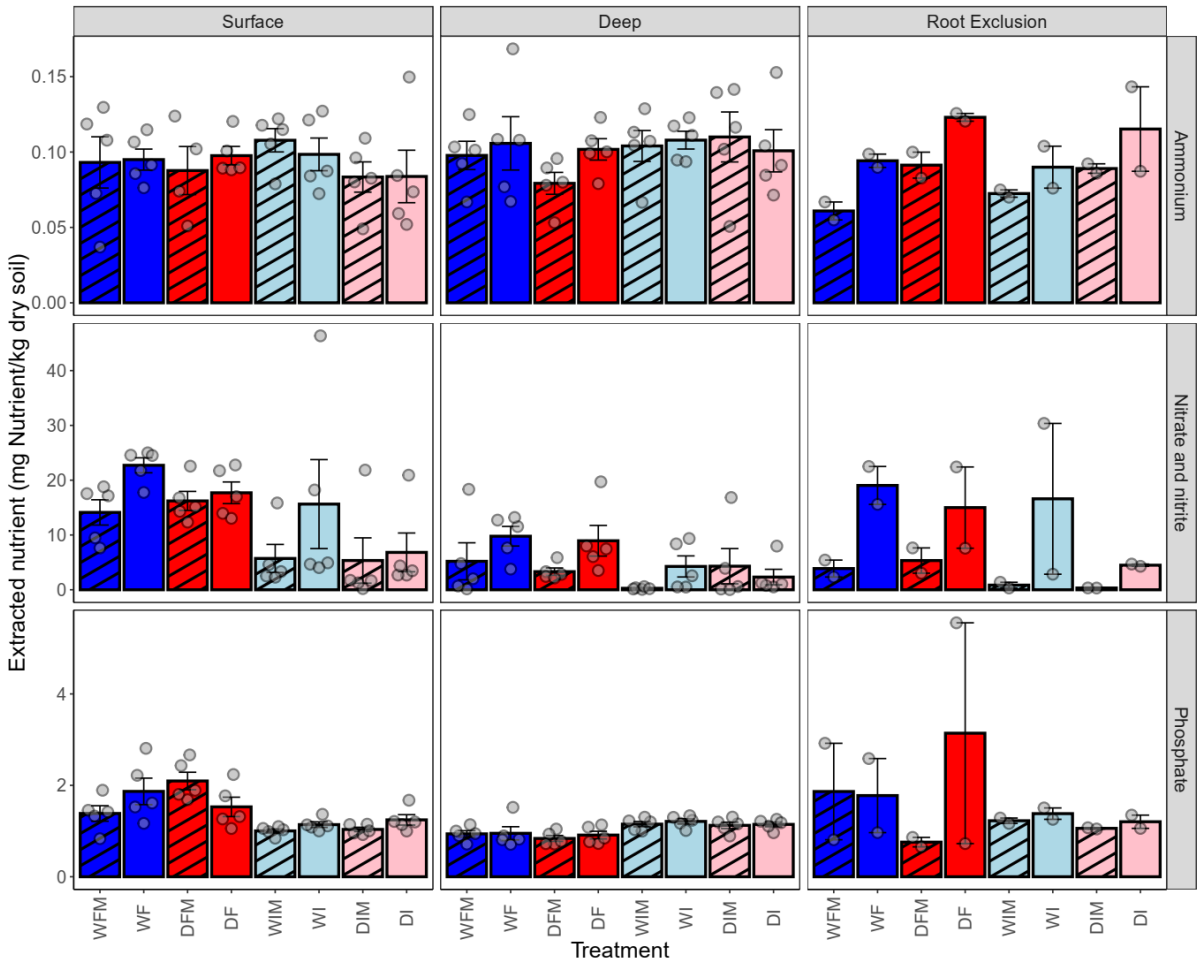

Figure SI 3.21: Extracted nutrients (mg) per kg dry soil across different treatments from soil extractions collected in the end of the experiment. Pannels present different nutrients measured on the rows and different soil locations on the columns. Data are mean ± SE (n = 10). Blue and red colors represent wet and dry treatment respectively and patterns are added when AMF is present. W=Wet, D=Dry, F=Fertile, I=Infertile, M= Mycorrhizal presence.

Figure SI 3.22.

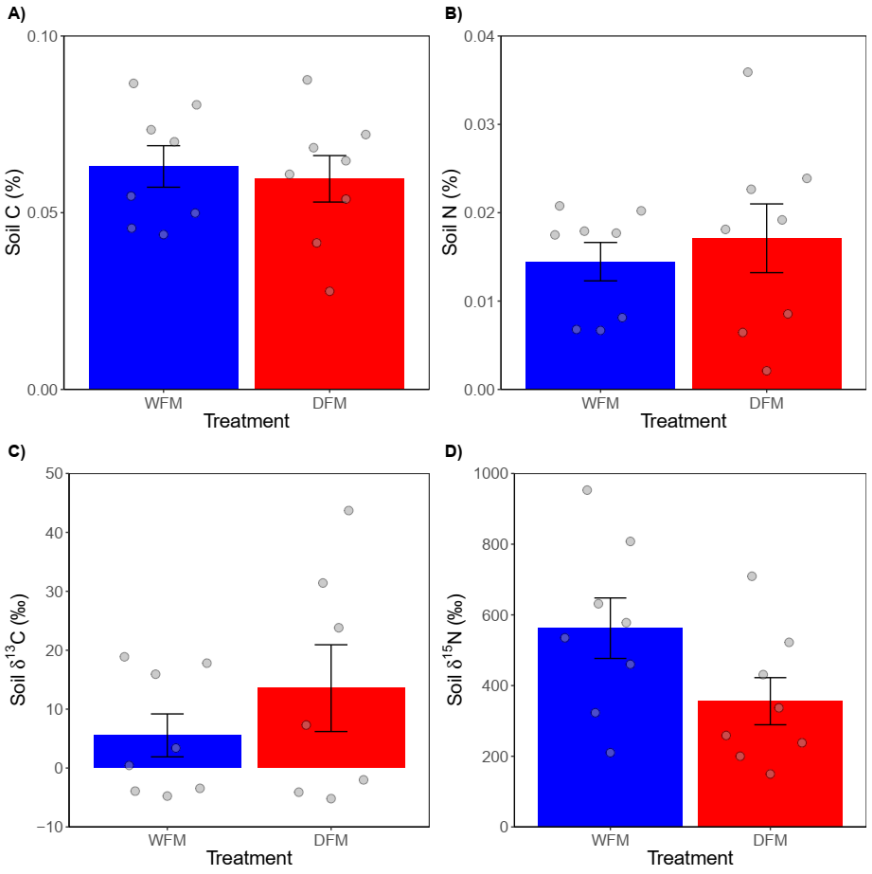

Figure SI 3.22: Soil chemistry across different treatments analyzed in the end of the experiment. A) Soil C (%), B) Soil N (%), C) Soil δ ^{13}C (‰) and D) Soil δ ^{15}N (‰). Data are mean ± SE (n = 10). Blue and red colors represent wet and dry treatment respectively and patterns are added when AMF is present. W=Wet, D=Dry, F=Fertile, M= Mycorrhizal presence.

Supplementary tables

Table SI 3.1: Master spreadsheet of raw data. This table serves as a master spreadsheet that consolidates raw data recorded for each plant and pot across varying treatment conditions. It contains variables including metadata details, harvest measures, plant morphology, plant tissue chemistry, photosynthesis, exudates and soil extractions analyses.

Table SI 3.2: Principal Component Analysis of Plant Traits. This table displays the loadings from a PCA that examined only plant trait variables. These variables include biomass from different tissues, leaf area, shoot height, rooting depth, root length, specific leaf area, below-to-aboveground biomass ratio root diameter, specific root length, and root tissue density for root orders 1-2, 3, 4, and 5, %C and %N in mature leaves, shoots and root orders 1-3, 4, and 5, extracted DOC and TDN from different soil locations, total photosynthesis and instantaneous photosynthesis. Each principal component is associated with a loading score for these variables, indicating their contribution to the component. The table also includes the proportion of variance explained by each component, the cumulative proportion with the addition of each component, the standard deviation, and eigenvalues.

Table SI 3.3: Results from MANOVA and multivariate post hoc tests are given, using Hotelling's T – squared test for differences indicated in MANOVA. Results are given across treatments. W=Wet, D=Dry, F=Fertile, I=Infertile, M= Mycorrhizal presence. Variables in the final MANOVA included: Total plant biomass, SLA, below/aboveground biomass ratio, root diameter absorptive, root diameter transportive, SRL absorptive, SRL transportive, RTD absorptive, RTD transportive, %C in mature leaves, %N in mature leaves, %C absorptive root, %N absorptive root, %C transportive root, %N transportive root, %C shoot, %N shoot.

Table SI 3.4: Principal Component Analysis encompassing a range of variables measured in the study. This table displays the loadings from a PCA that examined plant traits variables across all plant tissues including root orders separately as well as photosynthesis measured when plants were harvested and soil extractions collected in the last day of the experiment. These variables include root morphological traits like specific root length (SRL), root tissue density (RTD), and root diameter, as well as chemical traits such as nitrogen (N) and carbon (C) content for both absorptive and transportive roots as well as below-to-aboveground biomass ratio, total plant weight, and specific leaf area (SLA). Each principal component is associated with a loading score for these variables, indicating their contribution to the component. The table also includes the proportion of variance explained by each component, the cumulative proportion with the addition of each component, the standard deviation, and eigenvalues.

Table SI 3.5: ANOVA Summary table for multiple variables. The table provides statistical results from ANOVA tests for multiple variables (Response variable), with predictors including moisture, fertility, and mycorrhizal fungi (AMF) treatment, plus their interaction if significant. Degrees of freedom (Df), sum of squares (Sum Sq), mean squares (Mean Sq), F-values, and the p-value (Pr(>F)) are reported.

Table SI 3.6: Tukey HSD test results for multiple variables. This table presents the estimated marginal means (emmeans) for variables under different conditions of moisture availability (Dry

or Wet), soil fertility (Fertile or Infertile), and the presence or absence of mycorrhizal fungi (Myc or No_myc). Standard Error (SE), degrees of freedom (df), and confidence limits (lower.CL and upper.CL) are included. Tukey groupings are denoted by letters, where means that do not share a letter significantly differ at the $p<0.05$ level.

Table SI 3.7. Slopes and intercepts from regression analysis of $\delta^{13}C$ (‰) isotope composition in various plant tissues over an 8-day harvesting period when plants were exposed to atmospheric lighter CO2 (larger $^{12}C/13C$ ratio) after going inside a chamber with smaller $^{12}C/^{13}C$ ratio for ~4 months. The table presents intercepts and slopes derived from linear regression models, showing $\delta^{13}C$ in plant tissues versus plant photosynthesis.

Table SI 3.8: Results from Comparative Regression Analysis of $\delta\ ^{13}C$ (‰) Isotope Dynamics in Plant Tissues. This table summarizes the statistical evaluation of the slope and intercept for the relationship between the day of harvesting and $\delta\ ^{13}C$ content in various plant tissues (leaf, root orders 1-3, 4, and 5, shoot), as well as the slopes of the $\delta\ ^{13}C$ relationships between different root orders and leaves. Degrees of freedom (Df), sum of squares (Sum Sq), mean squares (Mean Sq), F values, and associated p-values (Pr(>F)) are provided for each predictor—moisture, fertility, mycorrhizal fungi (AMF) and plant tissue.

Table SI 3.9: Summary of Soil Chemistry. This table presents the mean values and standard errors (Mean + SE) for soil chemistry variables, categorized by the moisture levels (Wet, Dry), soil fertility (Fertile, Infertile), and mycorrhizal fungi presence (Mycorrhizal, No Mycorrhizal).

APPENDIX 4: SUPPLEMENTARY MATERIAL FOR CHAPTER 5

Supplementary table

Table SI 4.1: TropiRoot 1.0 complete database.